



University
of Glasgow

Hu, Wei. (1995) *Physical modelling of group behaviour of stone column foundations*. PhD thesis.

<http://theses.gla.ac.uk/817/>

Copyright and moral rights for this thesis are retained by the author

A copy can be downloaded for personal non-commercial research or study, without prior permission or charge

This thesis cannot be reproduced or quoted extensively from without first obtaining permission in writing from the Author

The content must not be changed in any way or sold commercially in any format or medium without the formal permission of the Author

When referring to this work, full bibliographic details including the author, title, awarding institution and date of the thesis must be given

**PHYSICAL MODELLING OF
GROUP BEHAVIOUR OF
STONE COLUMN FOUNDATIONS**

by

WEI HU

*A Dissertation submitted for
the Degree of Doctor of Philosophy*

at

University of Glasgow

Glasgow, June 1995

© *Wei Hu*

Frontispiece: Deformed model stone columns after penetration test



Physical modelling of ground behaviour of stone column foundations

WEI HU

SUMMARY

The stone column technique has been used as a method of reinforcement of soft ground over the past 30 years. Current design methods for calculation of load bearing capacity still remain essentially based on the behaviour of single isolated columns observed in the laboratory. Most popular analytical and numerical approaches tend to consider only a typical column and its tributary soil (unit cell) to represent the real situation of a group of columns working together.

This dissertation is concerned with the group behaviour of a soft clay ground reinforced by a large group of stone columns. A set of displacement controlled vertical loading tests has been conducted under laboratory condition to study the actual failure mechanisms of the granular column/clay system under a rigid circular footing. The influence of important parameters, including area replacement ratio, length of the column and the method of installation of columns, on the performance of reinforced ground was investigated through a total of 25 model tests. A limited number of tests under flexible loading were also performed.

The results clearly show that the load bearing behaviour of a group of columns is different from a single column, with particularly clear indication being provided in the shapes of the deformed columns. From these column casts it is evident that the interaction between columns and clay and between individual columns results in a general deepening of the failure mechanism following a conical wedge surface. The stresses and deformations in the foundation appear to be very complicated, however, some regional characterisation is possible. A realistic group failure mechanism is proposed in this dissertation. The area replacement ratio was found to be an extremely important parameter controlling the overall performance of the reinforced foundation: its value significantly affects the extent of column interaction, the degree of consolidation in the clay and the ratio of stress share between column and surrounding clay. Increasing the length of the column can also enhance the stiffness of the reinforced ground: a short column will punch into the clay below the column base in addition to developing localised bulging. This punching behaviour may be eliminated by increasing the length of the column. However, the effectiveness of the column length is limited to a critical level, beyond which the extra length of the column will not be of much benefit to the overall load bearing capacity of the composite ground. This critical level was found to be controlled by the ratio of column length to the diameter of the footing and hence by the overall failure mechanism rather than by the ratio of column length to the diameter of the column. It is also found that constructing columns using a displacement method will bring extra stiffness to the surrounding clay due to the lateral compaction during installation by comparison with a replacement method.

In parallel with this experimental investigation, finite element analyses were performed at University College Swansea using a homogenisation concept. Comparisons between numerical calculations and the model test results are made in this dissertation and comments are made concerning the different insights into the performance of the reinforced ground that the two approaches reveal. Results from relevant published centrifuge tests and field histories have been studied in order to validate the general findings from the present study, good general agreement was obtained.

After all, I still don't understand how do humankind generate their strength

To

Preface

During the preparation of this dissertation, many things have happened, which at times seemed as though it would never end ...What remains in me is their colour.

I am extremely grateful to my supervisor Professor David Muir Wood, for his active encouragement, stimulation and interest throughout my three years in Glasgow. I have derived great benefit from many inspiring discussions and suggestions during the period of preparation of this dissertation. His fast and logical way of thinking and his simple but precise engineering philosophy have influenced me strongly. I appreciate the value of these beyond what I managed to include in this dissertation itself. I would also like to thank Dr. Bill Stewart for his enthusiastic support and many invaluable suggestions on the experimental work. My special thanks are due to Dr. D. Greenwood (Cementation Piling & Foundation), the leading expert in the stone column technique in the UK, for his continuous interest in my research and for many useful discussions I have had with him. The generous access to his time and case histories have been much appreciated. The positive response and useful suggestions and visits from Dr. A. Bell (GKN Keller Foundation) are also gratefully acknowledged. I am also indebted to the people of Geotechnical Consulting Group, in particular Dr. R. Mair and Dr. D. Hight for their encouragement and generous financial support during the preparation of this dissertation, my friendship with them will always be maintained.

The work by University College Swansea forms a related part of the investigation carried out at Glasgow into the group behaviour of stone column foundations. Professor G. Pande, Dr. J. Lee and Dr. G. Amaniampong have provided many useful numerical results and their contributions are acknowledged. I would also like to thank: Dr. P. Smart and Dr. D.X. Luo (Glasgow University) for help in processing data using the Image Analysis System; Dr. M. Bolton and Dr. Sharma (Cambridge University) for help in using the Film Measuring Machine; and Dr. Magaverly (Royal Observatory Edinburgh) for the film scanning.

I would also like to thank Dr. R. Goughnour (formerly vice president of Vibro Flotation Company USA, now vice president of Geotechnic America Co.) for his sincere interest in my research and the generous time he spent with me during my visit to the United States. Co-operation and discussions with, and receipt of information from several enquires is also much appreciated: Professor R. Barksdale (Georgia Tech.); Dr. G. Munfukh (Parsons Brinckerhoff, New York); Hayward Baker, California; Dr. M. Terashi (Nikken Sekkei Geotechnical Institute) and Mr M. Kitazume (Japan PHRI) and Professor J. Mitchell (formerly U.C. Berkeley, now Virginia Tech.).

The experimental work lasted more than two years and was extremely intensive. I am grateful to Mr. J. MaGuire, for his diligent and enthusiastic assistance with great interest throughout the period of experiments. Technical assistant from Mr. T. Montgomery, Mr. W. Henderson and Mr. J. Tran (Soil Mechanics Laboratory); Mr. A. Yuill (Electronics) and Mr. A. Burnett (Department Superintendent), and general secretarial support from Miss B. Grant; Mrs J. Lawn and Mrs T. Bryden are also appreciated deeply.

My special gratitude is to my friends and colleagues for their consistent encouragement and warm friendship throughout the period of preparation of this dissertation. The "FTS" from Mr. Alsayed is specially remarkable. After all, the attitude to life of Miss Nicole Schwarcz is particularly unforgettable.

The experimental research described in this dissertation was funded by the Engineering and Physical Science Research Council. Data interpretation and preparation of this dissertation were supported by the Civil Engineering Department, Glasgow University. Again, I am grateful for Professor D. Muir Wood for his supportive and understanding attitude. Finally, I would like to thank the Civil Engineering Department for the facilities provided during my three years in Glasgow University.

My last and the most important acknowledgement is to my parents and my sister for their sincere endless love and deep understanding, which have been vividly supporting me through all these years whatever I do and wherever I go.

I certify that, except where specific reference is made in the text to works of others, the contents of this dissertation are original and have not been submitted to any other university. This dissertation is the result of my own work and includes nothing that is the outcome of work done in collaboration.

Wei Hu

June 1995



Contents

Summary

Preface

Chapter 0	Introduction and Outline of this dissertation	1
0.1	Introduction	1
0.2	Outline of this dissertation	2
Chapter 1	Reviews	4
1.1	Stone column foundation	4
1.1.1	The brief history	4
1.1.2	Equipment and system	5
1.1.3	Stone column construction	5
1.1.4	Application of stone columns	7
1.2	Previous research works	8
1.2.1	Introduction	8
1.2.2	Laboratory modelling	8
1.2.2.1	The work of Hughes and Withers	8
1.2.2.2	The work in Georgia Institute of Technology	9
1.2.2.3	The works of others	11
1.2.3	Full scale field tests	11
1.2.3.1	Single column tests	11
1.2.3.2	Group columns tests	12
1.2.4	Numerical and analytical analysis	13
1.2.4.1	Introduction	13
1.2.4.2	The unit cell based analysis	14
1.2.4.3	Homogenisation methods	16
1.3	Theories and present design methods	17
1.3.1	Introduction	17
1.3.2	Ultimate load bearing capacity	18
1.3.2.1	Single column analysis	18
1.3.2.2	Group column analysis	21
1.3.2.2.1	Single column based approaches	21
1.3.2.2.2	Homogenisation approaches	22
1.3.3	Settlement reduction analysis	24
1.3.3.1	Unit cell	25
1.3.3.2	Stress concentration	25

1.3.3.3	Methods of Greenwood and Hughes & Withers	26
1.3.3.4	Priebe's method and other similar approaches	27
1.3.3.5	Incremental method	28
1.3.3.6	The equilibrium method	30
1.3.4	Summary	32
1.4	The objectives of this dissertation	33
Chapter 2 Design and construction of test apparatus		35
2.1	Introduction	35
2.2	The materials	35
2.2.1	Clay	35
2.2.2	Sand	37
2.3	Modelling at reduced scale	38
2.4	Apparatus and their design	42
2.4.1	General requirements	42
2.4.2	Consolidation tank and pressure supply	42
2.4.3	Sand column installation	45
2.4.4	Loading facilities	47
2.4.4.1	Loading through rigid footing	47
2.4.4.2	Loading through flexible footing	48
2.5	Instrumentation and data acquisition	49
2.5.1	The displacement transducers (LVDTs)	49
2.5.2	Load transducer	49
2.5.3	Miniature Pressure Transducer (MPT)	50
2.5.4	Pore-water pressure transducers	51
2.5.5	Data acquisition	52
2.5.6	Photograph and Camera	52
2.5.7	Film and Measurement	53
2.5.7.1	Image Analysis	53
2.5.7.2	Film Measuring Machine (FMM)	55
Chapter 3 Experimental procedures		56
3.1	Sample preparation	56
3.1.1	Mixing of slurry	56
3.1.2	Consolidation	56
3.1.3	Clay bed preparation	59
3.2	Installation of sand columns	60
3.2.1	General	60
3.2.2	Densifying sand columns	60
3.2.3	Installing columns by replacement method	61
3.2.4	Installing columns by displacement method	62
3.2.5	The pattern and sequence	63
3.3	Loading test	64
3.3.1	Rigid loading tests	64
3.3.1.1	Loading: method and rate	64
3.3.1.2	Testing	65

3.3.2	Flexible footing tests	67
3.3.2.1	First layer (test TL01-1)	67
3.3.2.2	Second layer (test TL01-2)	68
3.3.3	Test of plain sand	68
3.3.3.1	Sample preparation	68
3.3.3.2	Testing	70
3.4	Post-loading investigations	71
3.4.1	Shear vane testing	71
3.4.2	Water content testing	72
3.4.3	Discovery of the deformed column shapes	73
3.4.3.1	Resin grouting	73
3.4.3.2	Section slicing	74
3.4.3.3	Plaster casting	74
Chapter 4	Presentation of the results and discussions	76
4.1	Introduction and testing programme	76
4.2	The measurements	79
4.2.1	Introduction	79
4.2.2	Load-displacement relationships	79
4.2.3	The surface displacement	82
4.2.3.1	Vertical displacement	82
4.2.3.2	Horizontal displacement	86
4.2.4	Measurement from Miniature Pressure Transducers (MPT)	87
4.2.5	Shear vane and Water content tests	90
4.3	The failure mechanisms under a rigid footing	93
4.3.1	Introduction	93
4.3.2	Deformations and characteristics	93
4.3.2.1	Model with short columns	93
4.3.2.2	Model with long columns	94
4.3.2.3	Parametric variations	95
4.3.3	The mechanism of failure	97
4.3.3.1	Zone "I" (elastic zone)	97
4.3.3.2	Zone "II" (plastic zone)	98
4.3.3.3	The potential failure surface A	99
4.3.3.4	Zone "III" (retaining zone) and Zone "IV" (extension zone)	101
4.3.4	Discussion on the load bearing behaviour of an axial symmetry system	102
4.4	Summary	104
4.5	Results from flexible loading test	105
4.5.1	The measurements	105
4.5.2	Discussion of the failure mechanisms	106
Chapter 5	Discussion of results of model tests compared with published numerical results	108
5.1	Introduction	108
5.2	The load displacement relationship under a rigid footing load	109

5.2.1	The load bearing characteristics	109
5.2.2	The effect of parametric variations	109
	5.2.2.1 Effect of area replacement ratio (A_s)	111
	5.2.2.2 Effect of the column length	112
5.3	Stress and deformation characteristics in a composite ground	115
	5.3.1 Stresses and deformations under a rigid footing	115
	5.3.2 Stress concentration in a composite ground	117
5.4	Settlement and consolidation	119
	5.4.1 General consolidation analysis	119
	5.4.2 Foundation under a flexible loading	121
	5.4.2.1 Stresses and deformations	121
	5.4.2.2 Consolidation under a flexible loading	122
	5.4.3 The consolidation due to column installation	124
5.5	Summary	125
	5.5.1 Evaluation of the Swansea homogenised analyses	125
	5.5.2 Further points drawn from various FE analyses	126

Chapter 6 Discussions of results of model tests compared with published results from centrifuge and field tests 127

6.1	Introduction	127
6.2	Centrifuge test results	128
	6.2.1 The test carried out at PHRI (Failure mechanisms)	128
	6.2.2 The test carried out in TIT (Width study)	129
6.3	Field case histories	131
	6.3.1 Stone column reinforced foundation under a rigid footing load	131
	6.3.1.1 Stress concentration	131
	6.3.1.2 Case history I: Hampton field trial	132
	6.3.2 Stone column reinforced foundation under an embankment loading	136
	6.3.2.1 General deformation characteristics	136
	6.3.2.2 Case history II: East Brent Trial Embankment	138
6.4	Summary and Conclusions	142
	6.4.1 Foundation under a rigid footing load	142
	6.4.2 Foundation under an embankment-like flexible loading	143

Chapter 7 Conclusions and Recommendations 144

7.1	Conclusions	144
	7.1.1 Foundation under a rigid footing load	144
	7.1.2 Foundation under flexible loading	146
7.2	Recommendations for future research	147

References

Figures

Plates

Chapter 0

Introduction and Outline of this dissertation

0.1 Introduction

In modern earth construction, there is an ever increasing need to utilise marginal sites and poorer soils as the availability of suitable construction sites decreases. In recent years, among the growing methods of soft ground treatment techniques, stone column foundations, or vibroflotation, have been generally recognised as a useful technique to reinforce cohesive soils for structural foundations. The principal concept of stone columns reinforcement involves the replacement of 10 to 35 percent of the weak soil with coarse granular material such as stone, or sometimes sand, in the form of columns. Two ways of forming the granular columns are known as "wet vibro-replacement" method and "dry vibro-displacement", or "vibro-compaction" method respectively. The inclusion of stiffer, relative incompressible granular material in a soft ground increases the load bearing capacity of the foundation and reduces the settlement of the structure as it is loaded. The presence of the columns of granular material also helps to speed consolidation effects in the soft ground.

Theories concerning the behaviour of stone column reinforced ground have been developed over the last 20 years world wide, mostly in Europe and USA. The load carrying behaviour of a single isolated column has been well understood (Hughes and Withers 1974). The complexity of column-soil and column-column interaction in a large group of stone columns under load has been recognised to some extent (Barksdale & Bachus 1979, Priebe 1989). To solve realistic engineering problems, many of the complexities of the problem have been simplified. For calculation of load bearing capacity, a column in a group is normally assumed to behave similarly to a single isolated column so that the load capacity of a group of columns is estimated from single column ultimate capacity multiplied by the number of columns in the group. Most settlement prediction methods neglect the boundary

conditions and analyse a typical column and its tributary area (unit cell) to represent a large area reinforced by a group or groups of stone columns (Priebe 1976, Baumann & Bauer 1976, Balaam 1978, Goughnour 1979). In most analyses, the stress redistribution between soil and stone column is assumed very approximately to be a constant stress concentration ratio, which is normally obtained from field measurement at the surface of the column or sometimes based on past experience (Mitchell 1981). As a consequence, engineering design of stone column foundations still retains its empirical and semi-empirical flavour. (Mitchell 1981, Greenwood & Kirsch 1983, Barksdale & Bachus 1983, Greenwood 1994, Munfakh 1994). So far, there is no rational design approach available to realistically introduce the group interaction effect for stone columns into the practical design in a simple manner.

This dissertation examines the behaviour of a soft cohesive ground reinforced by a large group of stone columns under a rigid footing load. Some attention is also given to the behaviour of foundations subjected to a uniform flexible loading. The investigation tool used is physical laboratory modelling at reduced scale. Overall twenty four model tests were conducted at Glasgow University by the author over a period of two years. Field tests data supplied by specialist contractors and some published case data are also re-analysed in the light of the failure mechanisms of groups of columns extrapolated from the model tests. Investigations concerning current design methods for stone column foundations have been made by the author through an intensive literature review and visits to specialist contractors in UK and USA. The final aim of this dissertation is to discover the group failure mechanisms of stone column reinforced foundation and to understand the influence of the major variables including area replacement ratio, column length and method of installation on the performance of reinforced ground.

0.2 Outline of this dissertation

Chapter 1 provides brief background information of stone column foundations and reviews previous research work relevant to the subject of the present study. Most existing theories and approaches currently being used in design practice will be intensively reviewed.

The design and manufacture of testing apparatus and instrumentation used in this model study will be presented in Chapter 2, and Chapter 3 will describe the specimen preparation and general procedures used for the model testing.

The testing programme designed to discover the effect of varying some important design parameters will be described in Chapter 4. Also, the measurements from all the model tests will be presented in this Chapter together with author's interpretation. The failure mechanism for a stone column reinforced foundation under a rigid footing load is presented on the basis of information deduced from the deformed shapes of columns after tests together with other findings from the measurements.

Chapter 5 will compare the results obtained from model tests with those obtained from a finite element analysis developed at University College Swansea using a homogenisation method. Other published numerical results will also be used to compare with the findings from model tests and to gain further understanding of the behaviour of stone column reinforced foundations.

Relevant results from published centrifuge tests and field studies will be used to further validate the findings from present model study in Chapter 6. Discussions concerning stone column foundation subjected to embankment-like flexible loading will also be presented in this Chapter.

Finally, a brief summary will be presented in Chapter 7. Some unsolved problems will be highlighted and recommendations for further research will also be made.

Chapter 1

Reviews

1.1 Stone column foundation

1.1.1 The brief history

Stone columns were possibly first used by French military engineers to support the heavy foundations of an ironworks on soft estuarine deposits in 1830 (Moreau et al 1835). The technique was forgotten until 1933 when Serzey Steuerman with Johann Keller patented a basic vibratory machine for ground immersion in Germany. The first true vibro-flotation job in the style of today was undertaken by Keller in Berlin 1937 to compact a 7.5m depth of loose sand in situ by vibration. The bearing capacity was reported as being doubled with relative density increased from 45% to 80%. At about same time, Serzey Steuerman formed his own Vibroflotation Foundation Company (V.F.C) in Pittsburgh USA. Since then, the development of vibro-flotation has been split into two part between Germany and USA during the 1940s and 1950s

By the late 1950s, the depths of treatment were in excess of 20 metres. It was about this time that the vibro compaction process was introduced into Britain when the use of Steuerman's American system was purchased by Cementation from VFC in 1957. Facing the fact that majority of sites in Britain that need treatment consist of finer and more cohesive soil, both Cementation and Keller have developed the technique of backfilling stone material by either a wet or dry method to suit the sites and economics. This has formed the basis of the wet vibro-replacement and dry vibro-displacement techniques used today. A more detailed history of vibro-flotation has been given by Greenwood (1976).

1.1.2 Equipment and system

The basic tool used in vibroflotation is a torpedo-shaped poker vibrator (Fig. 1.1) with dimensions normally in the range of 300 to 400 mm in diameter and 2 to 3.5m in length. Weights of the poker vary from 2 to 4 tonnes according to size and purpose. The vibrator contains an eccentric weight mounted near the bottom on a vertical shaft directly linked to a motor in the body of the machine. Vibratory motion is therefore horizontal with the body cycling around the vertical centre axis. Energy is applied directly to the ground through the tubular casing of the machine with constant output. Flushing jets are located in the nose cone and sides of the poker, and fins are provided to prevent rotation of the poker.

The machine is suspended through a flexible vibration damping connection to a follower tube which provide extension pieces to allow deep penetration into the ground. Power and flush supply lines are accommodated within the follower tubes. The machine can be electrically or hydraulically driven. The whole unit is lifted by a crane which may additionally carry the machine's driving system in the form of a power pack so that the whole system is a mobile self-contained unit.

The common power used is in the range of 35 to 100 kW. Recently developed machines can provide power up to 160 kW. Frequencies of vibration are usually fixed arbitrarily at either 30 or 50 Hz. Lateral impact forces have been from 5 to over 30 tonnes. Vibroflot sinking rates of 1 to 2 m/min and withdrawal/compaction rates of about 0.3 m/min are typical. Water pressures of up to 0.8 MPa and flow rates up to 3000 l/min can be used to facilitate penetration. Quite often the vibrators are provided with an automatic system for continuous recording of power output and depth of penetration. Additional details are presented by Brown (1977), Bauman and Bauer (1974) and Greenwood & Kirsh (1983).

1.1.3 Stone column construction

The stone columns are normally installed by either the vibro-displacement wet method or by the vibro-displacement dry method depending on the ground conditions and other construction details. Fig. 1.2 schematically illustrates the process of these two method in the field.

In the vibro-replacement method (Fig. 1.2a), the machine is run using the lower water jets to aid penetration under the weight of the vibroflot and the follower tube.

Soil is displaced by the jetting process and transported to the surface in the water flow during the formation of the borehole. Once the desired depth is reached, the poker is surged several times to clear the loose soft soils from the hole while water is kept flowing throughout construction to help stabilise the side walls of the hole. Then the backfill material is dumped into the annular space between the poker and the sidewalls of the hole from the ground surface as the poker is slowly withdrawn in controlled steps (lifts). Compaction of the stone is accomplished by re-penetration of each lift by the poker, a process which drives the stone laterally into the sidewalls of the hole and thus enlarges the column. The column normally finishes at a diameter between 0.8 to 1 m depending primarily on the strength of the subsurface soil. The softer the ground the larger the diameter. In addition, exceptionally large diameter columns can be formed by coupling vibrators together.

The vibro-displacement method (Fig. 1.2b) uses compressed air to aid the penetration (hole making) both by vibratory impact and by machine weight itself. There is no soil removed during this process. Instead, the soil is displaced laterally as it is around a driven pile to form an open hole. The diameter of the bore is usually about 0.6m, which is smaller than the hole typically formed using the vibro-replacement method. To avoid the need to remove the probe from the hole and to protect against collapse of the hole in softer soils, a new system of feeding the stone directly from the tip of the poker, the so-called bottom-feed system, was developed in Germany. This technique permits the construction of stone columns by vibro-displacement in soft liquefiable soils. The detailed description of this "bottom-feed vibrator" system and its modification for construction of both dry and mortared stone columns have been presented by Jebe and Bartels (1983)

The principal difference between the wet process and dry process is in the way in which the holes are formed. In the wet process, the removed soil space can be seen as being occupied by the stone, and the compaction pushes the stone further into the periphery soil until an equilibrium is reached. Therefore, the surrounding soil undergoes less significant shear strain as a result of the attenuation of both vibratory stresses and the ramming pressure. Whereas in the dry process, since the soil is being pushed sideways and not removed from the hole, the local shearing inevitably takes place (providing there has been no collapse of the bore) and hence permanent plastic deformation remains in the soil.

Some other techniques have been developed which involve concepts similar to these wet and dry methods. Rammed stone columns are used primarily in Belgium. After a

hole is created by driving a pipe or boring, backfill material is compacted in-situ by means of a heavy falling weight. In Japan, large diameter sand compaction piles are constructed by driving a casing pipe to a desired depth in the ground using a vibratory hammer and placing the sand inside this pipe in lifts as the pipe is partially withdrawn with the aid of compressed air and redriven to compact and enlarge the sand pile in the ground (Aboshi et al 1979). A combination of stone columns and dynamic compaction is used in France to treat soft unstable sites (Liausu 1984). This dynamic-replacement method is capable of improving soil both underneath the proposed footings and in adjacent areas through horizontal densification (Gamin 1984). However, these techniques are beyond the scope of this dissertation.

1.1.4 Application of stone columns

All ground treatment methods are developed to solve specific construction problems. The stone column technique is normally used to:

1. reduce the total and differential settlement of soft cohesive ground due to the applied load.
2. reduce the time required for consolidation settlement to occur.
3. increase the load bearing capacity of the soft ground.
4. increase the shear resistance of the cohesive material and reduce the potential for slope instability.
5. density cohesionless material and protect it from potential liquefaction under seismic loading.

However, this technique is not universally applicable to all sites. It is limited to certain ground conditions and other construction details. According to experience from specialist contractors and engineers in Europe and USA, normally subsurface soils whose shear strengths lie in the range 10 to 50 kPa are considered to be candidates. Vibro-replacement is normally used for sites with high ground water level. Greenwood (1983) suggested that the vibro-displacement method can be applied in stable insensitive cohesive soils whose shear strength lies in the range 30 to 60 kPa with a relative low ground water level. Barksdale & Bachus (1983) commented that stone columns work most effectively when they are used for area stabilisation rather than for a structural foundations. Most recommended treatment depths are in the range of 6 to 15 m although columns have been constructed to a depth greater than 30 m. It is not usually recommended to "float" columns in weak subsurface soils and a competent end bearing for stone columns is generally

specified. A blanket of sand or gravel over 0.3 m in thickness is usually placed over the top which serves both as a drainage layer and to distribute stresses from the structure or structures above.

1.2 Previous research works

1.2.1 Introduction

During the last three decades, the complexities of column-soil and column-column interaction have been approached by a number of investigators in various ways. The analytical techniques used in these approaches have been laboratory modelling, full scale testing and numerical/analytical methods.

1.2.2 Laboratory modelling

1.2.2.1 The work of Hughes and Withers

Possibly the most influential laboratory model study in today's understanding of the load carrying capacity of individual stone columns is the one reported by Hughes and Withers (1974). A series of single isolated model sand columns (150 mm in length and diameter at the range of 12.5 to 38 mm) constructed in one-dimensionally consolidated kaolin clay beds were tested in Cambridge. Stress controlled load was slowly applied to the column area. Radiographic techniques were employed to determine the displacement of pre-placed lead shots in the clay and column at various levels (Fig. 1.3).

Hughes and Withers found that under vertical load, a single isolated column bulges near the top in order to generate extra lateral confining stress (Fig. 1.4). The authors stated that the column's ultimate strength is governed primarily by the maximum lateral reaction of the soil in the bulging zone and that the extent of vertical movement within the column is limited. The authors idealised such bulging behaviour as similar to the expanding of a pressuremeter. When the horizontal resistance of the soil reaches its limiting value, indefinite expansion of the column occurs and it fails. By adapting Gibson and Anderson's elasto plastic theory for expansion of a cylindrical cavity, the authors established a simple method to estimate the load bearing capacity for a single isolated stone column in terms of the undrained shear strength of the clay and the internal friction angle of the column

material. Also, a simple plasticity method was developed to determine the vertical stress distribution by assuming that the limiting value of shear stress along the side of a column is equal to the initial undrained shear strength of the clay, and that it is constant over the column depth. As a result of this analysis, the authors defined a critical length at which end bearing and bulging failure will occur simultaneously in a single column which is about four times the column diameter. Furthermore, the authors stated that the additional length of a column beyond this critical length will not enhance the load bearing ability but may remain useful for reduction of settlement.

This work provided a significant understanding of the behaviour of single columns and has had a great influence on many other approaches which have been developed later. The plasticity theory itself proposed by the authors is simple and straightforward and it is still being used in today's practice.

1.2.2.2 The work in Georgia Institute of Technology

In 1983, G.J.Kaffezakis (1983) conducted a series of model stone column tests that were later described by Bachus and Barksdale (1984). In this experimental work, again, fine sand and kaolin clay were used for modelling stone column foundations. Tests with single end bearing columns (29 mm and 53.3 mm in diameter) were performed in a "real unit cell" chamber (108 mm diameter. x 305 mm high, Fig. 1.5a) (the unit cell concept is presented in Section 1.3.3.1). The load is applied one-dimensionally using a rigid piston. In addition, both stress and strain controlled loading tests on a small group of floating columns under a rigid strip footing (3 x 1 or 3 x 2, 29 mm in diameter) were conducted in a rectangular box (173 mm wide x 505 mm long x 305 high, Fig. 1.5b). And further, a special shear ring (64 mm ID x 102 mm high) was used to perform direct shear tests on a group of columns (Fig. 1.5c).

The results from unit cell tests showed that the ratio of vertical to lateral average stresses at end of each load increment was about 0.4 and approximately constant with the depth. The stress concentration ratio, n , (ratio of vertical stress on column to that on adjacent clay) was reasonably constant with time and load level, and in the range of 2.8 to 4.2. For samples having equivalent area ratio between 20 to 35%, the settlement at any load was reduced by about 30 to 45%. For specimens having equivalent area ratio of 7%, relatively small lateral bulging was observed, and most of the movements both in sand and clay were in the vertical direction (Fig. 1.6a).

The authors did not give any explanation of this phenomenon which rather contradicts the deformation behaviour observed by Hughes & Withers (1974). However, it is possible that for such a low area ratio the column may not be enhancing the load bearing capacity of the foundation. Also, Fig. (1.6a) shows that the sand and the clay deform almost uniformly, it would be only possible that the density of the model sand column is very low (column density was not reported).

A group of columns was centred adjacent to the sidewall of testing box, and this sidewall was taken as a plane of symmetry assuming zero shear stress on the vertical surface. The vertical loading tests showed approximately 40% increase of load bearing capacity compared with plain clay samples. The measured stress concentration value, n , lay between 1.5 to 5.0 at low stress levels but eventually converged to between 2.5 and 4.0 near to failure. The lateral stresses at high load levels were found to be concentrated near and above the column mid-height where pronounced bulges were visible on the radiographs (Figs 1.6b & 1.6c). Regarding the group effect, Kaffezakis (1987) noted that the lateral stresses within a stone column group are significant and increase as the number of columns within the group increases. But on the other hand, Bachus & Barksdale (1983) concluded that there is only a slight increase in the ultimate load carrying capacity per column with increasing number of columns (Fig. 1.7). In these tests, the effect of lateral confinement due to the proximity of the column to the faces of the testing box was quite noticeable (Fig. 1.6b) and it was taken into account for interpretation of the performance of the models.

The results from nearly undrained direct shear tests (performed with a displacement rate of 0.51 mm/min) were found to be influenced primarily by the area ratio. The authors concluded that for a specimen with an area ratio of 14%, the inclusion of columns was even weaken the shear resistance of original ground, and improvement only appears with an area ratio of 21%. For low normal stress, the rate of shear stress increase in the composite was greater than the rate of increase in the clay alone. Authors interpreted this as an indication that the clay and sand somehow move as a unit thus deriving the benefits of the stiffer sand. Authors also found that for the specimen having $A_s=21\%$ at high normal stress level, the rate of shear strength increase diminished and the composite strength approached the strength of the unimproved clay.

1.2.2.3 The works of others

Charles and Watts (1983) conducted large scale laboratory tests in a floating ring oedometer (1m in diameter) to assess the effectiveness of an isolated granular column in reducing vertical compression of soft clay (Fig. 1.8). They found that the principal stress ratio can reach a "peak" value with a small diameter column (low A_S value), but ratio is well below the "peak" value with a larger diameter column (high A_S value). This observation agrees with the results of small models obtained at Georgia Tech (Kaffezakis 1983). Also, Charles and Watts noted that to achieve a significant reduction in compressibility, a large area ratio is required.

In Japan, the compozer has been intensively studied. This is a method of improving soft ground by installing large diameter Sand Compaction Piles (SCP). Centrifuge tests have been performed to study the general failure mechanisms (Terashi et al 1991) and the effect of improvement width (Kimura et al 1983). Also, triaxial tests were conducted to study the stress and strain behaviour under controlled applied pressures (Ishizaki 1989). Since the compozer and stone column foundations have broad similarities with each other, the results from centrifuge tests are reviewed in detail in Chapter 6.

1.2.3 Full scale field tests

1.2.3.1 Single column tests

The load bearing characteristics of model single columns observed by Hughes and Withers (1974) were to some extent confirmed through the observation of the performance of a full scale fast loading test on a 730 mm diameter and 10 metre long column installed in soft silty clay ground (Hughes, Withers and Greenwood 1975). The rigid footing plate used has a diameter of 660 mm so that load was applied to the column only. Cambridge pressuremeter and Menard pressuremeter tests were conducted to determine the in-situ lateral stress and the radial pressure-deformation properties. An excellent agreement was reached between predicted and measured load-settlement curves and this demonstrated the occurrence of shear transfer between the column and surrounding clay. Also, a close match of column deformation shapes between model (Fig. 1.9a) and prototype (Fig. 1.9b) confirmed that bulging happens near the top of the column in a single isolated stone column.

In Santa Barbara, California USA, overall 6,524 stone columns were installed by vibro-replacement method to support a waste treatment plant situated within a historic tidal estuary. A total of 28 field loading tests were performed on individual columns to ascertain the design and performance criteria in association with a finite element analysis (Staal and Engelhardt 1976). Encouraging results were obtained to confirm that stone columns could provide an economical and adequate foundation. It should be noted that the loading covered both column and tributary clay so that the participation of the clay in supporting the load is taken into account (refer to section 1.2.4.3 for numerical comparisons). On the same site, the capability of stone columns to increase the horizontal shear resistance of the soil was evaluated by Engelhard and Golging (1975) through full scale in-situ quick direct shear tests. The result showed that the shear strength parameters of the combined mass of stone columns and native intervening soil are significantly higher than those prior to stone column installation.

1.2.3.2 Group columns tests

Munfakh et al (1984) reported a field study (for a project named Jourdan Road Terminal) on the effectiveness of stone columns in stabilising a deep deposit of very soft cohesive soil under a 3.4m height of embankment load. In situ shear tests showed that a peak internal frictional angle of 45° is achieved at the surface of an in-situ column. Approximately 40% of settlement reduction was achieved at the end of the embankment construction period. Significant lateral movements (maximum value of 60 mm) beneath the embankment were measured mostly occurring at mid-height of the column depth. It was reported that no significant lateral bulging was observed at the top of the stone columns. The failure of this testing embankment was accomplished by adding surcharge and excavation on the supporting side so that the ultimate failure mode was a combination of general shearing and local bulging.

Goughnour and Bayuk (1979b) reported a field test on a group of short columns (1.1m average diameter and 6.4m average length) in Hampton, Virginia. The long term vertical load test was performed to simulate embankment loading conditions. The in-situ shear vane results showed that the average undrained shear strength at a location within the stone column area lay approximately midway between lowest and median values of strength of original ground outside the column area. Load cells placed on top of columns and clay gave values of 2.6 to 3.0 for stress concentration ratio. The pore pressure measurements indicated that a large stress increase at the completion of loading occurred at a depth equal to half the width of the loaded area.

The test was stopped at a total settlement of 300 mm in the centre of tested area and no total failure of the ground was reported. The report of the test compared field measurements with predictions made using an elasto-plastic theory (Goughnour and Bayuk 1979a, see at section 1.3.4.4).

Now, having just mentioned two successful performances of stone column reinforced embankments, it is of interest to look at an unsuccessful case in East Brent, Somerset Levels in Southwest of England (McKenna 1976). A 70m x 189 m base size embankment was partially supported by a group of stone columns over an area of about 30 m x 30 m and the rest of the ground was left untreated. The embankment was built up to a height of 9.1 metre with side slopes of 3:1. Simply by comparing the settlement measurements between the treated zone and untreated area, McKenna et al concluded that stone columns had no beneficial effect on settlement reduction. Greenwood has long argued that the results obtained were misinterpreted and has proposed that the actual reason for this unsuccessful trial was that the columns were too short so that they acted like rigid piles transferring the loading penetration into deeper layers (Greenwood 1994).

So far as the author is aware, well instrumented field tests on stone column reinforced foundations have, until now, been extremely limited possibly because of their high costs. The embankment loading cases that have been presented only provide qualitative conceptual evaluation for specific theories or design methods, and the true group behaviour arising from the interaction between soil and column and between column and column has not been clearly revealed. Furthermore, field tests to study the behaviour of foundations reinforced by a large group of stone columns subjected to a rigid footing load have never been performed (Greenwood 1994). Results from the embankment trials mentioned above will be further analysed in Chapter 6 in the light of the findings from the present model study.

1.2.4 Numerical and analytical analysis

1.2.4.1 Introduction

The finite element method offers a powerful numerical technique for analysing complicated geotechnical problems and incorporating non linear stress-strain behaviour. The analysis of stone column reinforced foundations requires the consideration of the response of two quite different types of materials with different stress-strain behaviours with one showing time-dependent response through

dissipation of excess pore pressure and consolidation. To simplify the analysis, the majority of numerical methods that have been developed have adopted a unit cell approximation (see 1.3.3.1 & 1.3.3.2) where the variable boundary conditions of different unit cells are neglected (Balaam 1978, Balaam & Booker 1981 and 1985, Barksdale & Bachus 1983). Another type of numerical approximation considers the stone column reinforced ground as a homogeneous composite material (Mitchell & Huber 1985, Gerrard et al 1984, Schweiger & Pande 1988 and 1989, Pande et al 1994).

1.2.4.2 The unit cell based analysis

The unit cell method considers a typical column and its tributary soil within a large group with a fixed boundary condition (Fig. 1.10, for more details see section 1.3.3.1) and assumes that this would represent the general deformation behaviour of a large area reinforced by stone columns.

Balaam (1978) developed a finite element loading path method based on the load-settlement relationship of a single stone column which takes the slip at the column-soil interface into account. The behaviour of the stone column and the clay is approximated by assigning them different value of elastic Young's moduli E_1 , E_2 , and Poisson's ratio ν_1 , ν_2 respectively. The analysis treats both clay and stone as ideal elastic, perfectly plastic material obeying a Mohr-Coulomb yield criterion. The soil is taken to be purely cohesive while the column is treated as a purely frictional dilatant material which does not necessarily obey an associated flow law. The results agreed well with the results of a field test (Hughes et al 1975) when a purely adhesive column-clay interface was assumed. Concerning a group of columns, Balaam considered a single column and its tributary area as a combined unit on which the load is uniformly distributed on both clay and stone column. He found that significant reduction of settlement occurs only if the equivalent area ratio reaches 25%. The importance of a firm substratum to support the columns was emphasised. The consolidation rate is found to decrease dramatically with simultaneous reduction of column length and increase of column spacing.

An elastic analytical method in association with plane strain finite element analysis was described by Balaam and Booker (1981). This approach concerned the settlement behaviour of a large stone column foundation loaded by a rigid raft and the columns were assumed to be rested on rigid substratum. Again, the unit cell concept was utilised to simplify the problem. The assumption was made that the

stone column and clay remained elastic throughout the range of applied load and applied stress on the unit cell was still assumed to be uniform. The consolidation analysis adopting Biot's theory showed that the pore pressure flow mostly happens in the radial direction, and vertical flow is insignificant. The authors found that the stress concentration on the column initially increased rapidly with the ratio of column stiffness to clay stiffness, E_1/E_2 and proportional to the area ratio. No vertical stress distribution was presented. Due to the discrepancy of the stiffness between clay and stone material, the column normally carries more stress than the clay. This analysis found that initially, more load was applied to the clay than to stone, but the situation reverses as the load is increased (Fig. 1.11). Balaam and Booker interpreted such behaviour to indicate that initial undrained condition will cause the clay to behave as incompressible so that it is in fact "stiffer" than the stone column. However, this initial undrained settlement is relatively insignificant compared with the consolidation settlement. From Fig 1.12, the authors suggested that for a drained loading condition, a rigid footing is more efficient than a perfectly flexible raft simply based on the distribution of contact stress in a unit cell which obviously according to this analysis will apply to the whole footing. However, similar behaviour is also observed in an analysis of sand compaction piles in Japan (Asaoka 1994) using a coupled soil-water model. Comparing the results of this analysis with Priebe's elastic solution and with Greenwood's semi-empirical curves, a reasonable agreement is reached with the former but not with the latter.

Barksdale and Bachus (1983) presented a series of design curves obtained from a finite element analysis developed at Georgia Tech. The authors claim that this program can solve small or large displacement, axisymmetric or plane strain problems. For a non-linear analysis load was applied in small increments. Computations of incremental and total stresses were performed by solving a system of linear, incremental equilibrium equations for the system. By assuming the uniform stress condition in the stone and clay, only one vertical column of elements was used to model the stone and one to model soil. Field observations have shown that under surface loading, the column (as well as the clay) will deform horizontally (Manfukh 1989, Goughnour and Barksdale 1984): this implies that the rigid boundary assumption used in the unit cell analysis cannot be correct. To overcome this problem, an attempt has been made in the Georgia unit cell model to place a soft compressible boundary instead of the original rigid incompressible boundary to the unit cell (Fig 1.13).

In association with the findings obtained from the present model study, the results from Balaam's work and from Georgia Tech. will be critically reviewed in Chapter 5.

1.2.4.3 Homogenisation methods

Gerrard et al (1984) presented a constitutive model for soft clays reinforced with stone columns by combining the elastic-plastic behaviour of clay and stone column material. For soft clays the Tresca yield criterion was used while Mohr-Coulomb yield with associated flow rule was assumed to characterise the behaviour of the stones. This finite element modelling analysis was carried out for a flexible strip loading condition. In direct contrast with the work of Balaam and Booker (1980) and Balaam and Poulos (1982), this model was developed for an equivalent material that has homogeneously and uniformly distributed fabric of stone columns, in other words, using a mixture theory.

This method, in fact, has been further developed by Schweiger & Pande (1988 and 1989) to analyse the settlement problems for a large stone column reinforced area under a uniform loading. Most importantly, the present laboratory model study was established in direct relation with the latest developments of this mixture theory to investigate the load bearing behaviour of a large stone column reinforced foundation under a rigid footing. Data obtained from model tests performed at Glasgow University have been used to validate the numerical development which has been carried out simultaneously in University College Swansea (Pande et al 1994). This will be presented in Chapter 5.

Another type of homogenisation finite element method developed by Duncan at University of California, Berkeley was reported by Mitchell and Huber (1985). The axisymmetric program was specifically developed for predicting the load-settlement relationship for a single column within a group for comparison with the field loading tests conducted in Santa Barbara, California (Engelhardt and Golding 1975, Staal and Engelhardt 1976, Mitchell and Huber 1983). The program cannot precisely model a system of several stone columns surrounding a central column. Instead, the finite element analysis modelled the off centre columns as cylindrical equivalent rings of elements given material properties appropriate to the stone columns (Fig 1.14a). The dimensions of the concentric rings (thickness and radius) were calculated so that the relationship between stone column surface area to total surface area remained constant. The analysis only modelled a central column and one

surrounding ring whilst the load was applied to the whole surface since the assumption was made that each column in a group will behave in the same way. Mitchell (1994) confirmed that the column interaction is also assumed to occur in such way that there is no horizontal movement along vertical surface midway between columns because of the lateral confinement provided by surrounding columns. This is somehow identical to the assumption made in the unit cell idealisation.

However, the predicted overall settlement results agreed reasonably well with field measurements (Fig. 1.14b) despite the fact that the initial settlement calculation used undrained clay properties and drained properties for stone columns and the results were higher than the field observations. Mitchell argued that discrepancies could have been possibly caused by incomplete consolidation during each step in the field loading tests due to time limitation, however, the possibility of general horizontal expansion of the ground could not be excluded.

1.3 Theories and present design methods

1.3.1 Introduction

For a given load, the stress-strain relationships for granular material and for soft clay are different. Composite ground compels both materials to work together so that the loads are shared between clay and column material. The load bearing behaviour of composite ground is thus affected by the behaviour of both materials and their interactions. To theoretically analyse such a complex problem, certain idealisations for the individual materials are essential. Most existing theories consider stone and clay as perfect elastic or elastic-plastic materials (Hughes & Withers 1974, Priebe 1976, Baumann & Bauer 1976). Goughnour & Bayuk (1979a) considered the stone column to be elastic initially becoming perfectly plastic as load increases.

Most projects involving the stone column technique are in the following applications:

1. Single or sometimes double rows of stone columns under a long narrow strip footing such as building foundation.
2. A small group of columns (2 to 6 columns) under a rigid platform.

3. A large group of columns supporting a rigid structure such as cut and cover tunnels and caisson foundation.
4. A group or groups of columns supporting a large uniformly loaded area such as embankment, tank farm and fills.

Since stone columns always work together in a foundation, the reliability of the assumption that each column in a group will behave in the same way as a single isolated column on its own (Hughes & Withers 1974, Greenwood 1975, Maghav et al 1979) is questionable. Also, neglecting the participation of surrounding columns in a group (Barksdale & Bachus 1984) will not produce a true load carrying behaviour of stone column reinforced foundation. Priebe(1991) criticised such analytical assumption but was still unable to explain the true failure mechanism of group columns. The majority of theories deal with the settlement problems for stone column foundations. All theories have considered a typical column and its tributary area (unit cell see 1.3.3.1 & 2). On the other hand, except on high cost special projects, engineers and specialist contractors tend to adopt simple and straightforward approaches to perform routine foundation design. Hence semi-empirical methods in which most of the design parameters can be obtained from standard site investigation techniques become favoured regardless of the fact that those methods usually give conservative results.

Reviewing available literature, case histories and discussions with specialist contractors and engineers both in UK and USA, the Author has been able to briefly summarise the current state of design of stone column foundations in the following section.

1.3.2 Ultimate load bearing capacity

1.3.2.1 Single column analysis

Thorburn and MacVicar (1968) first attempted to present a purely empirical relationship between allowable working load on a single column and the undrained shear strength of the soil (Fig. 1.15). This chart is mainly based on the author's experience of stone column reinforcement applied to strip footings for foundation of low-rise buildings in Glasgow during the early 1960s. Interestingly, this chart is reasonably well supported by the approach later developed by Hughes & Withers (1974).

Most of the load bearing analyses have assumed that the stress state in a single column is triaxial and both column and surrounding soil reach their ultimate strength as it fails. Shear between column and soil (side friction) is generally neglected.

Hughes & Withers (1974) idealised the bulging type failure of a single column to be similar to the cylindrical expansion into the sidewall (clay) in a pressuremeter test (cavity expansion theory). Thus by adopting elasto-plastic theory given by Gibson and Anderson (1961), the lateral ultimate stress was expressed as:

$$\sigma_{rl} = \sigma_m + c \left[1 + \log_e \frac{E}{2c(1+\mu)} \right] \quad (1.1)$$

where σ_m , E , μ and c are, respectively, the total lateral stress, the elastic modulus, Poisson's ratio and the undrained shear strength of the soil. For simplicity, they further provided an approximated version of equation (1.1) as:

$$\sigma_{rl} = \sigma_m + 4c + u \quad (1.2)$$

where u is the pore pressure. Therefore, the ultimate vertical stress a column can carry as it reaches its critical state (bulging laterally) can be obtained as

$$q_{ult} = \frac{1 + \sin \phi'}{1 - \sin \phi'} (\sigma_m + 4c - u) \quad (1.3)$$

where ϕ' is the Mohr-Coulomb friction angle for the column material.

In practice, columns are usually analysed for drained conditions so that $u = 0$. This method still widely used because of its simplicity (Greenwood & Kirsch 1983).

Greenwood (1975) considered that the maximum column bearing capacity is achieved when the ratio of applied stress on the column to passive restraint at the critical depth is a maximum. In other words, the peak stress is first achieved at critical depth. On this basis, he provided an solution for estimating a single column bearing capacity in a group using passive earth pressure coefficient as:

$$q_{ult} = K_{ps}(\gamma z K_{pc} + 2c\sqrt{K_{pc}} + xqK_{pc}) \quad (1.4)$$

where: γ is the total unit weight of soil; K_{ps} and K_{pc} are the ratio of horizontal passive stress to vertical stress in stone column and in soil respectively; c is the undrained cohesion of the soil and z is the depth of soil. x is the critical depth where bulging and end bearing failure occur simultaneously (see 1.3.3.3).

The general cylindrical cavity expansion theory developed by Vesic (1972) includes both cohesive and cohesionless soil, and the behaviour of the material is assumed to be elastic initially and then plastically once the strength is reached. The expression for the ultimate lateral resistance is thus:

$$\sigma_{rL} = c F'_c + p F'_q \quad (1.5)$$

where F'_c and F'_q are cavity expansion factors, which are functions of the internal friction angle of surrounding soil and the Rigidity Index $I_r = G/(c + p \tan \phi)$, where G is the shear modulus of surrounding soil, and p is the mean isotropic effective stress at the equivalent failure depth.

On the basis of the Vesic's cavity expansion theory, Barksdale and Bachus (1984) presented an even simpler equation for calculation of the ultimate bearing capacity of a single column by introducing a bearing capacity factor \bar{N}_c .

$$q_{ult} = c_u \bar{N}_c \quad (1.6)$$

where c_u is the undrained shear strength of the cohesive soil.

Although the calculation of \bar{N}_c can be made from Vesic's theory by taking a value of E in the range of $5c_u$ to $10c_u$ (as recommended by Barksdale), from comparison with field measurements, the authors suggested that the value of \bar{N}_c should be chosen semi-empirically. It appears to lie normally in the range of 10-22 depending on the compressibility of the soil. They recommended a value of \bar{N}_c of 22 for soil having high initial stiffness such as non organic soft to stiff clays and silts, and a value of \bar{N}_c of 18 for those soils having low stiffness such as organic soils and clays with plasticity index great than 30. Mitchell (1981) recommends using \bar{N}_c of 25 for vibro replacement stone columns. Datye et al (1982) recommend using 25 to 30 for vibro replacement columns, 45 to 50 for cased, rammed stone columns and 40 for uncased, rammed stone columns.

Another approach based on Vesic's theory was made by Brauns (1978). He assumed no side friction existing between column and clay and no volume changes for a single stone column in cohesive ground, thus the ultimate lateral stress that can be mobilised in a stone column by surrounding cohesive soil is given by

$$\sigma_{rL} = c (1 + \log I_r) + \sigma_v \quad (1.7)$$

where $I_r = G/c_u$. A comprehensive comparison of these approaches based on cavity expansion theory was also made by Brauns (Fig. 1.16).

If a stone column is very short, there is a potential for end bearing failure rather than bulging. Barksdale and Bachus (1984) suggested that end bearing of a stone column can be considered by using conventional bearing capacity theories and adding the skin friction along the column side. Madhav and Vitkar (1978) presented a plane strain solution for a general bearing capacity failure of a trench filled with granular material in cohesive ground. Attention was also paid to the situation where surface load may be applied to both the granular material and the adjacent clay. For the three dimensional geometry of a stone column, the plane strain consideration is rather unrealistic. Winterkorn and Fang (1975) proposed the use of shape factors to correct the bearing capacity factors as an approximate axisymmetrical solution.

1.3.2.2 Group column analysis

1.3.2.2.1 Single column based approaches

Hughes & Withers (1974) considered a rigid strip footing supported by columns on a thin layer less than 6 m of thickness, overlying hard clay or rock. Two major assumptions are first that the stiffening effects of the bulging column on the clay and of the consolidation of the clay on the column can be ignored and second that the behaviour of a typical column within the group is the same as that of an isolated column (Fig. 1.17). This estimation concluded that stone columns are more effective in settlement reduction at small vertical effective stress level than at high stress level (Fig 1.18).

Greenwood (1975) considered a hexagon shaped unit cell for individual columns in a group and modified equation (1.4) by using an area replacement ratio parameter so that:

$$p_s = \frac{qA - K_{pc}aK_{ps}[\sigma_{vs} + xq]}{A - a} \quad (1.8)$$

where: A = the total area of the unit cell

a = the total area of soil in the cell.

others refer to function (1.4)

For a structure with low settlement tolerance, Greenwood suggested that all load should be considered to be carried by columns only in order to be on the safe side. Although equation (1.8) seems to consider the column and its surroundings since the

area ratio is introduced, the critical depth is still determined on the basis of the single column behaviour so that virtually no group effect was considered at all.

Barksdale and Bachus (1983) recommended that the load bearing capacity of a small group of stone columns under rigid footing can be estimated by multiplying \bar{q}_{ult} (as determined by equations 1.22 to 1.24, section 1.3.3.2) by the number of columns in the group. The ultimate bearing capacity of the tributary soil was recommended to be taken as $5c$ with upper limit of $\mu \cdot \sigma$ (see equations 1.23 & 1.24), the average stress on clay in unit cell according to the stress concentration factor n . Concerning the group effect in a small raft or strip footing foundation, Barksdale and Bachus provided a quantitative, linear relationship obtained from a statistical fit to result of model strip footing tests (refer to Fig. 1.7) for design consideration. For a column in a large group, the authors considered the possibility of bulging and lateral movement under vertical load and concluded that the ultimate load capacity will only be slightly larger than a single column. As mentioned in section 1.2.2.2, there are some limitations associated with the boundary effects in these model tests together with the general limitation associated with scale problems for small models, therefore, such direct extrapolation from low stress levels in the laboratory to high stress levels in the field may not be necessarily convincing. Most importantly, the authors did notice the group effect but the study did not go far enough to understand the failure mechanism of those group tests.

1.3.2.2.2 Homogenisation approaches

Priebe (1991) criticised the determination of the load bearing capacity of a group of columns based on the performance of a single column. Considering the composite ground in a homogeneous condition as it fails, Priebe recommended an approximate ground failure line (Figure 1.19) for a foundation under a rigid strip footing or small rigid raft. Thus by either adopting an average friction angle $\bar{\phi}_{comp}$ and mean cohesion for treated ground \bar{c}_{comp} , or extending the failure line below the footing and using the friction value of untreated soil (the dot lines also shown in Fig. 1.19), Priebe recommended that the bearing capacity could be estimated by normal bearing capacity factor methods. Priebe provide an equation to determine the value of $\bar{\phi}_{comp}$ as:

$$\bar{\phi}_{comp} = \tan^{-1} [m \cdot \tan \phi_s + (1 - m) \cdot \tan \phi_c] \quad (1.9)$$

$$\bar{c}_{comp} = (1 - m) \cdot c \quad (1.10)$$

where m is the proportion of the load carried by stone column and value of m were given by Priebe in a chart as a function of area ratio and stone frictional angle.

The two ways of calculating bearing capacity suggested by Priebe use essentially the same concept: which is based on one fundamental parameter, stress concentration ratio, which is normally determined from field loading tests (Mitchell 1981). This failure mechanism for rigid footings is not well supported by experimental observation. In fact, this approach was originally proposed by Priebe to estimate the contribution of stone column to overall shear resistance for a slope stability analysis which may have some significant difference from the rigid footing situation. The usage of such a method seems to be relatively little known.

By adapting Bell's (1915) local shear failure theories for a homogeneous soil, Barksdale and Bachus (1984) considered that a rigid strip footing or a small rigid raft supported by columns could fail on a straight rupture surface (Fig. 1.20). The authors assumed that the load is applied so fast that the undrained shear strength is developed in the cohesive soil (with the angle of internal friction being negligible). Also, the cohesion in the stone column is neglected, and the authors further assumed that the full shear strengths of both the stone column and cohesive soil are mobilised at failure stage. Barksdale (1994) explained that the improved soil could be idealised as a homogeneous composite material and its mean frictional angle could be determined from stress concentration ratio in a unit cell as

$$\bar{\phi}_{comp.} = \tan^{-1}(\mu_s A_s \tan \phi_s) \quad (1.11)$$

where the notation and unit cell concept are explained in section 1.3.3.2.

The ultimate stress q_{ult} is dependent on the ultimate lateral resistance σ_L of the block to the lateral movement and composite shear resistance, τ , developed along the inclined shear surface as illustrated in Fig. 1.20.

The calculation of σ_L for a square footing is adapted by the authors from Vesic cylindrical expansion theory presented in equation (1.5), whereas for an infinitely long strip footing, the authors employed the classical earth pressure theory for a saturated cohesive clay so that:

$$\sigma_v = \frac{\gamma_c \cdot B \cdot \tan \beta}{2} + 2c \quad (1.12)$$

where: γ_c = the saturated or wet unit weight of the cohesive soil

B = the foundation width

β = inclination of the failure surface ($\beta = 45 + \bar{\phi}_{comp.}$)

c = Undrained shear strength of the untreated cohesive soil

In both Priebe and Barksdale's homogenisation approaches, the possibility of a local bulging failure of individual columns is not considered. For an infinitely long strip footing (plane strain condition), this may be reasonable when the soil has rather high stiffness and low compressibility. For small raft, it is unlikely that the local bulging of columns can be avoided, especially when the reinforced ground is relatively soft cohesive soil. Regarding the assumption of straight rupture surfaces, both laboratory tests (Charles & Watt 1983) and field observations (Vautrain 1977) indicate that the soil does not fail in shear but remains in a state of plastic equilibrium so that the shear strengths in both clay and stone are not fully mobilised. Also, the assumption of clay developing only undrained shear strength is rather unrealistic in most field case because of the presence of effective drainage through the stone columns.

The homogenisation methods described above are, however, another extreme type of idealisation for the complicated soil/column system, and these do not provide rational rigorous solutions for stone columns either. However, these methods have taken one important aspect into consideration: the footing size, which is total ignored by all the design methods based on the performance of single columns. It is difficult to justify this homogenised simplifications in relation to analyses based on single columns because these suggested general failure modes are demonstrated neither by model tests nor by field histories. The only conclusion to be drawn is that today, design for foundations of small rafts or strip footings is still more or less based on the performance of single columns (Munfakh 1994, Greenwood 1994).

1.3.3 Settlement reduction analysis

For a large group of columns supporting loading from a structure or building, settlement control is normally the main design consideration; the consideration of load bearing problems only concerns those columns near the edge of the footing.

1.3.3.1 Unit cell

All settlement analysis approaches have considered a typical column in an infinitely large group with its tributary area of soil, a unit cell. The true hexagon tributary area is approximated as an equivalent circle (Fig. 1.21), thus the area ratio A_c is close to the square of the column diameter D over equivalent diameter of the equivalent unit cell D_c . For an equilateral triangular pattern of stone column arrangement $D_c = 1.05S$ and for a square pattern $D_c = 1.13S$, where S is the spacing between centre of the columns. By using a finite element method, Balaam (1978) has examined such approximations and concluded that they are accurate enough.

The basic assumptions in association with the use of the unit cell idealisation in analysis of settlement are:

- Vertical surcharge stresses are constant over an infinite loading so that the concept of a unit cell is theoretically valid.
- Shear stresses on the boundaries of the cell are insignificant so that boundaries can be approximated to be frictionless.
- Settlements for both the column and the clay are equal in the unit cell.
- The principal stresses in the unit cell are vertical, radial and tangential stress.
- The boundaries are rigid.

1.3.3.2 Stress concentration

Stress concentration ratio, n , is defined as the ratio of uniform average stress in stone column σ_c to the average stress in clay σ_e from the stress equilibrium. The following equation expresses the relationship between area replacement ratio and stress distribution.

$$\sigma = \sigma_c A_s + \sigma_e (1 - A_s) \quad (1.13)$$

$$\sigma_e = \sigma / [1 + (n - 1)A_s] = \mu_c \sigma \quad (1.14)$$

$$\sigma_c = n\sigma / [1 + (n - 1)A_s] = \mu_s \sigma \quad (1.15)$$

where μ_c and μ_s are the ratio of stresses in the clay and stone, respectively, to the average stress σ over the tributary area.

On the basis of a model test on a group of columns and K_0 consolidation tests on a single column, Aboshi (1979) suggested that the range in which this stress ratio falls when the column and clay yield, n_y , is

$$\frac{1 + \sin \phi_s}{1 - \sin \phi_s} \leq n_y \leq \frac{1 + \sin \phi_s}{1 - \sin \phi_s} \cdot \frac{1 + \sin \phi'_c}{1 - \sin \phi'_c} \quad (1.16)$$

where n_y is the stress concentration ratio at yield, and the ϕ_s and ϕ'_c are the internal friction angle for sand and effective angle of shearing resistance of the clay respectively.

Knowledge of stress concentration ratio is essential for all the existing settlement approaches. It is dependent on a numbers of variables including the relative stiffness of column and soil material, column length, area ratio and other construction details. Theoretical calculations could not possibly consider all these factors, and the value of the stress concentration ratio is normally chosen either from field measurement (usually by placing load cells on top of the column and surrounding clay) or according to past experience (Mitchell 1981, Barksdale and Bachus 1983). Its value is in the range of 1 to 5 and 3 to 4 are commonly used.

1.3.3.3 Methods of Greenwood and Hughes & Withers

Greenwood (1970) provided preliminary, empirical curves giving the settlement reduction due to ground improvement with stone columns by vibro-replacement method as a function of undrained shear strength of soil and spacing between columns (Fig. 1.22). It is very useful chart for primary study because of its simplicity. This chart considers both the situations of a strip footing supported by a single row of stone columns and a group stone columns beneath a widespread load and employs a simple lateral earth pressure approach to estimate permissible column loads. The curve for widespread load is purely empirical. Greenwood (1983) noted that care must be exercised when contemplating designs outside the range of data from which the curves have been developed. Despite the fact that it is an empirical approach, it is worth noting that comparison made with many other more recently developed theoretical and numerical approaches indicate that this design chart maintains its important value today. (Baumann and Baure 1974, Meghav et al 1979, Van Impe & De Beer 1983, Balaam & Booker 1981, Barksdale and Bachus 1983)

Hughes and Withers (1974) provided a simple elastic method to calculate the linear distribution of vertical stress by simply taking the limiting stresses up the side of a single column to be the undrained cohesion of the soil so that at depth z

$$\sigma_{vz} = \sigma_v + (\rho d - 4c_u) \quad (1.17)$$

where d is the diameter of the column. From this critical depth at which end bearing and bulging failure occur simultaneously was determined to be about $4.1d$. Such a result is supported by Matt and Poulos (1969) in their linear elastic analysis for a single floating compressible pile where the "pile stiffness factor" for a stone column is to be taken to be in the range of 30 to 50 (More details see Matt and Poulos 1969).

Greenwood's (1975) passive resistance theory (refer to section 1.3.2.2.1) uses K_{pc} and K_{ps} values to calculate the average stress in the soil near the column in the unit cell. Settlement predictions can then be simply made by calculating the settlement of the clay since equal strain in soil and column is assumed.

1.3.3.4 Priebe's method and other similar approaches

Priebe (1976) analysed the settlement of an infinite grid of stone columns beneath a rigid raft by considering a stone column within a cylindrical elastic half space with no change in lateral stress with depth. The columns are assumed to be founded on a competent bearing stratum. Stone column material is assumed to be incompressible and the columns are allowed to deform in shear failure only, whereas the surrounding soil still behaves in a quasi-elastic stress-strain manner. Priebe defined an improvement factor as the ratio of settlement of untreated to treated ground s/s_t , which is expressed as

$$\frac{s}{s_t} = 1 + A_s \cdot \left[\frac{\frac{1}{2} + 2\nu \cdot \frac{1 - A_s}{\nu + A_s}}{K_{ac} \cdot 2\nu \cdot \frac{1 - A_s}{\nu + A_s}} \right] \quad (1.18)$$

where A_s is the area replacement ratio and K_{ac} is the active earth pressure coefficient of the column material. The Poisson's ratio, ν , is taken to be $1/3$. This solution is normally presented in the format of a design chart (Fig. 1.23a).

In the above calculation, the effective stress resulting from the soil overburden is neglected. Priebe claimed that this is on the safe side. However, comparing

prediction with some field observations, Priebe (1993) incorporated a depth factor in order to overcome the over conservative nature of the calculation, and made an assumption of identical unit weights of soil and columns. In this paper, he also recommended a correction factor (Fig. 1.23b) as a function of the ratio of the compression moduli of the soil and column materials.

As a result of its simplicity and reasonable accuracy, Priebe's method has been widely used in USA by Hayward Baker and UK (Keller foundations and Cementation). However, comments have been made that this approach appears to over predict the beneficial effects of stone columns in reducing settlement (Barksdale & Bachus 1984).

Baumann & Bauer (1974) considered the total settlement divided into two parts: one, the immediate settlement of the stone, s_1 , for which no volume change of the soil is assumed, and consolidation settlement, s_2 , where Terzaghi's classical one-dimensional consolidation theory is adopted. The approach is basically similar to Priebe's (1976) early method but uses a weighted elastic modulus as a modification. In this approach, Grasshof's proposal (1955), which considered the load only applied to the column area, was adopted to determine the vertical stress distribution under the centre line of a circular footing. This is quit an unrealistic representation of the field situation. Therefore, the authors confessed that the approach is only an "analytical model".

1.3.3.5 Incremental method

An important extension of the above approaches was developed in a theoretical study by Goughnour and Bayuk (1979a). The theory idealises the stone as behaving elastically from the beginning of loading right up until the completion of consolidation of the clay, then the stone undergoes plastic strains and it is left in a state of plastic equilibrium (Fig. 1.24a). The analysis assumes that a unit cell idealisation is valid and it can be used to represent a large loaded area. The column material was assumed to be incompressible so that volume change only occurs in clay. Both vertical and horizontal consolidation is considered. A modified Terzaghi 1 - D consolidation equation is used to estimate the volume change of the clay due to radial consolidation. The vertical strain and vertical and radial stresses are calculated for each small increment of radial strain assuming that all variables are constant over the increment.

The effective stress path of the clay has been assumed to start always on the K_0 line and is assumed to be bi-linear as stresses increase and consolidation progresses: The path is confined between the K_0 and $1/K_0$ lines (Fig 1.24b). This distinguishes this analysis from most previous plastic approaches (Hughes et al 1975, Baumann and Bauer 1974), which all assuming the vertical stress in the stone to be equal to the radial stress in the clay times a constant K_0 (the coefficient of initial lateral stress in the clay). The final solution for vertical strain from the plastic analysis is expressed as:

$$\varepsilon_v = (1 - a_s) \frac{C_c}{(1 + e_0)} \log_{10} \frac{(\sigma_0)'_{vc} + \Delta\sigma'}{(\sigma_0)'_{vc}} \quad (1.19)$$

$$\Delta\sigma' = \frac{\Delta\sigma'_{vc}}{1 + 2K_0} \left[1 + K + K_0 \left(\frac{K: \text{ if } K > 1}{1: \text{ if } K \leq 1} \right) \right] \quad (1.20)$$

and the elastic analysis simply calculates the total load on the unit cell as:

$$P_t = E\varepsilon_s a_s + \Delta\sigma'_{vc} a_c \quad (1.21)$$

where $(\sigma_0)'_{vc}$ is initial vertical effective stress in the clay, $\Delta\sigma'_{vc}$ is the vertical stress increment in the clay, $\Delta\sigma'_{vc}$ is the effective stress increase in the clay, e_0 is the initial voids ratio of the clay and C_c is the compression index of the clay. E is the Young's modulus applying to the stone column and K is the ratio of the radial stress increment in the clay to the vertical stress increment in the clay. a_s and a_c are the cross sectional area of stone column and clay respectively.

Equation (1.20) appears to be independent of the stress strain behaviour of the stone. These simultaneous equations can be used for plastic and elastic states depending on whether the vertical strain ε_v is plastic or elastic. This solution thus allows the choice of the maximum value of vertical strain for a given stress increment on the clay. The assumption of rigid boundaries to the unit cell gives some degree of constraints to the calculation of ground vertical strain in the elastic range, while in the plastic range when the stone column fails, the assumption is made that both stone and clay material are in a state of plastic equilibrium. The composite stress strain behaviour therefore can be constructed and the depth of plastic zone in the column determined, together with the ratio of column and soil stresses to carry the total load at any stage of loading and consolidation.

This approach was examined in a field load test in Hampton, Virginia (Goughnour and Bayuk 1979b see section 1.2.3). Excellent agreement of settlement between prediction and field observation has been reached in the centre columns. The

prediction for the columns at the corner, however, appears to overestimate the settlement. The predicted stress ratio between column and clay has been reasonable matched. However, pore pressure measurements imply a quite different mechanism from the assumption of the unit cell. Again, noticeable horizontal movements were observed at depth in the columns. More information is presented in Section 6.3.1.2.

This analysis is very complex requiring an iterative procedure for the solution of the equations solution. A computer program was therefore developed by Goughnour for the formal Vibroflotation Foundation Company of USA to introduce this approach into practice. The usage of this computing program is rather little (Goughnour 1994). Goughnour (1984) presented a series of design charts for hand calculation of settlement reduction for widespread loaded stone column foundations. However, there are still quite a few parameters requiring careful measurements from laboratory tests.

1.3.3.6 The equilibrium method

This simple but yet effective theory is used in Japan for the prediction of the settlement in composite ground reinforced with sand compaction piles under a flexible raft. It was initially provided by Aboshi et al (1979). Barksdale & Bachus (1983) recommend that this method also offers a very simple and yet realistic engineering approach for estimating the settlement reduction provided by the installation of stone columns.

Again, the unit cell assumption is assumed to be valid, which basically indicates that an equilibrium condition is maintained in the column/clay interface. From conventional 1-D consolidation theory, the settlement reduction ratio, the ratio of settlement of the stone column treated ground, s_t , to that of an untreated ground, s , in a given vertical increment is expressed as:

$$\frac{s_t}{s} = \frac{\log_{10}\left(\frac{\bar{\sigma}_0 + \mu_c \sigma}{\bar{\sigma}_0}\right)}{\log_{10}\left(\frac{\bar{\sigma}_0 + \sigma}{\bar{\sigma}_0}\right)} \quad (1.22)$$

where the $\bar{\sigma}_0$, σ , and μ_c are the average initial effective stress in the clay layer, the effective stress due to the load and ratio of stress in the clay and the column respectively.

An indication from equation (1.30) is that the level of settlement reduction is proportional to the length of the column (presented as $\bar{\sigma}_0$ which increases with column length) when other factors are constant. For the case of long column with small applied load, Barksdale & Bachus noted that the settlement ratio relatively rapidly approaches the value of μ_c (equations 1.14 and 1.15 in section 1.3.22), which is possibly only useful for very preliminary studies.

This simple solution makes the level of settlement reduction of stone column foundation a function only of stress ratio, the initial effective stress and the magnitude of applied stress. Barksdale and Bachus also recommend that the stress ratio should be estimated from field measurements since there is not any realistic analytical solution yet available. Therefore, this approach has become a semi-empirical method, Barksdale and Bachus recommended that this method is suitable for some stiff to firm cohesive soils.

1.3.4 Summary

For the convenience of further reference, the relevance and application of most of the design approaches that have been described in the previous sections are summarised in Table 1.1.

Design approach	Single Column		Group Columns		
	Capacity	Settlement	Capacity	Settlement	
				Flex Raft	Rigid Raft
Thorburn & McVicar (1968)	X				
Mattes & Poulos (1969)	X	X			
Greenwood (1960)	X		X	X	
Hughes & Withers (1974)	X				X
Baumann & Bauer (1974)					X
Greenwood (1975)			X		X
Thorburn (1975)	X				
Hughes et al (1975)		X			
Priebe (1976)		X			X
Balaam et al (1977)		X		X	
Madhav & Vitkar (1978)	X		X		
Brauns (1978)	X				
Goughnour & Bayuk (1979)					X
Aboshi et al (1979)				X	
Maghav et al (1979)	X	X	*		*
Balaam & Booker (1981)					X
Van Impe & de Beer (1983)					X
Barksdale & Bachus (1983)			X	X	X
Balaam and Polous (1985)	X	X			
Gerrard et al (1984)				X	
Asaoka et al (1984)				X	X
Pande et al (1994)			X		X

Table 1.1: Summary of existing design approaches for stone column foundations

1.4 The objectives of this dissertation

Having reviewed most of the existing theories and design approaches for stone column foundations, one can see that all these approaches have neglected the column-column interaction in order to simplify the analysis, particularly in the calculation of the load bearing capacity of ground containing a group of stone columns. In reality, the format of stone column foundations always consists of a number of columns which will work together and interact with each other. The homogenisation method (Preibe, 1991 and Barksdale & Bachus, 1983) has suggested general failure modes but they have not been supported by experimental observations.

For unit cell idealisation, stress concentration ratio is most important factor and yet there is no a rigorous solution available to give a rationally estimate of this ratio, so that it has to be chosen either by empirical estimation on the basis of field measurement by means of load tests or from an engineer's experience. Many loading tests have been performed under rather quick loading, and these are of limited value in estimating the ultimate anticipated settlement. On the other hand, normal practice uses a constant value of stress concentration ratio, n , for simplicity, whereas a matter of fact, the variations of n value with depth and time could be very significant (Vautrain 1977). Some have even criticised such stress ratio estimation as "total ignorance" (Schlosser 1979).

Finally, the unit cell assumption has the overall effect of ignoring shear stresses along the unit cell boundaries which will weaken the composite structure and hence lead to lower estimates of settlement. Further, the assumption of rigid boundaries to the unit cells prevents the columns and soil from moving laterally under vertical load so that the overall settlement may be lighter than predicted. However, the justification of any likelihood of self compensation is difficult since there is no other alternative rigorous theory that has been developed yet.

In this dissertation, a research programme that has been formulated in order to study group effects in a large stone column foundation is described. The objectives of this research can be summarised as followings:

1. to perform a series of displacement controlled rigid loading tests with various value of important parameters such as area replacement ratio, column length to diameter ratio, clay block strength and installation method, and to assess the

influence of these parameters on the performance of a large area of soft cohesive ground reinforced by a group of stone columns.

2. to conduct tests under uniform flexible loading to examine the influence of the footing flexibility on the performance of a large stone column foundation
3. to investigate the soft soil beds before and after loading and to discover the deformed shapes of columns in order to understand the failure mechanisms of a group of columns under vertical loading.
4. to validate the finite element program developed at University College Swansea by direct comparison. Also, to further compare the findings from model tests in association with other published numerical results in order to reveal the group behaviour of a stone column reinforced foundation in depth.
5. to validate the findings from the model tests by comparing with relevant published results from centrifuge tests and field observations.
6. to provide basic knowledge of the group effect of stone column foundations in order to propose the way a more rational method of designing a large stone column foundation under a rigid footing load.

Chapter 2

Design and construction of test apparatus

2.1 Introduction

It is extremely difficult to create a precise laboratory model of a particular prototype situation involving a foundation reinforced with stone columns. In order to tackle the main issues such as identifying basic mechanisms of failure and determining the influences of major design parameters, the complexity of the dynamic vibro-process used for column installation in the field combined with non-homogeneity in typical natural ground condition was simplified to a 1-dimensionally consolidated bed of homogeneous clay reinforced with a regular array of fine sand columns. It was decided that a set of axisymmetrical footing tests conducted at reduced scale would be a sufficiently simplified version of the real situation to be able to discover basic information of stresses and deformations on which new methods of interpretation and analysis might be based.

2.2 The materials

This modelling investigation is concerned with the fundamentals of the mechanics of stone column foundations so that it is appropriate to use well-defined materials. It was decided to use Speswhite kaolin clay reconstituted from slurry and Loch Aline sand to build the model.

2.2.1 Clay

During the past three decades, kaolin clay has been widely used in soil modelling for fundamental geotechnical problems, and its mechanical properties and stress-strain behaviours have been intensively studied under well controlled laboratory conditions. Data are available from tests using various stress-paths in conventional triaxial, true triaxial, biaxial and simple shear apparatus (Roscoe & Burland 1968,

Wood 1974). The majority of those researches studied Spestone kaolin. Due to the shortage of Spestone, Speswhite kaolin was introduced as a substitute in the later 70s. Mair (1979) has compared the engineering properties between these two type of kaolin and concluded they are almost identical.

Al -Tabbaa (1987) has specifically investigated the permeability and mechanical characteristics of Speswhite kaolin during anisotropic consolidation. She found unique linear relationships on double logarithmic scales between the vertical and horizontal permeability and void ratio, those relationship are independent of the overconsolidation ratio. Her theoretical and numerical solutions for axisymmetrical problems of consolidation with radial drainage to inner and outer fixed boundaries are particularly relevant to the consolidation behaviour of stone column foundations. Also, she developed a new elasto-plastic "two-surface" strain hardening/softening model within the framework of critical state soil mechanics based on observations made from the triaxial tests and oedometer tests. Such a model might be useful in the concept of the present study for extrapolating the behaviour observed at low stress levels in laboratory model tests to the high stress levels of prototype situations.

The Speswhite kaolin powder used in this present stone column model study was supplied by ECC international (John Keay House, St. Austell, Cornwall, England). Tables 2.1 and 2.2 list the general properties of Speswhite kaolin as reported by Ponniah 1984.

Type	% by weight
SiO ₂	47.0
Al ₂ O ₃	37.8
Alkalis	1.2
Fe ₂ O ₃	0.6

Table 2.1: Chemical properties of Speswhite kaolin (after Ponniah 1984)

Property	Tested according to BS1377
Specific gravity	2.62
% of finer than 2 μ	60
Plastic limit (%)	36
Liquid limit (%)	63
Plasticity index	27
Activity	0.45

Table 2.2: Physical properties of Speswhite kaolin (after Ponniah1984)

2.2.2 Sand

The material used for modelling the stone in the model stone columns was a local fine silica sand, Loch Aline sand which has a silica content of 99.78% (Mesdary 1969). This type of sand has been used for a number of studies at Glasgow University (Mesdary 1969, Belkheir 1993).

Information based on previous investigations (Kirkpatrick 1954, Mesdary 1969 and Belkheir 1993) of the physical properties of Loch Aline sand indicates that this is a uniform, fine-grained sand with predominantly sub-rounded particles ranging from 0.2 mm to 0.6 mm. Note that the particle size distribution curve of Loch Aline sand is similar to that of Hostun sand (Fig. 2.1), a sand which was proposed initially for this research because of its well studied mechanical properties (Pande et al 1992). The uniformity coefficient d_{50}/d_{10} of Loch Aline sand was 1.3 and the mean particle size, d_{50} , was about 0.32 mm. Using the methods proposed by Kolbuszewski (1948), Mesdary (1969) found the maximum and minimum void ratio were 0.445 and 0.357, respectively. The specific gravity of this sand was 2.65.

2.3 Modelling at reduced scale

Consider the situation illustrated at Fig. 2.2. A rigid footing with diameter of D rests on the surface of a soft homogenous clay bed containing a group of columns. Dimensional analysis can be used to deduce that it could be expected that the load required to produce any specific settlement for such a composite ground will be influenced by the following independent quantities:

s	(mm)	the penetration of footing
c_u	(kPa)	the undrained shear strength of clay
D	(mm)	the diameter of footing
L	(mm)	the length of columns
d	(mm)	the diameter of the columns
S	(mm)	the spacing between columns
ϕ'	(-)	angle of internal friction for column material
G_v	(kPa)	the elastic shear modulus of sand
G_c	(kPa)	the elastic shear modulus of clay
γ_s	(kN/m ³)	the unit weight of sand
γ_c	(kN/m ³)	the unit weight of clay
d_g	(mm)	the average particle size of column material

To experimentally determine the load-settlement characteristic of such a composite ground, rigorously speaking, a model has to be designed in such way that all geometrical dimensions and material properties should be reduced by appropriate scale factors and they should be completely similar to those found in the prototype. In no physical model is it possible to maintain complete similarity of all parameters that govern the prototype response. Modelling with a geotechnical centrifuge (Schofield 1980) would provide the possibility of maintaining prototype stress levels but this approach was not available for the present study.

It is because of the inclusion of the stiffer, relatively incompressible stone material that soft ground treated with stone columns increases its load bearing capacity and lead to reduced settlement under the load. Previous researches of mechanical behaviours and theories of this composite soil-stone column system have been reviewed in Chapter 1 of this dissertation. It is possible to categorise parameters influencing response in two groups: first those believed to give major influence on the load-settlement curves and remainders giving only secondary effects. This may be expressed in terms of the link between ultimate load bearing capacity expected in

a dimensionless form as a combination of two (unknown) functions of a series of dimensionless groups of the influencing parameters:

$$q_{ult}/c_u = f_1(s/D, L/D, L/d, A_s, \phi', G_c/G_s) \cdot f_2(G_s/c_u, \gamma_s/\gamma_c, d_g/d_c, D_B \cdot \gamma_c/c_u)$$

where the column spacing S is presented by the area replacement ratio A_s

$$A_s = \left(\frac{d}{mS}\right)^2$$

where m is a shape factor depending on the pattern of arrangement of the columns (see section 1.4.3.1). The function f_1 represents the dominant variables and the function f_2 of the less significant quantities.

In spite of the fact that there is not a specific prototype situation in mind, Fig. 2.2 still can be seen as a laboratory model of a large rigid footing resting on soft cohesive ground reinforced by a group of stone columns in the field. Given the typical value used in the field and in the designed model (Table 2.3), for the dimensionless parameters L/d , L/D , A_s , and ϕ' in the first category, one can easily see that some similarities between model and prototype have been satisfied.

Shear modulus ratio G_c/G_s is an indication of the stiffness ratio between stone and soil, this could also be expressed by the ratio of Young's moduli E_c/E_s assuming that the soil and stone material have the same value of Poisson's ratio. In order to perform numerical modelling of the physical model tests, Lee and Pander (1994) chose a typical Young's modulus E_s for Speswhite kaolin clay as 11,057 kPa (Al-Tabbaa 1987) and E_c for Hostun sand (a similar sand to Loch Aline sand) as 189,243 kPa (Lade 1988, McCarron & Chen 1988), One can see that the ratio of E_c/E_s in model will then be 17, which falls into the range of 10-40, a typical range quoted for prototypes (Balaam 1978). Since it is true that deformation modulus is related to the mean stress level, the above argument then should be seen as a quantitative induction rather than an attempt at a perfect mathematical match.

Parameter (unit)	A_s (%)	L (m)	d (mm)	L/d	d_g (mm)	ϕ' (degree)
Prototype	10-35	10-20	600-1000	10-20	25-50	38 - 45
Model	10, 24, 30	0.11/0.17	11/17.5	10-15	0.2-0.4	36-39*

Table 2.3: Typical column parameters used in the prototype and in the models

* data from Belkheir (1993)

Most soft clay deposits in the field are at least lightly overconsolidated. For a given overconsolidation ratio (OCR), the elastic shear modulus of clay is proportional to its initial undrained shear strength c_u . Therefore, the dimensionless parameter G_c/c_u in the secondary category is accommodated by using undrained strength c_u to normalise the footing pressure providing the OCR profile is correctly established in the model. If Fig 2.2 is considered as a small model of a prototype, a ratio of typical column diameter between model and prototype will then imply a "scale factor" of about 60. Assuming a natural soft ground having an average undrained shear strength of 40 kPa, it is obvious that such scale factor in the present model is difficult to apply to the strength reduction in the model clay bed in order to satisfy a complete similarity. Since the clay will be heavily overconsolidated, it is not possible to reproduce the field gradient of stresses and histories in the model. However, controlled preconsolidation pressure will leave the clay with a rather uniform water content and hence strength in the model so that the ratio of the stiffness to strength could be expected to be independent of OCR value. The undrained shear strength was eventually chosen at the range of 10-15 kPa and the typical strength with depth profile was simulated by allowing swelling mostly on the top surface of the clay after its consolidation. Clearly, this scaling problem will inevitably cause troubles in directly applying the load-settlement curve obtained from model to a prototype. However, the reasonably similarity reached in the E_s/E_c ratio will still enable the model to reveal the fundamental characteristics of soil-column interaction in the field.

The scaling of the shear modulus of the column material $G_s G_c$, and yet the conservation of its internal angle of friction, ϕ' , were found to be compatible. G_s is affected mainly by the mean stress, p' , and the void ratio or relative density of the column material. On the bases of Janbu's (1963) suggestion, Wroth et al (1979) provided a relationship between G_s and p' as:

$$\frac{G_s}{p_a} = k \left(\frac{p'}{p_a} \right)^n$$

where: p_a : the atmospheric pressure
 k : constant
 n constant (between 0.5 to 0.9)

The reduction of G_s in the model will be likely less than the reduction of p' , but it is difficult to justify since the measurement of p' values in typical field stone column is

not available. It is author's intuitive belief that the departure from complete similarity in this particular scaling is not going to make a significant difference to the basic behaviour of the models. By slightly increasing the void ratio (decrease the density), additional reduction of G_s could be achieved, which would also tend to decrease the ϕ' value. This effect on ϕ' would, however, to be offset, by its tendency to increase with the decrease of mean stress level, p' .

Problems which involve formation of bands of localised deformation in granular material are strongly influenced by the ratio of particle size to the typical dimension of the problem (Stone and Wood 1988 and Bolton and Lau 1988) because such localisation typically have a thickness of 10-20 particle diameters (Wood 1994). If column diameters were in the range of 5-10 mm, use of Loch Aline sand for model stone column would make the ratio of d_g/d of the same order in the models (25-50) and the prototypes (27.5-55) (refer to Table 2.1). 5 mm diameter columns were found to be very difficult to prepare in soft clay bed. The diameters of 11 mm and 17.5 mm were finally chosen in the models, hence there might be scaling effects for the foundation of localisation in the large columns (17.5 mm). However, the nature of the failure zones that were actually observed in the model tests suggested that this is not a major effect.

Since conventional laboratory models operate in the condition of simple gravity on the earth surface, it is not feasible to correctly reduce the scale of the unit weight of clay and stone material, r_c and r_s without a centrifuge. The scale effect that come from the size of the model container of are also uncertain. Field situation have no such outer boundary. However, model tests are intended to provide data under well controlled boundary condition that can be used for validation of numerical analysis and not merely for direct extrapolation to prototype scale. Nevertheless, as Ovesen (1979) says: "the departure from complete similarity must be justified by means of experimental evidence". This evidence will be further discussed in Chapter 6 when comparison is made with the similar tests carried out on a centrifuge.

2.4 Apparatus and their design

2.4.1 General requirements

As discussed in previous section, the model was designed to approximately represent a typical field situation. The modelling technique was thus concentrated on those general requirements.

1. The clay bed had to be prepared from slurry and it had to be very soft but stiff enough to make it possible to install the sand columns.
2. The sand columns had to be prepared in such a way that the displacement and replacement nature of field installation methods could be simulated to a certain extent, and procedures of column installation should be repeatable from one column to another.
3. The footing load had to be applied slowly so that a relatively drained condition can be assumed.
4. A flexible footing had to be made such that a uniform load could be applied to the sample.

To ensure the quality of the model tests, a considerable amount of time has been spent on development of apparatus, testing methods and model site investigation procedures. In addition, two trial tests were specifically conducted to examine the performance of the apparatus and the general nature of the tests (Hu & Stewart 1993). It is not the intention to describe those experiments in detail in this dissertation. However, some of the relevant information will be presented appropriately in following sections as well as in Chapter 3.

2.4.2 Consolidation tank and pressure supply.

Following the successful experience gained from previous research (Ponniiah 1984), it was decided that the preparation of clay bed would adapt a system using a water pressure bag accommodated inside of a steel tank beneath a piston in order to perform one-dimensional deformation, with consolidation with two way drainage from kaolin slurry.

Consolidation tanks

A set of steel tanks were already in existence at Glasgow University including four large tanks (760 mm in diameter x 1200 mm in length); two small tanks (300 mm in diameter) with full length of 600 mm; four small tanks (300 mm in diameter) with half length of 300 mm; together with two large pressure bags and four small ones. Considering the nature of the tests and convenience for sample preparation, the set up of the consolidation tanks was designed in two ways depending on the position of pressure bag.

Two pieces of half-length small tank were assembled together and pressure bag was placed on top of the container in order to form a top downwards consolidation system (Fig. 2.3). The main concern of such a design was to produce a stable based clay bed with a final surface accessible for testing after the top piece (half-length tank and pressure bag) is removed. The full length tank (whether large or small diameter) was considered as a consolidation chamber on its own while the pressure bag was located on the bottom of the tank to provide a bottom upwards consolidation system (Fig. 2.4). Such a set-up resulted in a final level of clay bed at the top of the tank. Each tank was supported by four pieces of threaded rod (20 mm diameter) at about 250 mm above the floor.

As Fig. 2.3 and Fig 2.4 also illustrate, a solid steel plate of 6 mm thickness was fixed to the flexible latex pressure bag by a brass screw so that displacement will be uniformly transferred to the slurry through this rigid plate. (It may be worthwhile to note that it was necessary to use powerful epoxy glue, Araldite (CIBA-GEIGY), for the washers on both sides of rubber/steel plate joint to ensure a completely airtight seal). This piston-like system simulated an oedometer apparatus in order to achieve equal settlements over the contact surface providing no significant tilting occurs in the steel plate during the consolidation. To determine the settlement of the slurry sample and the magnitude of possible plate tilting, two brass rods were fixed on the plate and direct measurement could be then taken outside the tank as consolidation progressed.

Since the pressure bags had not been used since 1984, it was recognised that ageing of rubber material could cause possible leaks when they were subject to a pressure. To ensure the quality of consolidation, each bag was thoroughly examined and it was also subjected to a test pressure of 400 kPa with the bag was submerged entirely under water.

Two-way drainage for the consolidation was achieved by placing a saturated piece of porous Vyon discs on the top and bottom of the clay slurry. The diameter of the disc was made to be slightly less (1-2 mm) than the internal diameter of the tank. Drainage water was led by a flexible transparent plastic tube to an external container where a estimation of overall volume change of the sample could be made. The porous vyon sheet was supplied by Porvair plc, it has 1.5 mm thickness; pore size in the range of 9-95 micrometer; typical air flow at water gauge pressure of 2 kPa is $67\text{m}^3/\text{min}/\text{m}^2$.

Pressure supply

Consolidation pressure was supplied by a compressor machine (model: SR 20L23 manufactured by Fluidair LTD) produced for Departmental general use. The machine used a 700 kPa pressure cell monitor and self-adjusting its output at relatively constant air flow. A 400 kPa capacity pressure gauge with a minimum division of 1kPa and a manually adjustable regulator were used to control the desired pressure for consolidation.

It was decided to apply pressurised water into the bag for the consolidation so that an interface cylinder was required to mix the air pressure and water. To perform normal consolidation of slurry, each load increment should be applied only when a complete dissipation of excess pore water pressure has been achieved. Experience gained from trial tests indicated that such an operation could take more than 12 days for consolidating a clay bed subjecting to a maximum load of 160 kPa. The intensive testing programme (see Chapter 4) required a total number of 20 tests to be completed within a rather short period of time (about one year). Therefore, it is desirable to prepare a numbers of clay block at one time. A small metal cylinder used in previous research (Ponniah 1984) and trial tests was found to be too small to provide sufficient amount of pressurised water for a simultaneous consolidation process. A big cylindrical steel tank was therefore specially designed as an interface for a large quantity of water with the air pressure (Fig. 2.5) and this allows more than four tanks to be consolidated independently at the same time. An independent pressure gauge was fitted on this interface tank to indicate the final applied water pressure which goes directly to the rubber bag in each individual consolidation tank via a plastic pipe.

The entire consolidation set-up is shown schematically in Fig 2.6. Plate 2.1 is a photograph of the set-up.

2.4.3 Sand column installation.

Frame and drill

To facilitate the positioning and installation of the sand columns, a steel frame was designed to support a drill rig which in turn could be moved in two orthogonal directions. Fine screw rods were used for the supporting rails so that the location of the columns could be precisely controlled. For small tanks, the frame was made easy to handle, whereas for the large tank, the enlarged identical frame was inevitably heavy and has to be lifted by a small crane. The frames is square shape and each side can be bolted to the flange of the steel tank. The vertical movement control for installation of sand column was performed by a drilling rig (with attached depth scale) which can be easily assembled on a platform fixed on the steel frame(plate 2.2).

Thin-walled tubes and hole making

It is extremely difficult to precisely mimic the field vibroflotation system (as described in Section 1.2) to install the columns in laboratory condition.

1. It could be very expensive and time consuming to make a model poker at a scale of, say at least 1:60. It was also beyond the scope of present study.
2. A system of using vibrator or self-weight penetration with association of water flush could be relatively easier to establish. However, such a system would be likely to result varying diameter along the depth of a model column because of the softness of the clay bed, this would cause troubles for identifying the column deformation (bulging for instance) and test repeatability.

Therefore, it was decided that the model columns should be prepared in such way that following requirements should be met.

1. Field initial stress changes during either displacement or replacement method of installation had to be simulated to a certain extent.
2. A formed model column should have a uniformed cross section throughout the length.

3. The whole procedure of column construction should be easy to repeat from one to another.

The first requirement was achieved in such a extreme way that for replacement process, the entire clay volume in the column space was removed with minimum disturbance to the surrounding clay, whereas in the displacement process, clay was pushed out laterally by a closed end tube as hole-making progresses and the surrounding clay was subjected to a maximum lateral disturbances during the installation.

A thin-wall stainless steel tube with a 45 degree trimmed sharp edge at the base was used to make holes in the clay bed. The other end of this tube was held by the drill rig through an adapter. For replacement method installation, an auger was used to remove the clay from the inside of the tube as tube was penetrated. Lateral "pushing" in the displacement method of installation was achieved by placing a conical plug on top of this tube forming a close-end. The equipment described are shown in plate 2.3. The step-by-step installation procedures for both methods will be described in sections 3.2.3 and 3.2.4.

As mentioned in section 2.2, two diameters were chosen for the model columns. Table 2.4 lists the dimensions of all relevant equipment used to construct model columns.

Assumed model column finished diameter (mm)	11	17.5
Tube internal diameter (mm)	10	16
Tube external diameter (mm)	11	17.5
Auger mean diameter (mm)	8.7	15.8
Conical plug diameter (inside of tube) (mm)	9.8	not used

Table 2.4: Dimension of equipment used for installation of model columns

2.4.4 Loading facilities

2.4.4.1 Loading through rigid footing

The machine

Displacement controlled loading has been used to perform the majority of the tests. The load was supplied to a rigid (steel) footing by a 1 ton triaxial compression test machine (manufactured by Wykeham Farrance Engineering Ltd) which was fixed upside down to the top member of a reaction frame. The machine could provide a wide range of displacement rates, from 0.38 mm/min (fastest) to 0.0006 mm/min (slowest) according to the combination of driver/driven wheel size and gear position. Small tank tests used an existing frame (1.8 m in height x 1.8 m in width) which is directly fixed on the ground, whereas in large tank tests, a small reaction frame was made to be bolted on the flange of the tank (refer to plate 3.1).

The footing plate

All small tank tests used a 100 mm diameter (20 mm in thickness) plate which is 1/3 of overall diameter of the tank containing the clay bed. It should be noted that such close rigid boundaries may result in extra confinement (lateral) to the action area, a possible boundary effect. The extent to which this boundary influenced the observed behaviour was difficult to ascertain within the bound of present experimental programme. Cox (1962) noted under a circular footing load the influenced region in a clay ground would be contained within approximately $3D$ (D is diameter of the footing). Because the presence of sand columns enhances drainage in the clay beneath the footing, it is expected (and experimentally observed) that much of the action in these model tests will be contained in the clay beneath the footing than in an undrained failure of plain clay (More discussion on the axial symmetry will be presented in section 4.3.4). This is not to suggest that the ratio of 3 of tank diameter to footing will actually lead to no boundary influence. In the large tank, the ratio is 5 so that some comparison of this boundary effect is possible. However, as already noted, one of the aims of this model test is to produce data with defined boundary condition. What these boundary are is perhaps less important.

The compression machine supplied the load to a solid stainless steel plate via an extension solid steel rod (25 mm diameter with various lengths to suit the height of the samples). As the footing plate was to be directly in contact with the wet clay surface for a long period of time during nearly drained tests, corrosion might occur in the contact surface of the plate which would affect the smoothness of the footing

(increase the horizontal confining stress) during the test. Hence, the surface of the stainless plate was coated with a thin layer of silicone grease.

2.4.4 Loading through flexible footing.

In order to simulate the embankment-like loading condition, a Flexible Loading Device, FLD (refer to plate 3.2) was specially designed to supply a uniform load over the testing area.

As Fig 2.7 shows, air pressure was applied into a steel cell via a plastic tube which was connected to the same pressure source as was used for consolidation, and the rubber diaphragm fixed by a thin steel ring (2 mm in thickness and 5 mm in width) on the bottom of this cell then transferred the pressure to the clay surface. The shaped rubber diaphragm contains an extra flexible length so that it can follow the settlement of the foundation surface without imposing lateral restraint. Also, the elasticity of the rubber will ensure that a uniform stress is applied to the foundation surface regardless of the discrepancies of the settlements developed over the loaded area. To apply a vertical load, this FLD unit was screwed onto a reaction frame bolted on the flange of the tank which prevented the unit from raising (refer to plate 3.2). The surface settlements within the loading area were measured by three displacement transducers equally spaced on a diameter. Because of limited spacing inside the cell and the fixed position of the transducers, the settlement measurements hence only give the average profile across the section of the footing regardless of the relative position of each individual transducers (over clay or over a column). Holes were made to allow the bodies of transducers go through a top cover plate; these holes were completely sealed by rubber O-rings. It was found that under the high pressure environment, only AC/LVDTs can work normally.

Using a dipping technique, the rubber diaphragm was manufactured by the author in the laboratory from latex liquid. Its thickness was determined by the minimum strength required by the diaphragm to contain the maximum working pressure (350 kPa) and to follow the settlement without bursting.

2.5 Instrumentation and data acquisition

2.5.1 The displacement transducers (LVDTs)

The Linear Variable Different Transformer (LVDT) was the main displacement monitoring instrument. Most of the LVDTs were DC type and four of them (model LDC/1000A) were purchased from RDP for this research. The energising power supply was set at 10 V. DC or 15 V. DC. Considering the possible supply difference from test to test or during a test, every LVDT was calibrated in a micrometer at certain necessary stages, especially before and after its use to ensure the accuracy of the measurements.

As Section 2.4.2 described, four tanks were normally consolidated simultaneously. A 500 mm stroke DC LVDT (LDC/10000/C), together with another seven 200 mm stroke LVDTs were used to record the slurry settlements (two monitoring for each tank). The total consolidation settlement were generally in excess of the effective range of the 200 mm stroke LVDTs. This was solved by regularly re-setting during the consolidation period. For displacement controlled rigid footing tests, two DC/LVDTs were used to measure the footing descent and four to measure surface vertical displacement. As described in section 2.4.4, three AC/LVDTs were used in the flexible loading device to measure the foundation surface settlement profile across the centre section and again the surface vertical displacements were recorded by four DC/LVDTs. These LVDT are shown in plate 2.5 (a, b and c).

2.5.2 Load transducer

A 1000 lbs (4450 N) capacity load cell (plate 2.5e) was accommodated between the compressor machine and the rigid footing to monitor the total load applied to the footing. This total load cell is manufactured by Sangamo Weston Controls Ltd, model D91. Although the load cell was specifically designed for tension loading, the calibration results carried out from a Direct Load Compound Piston dead-weight Compression Tester(manufactured by Budenberg Gauge Co. Ltd.) show that in such a test, this load cell gives satisfactorily accurate compression response.

A signal conditioning unit connected this load cell to a data logging system. The function of this signal unit was to convert the AC reading from the load cell to a DC format input for the data scanner and also to supply an AC power to the load cell.

2.5.3 Miniature Pressure Transducer (MPT)

In order to discover the stress distribution underneath the footing area and the stress sharing between sand columns and clay at the surface of the footing, a number of quarter-bridge strain gauge pressure transducers, MPT (model 105S), were used. These load transducers are appropriate because of this extremely small size (3 mm in diameter and 0.5 mm in thickness, plate 2.4f). The ultimate design capacity for each transducer was 61 psi (413 kPa) although they could be loaded up to twice this capacity according to manufacturer's instruction.

Such small transducers are usually very sensitive, hence a calibration chamber was specifically made to determine the linearity and accuracy of each transducer independently from the figures provided by the UK dealer, H.Tinsley Co. Ltd. In fact, the MPTs were made by Precision Measurement Co. in USA. In order to eliminate the possible thermal effect in the transducers as they are energised, these were placed in direct contact with the steel base of the calibration chamber. The general results of those calibrations were not very satisfactory and some of the transducers were even found to be defective. However, for operational transducers, Fig. 2.8 shows, the linearity of the response appears to be in an acceptable range throughout repeated calibrations, but, the measured slopes are about 10-30% lower than the values quoted by the supplier. An explanation given by the US manufactures was that the transducers were initially calibrated in an oil pressure cell, so that air leaks could develop into stainless steel shell of the load cell, which is suppose to be fully sealed under a large air pressure. From author's point of view, this did not explain everything, and there were some other factors that should perhaps be taken into consideration such as the stiffness of the shell, sensitivity, temperature and so on, but that will be beyond the scope of this study. However, the conversion factors which translate the strain gauge reading to equivalent load were finally chosen as an average value from calibration loads in the range of 0 to 200 kPa, which was the approximate range of the typical pressure applied during a test.

As the ratio of diameter of the MPT to average sand size d_{50} is about 10, if those MPTs are in direct contact with sand, it is possible that large size particles might cause local contact stress concentrations and result in inaccurate average values across the measuring area of the transducer. Considering this fact, calibrations were thus also carried at such condition that transducers were placed in direct contact with sand in the calibration chamber. It was found that the transducer response contact with sand were of the order of 0.1% to 0.15% higher than that contact with clay,

which was in the experimentally acceptable range. Therefore, it was concluded that for Loch Aline sand, the effect of local contact stress concentration was negligible.

2.5.4 Pore-water pressure transducers

Attempt was made to measure the dissipation of excess pore pressure using four pore pressure transducers (Bell and Howell 4-327-L226). Each of these had a mounting block with a drainage path connection on each side (Fig 2.9). The block also provides a small screw cover for de-airing purposes. Powered by 10V DC supply, their output lay in the range of 0-100 psi (690 kPa). The pore pressure transducer with mounting block is shown in plate 2.4d.

In small tank consolidation, a transducer was connected to the tank wall at mid-height via a transparent tube (Fig 2.10). De-airing was achieved by applying low pressure (2 kPa) water from the other side of the mounting block while the top drainage hole was open, after all the air bubbles had escaped from the mounting block, the top drainage hole was screwed tight.

The small dimension of the model left very limited clay space between model columns, this made it difficult to install instrumentation to directly measure the pore water pressure at a known depth and location between columns without significantly disturbing the sample. The smallest available instrument, a Druck miniature pore pressure transducer has a head diameter of 6 mm which is still too big for the available space in the clay between columns, with a spacing typically about 10 mm. To solve this problem, attempts were made to use a steel hypodermic tube (2 mm in diameter) to lead the pore water pressure out of the sample via a small soft tube and connect it to a normal transducer where measurement could be made (Fig 2.11a). Several methods were tried to make a perfectly permeable tip and to position this tip at a desired depth. A cotton bung and a bottom supported positioning method were found to be most effective (Fig. 2.11b). Great difficulties were encountered in de-airing the system. A typical response from this measurement device is presented in Fig. 2.12, which shows that this device has not been able to transfer the correct excess pore water pressure response from measured points to the transducers. Therefore, this monitoring technique was abandoned after only two tests.

2.5.5 Data acquisition

As plate 2.1 also shows, the data scanner used was a Schlumberger 3531 Delta ORION data acquisition system. It has maximum scanning capability of 200 channels. A detached switch power box supplies alternative 10, 15 or 20 V constant DC power with the ability to power 10 devices. In addition, a total of 40 direct strain gauge connections were also provided on the other side of the board attached to the system. During each standard test, the scanning program took a set of reading of all 12 transducers with a period of approximately 0.5-1 seconds. The signals were read up to 0.0001mm accuracy, a very adequate level of accuracy for this research. In displacement controlled tests, each test lasted about 8 hours so that readings were usually repeated at a typical interval of 2 minutes, leading to a very large number of sets of data. For the flexible load tests, the interval of each reading varied from 5 seconds at the beginning of each increment to up to 10 minutes at later stages. Scanned data can be read from an attached printer instantly and also can be saved to a floppy disk simultaneously in ASCII format for subsequent processing.

2.5.6 Photograph and Camera

To understand the general failure mechanisms and soil deformation characteristics of ground under a load, the technique of recording the position of grids of small marks placed in a chosen section in the soil by means of photography or radiography has been often used in geotechnical research. In the present study, the set-up of the tests made it impossible to use such observations in a vertical section of the sample during a test. However, it was possible to look at horizontal displacements of the surface clay bed by means of direct overhead photograph.

After installation of the columns in the clay bed, 15 mm square grids of 2 mm black markers (painted steel balls) were placed on the surface of the clay bed over a half of the total area. Three reference points (those assumed have no movements during the test) made of perspex discs (20 mm diameter) with a fine cross were fixed on the flange of the tank, roughly equal distanced over the photograph area (refer to Fig 4.26). A 35 mm Nikon camera was mounted on a frame directly above the sample surface independently from the tank to avoid vibration and other movements (refer to plate 3.1). The distance between the camera and sample surface was adjusted so that the entire desired photograph area was included in the viewfinder through a 50 mm standard lens. The 50 mm lens provides an image with a minimum distortion which could be significant to the results of the film measurement since the overall

movement of the marker was not expected to be very big, especially for those outside the matrix centre of the lens. One method of film measurement used an Image Analysis technique (see film measurement section 2.5.7) carried out on the basis of grey level defection which required that all the photographs should be taken at a constant average light in the cross section of the photographed area. This was achieved by setting a fixed aperture and shutter speed in the camera for all the shots with a tungsten light as main lighting source.

2.5.7 Film and measurement

Films used for photograph were normal 35 mm acetate film, Ilford 400 Black & White. To measure the displacement of those markers from the photographs, two methods have been used.

2.5.7.1 Image analysis

The first method used was an Image Analysis system developed at Glasgow university (Dr. Peter Smart 1994). The system consists of a video camera (with various lens and aperture) and image analysis programme "Semper 6" installed on a Nimbus computer. The enlarged photograph (print) was scanned by the video camera, and the Particle Analysis programme identified particles (image of markers) according to given intensity threshold values. Each marker was assigned a unique identifying number and its properties such as size, area, coordinates of the centre were given by the analysis in ASCII format. Files from different stages of the test were processed in spreadsheet software and then the movement of each marker was calculated as the difference between the coordinates between two films.

It was found that the accuracy of such analysis was entirely dependent upon the quality of the print (contrast degree between black markers and white clay bed) and the uniformity of the "grey level" in a print and between prints. This required first, that all the photographs had to give a exactly constant exposure to the film during a test, and second, since the analysis system could not scan the images from the negative, the processing and printing of the film had to result in exactly uniform contrast and brightness throughout all the negatives and prints in a test. The efforts made to achieve such demands were:

- All the photographs were taken at a fixed aperture and shutter speed under a constant artificial light uniformly illuminating the photographed area throughout the test (no flash).
- Film was processed at constant temperature. Negatives were printed by a machine (instead of hand) at a fixed exposure time and the developing and fixing time were also constant for all the prints achieved using a professional laboratory.

Having described this long, rather complicated procedure, it can be seen that experimental errors could arise from all stages from photography, processing and printing to scanning (lighting). The calibration of such a comprehensive process was carried out by comparing the data from the same image scanned twice, and from two photographs taken from an unmoved image. It was found that errors from a such process could be in the range of 3 to 5 pixels, which was equivalent to ± 0.45 mm in the actual model. The estimated overall movements from a small tank were of the order of 1-2 mm, therefore, the accuracy was only about 30%, which was obviously not enough to be accepted for a realistic analysis. However, the measurement results indicated the general direction of the surface movement of the model tests and these results are presented in section 4.2.3.

Improvement was made by using a high resolution image scanner, the COSMOS at the Royal Observatory, Edinburgh to scan the images directly from the negatives at a resolution of 16 μm per pixel. The scanned images were processed by a VAX 11/750 computer with 8 MBytes memory. Such high density scans resulted large data files (4 Mb per image) which were stored in a type in order to transfer to the Semper programme for particle analysis. Unfortunately, the programme can only analyse a maximum image of a size of 512 x 512 pixels so that the COSMOS scanned image with average size of 1538 x 1280 pixels would have to be split to several small parts. It was unfortunately not possible to persuade further this measuring technique: it was concluded that the extra information gained concerning mechanisms of deformation would not justify the effort required. However, the resolution improvement from 48 μm per pixel in the Glasgow system to 16 μm per pixel in COSMOS indicated that the experimental errors could be reduced substantially. It is clear that this image analysis technique can provide a feasible method of measurement of small displacement.

2.5.7.2 Film Measuring Machine (FMM)

The second method of film measurement made use of Film Measuring Machine(FMM) at Cambridge University, Engineering Department with each negative being measured manually. This machine has been specifically developed for this type of task by James (1973), and has been used for radiographs of simple gravity models and for photographs taken from centrifuge tests. A program named "Strain" has been developed to process the data and plot displacement vectors, principal strains, zero extension lines and so on. The details of the program may be found in Britto (1983).

Regarding the accuracy of the measurement, Mair (1979) reported the errors could be limited to less than $\pm 10 \mu\text{m}$. Davies (1981) noted that using a new TV monitor, the error could even be reduced to $\pm 5 \mu\text{m}$. Errors associated with the strains computed from gradients of displacements could be more serious. Mair (1979) reported that shear strain could be accurate to a value of 2%, but for poor quality markers, errors could be within 4%. Taylor (1984) noted errors associated with shear and volumetric strains of about 5%.

The arrangement of the Film Measuring Machine and the "Strain" programme was designed for relatively small regular arrays markers (rectangular or square grid). The images from the present study had to be split into several sections. The reported experiences of the accuracy of the machine presented above were, however, based on the measurement from 70 mm medium size formatted negative with an approximately scale of 10:1 between model and image. Present study used 35 mm format film with a scale of 22:1 between model and image, the errors of measured displacement were found to be within $\pm 8\mu\text{m}$, which was then $\pm 0.17 \text{ mm}$ in the model. Considering the measured overall movement (between the film taken at the start and the end of the test) of 1.5 mm, such measurement gave a total accuracy of 11%. A typical measurement obtained will be presented in section 4.2.3.2.

Chapter 3

Experimental procedures

3.1 Sample preparation

3.1.1 Mixing of slurry

The Speswhite kaolin clay has several advantages for soil modelling such as low sensitivity, quick for consolidation, ease of saturation and so on. It was decided that the kaolin slurry had to be mixed to 120% water content which is approximately twice its liquid limit because it is likely that at such high moisture contents, the particles are free to develop their own random structure under a given system of applied pressures.

The mixer used was made by Croker Plant, Model RP 100. The machine performs the mixing by rotating the "stars" at a constant speed of 74 r/p/m. while the container rotating in other direction on a speed of 16 r/p/m. The capacity of the mixer is 113 litres. Two bags of kaolin power (25 kg per bag) together with 60 kg water were mixed at one time. Powder and water were stirred by hand before the motor was started to prevent dry powder caking to the star and side of the pan. The quality of the mixing was checked at middle stage by stopping the motor and any cake formed here were removed. For a saturated, well mixed kaolin slurry, each mix took 2 hours producing a quantity of slurry could fill one and half of small tanks. It required about 3 mixes of slurry to fill a large tank. For each mixed slurry, 3 samples of slurry were randomly taken for water content test.

3.1.2 Consolidation

During one-dimensional consolidation, the friction on the side walls of the chamber could prevent the loading stress applied at the surface from transferring to the bottom of the chamber (Roscoe and Burland 1969). From load cell measurements,

Cairncross (1973) found such stress reduction on the bottom could be up to 20% percent. To reduce this wall friction down to a very small magnitude, silicone grease was smeared on the side walls of consolidation tanks in present study on the basis of experiences described by Roscoe and Burland (1969).

As described in Section 2.4.2, four tanks were usually consolidated simultaneously. The preparation of these tanks was carried out before the mixing of the slurry so that the ready slurry was not exposed to the air for a long time. Rubber seals were commonly used in each joint between tank sections or between tank and base/top plate to ensure a proper seal during the use of the tanks. All pressure bags whether on top or bottom of the tank were initially in the deflated state and pressure pipes, connection parts and drainage tubes were also checked during the tank preparation. A piece of saturated porous disc (which had been submerged in the water overnight) was placed on the bottom of each tank.

After pouring the slurry into the tanks, a second piece of saturated porous disc was placed to cover the slurry surface and then the cover plate was bolted on. The possible leaks and other qualities of the tank assembly were checked after an initial load had been subsequently applied. This procedure was found to be vital to the final quality of the consolidation.

As a general rule, each increment of load should only be applied when excess pore pressure equilibrium has been reached in the slurry sample. The approximation of this equilibrium could be alternatively judged from when a relatively stabilised slow settlement rate had been achieved in the sample. Experience from two pilot tests found that to reach 90% of consolidation under a given load required much longer time than expected. Table 3.1 lists the typical settlement rate at the end of each load increment and the time it took in the pilot tests.

Test Number	Applied load (kPa)	Settlement rate at end of each load (mm/hour)	Duration from beginning of the each load(hours)
TS-01	25	1	30
TS-01	50	0.5	96
TS-01	100	0.1	129
TS-02	15	0.25	91
TS-02	30	0.25	70
TS-02	60	0.01	98
TS-02	120	0.001	68

Table 3.1: Typical settlement rates of consolidation in pilot tests

It was finally decided to set up a standard procedure as such that the load was doubled every other day from initial pressure 20 kPa or 30 kPa respectively according to the chosen maximum consolidation pressure 120 kPa or 160 kPa, until the final increment which was left on for four days, after which, the load was finally reduced back to its initial value. The total volume of drainage water was measured to confirm the overall settlement of the slurry sample at this stage. Typical load-time-settlement curves throughout the consolidation are shown in Fig 3.1.

After completion of consolidation, samples were normally allowed to remain in this stage until it was convenient for them to be used for further stages of the testing programme. This time period varied from one sample to another from a minimum of 2 days up to maximum of 30 days since tests were conducted in turn. It is believed that during this period of time, the samples had undergone a certain degree of swelling especially in the region near the top, since no surface load was applied, and this swelling resulted in an increase of initial undrained shear strength with depth in the consolidated clay bed. This can be seen from the results of the in-situ shear vane tests presented in Section 4.2.5.

The unequal time periods of "waiting for use" in these prepared samples consequently caused varied rates of swelling which inevitably results in different degrees of overconsolidation ratio in each sample. This problem was approximately overcome by allowing the samples that were used first and second to swell freely for an extra 2 and 1 days respectively at the stage when the top plate had been removed

and extra an layer of clay had been trimmed off and sample surface was by then covered by a piece of cling film to prevent it from drying out.

3.1.3 Clay bed preparation

The small tank used for top downwards consolidation formed by two half sections, resulted in a clay sample 80 to 100 mm thickness of layer clay after the removal of the top section. This layer was cut off by a wire cutter. A steel ruler was used to trim the surface to be completely flat and smooth. Three samples were taken for water content tests from this extra layer. The finishing surface was finally covered by a piece of cling film and the sample was then ready for the next stage.

The general problem for samples consolidated from the bottom upwards was that the pressure bag could not be removed from the tank since a clay surface near the tank top was required for the subsequent loading. A stable base for vertical loading test was therefore not naturally provided. An attempt was made in a pilot test to fix the rods which were attached to the steel plate at the bottom of the clay cake above the pressure bag to a thick steel cantilever bar bolted on the tank flange in order to support the base plate (and the clay bed) during subsequent vertical loading. It was found that the base had settled down by a maximum of 0.2 mm at the end of the test (Hu 1993). This settlement could substantially obscure the true load-displacement relationship in a sample.

This problem was finally solved by placing two wooden columns inside the pressure bag following the procedures described below:

- 1 Two rods were fixed to the top plate to hang the base plate independent support by the pressure bag. In the small tank, two clamps were used, whereas in the large tank, two small platforms were built on the top plate to hold the rods.
2. The tank was lifted about 1m above the floor, the water emptied from the bag, and the bottom plate was removed. It was necessary to use a large crane to lift the large tank because of its weight. A mini crane (3 tons capacity) was found sufficient to handle the small tanks.
3. Two wooden columns were placed inside the bag and the bottom plate was assembled back to its original position. The height of the wooden columns was made 5 mm less than the actual distance from the top of the bag to the surface of

the bottom plate in order to avoid the possible crushing of the clay surface during the re-assembly of the bottom plate.

Although the finished surfaces of these samples were found to be naturally flat after removal of the top plate, a 10 mm thick layer was anyway removed and same procedure described before was followed to produce a completely even and smooth surface.

3.2 Installation of sand columns

3.2.1 General

As mentioned in Section 2.4.3, the construction of model stone columns was intended to represent very approximately typical field situations. Two types of field stone column installation methods were modelled: for the replacement method, all clay was removed with a minimum disturbance to the remaining clay; whereas in the displacement process, clay were pushed laterally. To achieve a regularly inhomogeneous sample, all columns have to be formed in such an identical way that the disturbance to initial vertical and horizontal stresses in the clay due to installation, as well as the density of the sand columns could be reasonably assumed to be the same from one test to another.

3.2.2 Densifying sand columns

Since the clay was very soft, densifying the sand in-situ became a very delicate issue. Several methods of compaction were tried in pilot tests. In TS-01, compaction of sand after each lift was carried out by carefully hand tamping by means of a brass plug. It was difficult to control the tamping force and the procedure could not be precisely repeated from one test to another. Excavation after the test showed that the cross section of the formed column varied in diameter (see Hu 1993). Then in the next trial (TS-02), a modified "locking" system was used to improve the control of the compaction force. This system used the self-weight of the clamped brass plug to stop the sand moving up as tube was lifted up. The uniformity of formed column diameters was found to be much better. Most tests used the replacement method to form the holes, and as a result of removing clay through the tube, the moisture and the clay on the inside wall of the tube gradually caused the plug to be stuck in the middle of the tube, so that the plug had to be pulled out by "shaking" which

inevitably disturbed the surrounding clay significantly. This method therefore was eventually abandoned after being employed for samples TS03 and TS04. Detailed descriptions of these early experiments can be found in Hu (1993).

The method finally adopted was one of sand raining, with the sand being densified by free fall alone. Sand was poured from the top of the tube at about 450 mm height above the clay level with a constant flow. This method was found much easier to repeat and the uniformity of columns was also ensured. The densities of the sand columns were measured by performing identical free fall process into a density pot and the average value was about 1520 kN/m^3 , corresponding to a medium dense sand. The complete procedures for the installation of sand columns are described in the following sections.

3.2.3 Installing columns by replacement method

On the basis of the experience from the pilot tests, it was decided to use the replacement method to construct the columns in all tests except the one specifically designed for comparison of installation methods in the testing programme (see Section 4.1). The drill rig and a thin wall tube as described in section 2.4.3 (plates 2.2 and 2.3) supported and located in the two way (horizontally) controlled steel frame were used to construct the model columns. In order to minimise disturbance to the surrounding clay during the penetration of the tube, lubricating oil was smeared on the outside of the tube before the formation of every other column.

The standard procedure used for forming a uniform column is described as follows.

- stage 1: The drill rig was precisely located at the specified column position.
- stage 2: Using the drill rig, the open-ended tube was inserted into the clay bed to a depth of 20 mm.
- stage 3: The hand auger was located in the tube and clay inside the tube (20 mm depth) was carefully removed. The auger was then withdrawn from tube.
- stage 4: Stage 2 and 3 were repeated several times, depending on the desired column length in order to produce a lined hole in clay bed.

- stage 5: A small funnel with a 2 mm diameter hole was placed on an adapter connected to the top end of tube and sand was poured into this funnel.
- stage 6: The tube was slowly withdrawn at a constant speed, approximately of 2-3 mm per second, until it reached the surface. Thus a column was formed in the clay bed by the replacement method.

This procedure was repeated exactly in constructing all the other columns. Fig 3.2 is a schematic diagram of this construction process

3.2.4 Installing columns by displacement method

The displacement method was only used in preparing one test sample. Its major difference compared to the replacement method was that no clay was removed during the hole-making so that a plug with a conical end was used to close the end of the tube as it penetrated to the clay bed. The facilities used and sand compaction method were identical to those in the displacement method. However, the stages in the installation were as follows.

- stage 1: The drill rig was precisely located at the specified column position.
- stage 2: The plug with conical end was inserted into the tube to form a close end and the other end of the plug was fixed to a larger diameter handle which just rested on top of the adapter.
- stage 3: Holding the handle of the plug together with the adapter, the tube was inserted into the clay bed at a slow and constant rate, to the desired depth. The plug was then removed leaving a lined hole.
- stage 4: A small funnel with a 2 mm diameter hole was placed on the adapter connected to the top end of the tube and sand was poured into this funnel.
- stage 5: The tube was slowly withdrawn at a constant speed, approximately of 2-3 mm per second until it reached the surface. Thus a column was formed in the clay bed by the displacement method.

Again, this procedure was repeated exactly in constructing all the other columns. Fig 3.3 is a schematic diagram of this construction process

3.2.5 The pattern and sequence

The model stone column foundation was not designed to reproduce a particular prototype situation. Although columns are often formed in triangle patterns in the field, for the convenience of laboratory operation, it was decided to use a square pattern of model columns. The spacing between two columns was chosen dependent on the desired area replacement ratio, the ratio of column area to overall clay area. Intuitively, the columns outside the footing area would be likely to provide a certain degree of lateral confinement due to the interactions between columns and soil and between columns themselves. In all tests, the columns were extended 1 or 2 rows beyond the footing area.

The process of constructing small grids of columns in such soft clay beds inevitably lead to some disturbance of the original ground whose magnitude is unfortunately not easy to ascertain. The intention of the tests was therefore to work with a uniform level of disturbance as a the regularly inhomogeneous sample was produced. To assist this, installation of the columns was always started from the centre of the grid (and clay bed) and then progressed outwards in a symmetrical fashion.

The rapid removal of the lining (tube) and replacement by sand caused a rather sudden initial stress change for the clay near the boundaries (sidewall) of the column, especially in horizontal direction. An adjustment would then be expected to take place both in the clay structure and in the sand in this region and this process would finally reach a stable equilibrium stage over, presumably, a long time period since some movement of pore water in the clay would be required. In addition, the sand columns provide a drainage path which will introduce water from the soft clay to the dry sand and this wetting process could also last for a considerable long period of time. The time gap from completion of first column to the last was normally in the order of 4 to 10 hours, and the finished sample was then allowed to rest for at least 12 hours before the test in order to ensure an approximately equalised condition had been reached in all the columns in the sample.

3.3 Loading test

3.3.1 Rigid loading tests

3.3.1.1 Loading: method and rate

If a column bulges under load (Hughes & Withers 1974), the surrounding clay undergoes lateral compression. The presence of drainage through the stone column will in the medium term definitely turn the clay-column system into a drained situation. Therefore, it was decided that tests should be conducted in, ideally, a fully drained condition. Pilot test TS-01 was conducted under a set of small incremental loads by means of a pneumatic jack with the load increased only when a relatively stable settlement had been reached under the previous load. It was found that the stiffness increased steadily, and the ground (sample) yielded slowly without any clear discontinuity in the load-settlement-time curve (Fig. 3.4). Using this procedure, a reasonably large displacement (say 15 mm) could only be achieved over a quite long period of time (20 days approximately). This was obviously not feasible for the planned intensive test program. Therefore, it was finally decided to adopt a displacement controlled loading method for the test programme because a monotonous constant rate of penetration provides equal settlements during the same period of time in all tests, and this would be convenient for the analysis of parametric studies.

Barksdale and Bachus (1984) observed that the composite strength in similar samples increased as a function of the loading rate by varying the rate from 0.38-1.3 mm/min. This led to the conclusion that a fully drained test will result in the greatest bearing capacity. It was difficult to ascertain the rate for performing a fully drained test because of the absence of reliable pore water pressure measurements. A rate of 0.061 mm/min was finally chosen for the convenience of laboratory operations. Although the departure from a fully drained condition could not be claimed to be negligible, it was believed that the behaviour of the clay-sand system under a drained situation was adequately simulated so that extrapolations of basic mechanisms of the response of composite ground (stone column foundations) could be made.

3.3.1.2 Testing

Like field situation, the performance of the composite sample is very much dependent on the initial strength of the clay. Also, local variations of the clay strength play an important part in the scatter of the test results. It was considered important to take a set of shear vane readings through the sample before loading to obtain an independent average strength profile. For each sample, shear vane tests were performed at four similar positions so that the possible local strength variations caused by consolidation and other experimental variations were somehow equally investigated. More details of the shear vane tests will be found in Section 3.4.1.

After completion of column installation by replacement method, it was found that no significant heave occurred on the finished surface of the samples, whereas when the columns were installed using the displacement method, the process of pushing clay sideways resulted in the foundation of a small "hill" on the sample surface with a peak of 30 mm at the centre. It was then necessary to flatten this "hill" before the test could be started. Although a minimum volume was finally removed by a wire cutter, the amount of volume lost was, however, substantial for both clay and sand columns. A discussion of the effect of this lost volume will be found in Section 4.2.

To obtain a correct stress distribution and consequently to produce an even penetration in the clay bed, it was important to ensure that both sample surface and footing were perfectly levelled. Therefore, several positions on the sample surface were measured by a spirit level and necessary corrections were made by adjusting the four supporting screw rods in the bottom of the tank. The same actions were also taken for the footing and the reaction frame. Having said that, it has to be noted that the tanks were large and heavy, the adjustments made in the supporting rods were anyway of limited accuracy and the alignment may not have been perfect. The inevitable errors will be appropriately discussed in the presentation of the measurements (Chapter 4).

Photographs of surface clay displacement as described in Section 2.5.6 were only taken in one small tank test and one large tank test. The markers were placed over half of the surface area at this stage. In large tank test, the large numbers of markers took nearly 2 hours to place. Dirt and spots on the clay surface were carefully removed afterwards. The finished surface was then covered by cling film.

Miniature pressure transducers (MPTs) were positioned in the desired locations by means of a small stainless steel clip. It was found necessary to lightly insert the wires into the clay in order to prevent the light-weight transducers from possible relocation before they were in contact with the footing. The transducers were found to be extremely fragile so that care was also taken to avoid touching the transducer surface with any metal or sharp-edged objects. After all the MPTs had been positioned, a layer of sand (Loch Aline sand) of 3 mm thickness was placed over the footing area to mimic the field situation. This also served as a perfectly flat surface for the rigid footing. The total load cell was fitted between the piston of the compression machine and the footing. The two LVDTs used to measure the surface displacement and those used to monitor the footing descent were positioned by two separated perspex frames which were bolted on the flange of the tank. After placing the instrumentation, the footing was then slowly moved down towards the sand blanket by turning the handle of the compression machine. All the necessary initialisation for all the instruments was carried out and the moment of initial contact was controlled by the response given by the MPTs which could be read on the data logger instantly. Plate 3.1 shows the entirely set-up of the test.

The total displacement was set at 30 mm for most tests and each test took about 8 hours to complete. The whole procedure described above for instrumentation took about 1 hour. Considering the average temperature in the laboratory was in the order of 22-26 degrees, evaporation of moisture from the surface could result in some change to the profile of strength with depth in the sample. This was avoided by moisturising the sample surface from time to time throughout the period of preparation, instrumentation and testing. Photographs were taken every hour throughout the test and the tungsten light was switched on only during the time of photography (normally less than 10 seconds) to avoid water content loss at the surface because of the high temperature.

The machine (test) was stopped once a 30 mm displacement had been reached. The footing was subsequently lifted up and all the instruments were then removed from the sample. The finished sample was watered for the last time and finally covered by a piece of cling film waiting for the next stage, the post-loading investigations (see section 3.4).

3.3.2 Flexible footing tests

3.3.2.1 First layer (test TL01-1)

This flexible footing test was conducted in a large tank which had a 500 mm depth of clay bed. As described in Section 2.4.4.2, the incremental loading pressure (air) was supplied to the FLD device to apply a uniform load to the sample.

After levelling the surface, installation of the columns and positioning the MPTs, a slightly thicker sand blanket (4 mm) was placed on the footing area, this was mainly intended to reduce the contact stress caused by the rigid edge in the FLD (2 mm thick ring). Five LVDTs were used to monitor the surface vertical displacement. Again, the surface markers and photography set-up as described at Sections 2.6 and 2.7 were arranged to record the horizontal movement of the clay surface. Plate 3.2 is a photograph of the entire test set-up.

Like the rigid footing loading tests, the flexible footing test was considered to be conducted in a drained condition. In the absence of pore pressure measurement, the criterion for load increase was that each load increment should only be applied when a stable settlement had been reached. In each increment, the pressure was applied slowly at approximately constant speed of 1kPa/sec. Under initial pressure 30 kPa, settlement at the centre was quickly reduced to 0.00067 mm/min within 4.5 hours, a very satisfying rate. The second load of 60 kPa took 29 hours to reach a rate of 0.0022mm/min at the centre. After 184 hours (7.7 days) under the third load of 120 kPa, the settlement seemed to be reasonably stabilised at an average rate of 0.0021 mm/min in the centre. At this stage, consideration was given to reduce the increment to a smaller magnitude for the next load step to avoid the possible instability of the sample so that a small increase of 60 kPa was planned. As a result of the lack of experience in this initial attempt, catastrophic failure happened when 35 kPa extra load had just been put on and a shear surface quickly developed to the surface of the sample within approximately 4-6 seconds. (plate 3.3). During the test, photographs were taken at the beginning and end of each load increment, but because of the unexpected sudden quick failure, it was pity that the entire failure process could not be recorded by the camera.

3.3.2.2 Second layer (test TL01-2)

The experience from this first failed test provided useful information for the control of loading rate, it was clear that doubling the load in each step was not suitable for such tests. In addition, the general failure of the foundation caused a loss of vital information concerning the deformed shape of the columns, which would be extremely useful to determine the failure mechanisms of samples under flexible load. Therefore, after post-loading investigations (see section 3.4), the top layer of 250 mm was cut off leaving a second layer of 250 mm thick clay cake which could be used for another test.

After re-levelling the second layer, the sample was again left for free swelling overnight (covered by cling film). It is true that the initial strength in the second layer had been influenced by the applied stress changes in the test carried out on the top layer, and the removal of the top 250 mm layer results in a different overconsolidation ratio profile. Since it was the intention to obtain more information concerning the mechanisms of failure and the influence of the loading rate, the effect of OCR and initial strength profiles could therefore be considered as a minor influence. However, the shear vane tests were again conducted at four locations through the sample after it had been prepared. The rest of the sample preparation procedures were the same as described for the upper layer test except that the markers placement and photography were eliminated.

The load was increased every 24 hours from an initial value of 30 kPa to 50, 70 and 120 kPa as the final load. For the last two increments, pressure was applied at very slow speed of 0.5 kPa per min in order to ensure a stable condition for the sample. The loading was finally stopped when a maximum settlement on one side of the footing reached 8 mm.

3.3.3 Test of plain sand

3.3.3.1 Sample preparation

In order to establish a comparison case for the effectiveness of stone column reinforcement, it was decided to perform a test in an extreme sample of plain sand. Consequently, the experimental procedure thus has to start from the initial sand bed preparation.

The sample preparation

The sand raining technique developed by Kolbuszewski and Jones (1961) was adopted to prepare a uniform sand bed. This technique has been successfully used in previous researches in Glasgow University (Stewart 1988) and the basic equipment already existed. The principal concept of this technique involves vertical deposition of sand (free fall) with controlled intensity. By varying both the height of the fall and rate of the flow, this system can produce a uniform sand bed over a range of densities.

As Fig 3.5 shows, the system used in the present study consisted of a circular hopper of 500 mm diameter with interchangeable base plate with a drilled grid of holes, the depth of the sand in the hopper and the size of the holes in the base plate thus decided the intensity of the deposition. Since the sand bed was formed in a small tank (300 mm diameter and 300 mm height), the extra area in the hopper beyond the tank area was covered to avoid spread of sand during the preparation. The base cover plate was made of a thin aluminium sheet with a handle attached and it was accommodated in slots on either side of the hopper. The hopper was simply hung from a small crane which provided an easy adjustment of the height of the fall. Plate 3.4 is a photograph taken during the sand bed deposition.

The density

It was decided to produce medium-dense sand beds for comparison loading tests with density corresponding approximately to the density measured in sand columns. For a container of the diameter of 500 mm (same as the hopper), Stewart (1988) determined that a relatively high intensity of sand deposition was required for a medium-dense sand bed with the height of fall chosen as 950 mm. Stewart also found that because the air was displaced upwards from the tank around its circumference, the updraught resulted in a slope near the boundary in each formed layer (Fig 3.6). However, on the basis of density measurements, Stewart concluded that the formation of sand layers shaped in this way did not affect the homogeneity of the resulting sand bed.

Although in general, the larger the height of the fall, the higher the density deposited, this does not apply indefinitely. Kolbuszewski (1948) used a height of pouring up to 2 m. Vaid et al (1988) noted that the influence of height of the drop on densification seems to be most significant in a height range of about 0 to 300 mm for

fine sand with $d_{50} = 0.4$ mm and 0.16 mm. Mulilis et al (1977) and Miura and Toki (1982) also obtained similar observations. Those evidences indicate that there must be a terminal height beyond which the height of drop becomes insignificant when other parameters are fixed. Belkheir (1993) concluded that the terminal height for fine sand including Loch Aline would be about 300 mm. This may not be a complete conclusion since the intensity and the particle size would definitely influence the density too. The present research was not intended to study such affect in detail, but these previous studied provided a guideline for the sand preparation process. The height of the fall, which was determined as the distance between the bottom of the hopper and the surface of the sample container, was fixed at 375 mm throughout all the preparations.

Once an intensity had been chosen, achieving a completely homogeneous sand bed also requires a relatively constant height of fall for each layer (which could be divided to an infinite numbers in the extreme) throughout the deposition process. A rigorous solution would require the upwards lifting of the hopper at a constant speed corresponding to the increase of the thickness of formed bed. This was quite difficult to achieve because of the heavy weight of the material and the hopper. Nevertheless, such an effect was investigated by examining the distributions of the density in depth against various intensity (with fixed height of hopper). The density tests were conducted using density pots. As plate 3.5 show, 6 density pots of diameter 75 mm and depth 50 mm were placed at various locations in the tank. For a fixed distance between the bottom of the hopper and the surface of the tank of 375 mm, Fig 3.7 shows that the scatter of the densities decreased with the decrease of the intensity (presented as the diameter of the holes of the base plate in the hopper). A test was also conducted at an increased height of 600 mm for a 2 mm base plate, as presented in Fig 3.8, such an increase in the height of the fall shows relatively little influence in the achieved density. Therefore, it was finally decided to use 4 and 5 mm diameter hole plates with fixed 375 mm height of fall to prepare the uniform sand bed for the tests. The maximum and minimum densities obtained from 4 mm base plates were 1569 and 1654 kg/m^3 respectively, and 1540 and 1608 kg/m^3 for the 5 mm plate.

3.3.3.2 Testing

The preparation of the sand bed was straightforward after the completion of the sand deposition. The tank was moved to the test site carefully with shaking and possible vibration avoided as far as possible. A perfectly flat surface was then achieved by means of a steel ruler. Finally, a spirit level was used to ensure a perfect match

between the sand bed and the penetration plate. Four vertical penetration tests using displacement control were performed. Although the rate should not affect the load-settlement curve since there was no drainage involved, three rates of 0.56 , 0.38 and 0.061 mm/min were used in those tests.

Again, the instrumentation used in those tests was identical to that in clay/column tests, namely load cell for the total load applied to the sample; miniature pressure transducers for the stress distribution beneath the footing and LVDT for the settlement of the footing plate. Only the surface displacement measurement method was different from the other samples. Great difficulties were encountered in using the LVDTs to monitor the surface movement since the self-weight of the monitoring rod and force applied by the spring in the transducer pushed the supporting "boat", a small brass disc, down into the sand bed as heave developed. Successful measurement of vertical movement was finally achieved by means of photography.

As plate 3.6 shows, two thin (1.5 mm) aluminium sheets clearly marked with 2 mm grid were placed on each side of the flat sand bed surface across the central axis before the test. The sheets left no gap to their contact with the surface of the sand. A 35 mm Nikon camera mounted on a tripod was used to record the interface between sand and the sheet. Photographs were taken at constant intervals during the test depending on the rate of the penetration, normally 12 photographs were made in a test. The actual surface vertical displacement could thus be measured physically from the enlarged prints of the photographs. It was true that such measurements might not necessarily have the same level of accuracy as could be achieved using LVDTs, nevertheless, a ± 0.5 mm accuracy was believed to have been achieved, which was an acceptable level for a qualitative analysis in comparison to the results obtained from the other samples. A presentation of these measurements and discussion can be found in Section 4.2.3.1.

3.4 Post-loading investigations

3.4.1 Shear vane testing

To identify the quality of the 1-D consolidation, the homogeneity of the clay bed and to verify the strengthening of the sand columns, a laboratory vane fixed on to the steel frame was used to determine the undrained shear strength of the samples as shown in plate 3.7. The vane was 12.7 mm wide and 12.7 mm long, which gave relatively small disturbance to the clay. The shear vane was rotated by a motor at a

speed of approximately 10 degrees/min. In order to measure the strength at depth within a borehole, the standard 15 mm long rod was extended to total length of 450 mm. Silicone grease was smeared on the rod to reduce the side friction along the length.

The in-situ shear vane tests were carried out in each sample before and after the test at various locations. To collect the maximum amount of data, several measurements were taken through the depth in each borehole. After completion of a measurement (no further change in torque), the motor was stopped and the vane was rotated back to its initial position by hand. The vane was then pushed down a 30 mm depth in order to perform another measurement. In general, 6-8 measurements were taken in each borehole so that a total depth of 250 mm clay was investigated. The measurements were normally taken in the clay between columns within the footing area as well as in a clay region without columns. Fig 3.9 shows a typical arrangement of the locations where vane test was conducted. It was a pity that without completely sacrificing a sample, the strength measurement could not be taken immediately after the installation of the columns. The vane tests carried out after the footing penetration tests presented a strength profile for a heavily consolidated clay due to the large load applied to the footing, so that the strengths measured would be higher than those resulting only from the column installation. However, in two tests (TS05, TS07) an extra 4 x 4 grid of columns was installed outside the footing area where the influence caused by the footing loading was expected to be much less than under the footing area. The presentation of these results and interpretation could be found in section 4.2.5.

3.4.2 Water content testing

Water content distribution in the clay can also give a indication of the strength change in the ground due to the inclusion of the granular column because the columns act like drainage paths and speed up the consolidation process in the clay. Similar to the shear vane tests, water content tests were carried out in the samples, mostly after the tests because it was feasible to sacrifice the clay beds before a test had been completed.

One method of investigation of deformation shapes of columns was to slice the specimen vertically (see section 3.4.3). Once a desired section had been made, water content samples were taken easily at chosen positions vertically and horizontally. A special brass tube with shape edge (8 mm internal diameter and 1.8 mm thickness)

was made for sampling the clays between the columns with minimum disturbances to the surrounding clay and deformed columns. This apparatus allowed 3 to 4 samples to be taken in a clay strip between columns. Overall 5 to 6 samples were taken on each axis (vertical and horizontal) including those taken from the region beyond the columns. The vertical line of the water content samples was close to the region where a series of vane tests had been conducted (Fig 3.9). Water content investigations were conducted in 5 clay beds. Once the plaster casting technique was being used to reveal the column shape (refer to section 3.4.4), it was found very difficult to take the clay samples because of the very narrow available space between columns and the importance of protecting the deformed shapes of the columns. Water content tests were only attempted in two samples where plaster casting was employed.

3.4.3 Discovery of the deformed column shapes

Due to the limitations of the instrumentation and the monitoring techniques in such small models, it was felt that much information concerning column-clay, and column-column interaction and general failure mechanisms could be learned by physically observing the deformed shapes of the model columns after tests. Several methods were tried to achieve this result and successful results were finally obtained by using a technique of plaster casting. The techniques used are presented in detail in the following sections.

3.4.3.1 Resin grouting

Epoxy resin liquid, Geoseal-MQ5 (supplied by Borden UK) was first used to solidify the failed sand columns in-situ prior to excavation. The Geoseal-MQ5 is often used in chemical grouting treatment in fine sands, gravel and fissured rock. It is a tannin/formaldehyde resin powder premixed with catalyst, it requires only mixing with water to prepare for use. It has the penetrability of 0.05 mm/sec.

Several methods were used to infiltrate the resin liquid into the sand columns such as injecting through a stainless steel needle from a syringe and top feeding by its own weight. Unfortunately, it was found that the solidified columns were not rigid enough to keep the perfect shapes of the columns after excavation. Therefore, this technique will not be presented in any further detail in this dissertation. However, relevant information can be found in Hu (1993).

3.4.3.2 Section slicing

Having unsuccessfully attempted to use epoxy resin, another method attempted to reveal the actual shapes of the columns was by vertically slicing through chosen sections. The specimen was lifted up above the surface of the tank by applying a pressure of small magnitude to the pressure bag on the bottom of the tank (refer to section 2.4.2). Then a wire cutter guided by two steel rods, which could be screwed on to a chosen position of the flange of the tank, was used to slice the specimen section by section (normally through the centre axis of a row of columns). Assuming that the columns all deformed axisymmetrically, the sliced section revealed a 2-dimensional formation of individual columns (plate 3.8). An advantage of this technique was that the finished section provided an ideal site for sampling of clays for water content measurement (refer to section 3.4.2). It was found that the result of this method of investigation did give a realistic image of the columns providing a perfect position was chosen for the wire cutter. Some of the images will be found at section 4.3.2.

However, the sliced section only provided a 2-dimensional picture of the column deformation instead of the true dimensional picture. The only assumption that could be made was that deformation in a column group was axisymmetrical. It was also found that the section through every column in a row was not necessarily precisely central because of the errors during the manual "cutting" operation and the errors in original installation would not be discovered either. Therefore, another method was developed which eventually resulted in a significant improvement, the plaster casting technique.

3.4.3.3 Plaster casting

The idea of this technique was to take away the sand and make a solid "column" by plaster without much disturbance to the surrounding clay. Here, the only problem was how to exhume the wet sand from the sample. It was found that a vacuum technique could be easily applied. A vacuum cleaner with a range of power (suction) was connected to a soft plastic tube (8 mm external diameter) through an adapter. Once a suitable suction (power) was found, the tube was able to "suck" all the damp sands with minimum disturbance to the surrounding clay leaving a perfect empty holes. Then the liquid plaster was poured into the holes. The solid plaster would then precisely record the shape of the deformed columns. The plaster casts of columns

were left overnight. The next day, by carefully excavating the clay around the solid columns, the perfect shapes of the deformed columns were revealed (plate 3.9).

It was an extremely simple and effective method to discover what exactly had happened at the stage of the end of the test. It is important to note several key factors during this process:

- It has to be admitted that because of the sudden stress drop as its support (sand) was removed, the clay near the columns would inevitably undergo certain plastic deformation, especially in lateral direction. To eliminate such experiment error, the time for the emptying all columns was controlled to the minimum, which was in the order of 10 to 15 min.. In addition to that, a minimum water content was also chosen for a fastest setting speed for the plaster liquid. Such water content was finally chosen as 150%. Finally, the time gap between the end of the emptying all the columns and pouring the plaster was of course kept to a minimum.
- During the excavation, it was found the plaster casts of the column were very brittle because of their slender shape so that certain reinforcement was necessary in each column to strengthen the plaster. This was achieved by inserting a spiral shaped metal bar in the hole prior to the casting.
- The high water content in the plaster liquid might have some effect on the surrounding clay during the setting process. The clay had a relatively lower moisture content (in the order of 45 to 55%) some diffusion might occur and the results of the water content tests on those samples might be high. The magnitude of such moisture increase in the clay could not be determined. However, as the study only required a quantitative indication from these measurements, it was assumed that such effects were negligible.

The information deduced from these plaster casts provided vital information for a rational understanding of the failure mechanisms of the composite ground and the interaction between column and clay and between columns. These results will be presented in section 4.3.3. Comparing all the methods described in the previous sections, the plaster casting was clearly the most successful technique.

Chapter 4

Presentation of the results and discussions

4.1 Introduction and testing programme

The primary intention of the present physical modelling study was to provide data to validate the results from a numerical model, which was being simultaneously developed in University College, Swansea (Pander, et al 1991). However, the laboratory testing programme was established in such way that the behaviour of soft ground reinforced by a large group of stone columns under a rigid footing could be investigated independently by means of a set of model tests.

As reviewed in Chapter 1, the complexities of stone column foundation have not yet been fully investigated (Schlosser 1979, Barksdale & Bachus 1983, Greenwood 1994). The group effect of stone column foundations is associated with a number of parameters such as the arrangement and size of the stone columns, the ground conditions as well as the footing flexibility, and limited time has not allowed the present studies to cover all the relevant aspects. It was finally decided that the testing programme (as well as the numerical investigation) would concentrate on those fundamental factors which had been recognised as having the most influential effect on the improvement of ground using stone column technique. They are listed as follows:

- The column diameter and spacing (which can be combined in the area replacement ratio A_s)
- The length of the columns
- The effects of the column installation method
- The clay bed strength
- The flexibility of the footing

As presented in Chapter 2 & 3, each model test inevitably required a considerable amount of time. It was found much easier and less time consuming to prepare the model in the smaller tanks. As section 2.3 mentioned, it is believed that the size of the small tanks will not significantly affect the general observed behaviour of the model and the influence of the various key parameters. It was therefore decided to perform most of the tests in small tanks.

Table 4.1 provides a summary of the testing programme and indicates the values of each of the key variables in each test. All rigid footing tests were conducted by means of displacement controlled loading. The main parametric variation of three area replacement ratios (10, 24 & 30%), two column lengths (100 & 160/170 mm) and two installation methods (replacement and displacement) were studied in a combination of 11 tests (TS03 to TS18). TS21 was performed as a duplicate of TS08 in order to check reproducibility of results. In those tests, the maximum footing displacement was chosen as 30 mm and the deformed shape of the columns was discovered after this penetration. To understand the progress of the deformations in the columns, test TS20 was stopped at a displacement of 15 mm. Numerical predictions have found that the central column in the group tends to support a relatively small load (Pande et al 1992). Test TS19 was thus designed to study the behaviour of a foundation in which the central column was omitted. As section 2.2.1 mentioned, the boundary effect due to the proximity of the outer edge of the tank in small tank tests was to a limited extent investigated by performing comparison tests in a large tank (TL02) with key parameters given the same values as test in the small tank. To obtain the basic failure mechanism of the stone column foundation under flexible footing, an attempt was made in tests TL01-1 & TL01-2 in which incremental loading was applied. Columns were installed by replacement method in all the samples except those in TS15 & 18 where displacement installation technique was employed to study the effect of the installation method. Several tests were also performed for the two extreme situations, plain clay ($A_s=0\%$) and plain sand ($A_s=100\%$) to give a reference information for the interpretation of the behaviour of the composite models: TS11, TS20-2 (clay) and TS12, 13 14a & 14a (sand).

The programme summarised in Table 4.1 includes a total number of 24 tests, which were conducted over an intensive period of 12 months. The complex nature of the problems of stone column reinforced foundation indicates that this programme can not be regarded as adequately comprehensive for a perfect understanding of the problems. It, however, has touched on most of the sensitive aspects of stone column

foundations in some depth, and provides useful guidelines for possible future studies.

Test No.	P_c	c_u	d	S	L	L/d	A_s	Note
	kPa	kPa	mm	mm	mm	-	%	
Standard Tests: Replacement installation								
TS02	180	23	11	25.3	100	9.1	15	Trial
TS03	110	5	11	30.8	100	9.1	10	Bag-leak : very soft clay bed
TS04	160	16.5	11	19.8	150	13.6	24	
TS05	120	10.5	11	17.6	100	9.1	30	Extra 1/4 columns installed
TS07	120	8	11	30.8	150	13.6	10	Extra 1/4 columns installed
TS08	120	15	11	19.8	100	9.1	24	Casts taken from this test onwards
TS09	120	11.5	17.5	31.5	160	9.1	24	
TS10	120	11.5	17.5	28	100	5.7	30	
TS16	120	11.5	11	30.8	100	9.1	10	
TS17	120	14	11	19.8	160	14.5	24	
TS19	120	10	11	19.8	160	9.1	24	Centre column removed
TS21	120	10	11	19.8	100	9.1	24	Repeat of TS08
TL02	160	17	17.5	31.5	160	9.1	24	Large tank test
TS20	120	14	11	19.8	100	9.1	24	Load to 15mm of settlement
Displacement installation of columns								
TS15	120	9	17.5	31.5	170	9.7	24	
TS18	120	7	11	30.8	100	9.1	10	
Flexible Loading: large tank								
TL01-1	120	18	17.5	31.5	160	9.1	24	Load to failure
TL01-2	120	16	17.5	31.5	100	5.7	24	Load to 7 mm on 2nd half of sample
Plain clay								
TS-11	120	14						
TS-20-2	120	14						
Plain sand			Density kg/m³					
TS12			1540					
TS13			1590					
TS14a			1585					
TS14b			1590					

Note: P_c Maximum consolidation stress
 c_u Initial average undrained shear strength
d Column diameter
S Column spacing (centre to centre)
L Column length
 A_s Area replacement ratio

Table 4.1: Summary of testing programme

4.2 The measurements

4.2.1 Introduction

Most of the useful results will be presented and described in this section. Some unsuccessful data from various attempts will be found in the Appendix. To condense the description, certain terms have been abbreviated. These terms together with some notes are as follows:

- Except where noted, all tests were conducted by means of **displacement controlled** method at rate of 0.061mm/min under a **rigid footing**, and all the columns were installed by **replacement** method.
- **Short (Long) columns**: Two length ratio used in the presentation of the results are the ratio of column length to column diameter L/d , and the ratio of column length to the footing diameter L/D . **Short columns** are those having L/d and L/D equal to or less than 9.1 and 1 respectively, and **Long columns** are those having L/d and L/D equal to or over 13.6 and 1.5 respectively.

4.2.2 Load-displacement relationships

The effect of the inclusion of granular columns in a soft clay bed is quite clearly shown in all tests. A typical load-displacement relationship for reinforced clay is plotted in comparison with tests carried out on the samples of plain clay and plain sand in Fig. 4.1, which shows that reinforced ground develops a higher initial stiffness than unreinforced ground. The method of approximating the ultimate loading is also illustrated in Fig. 4.1. For a given $A_s=30\%$, the ultimate load of the improved ground is about 65% higher than the unimproved clay bed. Unlike the behaviour of the plain sand foundation, no significant discontinuity or softening could be seen in the load-displacement curve for the reinforced sample throughout the test, the deformation beyond the ultimate loading point tends to develop simultaneously with both elastic and plastic components. As the test approaches the final stage, the whole ground around the footing settled substantially without losing its overall stability (perfect plastic behaviour-failure). Similar behaviour was also observed in a pilot test TS01 when a slow incremental load was applied (refer to Fig. 3.4). Such behaviour might be caused by the presence of the columns acting as effective drainage path and inducing a rapid consolidation process in their surrounding soft clay, leading to a strength increase in the clay. Consequently, the

stiffer clay then provides a larger lateral confinement to the surrounding columns, which results in an increase of bearing capacity in the columns. It is difficult to quantify the extent of drainage condition in the clay under such slow displacement rate since no pore pressure measurements were available. On the basis of the trial tests and other researches (Kaffezakis 1983), it is conceivable that the ground is in fact nearly fully drained. If so, the volume of the composite ground will change as yielding occurs in the sample, compression is thus not occurring at a constant volume.

The load bearing capacity is very much influenced by the initial strength of the clay bed in a stone column foundation. Fig. 4.2 shows that for a given footing penetration of 10mm, two otherwise identical samples TS08 and TS21 with about 30% difference in their average undrained shear strength could lead up to about 20% of difference in their loading pressure. The strength differences for these clay samples were determined by means of a miniature shear vane to be around 30 to 35% (refer to section 4.2.5). Since this would certainly influence parametric study in terms of loading pressure-displacement relationships, the comparison are presented in dimensionless format with the loading pressure, p , was normalised by the average initial undrained shear strength of the clay bed, c_u . Since all clay beds have undergone the same stress history, it is expected that the general profile of effective stress and OCR with depth should be roughly identical in all samples. Therefore, it is believed that using the ratio p/c_u is appropriate, and will present a correct basis for comparison of bearing capacity between tests. To continue the requirements of dimensionless comparison, the footing displacements, s , were normalised by the footing diameter (D).

The area replacement ratio A_S is a function of column diameter and spacing between columns. It was found that the load bearing capacity of the reinforced ground is quite strongly influenced by the variation of the A_S value. Samples having $A_S = 10\%$ with short columns only results in a rather slight increase in the capacity compared with the unreinforced sample (Fig. 4.3). When the displacement reaches about 1/3 of footing diameter, a noticeable 30% increase of capacity is seen when A_S reaches about 24%, and 60% of increase of capacity was observed in samples having $A_S = 30\%$. A clearer view of the relationship between the capacity and the area ratio is observed in Fig. 4.4, which shows that the rate of load bearing capacity increase in the improved ground becomes higher when A_S reaches 24% and over. An A_S value of 10% seems to be a lower boundary of the effectiveness of the reinforcement. However, the initial stiffness of the clay is still somehow enhanced, which will

undoubtedly reduce the settlement. A similar effect is also seen in the samples having longer columns as showed in Fig. 4.5. It is concluded that the area replacement ratio, A_s , is a key parameter controlling the improvement level of the column inclusion treatment in a soft clay ground. Since the A_s value is directly related to the cost of the application of the stone column technique, it is an important parameter on which experimental observation should be concentrated. Its importance will be seen in most of the measurements presented in following sections.

If columns are very short, one would expect that columns may penetrate into the ground beneath like piles as a result of end bearing failure when the rigid footing has undergone considerably penetration, whereas for longer columns, this tendency may be limited. Results from the exhumed column casts do show such mechanism (plate 4.1a, sketch refer to Fig. 4.47). Therefore, if a link is drawn with conventional piled foundations, the question of the skin friction between the columns and the surrounding clays naturally comes into the discussion, especially for those short columns where relative movement is likely to occur as the columns penetrated deeper. Grouping curves according to L/d ratio, Fig. 4.6 shows that there was a modest 15% increase of capacity when L/d was raised from 5.7 to 9.1 at the point when footing total displacement reached 1/4 of footing diameter. However, with long columns where L/d ranged from 9.1 to 14.5, there is no noticeable increase in the load bearing capacity in any of the tests (Fig. 4.7). Such an observation might suggest that the skin friction is associated with the stability of the column base as well as with the loading stress level at the bottom of the column. Results from the exhumed long column cast show that the penetration in the base of the column is insignificant (plate 4.1b, sketch refer to Fig. 4.49). It is unfortunate that the vertical stress distribution along the depth of the column could not be measured: presumably, in the long columns, the vertical stresses due to the footing load would have been fallen to a much smaller magnitude at the column bottom level than in the short columns. This logically leads one to suggest that there may be a critical column length beyond which the increase of the column length will no longer be useful to enhance the load bearing capacity of the reinforced ground. Naturally, such simple experimental evidence is not enough to lead to a firm conclusion. More experimental evidence is to be found in section 4.3.

As section 2.3 mentioned, the principal difference between the replacement and displacement methods of installing columns is that the displacement method introduces extra lateral compaction to the surrounding clays during the installation. The effect of such compaction was examined in tests TS15 and TS18. The result was

quite dramatic. In sample TS15, 17.5 mm diameter columns were installed with an A_s value of 24%. Installation with such a close spacing caused a considerable amount of heave at the surface of the sample (plate 4.2). The test was carried out with footing loading on an level surface after the heave was removed. The removed clay was approximately 2.2% of overall clay bed volume. Considering that the total volume of the columns is approximately 4.5% of the volume of overall clay bed, it is clear that almost half of the displaced clay volume was squeezed out during the installation. As a consequence, excavation showed that the mean diameter of the formed columns decreased with depth to a maximum reduction of 20% in the bottom level (plate 4.3). Those factors would undoubtedly result in a stiffness reduction in the ground. The effect of such compaction shown in Fig. 4.8 is in fact the reverse, and the capacity of the composite ground is lower for the displacement columns than for the ones installed by the replacement method in tests TS17 & TS09. Such an effect might be also caused by the inevitable destrucuration or remodelling process in the clay. If so, the initial stiffness of the virgin ground could be reduced. This assertion need to be supported by more experimental evidence, some is to be found in section 4.2.3. The cause of the large surface heave might be partly due to the close confinement provided by the sample container (the small tank), which might not be the case in the field. However, the improvement of the clay bed capacity by means of compaction is not always absent. A positive improvement was observed when a larger spacing (and smaller column diameter) was chosen in sample TS18 as shown in Fig. 4.9. With a small area ratio ($A_s=10\%$), displacement installation (test TS18) produced a modest improvement in load carrying capacity by comparison with replacement installation (TS03 & TS16). This encouraging result provides positive evidence of the effectiveness of the displacement technique.

4.2.3 The surface displacement

4.2.3.1 Vertical displacement

Information on vertical displacement recorded by four LVDTs (five in large tank tests) on the surface of the sample along a radius (refer to plate 3.1) except for the tests conducted with plain sand samples where a photographic method was employed (refer to section 3.3.3). Transducers were positioned at regular spacing of 16 mm (20 mm in large samples) from the edge of the footing outwards.

A typical result from TS10 plotted as surface heave, h , versus footing penetration, s , is presented in Fig. 4.10, which shows that the development of the surface heave is

smooth. By comparison with the total footing displacement of 30 mm, the magnitude of the surface heave is relatively small (less than 2 mm). Such an observation implies that the failure has not reached the ground surface in the end of the test. The ground initially descends with maximum displacement occurring near the footing and extending outwards in a radial direction as if the whole ground was dragged down by the footing penetration. Heave begins when the footing displacement reaches about 1/4-1/3 of footing radius and continues to develop with the eventual ground surface being above the original ground level. A clear image of this reversal of development of the vertical ground movement is illustrated in a 3-D plot (Fig. 4.11).

Comparing to unreinforced sample (TS-11, Fig. 4.12), the effect of the column inclusion is that the amount of the downwards displacement in the reinforced sample (Fig. 4.11) is much less. It is important to note that this comparison is made at roughly equal settlement even though the unreinforced sample had higher initial strength (refer to table 3.1). Another noticeable effect is that the reversal of the direction of surface displacement at a late stage of the test is much more significant in the reinforced sample. This phenomenon might be caused by the participation of the sand which has a relatively much lower compressibility than the clay. Sand dilates when it is subjected to shearing. As Fig. 4.13 shows for a footing on plain sand, the amount of heave is much more significant (about 6 times higher at its maximum value) at the same settlement and loading level compared with tests TS10 and TS11. However, rather small deformations were observed in the columns in tests TS10 and TS11 when they were exhumed after test, (see section 4.4.2), and it is difficult to justify that the dilatancy of the sand in the composite ground could cause the observed surface heave. Fig. 4.14 illustrates the relative surface heave modes and corresponding load-displacement curves for clay, reinforced clay and sand beds. It seems that unlike the "punching" failure in the soft clay (Fig. 4.14a) and the "total" failure in sand (Fig. 4.14c), the reinforced clay/column composite system (Fig. 4.14b) undergoes a rather "local shear" failure mode (the shear plane did not reach the surface) which presumably is due to the increase in stiffness as a result of the reinforcement. If this is the case, logically speaking, the profile of the surface displacement should be proportionally affected by the area replacement ratio. By plotting surface displacement, h , against footing displacement, s for samples with various area ratio from 10% to 30%, Fig. 4.15 outlines a general trend: samples with higher area ratio shown much less settlement than those having lower A_s value at same penetration level. Referring to the load-displacement relationships (section 4.2.2), the magnitude of settlement seems to be related to the stiffness of the ground.

Measurements of surface movement near the tank wall provide same indication of the effect of the boundary confinement. To determine the extent of such boundary effect, comparison is made between surface profiles taken from the tests carried out in large tank (TL02, Fig. 4.16a) and small tank (TS10, Fig. 4.16b), which shows that the influence of the central loading would not affect the region beyond $2.3D$ (where D is the footing diameter). The rigid boundary in the small tank is at about $1.5D$ from the centre, and the effect of the extra lateral confinement can thus be seen clearly in Fig. 4.16b. However, in comparison with the overall footing settlement of 30 mm, the amount of heave at the edge of the footing has been very low. It is likely that confinement would be more effective when a heave is beginning to develop in the sample. At that time, the footing has settled considerably. It is conceivable that such boundary effects might slightly affect the overall stability and capacity of the ground, but the general behaviour of the sample would not be significantly altered.

Another way to present surface displacement data is by plotting the total surface volume change V_{surf} (settlement positive) and the total penetration volume of the footing V_{foot} . V_{surf} is calculated by approximating a straight line between the measurements of adjacent LVDTs under the assumption that the movement of the ground surface is axisymmetric. Fig. 4.17 illustrates this assumption.

Fig. 4.18 shows plots of V_{foot} and V_{surf} for tests on sand (TS14b), clay (TS11) and reinforced clay (TS10) with superimposed lines perpendicular to the $V_{\text{foot}} = -V_{\text{surf}}$ line where $\Delta V = V_{\text{foot}} + V_{\text{surf}} = 0$. If the path followed the $\Delta V = 0$ lines, the sample would be deforming at a constant volume with the amount of heave developed in the surface outside the footing area equal to the footing penetration volume: this should correspond to undrained failure. For the sand sample, the curve lies below the $\Delta V = 0$ line indicating the increase of the volume due to applied load, $\Delta V > 0$, in another words, the sand dilates. In the reinforced clay and clay samples compression tends to reduce the volume of the sample ($\Delta V < 0$) initially. Such volume reduction does not appear to be directly related to the drainage in the sample since the reinforced sample (TS05) suffered less volume reduction than the plain clay sample (TS11) where no drainage is expected. By comparing similar curves with varying area ratio, Fig. 4.19 indicates that the volume reduction due to the loading is somehow inversely proportional to the area ratio, and hence the stiffness of the ground and the amount of dilatant sand present. As the load increases, the volumetric reduction tends to reduce in proportion to the development of the load bearing capacity in the ground. The initial elastic deformation is replaced by elasto-plastic deformation as

indicated in the load-displacement relationship and this leads to a change in the gradient of the $V_{\text{surf}}:V_{\text{foot}}$ curve.

By looking at the link between the gradient ($\delta V_{\text{surf}}/\delta V_{\text{foot}}$) of the $V_{\text{surf}} : V_{\text{foot}}$ relationship shown in Fig. 4.19 and the load level p/p_{max} (Fig. 4.20), it is clear that the development of more plastic deformation leads the sample to tend towards an constant volume and possibly undrained failure with $\delta V_{\text{surf}} / \delta V_{\text{foot}} = -1$. However, the amount of deformation developed in the sample when the footing penetration has reached 30 mm is small and the condition of deformation under constant volume is not fully mobilised in most tests. It may be noted that the magnitude of the overall surface displacement developed in the samples is small compared to the total footing penetration, and the method of calculating the surface volume change (refer to Fig. 4.17) may not be particular accurate because of the limited number of points of measurement. Other minor factors such as the evaporation of moisture from the clay surface during the tests might also contribute to the observed overall volume change. Nevertheless, the general volumetric strain profile provides a reasonably clear image of the overall deformation process.

It can be concluded that for the clay beds used in these model tests, the larger the settlement, the less stiff is the composite ground. This leads to a interesting observation concerning the samples which used the displacement method of column installation in tests TS15 and TS18. Figs 4.21 & 4.22 plotted as the surface volume change V_{surf} against the footing settlement s normalised by footing diameter, D . By linking Figs 2.21 & 2.22 to the load-displacement relationship in early Figs 4.8 & 4.9 respectively, it is clear that the stiffness of the composite ground is indeed compatible with the amount of surface settlement developed: the removal of a relatively large amount of surface volume (TS15) after column installation has noticeably affected the initial stiffness of the sample, however, the increase of the stiffness at higher loading levels indicates that the compaction has not had a completely negative effect on the load bearing capacity (Figs 4.21 & 4.8). More significant improvement in the total stiffness as a result of such densifying process in TS18 is clearly shown in Figs 4.22 & 4.9. The observations of volume change support the conclusion that the displacement method of installation of the columns does have a positive effect.

4.2.3.2 Horizontal displacement

A rough estimation of the surface horizontal displacement, t , could be made on the basis of the surface vertical displacement, h , by assuming that the foundation undergoes a general shear failure. Fig. 4.23 demonstrates that the value of t would be in the order of 0.4 to 0.6 h (by assuming a average composite frictional angle, ϕ'_{comp} in the range of 45° to 30° respectively, and adopting a plain strain failure mechanism). The observed value of h have been relatively small: for a footing settlement of 30 mm, h is less than 1.5 mm in most cases, which leads to maximum expected t in the range of 0.6 to 0.9 mm. Notice the idealised relationship between h and t illustrated in Fig. 4.23 is based on a plain strain situation whereas the model in fact is axial symmetrical problem in which the failure slope might be steeper so that the t value is likely over estimated by this approach to some extend. The Author defines a factor, A , to take this influence of axial symmetry into account as indicated in Fig. 4.23. More discussion on the axial symmetrical failure behaviour is to be found in section 4.3.3.

As mentioned in section 2.5.7, the two methods of film measurement that have been used have not produced satisfactory result because of the small magnitude of the overall movement to be recorded in the photographs. Also, the errors arising during the measurement process lead to an accuracy of about 30%. Therefore, the results from either method can only be seen as giving a general indication of the surface movement rather than precise figures. Fig. 4.24 shows the measurement obtained from Image Analysis method where two photographs taken at the beginning and end of the test (TS05) were processed and overlaid on top of one another. It is clear that the surface soil was pushed outwards to radial direction, which agrees reasonably well with the observation of vertical displacement as illustrated in Fig. 4.25. Most observed movement of the lead shots is clearly below the average heave line.

Surface horizontal displacement vectors were also obtained by means of the Film Measurement Machine and the "Strain" plotting program (refer to section 2.5.7.2). Due to the technical limitation of the equipment, measurements were made only for a small section of the clay surface as indicated in Fig. 4.26 (TL-02). The displacement vectors for the sample tested in the large tank (TL-02) showed a similar pattern of outwards movement.

It is unfortunate that the amount of the surface horizontal movements was not adequate to provide more precise information concerning the developing mechanism

of deformation. Features such as the influence of the area replacement ratio and effect of the extra rows of columns beyond the footing will be further discussed in Chapter 5 when some relevant numerical predictions and centrifuge observations are adopted. The limited measurements of horizontal movement that have been made can not really distinguish between these different cases.

4.2.3 Measurement from Miniature Pressure Transducers (MPT)

MPTs were placed on the surface of the loaded area in the centre of the section of chosen columns and the clay mid-way between columns. They are very sensitive transducers and thus experimental errors such as slight inclination of transducer surface and off-centre position would be likely to affect the measurements, and this may be a principle reason for the scatter found in the information to be presented. Reviewing the data obtained from all the model tests, it is felt that the present testing programme has only been of limited success in identifying the influence on the contact stress distribution of column length and clay strength.

Plotted as the measured rate of stress increase against the footing settlement ratio s/D in Fig. 4.27, the records show a rapid response from the transducers as the load is increased. The stresses both in clay and sand column increase in a similar way which confirms the participation of both clay and sand column in supporting the load.

Fig. 4.28 shows a typical result from TL02 as measured contact stress normalised by the footing pressure, σ/p , against footing settlement normalised by the footing diameter, s/D .

1. Stresses in columns are in general higher than in the surrounding clay.
2. Stresses in columns increase more rapidly than those in clay, especially at higher loading stress levels.
3. The middle column tends to be more heavily loaded than the centre column and those near the edge of the footing.

The use of a rigid footing ensure equal settlement in both sand and clay. It is logical to propose that the stiffer sand in the columns tends to take more load than the relatively less stiff clay. This phenomenon is known as stress concentration. It was

mentioned in Chapter 1 that columns carry their load by bulging into surrounding clay. The 2nd and 3rd observations lead one to expect that deformation in the columns might be very small at low stress levels when the column (as well as the clay) behave like elastic materials. As the stress increases in the columns, bulging would be expected to occur in the column. The dilatancy of the sand may thus encourage the plastic yielding in the surrounding clay as the bulging develops. If so, the middle column should deform the most compared with the rest. The information obtained from the shapes of the exhumed columns supports such expectations of deformation characteristics (see section 4.3.3).

Now consider the clay/column system as a whole and look at the distribution of contact stresses across the footing radius. As Fig. 4.29 shows, the approximate stress distribution profile obtained from the plain clay bed (TS11, Fig. 4.29a) and plain sand bed (TS14, Fig. 4.29c) agree well with the typical pattern of vertical stress expected from classical theory for soft cohesive clay and medium to dense sand beds subjected to rigid footing loads. In reinforced samples TS21 (Fig. 4.29b), stress concentration over the columns causes a general stress fluctuation between sand and clay. It is expected that discontinuity of the vertical stresses at the boundary between clay and sand columns will exist throughout the length of the columns. This introduces a rather complex stresses condition at this boundary especially when deformation is occurring in the columns. No direct measurement was made in that region. This part of the mechanism will be discussed in a later section based on the deformation information obtained from plaster casts of the column and on some numerical analysis results.

Notwithstanding the likely stress discontinuity, an average line can be approximately drawn to outline the general profile of the surface contact stress from the measurements obtained from the samples with various area replacement ratio, A_s , namely, 10% (TS16), 24% (TL02) and 30% (TS10) in Figs 4.30a, b, and c. This shows:

- High stress concentration near the footing edge is noticeable for the low A_s sample (Fig. 4.30a) but this gradually disappears as A_s value increases.
- The middle column receives the highest proportion of the loading stress, especially in those samples having A_s of 24% and over (Figs 4.30b and c).
- The effect of area ratio increase tends to "even" the general distributions across the footing.

By comparison with a homogeneous clay bed, the smooth variation of the contact stress distribution in composite ground is interrupted by the presence of the columns, and this interruption is not uniform across the footing. Plotting the stress measurements from the central columns, σ_s^c , and middle columns, σ_s^m , normalised by the average loading pressure, p , against footing settlement s/D , Figs 4.31a and 4.31b respectively, it is clearly seen that the load carried by columns increases rapidly as the A_S value increases, especially in those columns located at middle radius (middle columns). In samples having A_S value of 10% (TS03, TS07 & TS16), σ_s^c/p and σ_s^m/p remain approximately constant as settlement progresses, whereas in samples with A_S of 24% (TS04, TS21), significant increases are seen clearly in the slope of σ_s^c/p or σ_s^m/p curves (Figs 4.31a & 4.31b). This partly explains the load-displacement relationships presented in section 4.2.2: significant improvement in load bearing capacity requires a relative higher A_S ratio value (24% for instance), whereas samples having low A_S value, for instance, 10%) are likely to offer a only slight additional bearing capacity since the strength of the column material does not seem to be utilised due to the larger spacing. Additional load bearing capacity may be the result of the strength increase in the surrounding clays.

The load carrying capacity of the clay involves the mainly radial consolidation process since the sand columns act like sand drains. The key parameter for an effective consolidation system is the distance to the drainage, which is related to the spacing of the columns (presented as A_S value) in this case. Fig. 4.32 shows an average of 120% increase in the loading stress carried by the clay for the samples having A_S value of 24% in comparison with those having A_S value of 10% when the footing settles about 1/3 of the footing size. A general increase of the gradient in the σ_c^m vs s/D curves is also seen in Fig. 4.32, especially at higher settlements and load (refer to Fig. 4.31). The stress increase in both clay and column tends to be much more rapid at lower settlements (lower loads), which indicates the drainage flow is occurring more rapidly at this stage. The drainage will be affected by the presence of the sand blanket placed directly on top of the transducers.

A stress concentration ratio, n , which can be defined as a ratio of the average stress in sand column σ_s to average stress in the surrounding clay σ_c . Values of n are calculated based on the stresses measured from the central column and middle columns, σ_s^c and σ_s^m respectively, divided by the stress measured on the nearby clay σ_c .

Values of n vary from 0.3 to 8, the average values be in the range 1 to 5. Plotted as n vs footing stress, p , normalised by the initial undrained shear strength, c_u , Figs 4.33 and 4.34 shows that average n value is lower than 1.8 for the sample having lower A_s value of 10%, and remains roughly constant as load increase. Higher n values of over 2.5 are observed in samples having A_s of 24%, and the value of n increases quite rapidly with increased load level (Fig. 4.33, $n = \sigma_s^c / \sigma_c$) with a more dramatic effect seen in the middle columns (Fig. 4.34 $n = \sigma_s^m / \sigma_c$). The different degree of bulging or shearing in the columns seen from the column casts (refer to section 4.3.2) indicates that the stress share between column and clay is related to the deformation behaviours of both material.

The effect on the stress distribution of the lateral compaction when columns installed by displacement method is presented in Fig. 4.35, which shows an average 250% of stress increase in the sand compared with the sample with columns installed by the replacement method. Note the comparison is made with a sample having a low area ratio of 10%, which has been seen to form a lower boundary of the improvement to the capacity using the replacement method. The pattern in the Fig. 4.35 is directly related to the change in overall capacity seen in the load-displacement relation (Fig. 4.9). As far as the profiles of stress concentration ratio, n , with the loading level are concerned, Figs 4.36 shows a generally decrease of n value in TS15 where significant amount of surface clay volume (heave) was removed, which again is seen as the capacity reduction (Fig. 4.8). However, the capacity improvement seen in Figs 4.9 and 4.35 (TS18) is clearly shown in the dramatic increase of stress ratio profile in Fig. 4.37. It is expected that the stiffness and strength of the clay has been increased by the lateral compaction, which increases the capacity of the columns and leads to an overall improvement to the capacity of the composite ground.

Further discussion of the shearing of footing stress between clay and columns will be provided in Chapter 5 when published numerical analysis are reviewed.

4.2.6 Shear vane and water content tests

Shear vane tests were conducted in each clay bed after its consolidation. The majority of the samples were consolidated to a maximum pressure of 120 kPa; two others were loaded up to 140 kPa. The average undrained shear strength variations in clay beds consolidated to 120 kPa were found to be about 15-20% (Fig. 4.38b) even though all samples experienced nominally the same stress history (consolidation pressure). One extremely clay bed (TS03) was obtained when the pressure bag

suffered a major leak during the consolidation. Less scattered results were obtained from samples subjected to the higher consolidation stress of 140 kPa (TS-04 and TL-02, Fig. 4.38a). The strength variation may be partly caused by the friction between steel plate and the tank side wall when the applied pressure is low. However, the homogeneity of the clay bed appears to be acceptable.

After loading tests, shear vane tests were conducted in each block of clay and water content samples were taken from limited number of locations, mainly in the region where the columns had been installed. From the data selected from more or less identical locations shown early on in Fig. 3.9b, a direct link between undrained shear strength, c_u , and water content, w_c , was found to be approximately (Fig. 4.39)

$$w_c (\%) = 70 - 2.1c_u$$

The scatter was probably because the vane tests and sampling of water content were not carried out at precisely the same locations. The results appear slightly higher than the data obtained from laboratory vane test on speswhite kaolin (Wood 1987) for which an average relationship is plotted in Fig. 4.39.

The effect of the column improvement is clear by comparing the c_u profiles obtained before column installation (initial) and the after loading test, mainly under the footing area. Fig. 4.40 shows the influence of the area replacement ratio A_s on the c_u profile. The inclusion of the columns in the clay bed produces a noticeable strength increase, mainly within the region of installation of columns. The columns act as drainage paths (like sand drains) in the clay bed and speed up the consolidation process in the surrounding clay, especially in the radial direction.

It is also seen in Fig. 4.40 that such strength increase is proportional to the area ratio: data are gathered in Fig. 4.41 showing an approximate relationship between the average c_u values over the column length (normalised by its initial value, c_{uini}), and the A_s ratio. This relationship between A_s and increase of the c_u can be understood in a quantitative way by adapting the Terzaghi one-dimensional consolidation theory for radial flow as illustrated in Fig. 4.42. The rate of the consolidation in the radial direction at a fixed time, U_r , can be approximately estimated by:

$$U_r = \frac{2}{\sqrt{3}} \sqrt{T_v} \quad (4.1)$$

$$T_{vr} = \frac{C_{vr} \cdot t}{(H/2)^2} \quad (4.2)$$

where: T_{vR} = the time factor for radial flow
 C_{vR} = the coefficient of consolidation in radial direction
 t = the consolidation elapsed time
 H = shown in Fig. 4.42

The area ratio A_s directly affects the time factor T_{vR} , which directly influences the U_r while other factors remain unchanged. Equations (4.1) and (4.2) only describe a simplified two-dimensional solution, whereas the actual consolidation process would involve a 3-dimensional space with an irregular boundary, as well as the vertical drainage flow. Exact analysis of this situation has not been attempted. Further discussion is to be found in Chapter 5.

The shear strength profiles presented above are taken from the region where the clay has experienced vertical stress due to the footing load. The undrained shear strength of the sample was also studied in test TS05 and TS07 where extra rows of columns were installed out side the footing. Fig. 4.40 implies that the clay under the load experienced a 6 to 12% increase in strength value in addition to the strength increase caused by the installation of the columns. It appears that strength increase due to the loading stress is not much affected by the variation of the area replacement ratio ($A_s=30\%$ in TS05, $A_s=10\%$ in TS07) but is primarily linked with the stress level.

The displacement method of constructing columns causes lateral compaction of the surrounding clays. For samples having a low area ratio of 10% (TS18), Fig. 4.43 shows that such compaction has caused a significant improvement in clay strength by about 50% in comparison with the replacement method (TS16). On the other hand, for sample having A_s of 24% (TS15), the displacement installation has caused a noticeable reduction in load bearing capacity comparing to the one used replacement method (TS09, refer to Fig. 4.8). However, Fig. 4.44 clearly indicates a strength increase in this test too. It may be suggested that for the sample TS15, the volume lost is the main reason for the reduction of the capacity. On the basis of peak and remoulded measurements of undrained shear strength, the average sensitivity of the kaolin was found to be 2.3 (Fig. 4.45), which is reasonably low. The severe disturbance caused by installing sand columns by displacement method would be expected to destroy any structure that the clay had, particularly in the region near the column/clay boundaries. This destructruation would be expected to increase as the area ratio increased. If the soil has a high sensitivity, the installation of column by

displacement method may cause a negative effect to the bearing capacity. It is generally recommended that vibro-displacement is not suitable for soil with sensitivity over 5 (Greenwood 1987, Mitchell 1984).

4.3 The failure mechanisms under a rigid footing

4.3.1 Introduction

Previous studies have suggested that a single isolated stone column takes the load by bulging into the surrounding clay in the region about $4d$ (column diameter) below the surface in order to mobilise extra lateral confinement (Hughes & Withers 1974). In the present study, the observations made from the excavated plaster casts which recorded the deformed shapes of individual columns rather well have indicated a quite different deformation pattern in columns in a group, which implies a difference in the mechanisms of failure in individual columns.

The failure mechanisms discussed in this section will be mainly based on the information deduced from the column casts. Measurements of the column deformation such as penetration depth, level of failure by bulging or formation of shear plane and average portion of central axis of the column were taken from enlarged (250 %) photography of the central section of the casts. A professional Image Editing software (Aldus PS-2) was also employed to assist the analysis of the deformation patterns from scanned images. It is estimated that the accuracy of the measurements is about ± 0.5 mm.

4.3.2. Deformations and characteristics

4.3.2.1 Model with short columns

Photographs of the central section of typical column casts from models TS08 ($L/d=9.1$ and $L/D=1.0$) are presented in plate 4.4, which shows:

- The central column deformed the least while the middle columns were noticeably pushed outwards in the lower region. Columns close to the edge of the footing suffered largest deformation with normally a clear shear plane being seen.

- There is a clear roughly conical region immediately below the footing where no noticeable change of column diameter occurred.
- Columns under the footing have generally shortened in length and their lower end have penetrated into the underlying clay.

To help understand the development of deformation during loading, test TS19 was stopped at 15 mm of footing settlement but was otherwise identical to TS08 & TS21. The deformations of identical columns are shown in Fig. 4.46 plotted as depth normalised by the footing diameter, Z/D , against the lateral displacement, n , from the central axis of the column, normalised by the total footing displacement at which the test was stopped, s . The edge columns bulge most near the top. The middle column bulge less and at a lower level, whereas the central column remains almost vertical and bulges slightly near the bottom. As the footing penetrates further, lateral deformation continues in a constant pattern, but a clear rupture plane develops in the top of the edge column associated with large outwards lateral displacement. The middle columns bulged over the lower 2/3 of its length and was displaced laterally. The central column still remained relatively straight but bulged near the bottom. Columns outside the loaded area shared modest lateral displacement. Linking the levels where most deformation occurred, it appears that the failure began at the edge and propagated forwards the centre as shown in Fig. 4.47. The bottom penetration of the columns varies with radius and is greatest under the centre of the footing. The radial bulging and vertical penetration of columns develop simultaneously.

4.3.2.2 Model with long columns

Plate 4.5 is a column cast obtained from sample TS17 ($L/d=14.5$, $L/D=1.6$), and shows no clear penetration of the end of the columns. The general profile of radial displacement of the central axis of long column under the footing appears rather similar in the upper part to that of short column (Fig. 4.48). However, the large footing settlement has little influence on the lower part of the columns below a depth of about $1.2D$ where columns show no noticeable bulging or radial or vertical displacement. Instead of being pushed outwards as with short column (TS21), the long columns in TS17 appear to be suffering a "buckling" failure over the section (1D)-like a slender elastic column (Fig. 4.49). Notice that the "wedge" failure mechanism is still rather similar to that found for short columns (compare Figs 4.47, 4.49).

4.3.2.3 Parametric variations

The terms "long column" and "short column" have been used in a rather vague way with reference to the ratio L/d of column length, L , to the column diameter, d , and to the ratio L/D of column length L to the footing diameter, D . Clearly both these ratios will influence the column deformation, particularly the penetration of the column base.

Plate 4.6a shows the deformed columns from the central section of the models TS08 and TS09 where all parameters are identical (including $L/d = 9.1$) except for the value of the ratio L/D equal to 1 and 1.6 for TS08 and TS09 respectively. Penetration of the column bases occur only in the sample having the lower L/D ratio of 1 (TS08). On the other hand, if the L/D ratio is fixed at 1.6 and the L/d ratio is varied (models TS17, $L/d = 13.6$ and TS09, $L/d = 9.1$), no indication of column penetration in the bottom level is seen from either model (plate 4.6b). Such comparison is achieved by varying the column diameter between 11 mm and 17.5 mm with constant footing diameter. To avoid the errors raised from the influence of column diameter variation in this deductive reasoning, tests TL02 and TS09 are compared in which both models used same 17.5 mm diameter columns with L/d ratio of 9.1, the different footing diameters 150 mm and 100 mm giving result of L/D equal to 1.1 and 1.6 in TL02 and TS09 respectively, it is then again seen that only with the lower L/D ratio (TL02) do the columns punch into the underlying clay (plate 4.6c). These effects are summarised in Fig. 4.50, and it is quite clear that it is the ratio L/D and not L/d that governs the occurrence of column bottom penetration into the underlying clay.

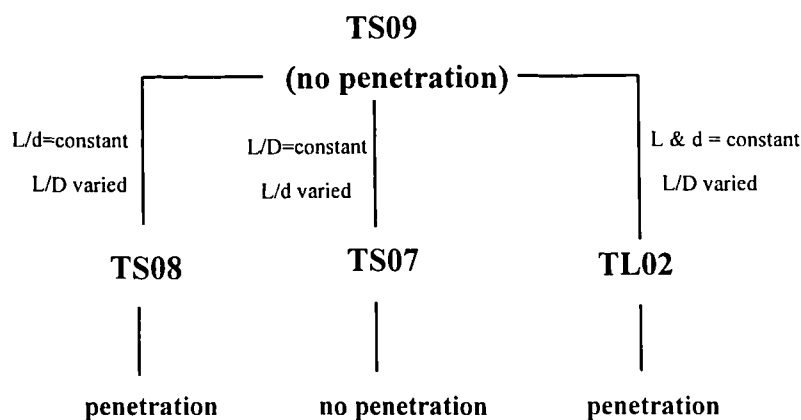


Fig. 4.50: Diagrams of the deductive inference for the effect of the column penetration due to L/D and L/d

This discussion has looked at the three basic parameters, namely the footing diameter, D , column diameter, d , and the column length, L . Since most of the tests were carried out in the same small size of tank (with footing of 100 mm in diameter), the influence of the parameters d and L on the deformation behaviours of the model could be studied using the column casts. As plate 4.7 and Fig. 4.49 show, in the thin long columns model (TS17), the middle columns suffered a buckling-like failure with no significant bulging/shearing in the failed region, whereas in bigger column model TS09 (plate 4.8), much bulging occurred with eventual formation of a clear shear planes. One could expect that flexural rigidity of the columns, which is controlled by the diameter, might influence the mechanism of failure as illustrated in Fig. 4.51a, particularly in those long columns in which no penetration of the base of the column occurred. The shear rupture in the large columns (plate 4.8a) is almost identical to the typical failure seen in the triaxial apparatus (plate 4.8b). This is not surprising since the columns are subjected to an axial stress increase with confining stress provided by the surrounding clay (reinforced by the group of columns) (Fig. 4.51b).

The mechanism of column base penetration can be introduced further by plotting the penetration, N_p , normalised by overall footing settlement, s , against the radial position of individual columns r , normalised by footing diameter, D , with the base penetration of columns outside the footing assumed to be zero. The penetration profiles with various area replacement ratio, A_s are summarised in Fig. 4.52. The depth of penetration in each model increases towards the centre. The columns near the edge are evidently shortening more. The central column has benefited the most from its surrounding columns in the group. The depth of penetration increases as the area ratio (A_s) increases (Fig. 4.52). The slope of the curve tends to be flatter as A_s increase implying that the column/clay system would punch into the deep layer as one solid unit if the area ratio reached a sufficiently high value. The higher area ratio brings the action down to a deeper level. A similar conclusion can also be drawn by plotting the level of greatest column deformation (bulging/shear plane), L_f , normalised by the footing diameter, D , against the radius, r , normalised by D (Fig. 4.53).

A general indication of the shape of the "conical wedge" failure mechanism seen in the column casts (plates 4.4 and 4.5) can be seen in Figs 4.52 & 4.53. The wedge line defines the region in which most of the bulging or shearing or lateral deflection occurred. Section 4.2.2 concluded that the load bearing capacity increase as the area ratio increases, here it is shown that the depth of the failure wedge goes deeper as the

area ratio increases, which implies that the less deforming region (above the "wedge" boundary), is increasing in volume. This deepening mechanism is associated with reduced lateral deformation both beneath the footing (Fig. 4.54a) and beyond (Fig. 4.54b).

4.3.3 The mechanism of failure

The footing used in the model tests was restrained from free tilting and was punched in under deformation control so that the stability of the ground was protected. On the other hand, previous discussion has shown that the 30 mm of total settlement may not have been large enough for the full development of a failure mechanism. However, based on the results of the measurements presented in previous sections and other characteristics of the column/clay system, the general mechanism of failure of the composite ground is as proposed in Fig. 4.55a. The failure begins at the edge of the footing and propagates into the clay axisymmetrically along a conical surface, A. Further failure then develops along the surface B and, if deformation were continued far enough, would reach the ground surface through C. This failure mechanism could be expected to develop on both side of the footing.

To help the analysis of such mechanism further, the propose failure mechanism (Fig. 4.55a) divides composite ground into four basic "zones" according to the predominant deformation character in those regions, namely elastic, plastic, retaining and extension zone.

4.3.3.1 Zone "I" (elastic zone)

This is a "conical" unit directly beneath the footing defined as an elastic zone. In this region, the columns are sufficiently confined by the surrounding clay that no lateral movement (bulging) occurs in the columns and the whole region acts like an "elastic cone" and penetrates downwards as footing settlement progresses (Fig. 4.55b). The relative vertical movement between clay and columns is negligible so that the frictional shear force in the column/clay boundaries is probably not mobilised. No significant lateral deformation occurred in clay/column boundaries, the clay and columns in this region could be seen as move together as one unit. Therefore, regarding the stress condition, it seems reasonable to assume that column (and clay) have undergone isotropic compression under the applied load so that the stress ratio $\Delta\sigma_v/\Delta\sigma_h \cong 1$ for both column and clay, which means that the lateral stress increases in proportion to the increase of vertical stress (Fig. 4.55b).

The volume of the region, which partly indicates the level of improvement provided by the columns, can be represented by the angle β_I , which should be dependant on the following parameters:

$$\beta_I = f(A_S, \phi_C'/\phi_S', c_u, G_S/kG_C) \quad (4.3)$$

Where all others symbols has been previously defined except the G_S/kG_C , which is the stiffness ratio of column material and the clay, and k is the constant which represents the stiffness change in the clay due to the column installation including the effect of consolidation, compaction/remoulding and so on.

4.3.3.2 Zone "II" (plastic zone)

This is the region where most of the horizontal deformation occurred in columns, as well presumably as in the clay (Fig. 4.55c). The term "plastic" here specifically refers to the deformation developed in the columns, The stress situation in this region is complicated because of the development of plastic deformation in both vertical and lateral directions. Most of the axial shortening of the columns due to the footing settlement occurs in this region. It was noticed in Figs 4.52 and 4.53 that the depth of such deformation increases as the position of the column is near the centre axis. This phenomenon reflects the horizontal interactions within the clay/column system.

Three modes of deformation of columns are seen: bulging/shearing, bending or buckling, presumably due to the insufficient confinement from the surroundings, and punching as the result of end bearing failure in a column base. Fig. 4.56 suggests the stress conditions in these 3 basic types of deformation in a column. For types (a) and (b), the column is under a triaxial stress condition initially; as the load increases, the column generates extra resistance along the column/clay boundaries either by bulging/shearing, or by penetrating into deeper clay, both effect being the result of the relative movement between column and clay. The buckling failure mode in case (c) (Fig. 4.56c) tends to mobilise lateral resistance over a rather larger depth. Deflection is associated with much less significant axial bulging. Horizontal interactions between columns also provide extra confinement, and the extent of this interaction is proportional to the number of the neighbouring columns. That is why the axisymmetrical nature of the problem lead to an increase in such interaction towards the centre: the central column has undergone the least deformation at the lowest level.

The lower boundary of this "plastic" zone is thus defined to cover most of the action in the clay/column system. As Fig. 4.55a illustrates, the equilibrium of this conical unit is the result of the column-clay, column-column interaction through their relative movement to mobilise sufficient resistance. When equilibrium is reached, columns and clay in the unit then move as one block. If the column is not long enough to reach this boundary, penetration inevitably occurs in addition to bulging. On the other hand, if the column length takes it beyond the boundary, the extra part of the length is no longer beneficial to its load carrying capacity. Therefore, the lower boundary of this zone, E in Fig. 4.55a, provides a criterion to justify the effectiveness of the length of the column on the load capacity. The corresponding depth is named the effective depth, which is related to the effective length of the column L_e . Nevertheless, the definition of the lower boundary E does not necessary mean that columns should be installed with different lengths to follow the shape of this boundary since other fundamental aspects such as overall the stability and stiffness are also of importance: those will be discussed later in association with the mechanisms in Zone "III" and "IV". The effective depth, which is related to the effective length L_e for all the columns, is defined as the minimum depth for which the column/clay system would carry the load without punching into the deep clay layer, as an equivalent total end bearing failure. Column length beyond this level would be mainly of benefit to reduce the total settlement of the foundation.

The only parameter for defining the zone "II" geometrically is L_e , which can be represented by the angle β_e : $L_e = D/2 \cdot \tan\beta_e$ (Fig. 4.55c). For a given area ratio, the penetration is governed by the ratio L/D (Fig. 4.50 and section 4.3.2.3). There are other parameters which could also influence β_e :

$$\beta_e = f(A_s, \phi_c'/\phi_s', c_u, L/D, E_s I_p, G_s/kG_c) \quad (4.4)$$

where: $E_s I_p$ = the "flexural rigidity" of the column

4.3.3.3 The potential failure surface A

Having understood this "plastic" region a bit better, it is then possible to define with more confidence the potential failure plane, A, to be within the Zone "II". The stresses in columns and clay along this surface would be assumed to reach their ultimate values within the composite system. The stiffness of the sand and clay are quite different, and the local failure angle in sand, β_s , and in clay, β_c , should also be different as illustrated in Fig. 4.57, and will be affected by various factors such as

internal friction angle, ϕ' , the stress level and the degree of drainage. Therefore, the total failure surface, A , should be seen as an average failure surface for this composite ground, as presented by an average failure angle β_{cri} , representing a comprehensive failure of this sand/clay composite system under the rigid footing load (Fig. 4.57).

The value of β_{cri} can be estimated from the column casts (Fig. 4.58). Typical failure angles measured from failed column cast are about 70° , corresponding to an internal friction angle of 50° for the presumably drained and dense sand. Using the internal friction angle ϕ' value obtained from drained triaxial tests (Al-Tabbaa 1987) of 23° for speswhite kaolin, the failure angles β for undrained clay and drained clay should be 45° and 56.5° respectively using Mohr-Coulomb rupture theory as:

$$\beta = 45^\circ + \frac{\phi'}{2}$$

Measured values β_{cri} from several model tests are shown in Table 4.1, and plotted against the area replacement ratio, A_s in Fig. 4.59. The effect of the presence of columns is then clear. In the sample having lower area ratio ($A_s=10\%$), it is likely that clay is only partly drained, the stiffness of the sand material is thus not fully utilised for the overall stiffness of the composite ground due to the rather insufficient lateral confining stress from the clay. Significant improvement of the total stiffness of the composite can only be seen when the A_s value reaches 24%: the average failure angle is beyond the value expected for the drained clay, and this improvement increases rapidly to the upper limit, the β value for drained sand, as the A_s value increases. Such observations agree well with the load-displacement relationships presented in section 4.2.2. It would be attractive to be able to use this average failure angle to estimate the load bearing capacity of the foundation by adopting limit equilibrium theory.

The measured β_{cri} value (Table 4.1) is rather a rough figure, and theoretically determined β_{cri} values require further analysis. It is likely that value of β_{cri} might be controlled by:

$$\beta_{cri} = f(A_s, \phi_c'/\phi_s', c_u, L/D, E_s I_p, G_s/kG_c, \gamma_s/\gamma_c) \quad (4.5)$$

4.3.3.4 Zone "III" (retaining zone) and Zone "IV" (extension zone)

Zone "III" is a region where most of the lateral movement in the column is observed, and no noticeable bulging could be seen in the columns. The columns, as well as the clay, are pushed outwards. This region is expected to provide the main lateral support to the action directly under the footing in the Zone "I" and "II" like a "retaining" unit. The horizontal stiffness of this region is thus critically related to the overall settlement of the foundation under the footing as illustrated in Fig. 4.60. It is beneficial to have columns present in the region beyond the boundary B. In fact, even in the region beyond the footing area, the existence of the column would also contribute to the overall stiffness of the clay under the footing. Experimental evidence and numerical analysis have demonstrated such effects, which will be discussed in Chapter 5.

The diagram Fig. 4.60 indicates that the lateral stress is the major principal stress in this region. The lateral effective stress increase due to the load is likely to decrease outwards, leading to a corresponding decrease of lateral displacement. The vertical stress in this region is much smaller than in Zone "II". The clay/column system in this region undergoes some sort of horizontal anisotropic compression. Although the direction of consolidation is different in this region from that found in Zone "I" and "II", the shear vane results shown some increase in strength in this region too (see Fig. 4.40).

Fig. 4.61 has located the failure boundary in zone "III" beginning as a continuation of the boundary A in zone "II" and propagating upwards along the curve surface B. Extrapolation on the basis of the average failure angle β_{CRI} in section 4.3.2.2 could lead one to choose a corresponding average internal friction angle ϕ_{comp} to define the shape of the curve B.

Finally, the zone "IV" is similar to the passive zone defined in conventional failure mechanisms. The potential failure surface C, is an extension of the surface B as also illustrated in Figs 4.55 and 4.61.

The failure mechanism proposed in Fig. 4.55 is very much based on the conventional load bearing behaviour of a plane strain condition, whereas the arrangement of the present experimental models clearly presents an axial symmetrical situation. It is therefore necessary to explore the difference between these two cases in order to see whether it will have a significant influence on the true

failure mechanism. However, a factor, A, is defined by the Author to take the influence of axial symmetry system on this plane strain based approach into consideration as indicated in Fig 4.61.

4.3.4 Discussion on the load bearing behaviour of an axial symmetry system.

Cox (1962) compared the deformation characteristic of a infinite heavy mass of cohesive frictional soil under a circular footing (axial symmetrical) with that under a strip footing with infinite length (plane strain) through a plastic analysis. The calculated networks of planes of mobilisation of maximum friction (characteristics) (Fig. 4.62) indicate that the width of the influenced zone in axial symmetry (Fig. 4.62a), represented by the ratio OB/OA, is less than that in plane strain (Fig. 4.62b) for the same footing width. Cox also suggested that the ratio OB/OA is affected by the frictional angle, ϕ , and the weight of the soil. The weight of the soil is represented by a parameter, G:

$$G = \frac{\rho \cdot g \cdot R}{c^*} \quad (4.6)$$

where: ρ the bulk density of the soil
 g Acceleration due to gravity (9.8 m/sec²)
 R the radius (half of the width) of the footing
 c^* the relative cohesion of the soil ($c^* = c + p_a \tan \phi$)
 c cohesion of the soil
 p_a the atmospheric pressure

In order to quantitatively estimate the departure of failure mechanism proposed in Fig. 4.55 from axially symmetric reality, the Author defines an influence parameter N as the ratio of the value OB/OA in plane strain to that in axial symmetry.

$$N = \frac{(OB/OA)_{plane \cdot strain}}{(OB/OA)_{axial \cdot symmetry}} \quad (4.7)$$

Fig. 4.63 shows N plotted as a function of ϕ , and shows that the N value increases with ϕ . Assuming $\phi = 23^\circ$ for kaolin clay (Al-Tabbaa, 1987) and $c = 10-12$ kPa, the G value in the present model lies between 5 to 7. Section 4.3.3 suggested using an

average frictional angle, ϕ_{comp} , to calculate the load bearing capacity of the composite foundation:

$$\phi_{\text{comp}} = 2 \beta_{\text{cri}} - 90 \quad (4.8)$$

This ϕ_{comp} value may be used in Fig. 4.63 as the value of ϕ . According to the measured angle of shear plane from column casts listed in Table 4.1, the ϕ_{comp} value is likely to be between 35° to 50° in the composite ground of the present study. Therefore, the axis symmetry influence parameter, N , would likely lie between 1.25 to 1.5. This figure should be seen only as a very rough guide for the analysis of the model situation.

On the other hand, a same experimental observation which can be compared with the deformations produced in the present model tests can be obtained from study of cone penetration tests in purely cohesive soil performed by Houlsby (1981). Based on the calculated displacement fields (Fig. 4.64a), he constructed a network of stress characteristic for cone penetration in a cohesive clay bed (Fig. 4.64b). If this is compared with the wedge failure surface defined in Fig. 4.55, the deduced character of the behaviour in the cone test might be seen as an indication that: the slope of the failure zone in Zone II and IV proposed in Fig. 4.55a should be steeper than that formed under plane strain conditions, and the influence region due to circular footing loading on stone column reinforced ground may be less wide than in a plain clay bed. There will be a difference in the compressibility of a steel cone in a cone penetration test and the fictitious quasi rigid cone of clay and columns under the footings in the present models, and it is difficult to apply the analysis quantitatively from one to the other. However, it is at least clear that the slope of the failure mechanism ABC defined in Fig. 4.55a should be considered to be steeper as a function of angle of friction because of the axial symmetry in the present models.

4.4 Summary

An attempt has been made to give a comprehensive presentation of the measurements and their interpretation. The basic findings for a reinforced clay/column composite system under a rigid footing could be summarised as follows:

- The reinforced ground initially undergoes elastic deformation with a higher stiffness than unreinforced sample. As load progresses, further deformation is elasto-plastic and the overall stiffness become smaller.
- The group of columns behaves differently from a single isolated column: the interaction between column and clay and between column and column tend to improve the load bearing capacity more efficiently and transfer the loading action deeper.
- The area replacement ratio is an extremely important parameter controlling the level of the improvement. Lower area ratios around 10% only improve the composite ground slightly. A significant increase of load bearing capacity require a ratio of over 24% and, beyond that, the effectiveness of the improvement rises rapidly.
- Short columns suffer local end bearing failure at their base and consequently become effective in improving bearing capacity. There is a finite effective length of columns which is dominated by the footing size.
- The clay participates in carrying the load in the composite ground; the high stiffness of the column material is much more apparent when a close spacing is chosen. The loading stress share between columns and clay (stress concentration ratio) at the surface of the ground is not constant: it generally increases as the load increase with most significantly increase in the samples having larger area replacement ratio.
- Installing the columns by displacement method strengthen the soft clay and contributes substantially to the overall effectiveness of the reinforcement.

4.5 Results from flexible loading test

4.5.1 The measurements

The load-time-displacement relationships of both tests are plotted in Fig. 4.65. The loading rate is crucial to the overall load bearing capacity and the stability of the foundation. A slow rate allows the ground to become much stiffer at higher loading level than under a fast load. Test TL01-2 (slow rate Fig. 4.65b) settled only about half as much as test TL01-1 (fast rate, Fig. 4.65a) for a load of 120 kPa. Such sensitivity of the stiffness to the loading rate is presumably related to the degree of consolidation in the clay. The slow loading rate leaves the sample a longer time for primary consolidation and increase of the strength in the clay around the columns. In general, the stiffer the clays are, the larger the lateral confinement they can provide to the columns and the more load can be taken by the columns.

From the finished surface of test TL01-2, it was found that clay and sand columns settled about the same amount. Similar observations were also made in the field (Vautrain 1977). The development of stress in both clay and sand column can be seen in Fig. 4.66 where they are normalised by the total applied pressure. The slope of the curve tends to flatten as the load is increased, and a relatively steady condition occurs when load reaches about 120 kPa and a large surface settlement develops (refer to Fig. 4.65a). This appears that initially, the stiffness of the ground increases rapidly as the result of the rapid primary consolidation so that the ground behaves more like an elastic material. Under higher loads, both elastic and plastic deformations occur. But with a high rate of loading, the degree of drainage that can occur tends to reduce. Eventually, a complete undrained failure occurred in test TL01-1 with rather too rapid loading.

Regarding the stress share between column and clay, Fig. 4.67 shows that the average value of stress concentration ratio in the central region, n , is between 1.8 to 2.5, and is very sensitive to the loading level. The n value tends to drop as load progresses, even under unloading condition Fig. 4.67b. The rate of loading does not affect on the stress concentration ratio as much as on the total capacity. Stress development in both clay and column is simultaneous and intimately dependant on each other.

Similar to the rigid footing, the surface of adjacent ground is generally dragged down by the action in the centre, so that overall deformation is certainly not constant

volume (as assumed in many settlement analysis methods, refer to Chapter 1). The total volume change, V_{surf} , vs time, Fig. 4.68 shows that fast loading produce a much greater volume increase, with eventual total failure, whereas the slow loading shown a more gentle response at the same loading level.

No pore pressure measurement was taken in the tests. However, the surface settlement records made outside the loading area in the fast loading test TL01-1 suggest a profile of dissipation of the excess pore pressure as shown in Fig. 4.69a. The load increment instantly leads to a heave in the adjacent ground surface, and this heave fall as consolidation occurs. The rate of descent is more rapid than the settlement under the load. The sudden load increase is transferred to the region adjacent to the action area through the saturated clay indicating an undrained response. The consolidation in the region under the footing also affects the area outside the footing so that the ground settles as the clay behaviour becomes more "drained" overall although drainage paths in the unreinforced region may not actually allow total drainage. These effect of central drainage beyond the footing are limited, and only observed under fast loading. The effect is less evident in the slow loading test TL01-2. (Fig. 4.69b), implying that the slow rate has much less affect outside the loaded area.

4.5.2 Discussion of the failure mechanisms

Insufficient flexible loading tests have been performed to obtain much information from the exhumed column casts. The fast loading test (TL01-1) caused a catastrophic failure when the load was raised from 120 to 140 kPa, and only limited deformation remained below the failure surface (plate 4.9a). On the other hand, the slow loading test (TL01-2) did not cause noticeable deformation in the columns (plate 4.9b) after load was reduced from maximum 120 kPa to 30 kPa.

The settlement measurements indicate that the development of the deformation around the loaded area is not symmetric (refer to Fig. 4.65). The impression from plate 4.9a is that the failure might have occurred first from the edge of the footing where columns are less restrained by the surroundings. Columns under the footing generally bulged at depth and the shear plane with maximum deformation is located at a depth of approximately $5d$ (column diameter). The central column obtained most lateral confinement and its bulging occurred at a greater depth as seen under the rigid footing (although perhaps less obvious in flexible loading tests). Although

no information concerning the deformation pattern immediately beneath the footing is available, it is likely that the interaction between column/clay and column/column would provide sufficient lateral confinement to the columns and prevents the bulging occurring. Fig. 4.70 suggests an interpreted mechanism of failure.

By comparison with the deformation patterns seen under the rigid footings, the shear surface direction revealed in the casts of TL01-1 showed a rather random mode, especially for columns at mid-radius. It might be suggested that for a large loaded area, the columns in the central part would behave in a rather similar way in terms of the stresses and deformation (such as bulging) with similar stresses in both axial and radial directions. Columns near or under the edge of the loading zone would experience a very different stress state since the group effect would be much less, which is why the columns central axis tends to spread outwards radically more significantly than circumferentially. Naturally, the function of the columns outside the loaded area tends to prevent such an instability, which will benefit the overall settlement performance of the loaded ground.

This discussion is intended to suggest a concept for dealing with the problems of a larger uniformly loaded ground reinforced by stone columns. Design should divide the whole ground into several zones in which there are different general stress-strain characteristics. More details about this concept are presented in Chapter 6 where case histories are reviewed.

Chapter 5

Discussion of results of model tests compared with published numerical results

5.1 Introduction

Chapter 1 has briefly outlined the various numerical approaches developed for estimating the capacity and settlement of stone column reinforced foundations, and these methods can be categorised into two types:

1. The unit cell method in which only a typical column and its tributary clay in the foundation is analysed.(Balaam 1978, Balaam & Booker 1983, Barksdale and Bachus 1984),
2. The homogenisation method in which the mechanical properties of the column material are smeared into the reinforced soil to simplify the analysis (Mitchell & Huber 1985, Schweiger and Pander 1988, 1989).

The present physical model study has been carried out in collaboration with a series of finite element analyses at Swansea University in which the clay/column system was treated as a mixed composite ground (Pande et al 1994). The major geometric parameters and the material mechanical properties used in both physical and numerical model are compatible. In this Chapter, this numerical method is evaluated by comparing the numerical results with these obtained from the physical model tests. Because the individual columns are not present in the homogenised FE mesh, certain features studied in the physical model can only be compared indirectly, particularly aspects concerning the localised deformations of individual columns and the mechanisms of failure.

The unit cell method applies the single column solution to problems like bearing capacity of a soft clay bed reinforced by a small or large group of columns under a

rigid footing load, and the settlement calculation of a large area reinforced by stone columns (Balaam 1978, Barksdale & Bachus 1984). These results are critically reviewed in this Chapter in association with the findings from the present model tests.

In addition, other published numerical results used in Japan for soft ground treated with large diameter sand compaction piles are reviewed in relation to stone column foundations, and some of these numerical results are used to interpret the experimental findings further. The discussion is extended to the behaviour of a stone column reinforced foundation under a flexible loading for which only limited tests were performed in the present study.

5.2 The load displacement relationship under a rigid footing load.

5.2.1 The load bearing characteristics

A typical load-displacement curve obtained from the Swansea mixture theory analysis (Pande 1994) is compared with the result obtained from physical model test TS10 in Fig. 5.1. The numerical analysis appears to over predict the total bearing capacity by approximately 20%. The stiffness of the reinforced ground is also overestimated by an even large proportion. In addition, the numerical load-displacement relationship shows that the composite ground tends to behave elastically all the way through the loading until it reaches a clear collapsing point, followed by a generally softening pattern and progressive plastic deformation. The non-linear stress-dependent hardening behaviour observed in all the physical model tests is not shown in the numerical solution in spite of the fact that the analysis has assumed that both clay and column material behave elasto-plastically with different yielding criterion, namely, Mohr-Coulomb criterion for sand and Modified Cam clay model for the clay. Lee & Pande (1994) explained that the softening behaviour after peak load and progressive plastic yielding afterwards is due to the stress path which generate tensile stresses beneath the periphery of the footing. The stress states in this region reached the dry side of the critical state line of the modified Cam clay model used to describe the clay. The results are also influenced by the non-associated flow rule of the Mohr-Coulomb yield criterion used for modelling the column material. Also, Pande and Pietruszczak (1986) have pointed out that it is a general known feature that numerical analysis adopting the Cam clay models for describing the soft clay tends to overpredict the stiffness of the soil.

From the Author's point of view, this unrealistic load-settlement behaviour presented by the numerical analysis may well be caused by the disadvantage of the mixture theory which is probably incapable of simulating the correct consolidation process for the clay constituent of the composite, particularly in the radial direction because the "equivalent composite material" does not specify a drainage path and of course, no direction of the flow either. In fact, such a homogenisation technique is very much dependent upon the pre-defined stress-strain response of the composite material (Lee & Pande 1994). The reality is likely to be far more complicated than the assumed model: during shearing the clay compresses and sand expands, the composite response will be complex.

Balaam (1978) proposed a linear elastic analysis for the calculation of the bearing capacity of a rigid footing resting on a small group of stone columns on the basis of the unit cell concept. He introduced interaction factors, α_f , to estimate the average load in a column in the group, S_g , so that the estimation of the load and settlement of the group of columns could be computed by multiplying S_g by the total number of the columns in the group (Fig 5.2). This is a typical method based on the performance of single columns. The α_f values were computed from an elastic analysis of interaction of two identical piles (Poulos, 1968). The contrast between the behaviour of essentially rigid piles and the extremely deformable behaviour of stone columns, where bulging and volume change of the column material will be significant, is large. It is not really to be expected that such an analysis would provide a realistic estimation for the load carrying capacity of a group of stone columns. In fact, comparison was made between the results obtained from this analysis and results obtained in a model test conducted by Balaam (1978) himself (Fig 5.3), which shows a very different behaviour. It seems that unit cell based analysis should not be applied to cases where boundary conditions cannot be ignored, columns in a group for instance, where the response will be likely different according to the location of the column in the group.

However, having criticised the accuracy of predicting the load-displacement relationship for the stone column reinforced foundation under a rigid footing, it is important to note that numerical analysis has its advantage in providing a comprehensive approximation to complicated problems so that information can be obtained which other methods are unable to offer. Some of these possibilities are further reviewed in the following sections.

5.2.2 The effect of parametric variations

The model study has revealed the influence of various parameters like area replacement ratio and column length on the effectiveness of the stone column improvement (section 4.2.2). Numerical analysis can estimate such effect in a rigorous mathematical manner.

5.2.2.1 Effect of area replacement ratio (A_s)

Swansea homogenised analysis suggests that the capacity of the reinforced ground would increase by about 20% with a relative area replacement ratio of 10%. The higher area ratio of 24% tends to be the upper limit of the reinforcement beyond which, the column installation in the ground tends to be much less effective in terms of bearing capacity increase (Fig 5.4b). This pattern does not agree with the observations in the model tests where significant improvement was only seen for area ratios above 25%: low area ratios such as 10% produce only a modest increase in the ground load capacity (Fig 5.4a). The precise reason for such discrepancy between numerical analysis and physical model in this respect is not clear, yet it is beyond the scope of this dissertation. However, information deduced from column casts in the physical model have determined that for samples having low area ratio of 10%, the clay in fact is only partly drained, whereas the degree of consolidation of the clay increases rapidly with the increase of the area replacement ratio (refer to Fig 4.59). Therefore, a homogenised analysis used using fully drained material properties for both clay and column material will inevitably make not be able to distinguish between the actual drainage condition.

Now look at the results obtained from unit cell analysis. The results of both elastic (Balaam & Booker 1981) and elastic-plastic (Balaam & Booker 1984) analyses have indicated that the stiffness of the unit cell (reinforced ground) could be increased significantly by increasing the size of the column simultaneously in horizontal (diameter/area replacement ratio) and vertical (length) directions, and a significant reduction of the settlement of the unit cell under a uniform load could only be achieved when the equivalent area replacement ratio reached about 25%. By superimposing the data from present model tests on the curves of settlement reduction versus area replacement ratio presented by Balaam's elastic unit cell analysis, Fig 5.5 shows that the agreement between the results from analysis, unit cell tests and group tests is reasonably good.

A disadvantage of Balaam's unit cell model is the assumption of a rigid boundary (refer to Fig. 1.10), which would be likely to provide extra lateral confinement so that the load bearing or settlement deduction due to the column inclusion could be over estimated by such analysis. A modification was made in another unit cell model developed in Georgia Tech (Barksdale and Bachus 1984), where a compressible "wall" is placed in the boundary of the unit cell (refer to Fig 1.13). The stiffness of this boundary is rather significant to the results of the analysis as shown in Fig 5.6, particularly for very compressible soft soil. To determine the effect of the area replacement ratio on the improvement level by this analysis, Fig. 5.7a shows load-displacement curves for different value of area ratio (data deduced from the design charts Fig 29-37, Barksdale and Bachus 1984). It is clear in Fig. 5.7a that for a very compressible soft boundary, a column with relatively less lateral confinement, the increase of the stiffness is almost proportional to the increase of the area ratio, whereas for a more incompressible boundary, or a rigid boundary, the overall stiffness of the unit cell increases rapidly in the A_s range of 25% to 35%, especially at high stress levels. This result agrees well with Balaam's curve (Fig 5.5). In comparison with the curves showing the effect of area ratio on load bearing obtained from present model tests (Fig 4.4), it is therefore concluded that the area replacement ratio is indeed an important parameter controlling the overall effectiveness of the reinforcement.

Another aspect analysed by the unit cell model of Barksdale & Bachus is the effect of the compressibility of the virgin ground on the improvement level due to stone columns. Fig 5.7b shows that the rate of improvement is much greater for a highly compressible soft ground compared with a stiffer ground when the area replacement ratio increases. This numerical observation confirms a fact which has also been seen in the physical model tests that the initial stiffness of the ground is vital to the efficiency of the column reinforcement (refer to Fig 4.2), because the lateral confinement provided by the surrounding soil is critical to the load bearing of the column (Burland 1974).

5.2.2.2 Effect of the column length

Results from Swansea homogenised analyses

The effect of varying column length can be presented in two forms in a dimensionless analysis, the ratio to the column diameter L/d and the ratio to footing width (diameter) L/D . The influence of these two ratio on the load-settlement

relationship is different. Model tests have determined that for a rigid footing problem, the L/D ratio tends to be more significant for the overall load bearing behaviour of the foundation (section 4.3.2).

For columns with L/d ratio less than 9, model tests have shown some difference in the load-settlement curves (refer to Fig 4.6) and once the L/d ratio is beyond 10, this influence becomes less significant (refer to Fig 4.7). Considering the homogenisation technique, it is understandable that the L/d ratio virtually does not exist in the analysis since the columns are not present individually. Hence the effect of L/d seen in Fig 4.6 is not shown in the mixture analysis (Fig 5.8). This is because the overall controlling parameters for this analysis, the L/D ratio and the area replacement ratio, A_s , are identical in both samples TS05 and TS10. The unique features of the mixture theory do not stop the analysis from providing useful guidelines in this respect. The corresponding stresses and deformation information obtained from this mixture analysis are important for a better understanding of the problems. More discussion is included in Section 5. 2.3.

The Swansea mixture analysis found that higher value of the vertical stress are concentrated near the footing edge, and the vertical stress distributed in the central region of the footing is relatively low. Analysis was performed to examine the effect on the load-settlement behaviour when the length of central column is reduced. The result appears to show that this reduction in column length is beneficial to the overall load bearing behaviour of the composite foundation (Fig 5.9a): the general amount of softening after the peak load seen in the constant length model was eliminated. Also, the overall load capacity was not affected by the length reduction in the central column. Therefore, a proposal was made based on this numerical observation that foundations could be designed with shorter central columns in order to reduce the cost of stone column reinforced foundations (Pande 1994).

The contact stresses measured in the model tests do indeed show that the central column tends to take less load than those near the edge (refer to Fig 4.28). To validate the length reduction proposal made by the numerical team, a model test, TS19, was specifically conducted in which the central column was completely omitted. The comparison result is presented in Fig 5.9b, which shows that the total bearing capacity does not seem to be much affected by such omission, but the stiffness of the composite ground is noticeably reduced by about 15%. In the light of this experimental comparison, it is therefore believed that the numerical prediction is somewhat unrealistic. The exact reason for this is yet not determined. However,

given the general disagreement in the load-settlement behaviour discussed in section 5.2.1, it is likely that such numerical observation was simply from the individual soil models on which this homogenised material is constructed. The reduction of the central column length, in a medium size group of columns like the model arrangement, would be unlikely to make any significant difference to the construction costs in practice. Even with a large reinforced area where central column in the model tests should be seen as a group of columns in the central region, the reduction of the length of those columns appears to be unrealistic in terms of construction practice.

Results from unit cell analyses

The length effect studied by unit cell analysis is mainly shown in terms of settlement reduction, and this is another extreme where only the ratio of L/d is considered. It is generally recognised by the unit cell analysis that the settlement reduction increases rapidly with the increase of L/d ratio, and the length increase tends to be more effective for the settlement reduction when the area replacement ratio is higher (Figs 5.10 a & b).

Balaam's elastic analysis (1978) has covered the ratio of column length to column diameter up to 70, which corresponds to an extremely long column in the field. However, Balaam found the most sensitive length ratio L/d is in the range 5 to 20.

The results from the unit cell analysis of Barksdale and Bachus with a rigid boundary show that effect of increase L/d ratio on the settlement reduction is more significant in ground having higher initial stiffness, particularly for the modular ratio E_s/E_c range of 10 to 20 (Fig. 5.10b). Analysis of a highly compressive soil considered a soft boundary being placed in the unit cell. The curves in Fig 5.11 are deduced from the load-settlement curves proposed by the FE analysis for the soft cohesive soil (Barksdale & Bachus 1983 Figs 29-37), and show that the effect of the boundary stiffness is very noticeable for low area replacement ratio. This implies that the lateral deformation is influenced by the area ratio. Section 4.3.2.3 has noted that the consequence of increase of area ratio would be to direct the loading action inwards to the loaded area, in other words, to allow less horizontal deformation.

Notice the analysis of Barksdale and Bachus is carried out under the assumption that the columns are end bearing by a firm layer. It can be seen from Balaam's elastic analysis (Fig 5.10a), that such assumption tends to predict higher value of the

settlement reduction caused by stone columns. On the other hand, no information concerning the vertical stress distribution with depth of the column is provided in either of the unit cell analyses. The model tests have shown a tendency for the loading stress not to be fully transferred to a great depth. Unless the distribution of loading stress with depth is revealed, the effect of the column length can not be fully understood. In following sections, the stresses and deformation characteristics drawn from other relevant FE analyses are presented.

5.3 Stress and deformation characteristics in a composite ground

5.3.1 Stresses and deformations under a rigid footing

Finite element method uniquely offers the possibility to analyse the details of stresses and deformations within a stone column foundation. Fig 5.12 and 5.13 are typical results obtained from the analyses performed at Swansea using the homogenised method for the model tests TS05 and TS07 (Lee and Pande 1994). In terms of the average stress, Figs 5.12b & 5.13b show a significant concentration of vertical stress around the periphery of the footing, and relatively small magnitude of loads in the central region under the footing. The deformation pattern of the ground appears to be quite similar to that observed in the model tests, with the footing punching into the ground (Figs 5.12a & 5.13a).

For the model tests with short columns (TS05), the numerical result shows that significant vertical stresses are transmitted to the bottom of the columns (Fig 5.12d), which partly explains the phenomenon of column penetration observed in the physical model, whereas model with long columns (TS07), the stress transferred to the bottom of the column appears to be relatively small (Fig 5.13d). Quantitative plots for the column beneath the centre of the footing show that both vertical and radial stress (Fig 5.14) drop rapidly at the depth of $13.5d$ (column diameter), which is $1.5D$ (footing diameter). This explains why the lower ends of the columns hardly move as deduced from the casts of the model column (refer to sections 4.3.2.2 & 3). These numerical results further confirm the speculation made in section 4.3.3 that there is an effective length for the column beyond which the extra length of the column is no longer beneficial in contributing to the load bearing, but of course may still be useful for settlement reduction. As an engineering approximation, such effective length can be roughly estimated to be in the range of $1.5-2D$ (D : footing diameter) for a rigid footing foundation.

The lateral plastic strain plots show a similar pattern of yielding in the columns to that observed from the column casts (refer to section 4.3.2), the yielding beginning from the edge of the footing and propagating into the central region along a "wedge" (Figs 5.15a & 5.15b). The deformed mesh shows that lateral spreading increases from the centre outwards with the depth of maximum lateral displacement becoming deeper towards the centre of the footing (Fig 5.16a). A limiting equilibrium solution using a coupled effective stress/water pressure finite element analysis (Asaoka et al 1994) has produced the vectors for displacements in a soft ground reinforced by large diameter Sand Compaction Piles under a rigid footing (Fig 5.16b). All these numerical observations whether from an idealised homogeneous composite ground or from an idealised unit cell tend to support the wedge failure mechanisms proposed in Section 4.3.3.

All the unit cell based analyses have assumed that the state of the stresses in every column is axisymmetric as can be imposed in a triaxial apparatus (Priebe 1976, Balaam 1978, Barksdale & Bachus 1983, Goughnour 1979a). According to an elastic-perfectly plastic analyses, Balaam & Booker (1981) found that possible yielding in the clay will always be less than the yielding in the column assuming no shear stress at the column-soil interface, Balaam & Booker suggested that the clay will always behave elastically. Further, based on the results from analyses using the homogenised method, Lee and Pande(1994) noted that when load reaches a high level, the column will fail first. Both statements seems to have the same implication: the deformation is discontinuous between column and clay.

From the Author's point of view, this seems to be unconvincing. First, the triaxial stress state may only exist within a particular section of a column in a group (see section 4.3.3). If irrecoverable plastic deformation (bulging) occurs in the column, the clay in this region will be subjected to lateral compression and undergo the same amount of volume change in order to reach deformation equilibrium in this region, and this volume change will certainly not be recoverable (elastic). The direction of the major principal stress in the column-clay interface will be nearly horizontal, and the actual stress status in this interface will thus be extremely complex. It is difficult to believe that the shear stress in this interface could be ignored. On the other hand, the statement that the column fails first (while the clay still remains in non-failing equilibrium) may appear curious if a mixture theory was used to perform the analysis (Lee and Pande 1994). The failure of a column in the clay/column system cannot be considered to be independent of the surrounding clay because the load carrying ability of a column is always dependent on the amount of lateral support

provided by the surrounding clay. The nature of the problem concerns very complicated localised stress/deformation states and a rational approach needs to idealise this complex situation more realistically. The failure mechanisms proposed in section 4.3.3 suggest that the potential failure surface where the stresses reaches their critical state should be considered along a wedge surface through both clay and sand.

5.3.2 Stress concentration in a composite ground

The stiffness difference between soil and column material causes a stress redistribution, which is a stress concentration phenomenon. A rigid footing compels the soil and column to deform equally. For a foundation under a flexible footing, both the present model tests and full scale study (Vautrain 1977) have found that surface settlement in column and in-situ soil are also approximately the same. Therefore, in principal, the loading stress concentration in the composite ground should be proportional to the stiffness of the material, so that the stiffer column will always receive a larger proportion of the applied pressure than the surrounding soil. Such behaviour is clearly shown both in the numerical results (compare Figs 5.12 c & d; 5.13 c & d) and in the measurements taken with the miniature pressure transducers at the foundation surface in the physical model tests (refer to Fig 4.28).

Results from model tests have showed that the contact stress concentration ratios in the range of 1.0. to 5.0 (refer to Figs 4.33 & 4.34). Homogenised analyses (Lee & Pande 1994) indicate that the ratio of the average vertical stress in the column to that in the clay on the surface of the footing is of the order of 2.2 to 3. This stress ratio decreases by 20-40% with depth. Ishizaki's et al (1992) also found a generally decrease behaviour of the stress concentration ratio with depth (Fig 5.17a). However, Mitchell (1985) reported a homogenised non-linear analysis which estimates n values to be 2 to 3 for a specific soil type in Santa Barbara, and indicated that n value is approximately constant through the length of the column. To the Author's knowledge, published measurement data concerning the variation of stress concentration ratio down the column depth have been very limited. Aboshi (1979) reported measured results from a undrained model test showing that the stress concentration ratio appears to increase with depth (Fig 5.17b) with the difference between the n value on the surface and on the bottom of the column being about 50%. It phenomenon appears rather curious and yet difficult to explain. In practice, the stress concentration ratio, n , has often been assumed to stay constant with depth as a reasonable engineering solution (Mitchell 1981, Barksdale and Bachus 1983).

From the Author's intuitive point of view, the distribution of stress concentration ratio with the depth might be associated with the deformation profile of the column (as well as clay) along the depth. In the present model tests, measurements from miniature pressure transducers at surface of foundation have indicated that the rate of stress increase in a column is much greater than in clay. Therefore, it is possible that the stress concentration ratio in the region where column bulges would be higher than the region below. Also, as loading stress decreases with depth, the stress concentration ratio might also be affected in a similar way. However, it has to be admitted that there is not adequate information to support such speculation. Until a realistic analysis is performed to concentrate on this particular aspect, it is hard to justify or criticise the constant stress concentration ratio assumption in the design practice merely on the basis of measurements taken from the surface of the foundation.

Stress concentration ratio is affected by the major parameters of a stone column foundation such as area replacement ratio and length of the columns. The present model study has shown that the value of n increases significantly from area replacement ratio, A_s , raises from 10% to 24%, but as A_s increases further, the n value tends to sustain (Figs 4.33 & 4.34). Ishizaki et al (1989) also found a similar pattern in their triaxial tests (Fig. 5.18). These results lead one to expect that the degree of consolidation in the clay could be the key factor influencing the increase of the n value. For a low area ratio sample, the clay might be partly drained so that the strength developed in the clay would be less significant than that in a ground having a higher area ratio where clay could be treated as almost fully drained. However, once the area ratio reaches certain high value, 30% for instance, the extra strength increase between almost fully drained samples becomes less significant than that between drained and partly drained samples, and the stress concentration ratio tends to remain more or less constant.

Parameters such as the ratio of stiffness of column material and soil and the column length will also affect the distribution of the loading between column and surrounding soil. Barksdale and Bachus (1983) found a linear relationship between the Young's modulus ratio E_s/E_c and the stress concentration factor obtained from their non-linear unit cell FE analysis (Fig 5.19a), which indicates the important influence of the initial stiffness of the virgin ground on the stress redistribution in the stone column treated ground. Their analysis also shows that n value increases by about 30% when the ratio of column length to diameter, L/d , rises from 5 to 10, and an even higher increase in n value of 60% occurs when L/d is increased from 10 to 20

(Fig 5.19b). From the Author's point of view, such sensitivity of the stress concentration ratio to the increase of the column length might not be realistic in reality, and the assumption of end bearing of the column on a firm underlying layer in the unit cell analysis would tend to exaggerate the effect of the column length on the n value.

5.4 Settlement and consolidation

5.4.1 General consolidation analysis

Comparing to the behaviour of a conventional pile foundation, an important feature of the stone column foundation subjected to vertical loading is that the column will act like a sand drain to speed up the consolidation process in the surrounding soil. The strength and stiffness in the surrounding soils are thus increasing with the load, which consequently enhances their lateral confinement to the column. The shear vane and water content results obtained from the present model tests have indicated that the degree of the consolidation is affected by the column's area ratio, length, installation method and the loading level of the foundation (section 4.2.5). However, the consolidation progress was not fully determined in these tests due to the lack of reliable measurements of excess pore pressure within the foundation: numerical analysis results therefore provide useful guidelines.

Homogenised finite element analysis (Pande et al 1994) does not describe the consolidation process in the clay because the smearing technique leaves literally no possible for drainage in the composite (mixed) ground. A fully drained analysis approximates the situation by merely using the material drained properties regardless of other influential factors, which might not be able to give a rational solution to the problem, particularly in respect of ground settlement. Alternatively, the homogenised analysis could be performed on the basis of fully undrained clay response but this, which providing an extreme assumption, is nor likely to be realistic. Unit cell methods consider the consolidation nature of the stone column foundation more realistically.

Balaam (1978) has adopted both Biot's 3-dimensional consolidation theory and diffusion theory to calculate the settlement rate and average pore pressure dissipation in an idealised unit cell. He found the rate of the consolidation in the clay is increased dramatically by simultaneous reduction of the column spacing and increased column length (Fig 5.20) and a significant settlement reduction can only

be achieved when the area replacement ratio reaches about 25%. Adopting Biot's theory, Balaam's consolidation analysis results showed that the pore pressure flow mostly occurs in the radial direction, and vertical flow is relatively insignificant. Balaam also found that the degree of the consolidation in the clay is proportional to the degree of anisotropy of the consolidation characteristics of the clay.

Barksdale and Bachus (1984) proposed a finite element method by using modified Terzaghi 1-D consolidation theory to analyse both vertical and radial flow in a unit cell. The main assumption in this analysis are:

1. The soil is saturated with incompressible fluid
2. The mineral components (solids) are incompressible
3. Darcy's law is valid
4. The coefficient of permeability of the soil is a constant.
5. The coefficient of the compressibility of the soil is a constant for the applied load.
6. The void ratio e is a constant.
7. The drain is infinitely permeable and incompressible
8. Only vertical compression occurs (lateral flow of water takes place but on lateral strain)

Based on the behaviour observed in model tests, some of the assumptions made above are clearly unrealistic for stone column foundations. Assumptions 4 to 6 lead to a constant coefficient of consolidation in the analysis. In fact, the coefficient of consolidation is largely dependent on the stress level so that the accuracy of the analysis is virtually based on the simulations of the field stress condition in the analysis. Deformation under a constant volume (assumption 6) is obviously far beyond the reality. Finally, since lateral spreading has been observed in the model tests and in most of case records (some of which are presented in Chapter 6), the assumption of zero lateral deformation is again a problem for the unit cell analysis, which would likely lead to an underestimate of the settlement.

Nevertheless, in this analysis, the primary consolidation settlement problem for the stone column foundation was solved by considering the vertical and radial consolidation effects separately so that:

$$U=1-(1-U_z)(1-U_r) \quad (5.1)$$

Barksdale and Bachus also considered the continuing decrease in volume of the cohesive soil which would result in settlement occurring under a constant effective stress after the excess pore pressures caused by the initial loading have dissipated, in other words, the secondary consolidation settlement. The analysis was based on the observation that the relationship between secondary settlement and the logarithm of time can often be approximated by a straight line. In reality, Leonards (1962) has pointed out that secondary settlement does not always vary linearly with the logarithm of time. Secondary compression will also be complicated by factors other than simple 1-D consolidation settlement, which are beyond the scope of this dissertation. However, some field observations of long term settlement development under embankment loading are given in section 6.3.2.

The results of Barksdale and Bachus' analysis are presented in Fig 5.21, which shows that the vertical consolidation (Fig 5.21a) is much less significant than the consolidation in the radial direction (Fig 5.21b). Also, the area replacement ratio is extremely important to the degree of consolidation of the soil.

5.4.2 Foundation under a flexible loading

Data from flexible loading tests at the present model study has been very limited (see section 4.5). Because stone column reinforcement method has been widely used to improve soft ground under such loading condition, for instance, the embankment construction, it is thus useful to understand its basic mechanical behaviour. It is also author's belief that the findings from rigid footing tests at the present study will shed the light on behaviours of the foundation under flexible loading. Since no analysis was performed using homogenised method in Swansea, numerical results presented in this section are adopted from other relevant finite element analyses.

5.4.2.1 Stresses and deformations

Aboshi (1979) has presented results of a plane strain finite element study comparing the vertical stress distribution in a soft ground reinforced by sand compact piles with a homogenous soil (Fig 5.22). The same infinitely long, uniform strip loading was applied to each type of the soil. The unit cell concept of the stress concentration factor was applied to the analysis for the composite ground, whereas for the homogeneous soil, Boussinesq method was employed. The results show clearly the higher stress concentration in the column along the depth, which is the main cause of the increase of the stiffness of the reinforced ground.

The vertical stress contour in the clay indicates that the stress increase in the central region is in generally transferred deeper than in the region near the edge of the loading area. Although the stress information in the columns is not presented, considering the general stress concentration phenomenon, it is conceivable that the loading stresses in the columns could be compatible with these in the clay, in other words, the vertical stress contour in the clay would also reflect the distribution of vertical stresses in the columns: a generally deepening behaviour in the central column. This phenomenon could be seen as a indication that the column-column interaction (group effect) is transferring the loading into deeper layers. Similar behaviour was also deduced in the present model test from the shear deformation shapes of the columns (see section 4.5.1). The characteristic of the vertical stress distribution of this FE analysis provide supporting numerical evidence for the column group mechanisms proposed in section 4.4.2.

However, the similarities between the vertical stress distribution immediately outside the footing in the reinforced and unreinforced soils in Aboshi's plane strain analyses are curious (Fig. 5.22). Such a phenomenon is presumably caused by the assumption of zero horizontal displacement on the boundary of the unit cells. Asaoka (1994) has presented the results of a coupled soil-water finite element analysis applying limit equilibrium theory to the composite ground. The deformation mesh for the composite ground under embankment loading (Fig. 5.23) shows clearly that the horizontal displacement is significant at the failure stage, and the magnitude of such lateral spreading around the columns increases towards the edge of the embankment. More experimental evidence of lateral spreading of the stone column reinforced foundation will be presented in Chapter 6.

5.4.2.2 Consolidation under a flexible loading

Ishizaki (1992) has proposed a quasi three-dimensional FE method to analyse a larger area reinforced by sand compaction piles under a flexible loading. The analysis used a homogenisation technique to join individual unit cells described as "multi-link elements" in order to obtain a global view (Fig 5.24a) by taking both the stiffness of the pile and the drainage through the pile into consideration. Ishizaki found that the settlement ratio due to the consolidation is proportional to the area replacement ratio (Fig. 5.24b). The excess pore water pressure distribution contours obtained from this analysis show that most of the higher pore pressures are concentrated in the area beneath the load. Under the surface load, the excess pore pressure due to the load was found to dissipate rapidly in a short period of time,

especially for a ground having a high area replacement ratio. The measurements of adjacent surface vertical displacement in the Author's model tests TL01-1 & TL01-2 (Fig 4.69) show a similar pattern, which can be seen as an indication of the excess pore pressure dissipation profile under load. The numerical indication seems to be supported well by the experimental evidence. Such behaviour is caused by the important participation of the highly permeable column acting like drain in the clay to speed up the consolidation. As a consequence, the reinforced ground would likely develop its deformation more quickly than an unreinforced ground during the primary consolidation period. This lead to a speculation that the secondary deformation under a constant loading in a stone column reinforced ground would likely reach a relatively stable condition. Some field data and further discussions are presented in section 6.3.2.1.

As far as the influence of parametric variations such as area replacement ratio are concerned, section 5.4.1 has discussed the effect of length and area ratio on the clay consolidation. If the settlement is the most important in a design consideration, the effect of comprehensive parameter area ratio A_s may be considered separately in terms of the column diameter, d , and spacing between columns, S . Numerical analysis has indicated that the consolidation in the radial direction is very significant in a stone column foundation (Balaam 1978, Barksdale & Bachus 1983). By adopting the modified Terzaghi 1-D consolidation theory proposed by Barksdale & Bachus (1983), the consolidation time factor for radial drainage is given by:

$$T_r = \frac{C_v \cdot t}{(D_e)^2} \quad (5.2)$$

where: C_v is the coefficient of consolidation, and d_e is the equivalent diameter of the unit cell (for square pattern $D_e = 1.13S$, and for triangular pattern, $D_e = 1.05S$). Therefore, the degree of radial consolidation is essentially inversely proportional to the, S^2 . This analysis indicates that for a given reinforced area, stone columns with smaller diameter, d and closer spacing, S will be more effective for the settlement reduction than an improvement having same area ratio_s but with larger diameter, d and hence a larger spacing S . The concept here is similar as conventional sand drain theory. However, the difference between sand drain and stone columns is still rather distinguish , particularly in terms of load bearing behaviour.

5.4.3 The consolidation due to column installation

Shear vane investigations in the present model study have indicated that the displacement method of column installation results in a more significant increase of the strength of the clay in comparison with that obtained using the replacement method (section 4.2.5), which is presumably caused by the lateral compaction during the course of the column installation.

By applying the cylindrical cavity expansion using a velocity boundary condition, Asaoka (1994b) presented a rigid plastic deformation FE analysis for estimating the effect of undrained shear strength increase (set-up of the clay) in a soft ground due to the installation of a large diameter sand compaction pile in a soft soil, a displacement type of pile driving. In this analysis, the mechanical behaviour of the soil is assumed to follow the original Cam-clay model. The "set-up" behaviour was assumed to occur by plastic hardening which occurred in each finite element as a result of drainage.

The results of simulation of single sand pile driving obtained from Asaoka's limiting equilibrium undrained coupled soil-water analysis are presented in Fig 5.25, which show:

- 1 The spacing of the columns controls the amount of heave developed at the surface of the ground (Fig. 5.25a).
- 2 The size of the analysed region does not make significant difference to the profile of pore pressure distribution. The greatest degree of excess pore pressure dissipation occurs in the deeper layers of the ground (Fig. 5.25b).

The numerical finding 1 has been well demonstrated in the author's model tests TS15 & TS18 where columns were installed by using displacement method: large amount of surface heave was indeed observed in the model TS15 in which a close spacing of 31.5 mm ($d=17.5\text{mm}$, $A_s=24\%$, refer to plate 4.2), and much less heave was seen in TS18 where a large equivalent spacing of 30.5 mm ($d=11\text{mm}$, $A_s=10\%$) was used.

The numerical finding 2 indicate that consolidation occurred in the clay during the pile driving (column installation), and this will result in an extra increase on the clay strength. The extra improvement can not be achieved by the replacement method of

constructing columns. The undrained shear strength measurements obtained from vane tests in the present model tests also have clearly shown this effect (refer to Figs 4.43 & 4.44). The numerical analyses given a more quantitative picture of the benefit of the improvement when columns are installed by displacement method (Fig 5.25c). Note that all the numerical results were obtained for the case of driving a single pile; group pile driving would of course alter the profile to certain extent. It is likely that the group effect would results in an even significant improvement to the strength of the clay.

5.5 Summary

5.5.1 Evaluation of the Swansea homogenised analyses

By directly comparing the results obtained from physical model tests with those from the homogenised analyses performed by University College Swansea, it is clear that:

- homogenised analyses using mixture theory provides a simplified engineering solution to the complicated problem of the analysis of the behaviour of the stone column foundation, the basic concept of the homogenised analysis is particularly useful for the estimation of the ultimate load bearing capacity of a composite ground under a rigid footing load.
- The general profiles of stress and deformation s appear to be in reasonable agreement with the observations that can be made from the physical model tests. However, the present version of homogenisation technique tends to overestimate the effectiveness of the columns in improving stiffness and ultimate load bearing capacity by, say, at least 30%.
- The homogenised analysis combines stress: strain response of the two contrasting materials and has to treat them as either fully drained or fully undrained. Performed fully drained analyses neglect the progressive consolidation process which will occur in reality, which lead to a rather unrealistic prediction of the load bearing behaviour of the composite foundation under the rigid footing load and may also affect the results of variation of parameters such as area replacement ratio.

- The proposal made on the basis of the numerical analysis that the length of the central column should be reduced may not be a rational engineering solution in order to achieve the economic goal.

5.5.2 Further points drawn from various FE analyses

Both mixture analysis and unit cell method of finite element analysis have provided useful information which assists the development of a rational understanding of the behaviour of stone column foundations. The discussion presented in this Chapter can be summarised as followings:

- The area replacement ratio is an extremely important parameter governing the overall effectiveness of the reinforcement in terms of load bearing capacity and settlement reduction in a stone column reinforced foundation. It also affects the basic elements of the improvement such as the degree of consolidation degree of the clay and the distribution of load between soft clay and stiff columns, the stress concentration ratio.
- The column length is also a key parameter in the performance of the reinforced ground under the load. However, as the column length is increased beyond a certain point, the extra column length ceases to have any effect on the load bearing capacity.
- The improvement due to increase of area replacement ratio and increase of column length is interactive.
- The interaction between columns should not be ignored in a rational analysis.
- A constant stress concentration ratio through the depth of the composite ground is not yet been conclusively demonstrated from numerical analyses.
- The failure mechanisms proposed in section 4.3.3 have been further supported by the evidence of the numerical analyses. Therefore, it seems to be possible to calculate the ultimate load bearing capacity of the composite ground under a rigid footing load by adapting the standard limit equilibrium theory as an engineering approximation: calculation the mobilised shearing resistance along the edges of the footing soil whether the failure surface passes through clay or column.

Chapter 6

Discussions of model test results compared with published results from centrifuge and field tests

6.1 Introduction

So far, the interpretations of the present experimental study have drawn a general profile of the mechanical behaviour of a foundation reinforced with a group of stone columns under a rigid footing load. Section 2.3 has discussed the limitation that the modelling technique adopted in these experiments could not completely achieve full similarity of the mechanical properties and satisfaction of scaling laws between model and the prototype situation. Therefore, the discovery of the group affect from the model study needs to be further validated from full scale field tests and other model tests.

In Japan, the mechanical behaviour of soft ground reinforced with large diameter sand compaction piles has been extensively studied. The principles of stone columns and sand compaction piles are similar. In this Chapter, results from two centrifuge tests carried out in Japan are selected to compare with the findings drawn from the present single gravity model tests.

Chapter 1 has indicated that up to now, the available full scale studies of the group effect in stone column behaviour have been very limited, especially for the problem of a rigid footing supported by a group of stone columns that has been the subject of the present model study. In this Chapter, two published field cases, one under a semi-rigid loading and another under a flexible loading are reviewed and compared with the aspects of behaviour of groups of stone column that have been discovered in the present study.

6.2 Centrifuge test results

6.2.1 The test carried out at PHRI (Failure mechanisms)

A set of centrifuge tests was conducted at the Japanese Port & Harbour Research Institute (PHRI) to examine the load bearing behaviour of soft ground reinforced with large diameter sand compaction piles under a rigid footing load. The vertical loading test set up is showed in Fig 6.1a. The ground was modelled using kaolin clay and Toyoura sand was used for the model piles. The test described here was performed at a constant footing penetration rate of 17.5 mm/min under 50g condition (More details are given by Terashi et al 1991).

The Toyoura sand is a fine sand having d_{50} of 0.24 and d_{50}/d_{10} of 1.5. Referring to the D_{50} of 0.32 and d_{50}/d_{10} of 1.3 for the Loch Aline sand used in the Author's models, the materials used in both sets of model tests can be considered to be roughly similar. Furthermore, the general geometric parameters of the centrifuge model and of the Author's model TS17 are listed in Table 6.1, which shows that these two tests are rather closely comparable. As far as loading rate is considered, a relatively undrained situation might be expected in the centrifuge test, but it should be appreciated that in a centrifuge test at 50g, consolidation will occur 2500 times faster than in the corresponding prototype and 50 times faster than in a 1g model with the same dimensions. Even allowing for this more rapid consolidation, the equivalent penetration rate is almost 50 times faster in the centrifuge test than in the 1g model tests of the present study.

	A_s %	c_u kPa	d mm	D mm	L mm	L/D -	R_p mm/min	s_{max} mm
Centrifugal model (50g)	28	10	20	100	175	1.75	17.5	25
Physical model (1g, TS17)	24	14	11	100	160	1.6	0.061	30

Note: all the symbols are defined in table 2.1, except:

R_p : the footing penetration rate.

s_{max} : the maximum footing displacement

Table 6.1: The major geometric parameters in the centrifuge model test and in the Author's test TS17

For the convenience of further discussion, the displacement vectors for the deforming ground obtained from the centrifuge model, Fig 6.2a, are presented alongside the failure surface defined by the Author (Fig 6.2b). Also, typical photographs of deformed columns from conventional and centrifuge models are presented together in plate 6.1.

The symmetrical sliding wedge directly beneath the footing deduced from the centrifuge displacement vectors (Fig 6.2a) appears to be very similar to the wedge surface zone I and II defined by the Author in sections 4.3.3.1 & 2 (Fig 6.2b). The direction of the relatively larger displacement vectors in the region immediately beneath the footing is roughly vertical: this is the region penetrating with the footing as a more or less rigid wedge (corresponding to Zone I). The magnitude of the vertical movement below this region tends to decrease rapidly with depth within a second wedge (corresponding to Zone II). The directions of the displacements outside the sliding wedge Zone I and II are mainly horizontal, and the propagates to the ground surface with much smaller magnitudes of displacement. The author has proposed (section 4.3.3.4) the presence of a retaining zone (Zone III) and extension zone (Zone IV): these compared more or less with the observations from the centrifuge model through the movements in most of the region IV seems to be rather horizontal. Furthermore, the deformation patterns revealed in photographs of the columns from two models are basically similar (plate 6.1). Notice an rotating free ball joint was placed between the footing and the loading device in the centrifuge test (refer to Fig 6.1a) rather than the rigid joint used in the Author's test, and this allows the footing to tip over to one side as the failure develops.

In the centrifuge model, the bases of the columns are supported by a sand layer. Notice the column length to the footing diameter ratio, L/D , in the centrifuge model is 1.75, which corresponds to the long column group in Author's test. Fig 6.2a shows approximately zero movement in the lower 20% of the depth of the model, which implies that the loading stress distributed to this level has been relatively insignificant. The concept of the effective column length in terms of the load bearing and transfer suggested in Section 4.3.3.2 is thus further validated.

6.2.2 The test carried out in TIT (Width study)

The proposed failure mechanism suggests that the columns installed outside the footing area (in Zone III) would act like a retaining unit to provide some horizontal resistance, which would consequently be beneficial to the overall load bearing

improvement (refer to Fig 4.60). Such an effect can be seen in the normalised load-displacement relationship in Fig 6.3a where two otherwise identical tests TS05 and TS10 are compared.

At Tokyo Institute of Technology, a set of centrifuge tests was performed to examine the effect of the width of the area of stone columns (or sand compaction piles) outside the footing area on the performance of the reinforced soft ground. The arrangement of the centrifuge test is shown in Fig. 6.1b. The materials used are Kawasaki clay for the soft ground and Toyoura sand for the sand compaction piles. Displacement controlled tests were conducted with a footing penetration rate of 0.1 mm/min under 50g gravity condition (More details are given by Kimura et al, 1983).

The parameters whose effects were studied included three improvement widths, W , of 1B, 2B, 3B (where B is the footing width) and two area replacement ratios of 23% and 36%. The corresponding load-displacement curves shown in Figs 6.3 b & c indicate that the stiffness of the improved ground increases roughly in proportion to W for a medium area ratio sample (23%), whereas for sample having higher area ratio value of 36%, W equal to 2B appears to be the upper limit of the effectiveness beyond which, extra width of the column reinforced zone would no longer be beneficial. Referring to the displacement vectors obtained from the centrifuge tests (Fig 6.4), the following points can be made to support the proposals for failure mechanisms presented in section 4.3.3:

- The main function of the columns beyond the footing area mainly is to resist the lateral movement in the ground due to the footing penetration (the function of Zone III). The effectiveness width of the improvement is limited within the region affected by the loading.
- The increase of area replacement ratio causes the action of penetration of the footing to be contained, so that movements extend less far beyond but further below the footing, which consequently reduce the effectiveness of the extra column width outside the footing area on the overall performance of the reinforced ground subjected to vertical load.

The experimental evidences from centrifugal investigations have supported and can be explained by aspects of the mechanical behaviour of the stone column reinforced foundations drawn from the author's conventional single gravity model tests as presented in section 4.3.3. Although the tests were carried out under a rigid footing,

the principle mechanisms of group column behaviour are able to shed light on rational approach to more complex engineering problems. In the following section, some selected field case histories are reviewed.

6.3 Field case histories

6.3.1 Stone column reinforced foundation under a rigid footing load

As section 1.2.3 mentioned that up to now, field studies concerning a large area reinforced by a group or groups of stone columns under a rigid footing have been extremely rare. On the other hand, the set up of the model in the present study was not design to simulated a specific prototype. However, the group behaviour of the composite ground discovered at the present model study provides basic relationship in terms of stresses and deformation in a stone column reinforced foundation. In following sections, field measurement of stress concentration ratio is compared with that from model tests, also, a case study with close link to the model tests set up is reviewed.

6.3.1.1 Stress concentration

The ratio of the stress in the column to that in the clay, n , is often measured on the surface of a foundation, and the stress concentration phenomenon is observed in all the field studies (Mitchell 1981, Barksdale & Bachus 1983 and Greenwood 1991). Results from the Author's model tests have indicated that n value at the surface of the foundation is affected by the loading level and area replacement ratio. Field measurement of stress concentration ratio from Humber bridge field case (Greenwood 1991) is plotted together with the results measured from present model tests (TS21 & TS17, $A_S=24\%$) against the load in Fig 6.5. It is important to note that these field data are measured from top of a column in the centre of a large group columns with an area ratio estimated to be in the order of 20-26% (More details see Greenwood 1991), so that the results shown in Fig 6.5 are somewhat compatible. Fig 6.5 shows a good agreement between the result from the filed and from the present model: n value increases with the increase of the load in the range of 1.5 to 5. Greenwood (1995) suggested that the increase of the n value will reach a peak value and drop when the strain in the column reaches about 2%. The results measured from triaxial tests (refer to Fig 5.18) by Ishizaki et al (1989) indicates that the n value reaches the peak value when strain raises to about 5%. From the Author's point

of view, it is important to notice that the n value is dependent on the stress level, which in fact reflects the drainage degree in the clay (see section 4.2.4). But neither of these measurement or prediction reveals the true behaviour of the stress concentration phenomenon in a column because: the measurements showed in Fig 6.5 are obtained from the surface of the foundation, whereas the deformation in the depth of the column is quite different from that in the surface as revealed in the present model study. Some numerical analyses indicate that n value decreases with depth (refer to section 5.3.3), whereas measurements from laboratory model tests shown a rather contradicted behaviour: n increases with depth (Aboshi 1979). On the other hand, the result from triaxial tests only represents a particular section of column where the confining stress is constant along the depth, this may only be roughly referred to the region where column bulges. It is therefore to stress, again, that the stress concentration ratio is important aspects of the general behaviour of stone column reinforced foundation, the assumption of n to be constant everywhere in the foundation used in most of current design approaches may be too simplified to provide an rational solution.

6.3.1.2 Case history I: Hampton field testing

Goughnour and Bayuk (1979b) reported the results of a field test on soft clay reinforced with stone columns in Hampton, Virginia, USA. A group of stone columns (average diameter of 1.1 metre) was installed through 3.7 to 4.6 metres of very soft to soft silts and clay, and terminated in a layer of loose to medium dense sand at an average depth of 6.4 metres. Forty five columns were constructed by means of wet vibro-replacement method in a triangular pattern with an area replacement ratio of 36% (Fig 6.6a). Load was applied within 54 hours by placing 4 layers of concrete blocks on top of a 2 metre sand blanket. The instrumentation and test set-up is shown in Fig 6.6b. Long term observations lasted more than 85 days (More details are given by Goughnour and Bayuk 1979b).

The piezometer readings taken from the soil beneath the central loaded area at four different various depths are plotted in Fig 6.7 together with the prediction of the excess pore pressure dissipation profile produced by Goughnour and Bayuk using a unit cell analyses (Goughnour & Bayuk 1979a). The settlements measured at the centre and 4 corners of the test area are presented in Fig 6.9, which shows that the settlements measured at the centre of the loading area are about twice those measured at the corners throughout the loading period.

Although the intention was to simulate an embankment-like flexible loading, the concrete blocks were actually overlapped one on another for stability so that the force applied to the foundation surface was more like a semi-rigid loading. The total load of 115 kPa was applied within 54 hours and a central settlement of 79 mm was reported after this total load had been applied. The relatively fast loading rate might be expected to produce a nearly undrained settlement response in the ground. Field observation indicate that by then, bulging would have begun in the columns, although failure might not have been fully developed (see 6.3.2.1).

Section 5.4.2 has discussed the basic relationship between column geometry and the rate of radial consolidation, and equation 5.2 indicates that the dissipation of the excess pore pressure is a function of the coefficient of radial consolidation C_{vR} and the equivalent diameter of a unit cell, d_e . In this case, column spacing, S , is a constant so that the rate of pore pressure dissipation is essentially a function of actual diameter of the stone column, d . Then equation 5.2 can be expressed as:

$$T_r = \frac{C_{vr} \cdot t}{(Nd)^2} \quad (6.1)$$

where N is a constant.

Assuming that the formed columns have the same diameter before loading and that the proportion of vertical consolidation are the same for Piezometers 1, 2 and 3 (see Fig 6.6b), the rate of dissipation of the pore pressure generated by the surface load should be proportional to the value of C_{vR} of the soil layers, Soil No1 and No 2, and it may not be unreasonable to assume C_{vR} to be approximately equal to the quoted value of C_v . Therefore, if the columns did not bulge horizontally significantly, the fastest rate of pore pressure dissipation should have occurred in Soil No1 (Piezometer 1) where the C_v value is greatest (about 4 times higher than that in Soil No2, where Piezometers 2 & 3 are placed).

Fig 6.8 plots the pore pressure, U , measured from each piezometers (deduced from Fig 6.7), normalised by its maximum value, U_{max} , against time, which shows that the rate of pore pressure dissipation in Piezometer 1 is in fact about 3 times slower than that in Piezometers 2 & 3. It might be suggested that the bulging in the columns could be a major factor influencing the excess pore pressure dissipation shown in Fig 6.7. The degree of bulging in a column within a group is affected by the general mechanisms of the load bearing of the foundation, and the compressibility of surrounding soil.

Goughnour (1994) has assumed that a stone column in a group would always bulge near the top so that his predictions indicate that the most rapid dissipation of the excess pore pressure would occur in top layer Soil No1 (Fig 6.7a), which obviously is not the case (Fig 6.8).

For the sake of argument, the model test TS10 is selected to compare with this field case. The comparison of major parameters between these used in TS10 and in this case data is list in Table 6.1, which shows that a rough similarity exists in the column arrangement

Test	d (m)	D (m)	L (m)	As (%)	L/D	Note
TS10	0.0175	0.1	0.1	30	1	Square pattern, homogeneous clay with depth
Hampton case	1.1	6.3	7.4	36	1.2	Triangular pattern, several layer soils with depth

Table 6.1: The geometry of the column arrangements in test TS10 and the Hampton field test.

Note all piezometers were placed around the centre column (Fig 6.6b). The Author's model tests have demonstrated that the group effect would push the bulging of the centre column deeper into the ground. Superimposing the proposed failure mechanism defined in section 4.3.3 in the section of this field case, Fig 6.10 shows that the location of the Piezometer 1 is contained in Zone I where insignificant bulging is expected, and Piezometers 2, 3 and 4 are more or less contained in Zone II, which is the region where most significant bulging is expected both in the centre column and middle columns. The maximum increase in column diameter due to bulging in TS10 was found to be about 10%. According to expression (6.1), this would result in an increase of about 200% of rate of radial consolidation compared to zero bulging in a homogeneous soil layer (allowing for 2 bulged columns). This corresponds to a 150% of increase in the rate of excess pore pressure dissipation in the reading from Piezometers 2 & 3 compared to that from Piezometer 1 in Fig 6.7. Furthermore, the compression index, C_c , in Soil No 2 (Piezometers 2 & 3) was reported to be 1.04, which is about 3 times higher than that in the Soil No1 (Piezometers 1). It is expected that the column diameter increase due to bulging developed in Soil No2 would consequently be greater than that discovered in the Author's model TS10 and might be suggested as a factor contribution to the extra

150% increase in the rate of excess pore pressure dissipation shown in Fig 6.8. The relatively fast rate of dissipation observed in Piezometer 4 in Soil layer No 3 might be caused by the fast radial consolidation due to bulging in the column, and vertical consolidation due to the close distance to a much more permeable layer Soil No 4 ($C_v = 0.1 \text{ ft}^2/\text{day} = 0.009 \text{ m}^2/\text{day}$).

These arguments are only very qualitative because the field situation may be more complex. Factors like non-uniformity of the shapes of the formed columns with depth and uncertainties of precise location of the piezometers with respect to the actual column boundary will also influence the piezometer readings and the rate of dissipation.

Now look at the settlement readings. Although a 2 metre thick layer of sand blanket was placed between the concrete blocks and the foundation in this field test, the load would still probably be semi-rigid. A similar arrangement was used in Author's model tests (with a 3 mm layer sand blanket). The model studies have shown that the ratio of column length to the footing width, L/D , controls the load bearing behaviour of the stone column reinforced foundation. In this field test, the ratio L/D is about 1.1. The mechanism superimposed in Fig 6.10 suggests that for a such small L/D ratio, the column bottoms would be expected to penetrate into deeper layers as the footing is loaded, particularly the central column/columns for the floating columns used in the model test (as seen in the column cast of model TS10, plate 6.2). Despite the fact that the columns at Hampton were installed down to a loose to medium dense sand layer, the compression index of 0.1 in this layer would not entirely prevent the column from penetrating deeper as the load was increased.

The settlement measured from surface clearly indicates that the column (and clay) under the centre of the loaded area settled about twice as much as the columns in the corners (Fig 6.9). Notice the Fig 6.6a shows that the footing consists of several concrete blocks, as load applies, the ground surface in the central region can settle relatively independent from that in the corners, in other words, equal surface settlement condition in the model tests (refer to plate 6.2) is not applied to this field case. Therefore, the magnitude of the surface settlement may be contributed by the penetration occurred in the base of the columns (Fig 6.9).

It has to be admitted that the evidence from this field study is probably rather limited. However, the principles of the group behaviour discovered in the Author's model study have been reasonably validated, and the behaviour of the stone column

reinforced foundation can be explained by the mechanisms proposed in section 4.3.3.

6.3.2 Stone column reinforced foundation under an embankment loading.

The stone column reinforcement method has been used to reduce the settlement of soft ground under embankments. The limited information obtained from the few flexible loading tests conducted in present model study has been rather inconclusive. However, the mechanisms of deformation observed from the rigid footing tests may be able to shed some light on the general behaviour of foundations under flexible loading. In the following sections, the general behaviour of stone column reinforced foundation under embankment is discussed on the basis of findings from the present model study and other relevant published information. Also, a controversial case where stone columns was reckon to be of insignificant to the settlement control in East Brent (Mckenna et al 1976) is reviewed.

6.3.2.1 General deformation characteristics

It is generally observed behaviour that the construction of an embankment on soft clay results in lateral displacement in the ground, and the maximum horizontal displacement is likely to occur near the toe of the embankment (Bjerrum 1972, Holtz & Lindskog 1972 and Leroueil et al 1978). It has been found that the vertical settlement beneath the centre of the embankment can be linked with the lateral displacement near the edge, and typical deformation mechanisms are illustrated in Fig 6.11. The inclusion of the stone columns increases the overall stiffness of the ground in both the vertical and horizontal directions so that the deformation due to the embankment load is reduced. Such an effect was demonstrated in a field embankment trial carried out at the port of New Orleans in USA, from a project called "Jourdan Road Terminal". As Fig 6.12 shows, the lateral displacements caused by 1.5 m height of bank on the ground without stone columns (left side) were found to be greater than those caused by 3.5 m height of bank over the soil mass reinforced by stone columns (right side).

Fig 6.11 shows the maximum settlement δ_v^m (under the centre of the embankment) and the maximum horizontal displacement δ_h^m (under the toe). Tavenas et al (1979) found from many trial embankment that the ratio δ_h^m / δ_v^m had the typical value of about 0.18, 1 and 0.16 for the period of initial compression (Tavenas et al maintain that it is at least partially able to drain while the clay is initially over

consolidated), during the second phase of undrained compression (when the clay is partly or entirely normally consolidated) and during consolidation of the clay and dissipation of pore pressure after embankment construction period, respectively. For the stone column reinforced ground, the present model study has found that the stiffness increase of a stone column reinforced ground would hold the effect loading closely under the loaded area and not generate significant spreading of the load as would occur for an unreinforced ground (refer to Fig 4.63). Thus, the ratio δ_h^m/δ_v^m would be expected to be very low by comparison with a pure clay foundation: perhaps having a value of similar to that found for drained clay, namely around 0.18, throughout the embankment construction period. Due to the lack of field data at present, this is of course a somewhat speculative figure.

Almeida (1984) has performed a set of centrifuge tests on an model embankment partly founded by stone columns. The displacement vector obtained from one of his tests (Fig. 6.13) show that the lateral displacements are mainly located beneath the toe area of the embankment, the dominant direction of the displacements beneath the central section of the embankment is vertical, which is not surprise because of the symmetry nature. The column deformation shapes shown in the Author's flexible loading test (TL01-1) also indicate a similar pattern (refer to section 4.4.2). This evidence strongly suggests that the analysis of stone column foundation under a embankment-like flexible loading should give different consideration to the columns in the central region and to those near the edge. The unit cell concept generally assumes a rigid boundary to each cell, which seems to be only suitable for the settlement calculation under the central region of an embankment, whereas for the columns near the edge of the loading, horizontal displacement through the cells should not be ignored.

Tavenas et al (1979) have noted that during the period of an embankment construction, the initial stress-strain response in a clay foundation (unreinforced), which is often overconsolidated, can be treated as drained. At this stage, the lateral displacement is relatively small. Tavenas et al also pointed out that as a result of the initial consolidation, the clay would likely become partly or entirely normally consolidated and the foundation thus will subsequently experience an undrained deformation throughout the embankment construction period. Further deformations will occur at constant load after the completion of the embankment.

When a clay ground is reinforced by stone columns, the presence of the columns speeds up the consolidation in the clay throughout the construction period.

Therefore, under the embankment fill loading, the clays might quickly become nearly or completely normally consolidated, and the drained process in the clays would likely last longer than that in a unreinforced clay foundation. The development of the horizontal displacement and the link with vertical displacement could thus be expected to be more uniform throughout the embankment construction. Also, the fast consolidation process would likely cause the further development of deformations after the completion of embankment construction to reach a stable condition rather more quickly than in an unreinforced ground. In comparison with an unreinforced clay foundation, it is thus expected that the primary deformation which occurs in a stone column reinforced ground, during the embankment construction, would be a larger proportion of the overall long term deformation. Fig 6.14 plotted the data deduced from published long-term field measurements of lateral displacements under the edges of two embankments one built on top of a clay foundation, and one on stone column reinforced clay, which show that the lateral displacement developed during the embankment construction period is about 76% of overall (roughly) deformation in a stone column reinforced ground, whereas in unreinforced clay, the primary lateral displacement is only about 30% of overall long term deformation. It has to be admitted that the development of the deformation under an embankment loading is affected by various factors including loading rate, the soil properties and the geometry of the embankment. However, Fig 6.14 can still give a quantitative estimation of the effect of stone columns on the deformation behaviour of the ground under the embankment load.

6.3.2 .2 Case history II: East Brent Trial Embankment

Having a better background knowledge of the general behaviour of stone column reinforced ground under embankment loading, it is thus interesting to re-analyse a controversial case history.

Mckenna et al (1976) reported the performance of an embankment built on 27 metre of soft alluvium partly treated by stone columns at a site located at East Brent, Somerset, England. Using the Cementation wet vibro-displacement method, a group of columns (0.9 m in diameter and 11.3 m average) spaced at 2.45 m in a triangular pattern was installed at one end of the embankment. Three groups of instrumentation consisting of rod settlement gauges, piezometers and inductive settlement gauge were installed in left, central and right section of the trial embankment. The details of the site and construction layout are shown in Fig 6.15 (More details can be found in Mckenna et al 1976).

The settlement records made two days before the central section failed (Figs 6.16 a, b & c) show that the untreated end of the embankment settled considerably less than that with stone columns, and the untreated central section settled almost exactly the same amount as the stone column end. As a result, the engineers suggested that the stone columns were not performing satisfactorily. Mckenna et al postulated the reasons for that surprising poor performance to be: "smearing" at the column/clay interface blocked the drainage due to the remoulding of the clay in this region during column construction; the clay lost volume by squeezing into the column voids as it bulges.

Greenwood (1994) has long argued that the case was misinterpreted by Mckenna et al (1976). Greenwood (1976) provided piezometer measurements to prove that free drainage was taking place during the construction of the columns so that smearing affect could not have been significant. Greenwood (1976) also presented a magnified photograph taken from the excavated column/clay boundary, which shows only sand filled voids and no significant penetration of clay. An explanation for the poor column performance given by Greenwood (1991) was that the shear resistance (skin friction) between column and clay in the main peat layer has been demolished during the wet process, leading to the surface load being fully transferred to the toe of the columns so that columns act like a rigid pile penetrating into deeper layer. This hypothesis was supported by the profiles of the excess pore pressure measurement (Fig 6.16d). Using Hughes & Withers (1974) single column analysis (refer to section 1.2.3.3), Greenwood argued that the critical length over which the columns are effective in transferring load is about the same as the column length by taking an average undrained shear strength in the ground as 20 kPa. Therefore, Greenwood suggested that the poor performance of the stone columns in the East Brent trial embankment was caused by inadequate column length.

From the Author's point of view, Greenwood's rigid pile hypothesis might only partly explain the problem. Findings from Author's model tests certainly demonstrate the possibility of punching failure at the bottom of the columns for the short columns. The occurring of punching would certainly contribute to the ineffectiveness of the settlement control achieved using stone columns (refer to section 4.4.4). The performance of the stone columns in East Brent trial embankment might be, however, also affected by other factors.

First, the justification of ineffectiveness of the stone column was made by the Mckenna et al (1976) on the basis of the settlement measurements (Fig 6.16a) made

at various locations along the length of the embankment, namely, left-end, central (both unreinforced), and right end (partly reinforced). According to the site investigation report made by Mckenna (1968), 12 boreholes were sunk mainly in the region around the central section of the embankment for this particular job, and the general profile of the ground section shown in Fig. 6.15c was probably based on a previous site investigation near the embankment site (Loc. No.4765, Soil Mechanics) together with certain geological assumptions, particularly in the region on left side. After the failure of the central section, the slip surface was found immediately beneath the main peat layer, a depth shallower than that predicted by Mckenna (1968) by using a conventional total stress analysis, which indicated that the thickness of the main peat layer and the silty clay layer immediately below are likely to be most influential to the settlements. The marked settlement difference between the left and central sections (refer to Fig 6.16a) seems to suggest that the thicknesses of the peat and clay layers beneath the left end of the bank are less than in the central and right section. Such speculation is also supported by the pore pressure profiles (Fig 6.16d), which show that the depth of the maximum excess pore water pressure in the left end is about 3 to 4 meter less than in the centre and at the right end, giving evidence of the depth of the compressible layer or layers in that region. Therefore, the extent of the ineffectiveness of the stone columns under the right end of the bank deduced solely from the settlement observation might be a chance occurrence associated with unforeseen ground condition and insufficient information concerning the soft layer in the ground.

However, it cannot be suggested that stone columns were particularly significant in controlling settlements. The Author suggests that a further contribution factor may be founded in the geometrical arrangement of the stone column reinforcement in relation to the overall dimensions of the embankment. Notice that the stone columns were only installed in an area 30.5m x 40 m with a low area replacement ration of 12.5% symmetrically around the long axis of the embankment. The results of the present model tests have shown that under a rigid loading, the settlement of the loaded area is much influenced by the stiffness of the ground beyond the loading area (refer to section 4.3.3), and such influence was examined by Kimura et al (1983) by means of a set of centrifuge tests (section 6.6.2). Although the experimental evidences reported in this dissertation was observed under a rigid footing loading condition, it is the Author's intuitive belief that the deformation behaviour and mechanisms of deformation a ground loaded by an embankment fill would be rather similar as illustrated in Fig 6.17. In another words, this is to suggest that the effectiveness of the settlement reduction in a soft ground due to stone

column reinforced is influenced by the overall geometrical arrangement of the stone columns, and the reinforcement in the area near the toe of the embankment has an important influence on the settlement beneath the central region of the bank. Almeida (1984) has demonstrated such settlement behaviour by means of a set of centrifuge tests. By installing a group of granular columns of a low area replacement ratio of 10% beneath the embankment edge region only, Almeida found that the settlement in the central section (unreinforced) due to the embankment load is reduced by about 30% (Fig 6.18), the presence of the columns in the toe region of the bank results a much less significant of the horizontal displacement in this area (Fig 6.19b) than without the reinforcement (Fig 6.19a). It seems logical to assume that installing the columns only beneath the central region of the bank would not be completely helpful in reducing the lateral displacement near the toe of the embankment, and beyond. Consequently, following Tavenas et al (1979), the overall settlement beneath the central region would be unlikely to be reduced significantly.

Another plausible reason for the rather poor performance of the East Brent stone column trial might be the low area replacement ratio, namely 12.5%. Such a low area ratio would tend to result in a partly undrained condition in the ground (section 4.2.5). The discussion in Section 6.2.3.2 has suggested that the drainage conditions in a stone column reinforced ground would tend to lead to a faster rate of development of deformation than in an unreinforced ground both during the embankment construction period, and for the period after construction. The long term settlement observations made at the East Brent trial embankment (refer to Fig. 6.16a) show a rather identical settlement process in the reinforced and unreinforced sections, and it is thus conceivable that the area replacement ratio of 12.5% used in the stone column end did not significantly improve the drainage condition of the virgin ground.

Overall, the exact reasons for the poor performance of the East Brent trial embankment can still not be seen as completely understood because of the lack of site investigation information and other relevant measurements, however, the interpretation presented above might suggest some alternative possibilities.

6.4 Summary and conclusions

Findings from the present model study concerning the group behaviour of stone column foundations under a rigid footing load have been confirmed by results obtained from relevant centrifuge tests and field observations. Discussions of the general deformation behaviour of stone column foundations under an embankment-like flexible loading have provided further understanding. The significance of these discussions is to provide a understanding of some of the engineering problems related to stone column foundations, which can be summarised as follows.

6.4.1 Foundation under a rigid footing load

- The general character of the failure mechanisms presented in section 4.4 has been validated in both centrifuge tests and field tests.
- The effective column length is indeed controlled mainly by the size of the rigid footing.
- The extra provision of rows of columns or additional reinforcement outside the footing area plays an important role in the control of settlement. The effectiveness of the increasing extra width of reinforced area or provision of additional columns outside the loading area is reduced as the extent of unloaded reinforced area increases.
- The stress concentration phenomenon with greater load being taken by column than by the soft clay is valid in the field. However, the assumption of constant stress concentration ratio, n , with loading level and depth is questionable.

6.4.2 Foundation under an embankment-like flexible loading

- Stone column reinforcement is generally effective in the control of settlement of a soft ground under embankment-like flexible loading.
- A large proportion of the deformations in a stone column reinforced ground is developed during or shortly after the construction period.
- The lateral displacement in the ground is a significant factor to consider, particularly for the region near the edge of the loaded area. The unit cell concept

is only useful for the settlement prediction in the central region of a stone column reinforced foundations. It is important to distinguish the different mechanisms in the various region of the foundation; encouraging support for the regional design concept suggested in section 4.4.2 is provided by the field evidence.

- The general deformation behaviour needs to be studied further. However, the conventional strategy of column arrangement under an embankment might need to be modified with the provision of extra rows of columns outside the loaded area being considered as an important part of the design philosophy.

Chapter 7

Conclusions and Recommendations for future research

7.1 Conclusions

7.1.1 Foundation under a rigid footing load

The present investigation has revealed that the load bearing behaviour of a column within a group is different from that proposed for a single isolated column by Hughes and Withers (1974). The interactions between clay and column and between column and column are indeed important, and they should be considered in developing a realistic engineering approach. The mechanical behaviour of this complex clay/column system under a rigid footing load has been analysed based on a set of physical modelling tests. The "wedge" failure mechanism proposed in section 4.3 provides a basic guideline for a realistic analysis of the load bearing capacity of a stone column reinforced foundation subjected to a rigid footing load, and this proposal has been reasonably well supported by the evidence from various numerical analyses and other relevant experimental data.

Under a rigid footing load, the ground reinforced with stone columns initially behaves elastically, but as loading progresses, the composite ground develops irrecoverable plastic deformations. Vertical loading causes the columns to shorten vertically and consequently the columns expand horizontally at a certain depth, which is seen as bulging. The depth of the bulging in a column within the group is influenced by the lateral confinement from neighbouring columns. At the same time, the surrounding clay undergoes a rapid consolidation process because of the generally rather small lengths of drainage paths and there is a general increase in strength. The phenomenon of the surface stress concentrated being more on the columns than in the clay is clearly observed in all the model tests. The ratio of average contact stress in a column to that in its surrounding clay was measured in

the range of 0.5 to 5. Results from the present model tests and from triaxial tests (Ishizaki et al 1989) indicate that the strength increase in the clay would greatly enhance the stiffness of the composite column and clay.

The area replacement ratio, A_s , is an extremely important parameter controlling the overall performance of the stone column reinforced foundation. Significant improvement in the load bearing capacity requires a high value of area replacement ratio, generally over 25%. A low area replacement ratio, for instance 10%, would only improve the load bearing capacity slightly, however, the stiffness of the ground will still be enhanced. Balaam and Booker (1983) suggest that an A_s value of 4% is the lower boundary of settlement reduction in a stone column reinforced ground. As far as the group effect is concerned, increasing area replacement ratio will enable the composite ground to hold the loading action closer to the loaded area and transfer the load deeper (illustrated in Fig 4.60). The presence of stone columns in a soft clay ground will accelerate the speed of consolidation, and the degree of consolidation is directly related to the spacing of the columns, which is included in the parameter of area replacement ratio: for a given size of column, a low area ratio (larger spacing), 10% for instance, would likely result in a partly drained situation in the clay whilst in ground having a higher area ratio, a fully drained condition could be expected. The degree of consolidation also affects the degree of stress concentration: the stress concentration ratio, n (ratio of the stress in column to stress in clay), rises noticeably when the area replacement ratio is increased from 10% (clay partly drained) to 24% (clay fully drained). Once a fully drained situation is established in the clay, the further increase of A_s value, for example from 24% to 30%, might not influence the value of n any further.

In general, the overall stiffness of the reinforced ground rises with the increase of the length of columns. Unlike a single isolated column, the load bearing mechanism of a soft ground reinforced by a group of stone columns is significantly influenced by the size of the footing: if the length of the column is less than or equal to D (D : footing diameter), the base of the columns will transfer their load down to the deeper clay layers and develop end bearing failure, and such punching failure could occur simultaneously with the development of bulging in the columns. This penetration behaviour is related to the level of the vertical stress distributed to the column base. It is found that for columns having a length over $1.5D$, the penetration phenomenon at the column base is insignificant. If the columns are long and thin, the buckling failure may occur due to insufficient flexural rigidity of the columns. The observations made from the present model study and from other published

centrifuge results (Terashi et al 1991) suggest that there is an effective length beyond which the extra length of the column would no longer be beneficial to the bearing capacity of the composite ground, but still be useful to the settlement reduction. This effective length may be approximately estimated to be in the order of 1.5D to 2D.

Construction of columns using a displacement method produces an effect of lateral compaction to the surrounding clay and consequently generate additional stiffness in the clay. In-situ vane tests in the present study have demonstrated that the clay increases its strength as a result of the displacement method of column installation. With a suitable ground condition, installing columns using displacement method would result in a more effective improvement than using a replacement method. However, installing columns using a displacement method would cause heave on the ground surface. The magnitude of such heave is controlled by the spacing between the columns.

In a larger stone column reinforced area, installing columns beyond the loaded area would also be beneficial to the overall performance of the reinforced foundation. The effective width of this extra reinforcement region is inversely proportional to the area replacement ratio. This aspect is generally not recognised in field practice, and contractors tend to think that it may not be economically effective (Greenwood 1995). It is the Author's opinion that the effectiveness of extra reinforcement beyond the loaded area should be considered in relation to the overall failure mechanisms of the reinforced ground, and this has not yet been fully investigated. Based on the limited information from the present model study and from the failure mechanism proposed in section 4.3, the Author believes that it is possible that for supporting a large structure like an oil tank, installing columns in the region beyond the loaded area might be beneficial to the overall improvement, particularly in terms of settlement control.

7.1.2 Foundation under flexible loading

Only a limited number of tests under flexible loading have been performed in the present model study. However, it is believed that the findings from rigid footing tests can shed some light on the analysis of the behaviour of stone column reinforced foundations under flexible loading. In addition, information from published numerical analyses and other relevant experiments contributes to a basic understanding of the mechanisms of the foundation behaviour.

The group effect transferring the loading action deeper in the ground, which has been discovered from the rigid footing tests, might also be expected to apply to the case of flexible loading. Although it is difficult to define a clear failure mechanism due to limited available information, the motion of ground lateral spreading as a result of vertical loading (as illustrated in Fig 4.60) could be introduced into the stability analysis, particularly in the region near the edge of the loaded area. The horizontal displacement in this region is indeed so important that any settlement analysis adopting unit cell concept would likely misrepresent the true situation. Information from centrifuge tests (Almeida 1984) has confirmed that the principle displacement direction for the composite ground in the central region under the flexible embankment foundation is vertical, and that lateral deformations in the columns, as well as in the clay can be ignored. Thus, the rigid boundary assumption used in unit cell concept may be appropriate for the settlement analysis in this region only. The regional design concept mentioned in section 4.4.2 is valid and again should be used for a realistic engineering approach.

As far as parametric variation is concerned, it is believed that the area replacement ratio, A_s , and the ratio of column length to column diameter, L/d , significantly affect the degree of settlement reduction for the stone column reinforced ground. The effect of A_s and L/d on the improvement of stiffness are interactive. In order to achieve a substantial settlement reduction, a higher value of A_s of 20% or 30% might be required, and A_s equal to 4% tends to be the lowest boundary (Balaam 1984) in terms of settlement reduction. Values of the ratio L/d in the range of 5 to 20 are most effective (Balaam 1984, Barksdale & Bachus 1984). Again, the compaction force in the soil due to installation of columns using a displacement method would generally enhance the stiffness of the soil and result in a more substantial improvement than using a replacement method. It is also noticed that for a structure like an embankment, the arrangement of stone columns should follow the overall geometry of the loaded area, and perhaps even beyond. Local reinforcement would be likely to result in a less obvious improvement provided by the stone columns.

7.2 Recommendations for future research

The majority of studies concerning the behaviour of stone column reinforced foundations either by means of experimental testing or numerical analysis have been summarised in the Tables 7.1 and 7.2 respectively. It is clear that true group behaviour of stone column reinforced foundation has been studied for the first time

in this present research. Findings from the present study indicate that the group mechanism is indeed different from the response of a single column. The effects of various important design parameters on the performance of the reinforced foundation have also been discovered to a certain extent. It is the Author's firm belief that the present study has touched on, and presented a broad view of most of the sensitive aspects of the group behaviour for the stone column reinforced foundations. The findings from this study strongly challenge the existing analytical concepts and suggest that present design methods should be revolutionised. However, it has to be noted that the interaction between column and clay and between columns results in an extremely complex overall stress/strain relationship for the composite foundation. The scale of this study has been quite wide in terms of numbers of investigated factors, however, a rigorous solution to this complex reality requires the study to be extended to great depth. The findings from the present study can be used to provide initial suggestions for further work.

The failure mechanism proposed in section 4.3 has characterised a fundamental relationship between stresses and deformations in a stone column reinforced foundation subjected to a rigid footing load, and evidences in support of this mechanism have been found in other studies. There is clearly potential for further development of analysis based on this mechanism. The proposed failure mechanism has laid a foundation for calculation of load bearing capacity by adapting limit equilibrium theory: for instance, the analysis may treat the composite ground as a homogeneous material and apply classical bearing capacity solution to the problems. To do so, a rational estimation of average frictional angle, ϕ_{comp} , is the major issue. The suggestion made by Preibe (1991, see section 1.3.2.2.2) is merely based on an empirical stress concentration ratio, n , which ignores the group effect entirely. A realistic solution may consider the problems separately according to the characteristics of stresses and deformations defined in various Zones (Fig 4.55), in each of which the constitutive relationships between stress and strain for both sand and clay may be related through the rational rules of critical state soil behaviour. For foundations which have arrangements similar to that in the present model tests, the consideration of the significance of the distinction between plane strain and axisymmetrical situations also needs to be addressed.

The stress concentration phenomenon is generally recognised as an important feature of stone column foundations. Measurements from the present model tests indicate that the value of the stress concentration ratio, n , is affected by the loading level and by parametric variations (refer to section 4.2.4). The discussions in section 5.3.3 has

shown that the results from various numerical analyses and from a model study concerning the variation of n value with depth are rather contradictory. Table 7.3 lists some measurements of n value from laboratory tests and from the field, and it is clear that the assumption in current design methods (refer to section 1.3) of constant value of stress concentration ratio to describe the general load sharing characteristics between column and clay throughout the depth of foundation regardless of the influence of other design parameters, which is normally made on the basis of field measurements taken from the surface of the foundation, is by no means well founded. It would thus be extremely useful to understand more clearly the distribution of vertical stress with depth both in columns and in the soil.

Studies concerning the variation of vertical stress with depth in a stone column reinforced foundation will also help to improve understanding of the effect of column length on the overall performance of the reinforced foundation. For a rigid loading, the possibility of penetration of column base is controlled by the vertical stress distributed to this level, which is much influenced by the size of the footing. The concept of effective length mentioned in section 4.3.3 appears to be convincing with particular reference to the results from centrifuge tests (Terashi et al 1991). Since the length of the column is directly related to the economy of the reinforcement, a more detailed study on this particular aspect would be desirable.

The area replacement ratio, A_s , represents two independent parameters, the spacing and the diameter of the columns. In general, it is sufficient to use the composite parameter, A_s , for the analysis of stone column reinforcement. The results from the present study have given a general indication of the effect of A_s on the bearing capacity improvement. However, it is noticed that long, slender columns may undergo buckling failure like a thin long rigid column. Investigation regarding the flexural rigidity of the column in the soil could thus be useful. The columns cannot take tension stress but can develop movements through the presence of the axial compression stress.

The consolidation process in the soil throughout the loading is an unique and yet an important feature of the stone column foundation. The degree of consolidation in the soil significantly affects the stress redistribution between column and soil, which will consequently affect the overall performance of the composite ground. Moreover, the deformation behaviour of the soil/column system is also much influenced by the drainage situation in the soil. Therefore, studies concentrated on

the progress of the consolidation in relation to the various parameters and loading stress level would be extremely valuable for any type of loading situation.

Stone columns have often been used to support the foundation of low rise buildings in the form of pad footings or strip footings. According to the Author's inquiries to the specialist sub-contractors both in UK (Cementation and GKN Keller) and USA (GKN Hayward Baker), and from consolidation of available design approaches (section 1.3), it is understood that current design procedures for this type of foundation generally treat the columns as individual piles. Although the model setup used in the present study does not precisely match the prototype situation, some interaction between columns can be expected even under pad footing and strip footing foundations. In the light of the group behaviour discovered from the present model study, a similar model testing program could be devised to investigate the load bearing behaviour of a rigid pad footing supported by a small group of stone columns. It would be useful to extend such studies to well instrumented full scale trials at location such as *Bothkenner* where the ground conditions are well known.

Investigation of the mechanical behaviour of stone column reinforced foundation subjected to embankment-like flexible loading has been very limited in the present study. Although the possibility of using this stone column technique to control the settlement of a large flexibly loaded area has been generally recognised and applied in field applications, available analysis methods still have many limitations. It is the Author's belief that the deformation behaviour and stress condition under the edge of the loaded area is quite different from those under the centre area, and this difference must be understood in order to achieve a realistic and economical design. From a practical stand point, the present work could be extended relatively easily to study the deformation behaviour of stone column reinforced foundation under flexible loading by means of laboratory modelling. There remain questions about the scaling of the model tests that have been performed in the present study so that the precise field conditions to which the results of these tests are relevant are somewhat unclear. The performance of centrifuge model tests might overcome some of these problems: particularly if methods of installing model columns while the centrifuge is in flight could be devised.

Investigator & reference	Method of investigation	Foundation & Testing		Key observations			Main aspects of study				Reference in this dissertation
		Columns	Loading	Materials (Site)	Stresses & deformation	Consolidation	Failure mech.	Load & Settlement	Consolidation & Settlement	Parametric variations	
Hughes & Withers (1974)	Lab. modelling	Single, floating column	Rigid on the column area only	Kaolin for clay; sand for column	Lateral stress in clay; Displacements in column & clay with depth		Column bulges over top 4 diameter	Load : displacement response			Sections 1.2.2.1 & 1.3.2.1
Goughnour & Bayuk (1979b)	Field testing	Large group	Semi-rigid fast loading	Silt & Sandy clay Soft clay Loose sand	Surface settlement	Pore pressure measurement in depth		Load : displacement response			Section 6.3.2
Charles & Watts (1983)	Large lab. oedometer testing	Single end bearing column	Rigid incremental loading (drained)	Remoulded boulder clay & fine gravel	Total load, & lateral displacement of column	Pore pressure measurement in depth		Stress : strain response	Consolidation degree	A_s	Section 1.2.2.3
Bayuk & Barksdale (1984); Kafetzakis (1983)	Lab. modelling	Single & small group end bearing columns	Rigid stress and displacement controlled slow vertical loading; direct shear tests	Kaolin for clay and fine sand for columns	Total load & displacement, Displacement in clay & sand with depth		Noticed group effect, but not defined	Load : displacement response		A_s	Section 1.2.2.2
Kimura et al (1983)	Centrifuge modelling (50g)	Group end bearing columns	Rigid displacement controlled slow tests	Kawasaki clay & Toyoura sand for columns	Total load & displacement, displacement in clay & sand with depth		Shown in displacement vectors, but not defined	Load : displacement response		A_s & width of improvement	Sections 1.2.2.2 & 6.2.2
Ishizaki et al (1989)	Lab. triaxial tests	Single end bearing column	Triaxial compression & extension tests, Ko-consolidation tests (all drained)	Kawasaki clay & Toyoura sand for columns	Total stress and strain in the cell; Stress and strain in clay and column	Pore pressure measurements		Stress: strain response for average of clay & sand		A_s & confining stress σ_r	Sections 1.2.2.2 & 5.3.1
Terashi et al (1991)	Centrifuge modelling (50g)	Group end bearing columns	Rigid displacement controlled slow loading in vertical & horizontal direction.	Kaolin clay & Toyoura sand for columns	Surface load & settlement; Displacement in the depth of composite ground		Shown in displacement vectors, but not defined	Load : displacement response		Rate of penetration	Sections 1.2.2.2 & 6.2.3
The Author	Lab modelling	Large group floating columns	Rigid displacement controlled tests (slow rate) & Flexible incremental loading tests	Kaolin clay and Loch Aline sand for columns	Total load and settlement, contact stress in clay and sand, surface settlement in adjacent ground, Deformation of columns		Defined a wedge failure mechanism due to group affect	Load : displacement response		A_s , L/d , L/D , method of column installation & footing flexibility	Section 4.2.2

Table 7.1: Summary of experimental studies concerning stone column reinforced foundations

Investigator & key reference	Type of analysis	Foundation			Main aspects of study				Reference in this dissertation
		Type	Footing	Modelling method	Stresses & deformation	Consolidation & Settlement	Failure mech.	Parametric variations	
Balaam (1978)	F.E method drained	Single, floating column	Rigid & flexible	Elastic analysis using unit cell concept	Total stress and settlement in unit cell	Horizontal consolidation		$A_s, L/d, E_s, E_c$	Sections 1.2.4.2, 5.2, 5.3 & 5.4
Abosht (1979)	F.E method undrained; plane strain	Large group of columns	Flexible	Elastic analysis using unit cell concept	Stress distribution with depth				Sections 5.3.2 & 5.3.3
Balaam & Booker (1981)	F.E method drained	Rigid rafts	Rigid	Elastic-plastic analysis using unit cell concept	Load : settlement responses	Horizontal consolidation		$A_s, L/d, E_s, E_c, v_s, v_c$	Sections 1.2.4.2, & 5.3.3
Barksdale & Bachus (1983)	F.E analyses drained and undrained	Unit cell	Rigid & flexible	Non linear elastic & elastic-plastic analysis	Design curves for settlement estimation	Consolidation: vertical and horizontal		$A_s, L/d, E_s, E_c, E_c, E_b$	Sections 1.2.4.2, 5.2.2, 5.4.1 & 5.4.2
Mitchell & Huber (1985)	F.E drained analysis, axisymmetrical	A single column within a large group	Rigid	Homogenisation method using non-linear, stress dependent material properties	Load : settlement responses			A_s	Sections 1.2.4.3 & 5.3.3
Ishizaki (1992)	F.E analysis 3-D drained	Group of columns	Flexible	Semi-homogenised method using Multi-link elements	Stresses & deformation in clay & columns in depth	Consolidation settlements		A_s	Sections 5.3.3, & 5.4.2
Asaoka et al (1994a)	F.E drained & undrained analyses; plane strain	Group of end bearing columns,	Rigid & flexible	Soil-water coupled theory using Mod. Cam clay model for clay	Stresses & deformation in clay & columns in depth	Horizontal consolidation degree c_u increase ratio (clay set-up)	Deformation mass & displacement vectors	Footing flexibility	Sections 5.3.1, 5.3.2 & 5.4.2
Asaoka et al (1994b)	F.E drained & undrained analyses; plane strain	Installing a single column by displacement method		Soil-water coupled theory using Mod. Cam clay model for clay	Strength increase in the clay due to column installation (displacement)	Horizontal consolidation degree c_u increase ratio (clay set-up)	Deformation mass & displacement vectors	A_s	Section 5.4.3
Pande et al (1994)	F.E drained analyses; axisymmetrical	Large group of floating columns	Rigid	Homogenisation method using Modified Cam clay for clay, Mohr-Coulomb for sand	Stresses & deformation in clay & columns in depth		Deformation mass & displacement vectors	$A_s, L, d, L/D,$	Sections 1.2.4.3, 5.2 & 5.3

Table 7.2: Summary of numerical analyses concerning stone column reinforced foundations

Type of test	Column length (m)	A _s (%)	n (measured from surface)	Time variation of n	Variation of n with L	Variation of n with A _s	Reinforced soil condition	Reference	Site
Embankment	6.7-8	25	2.8 (aver.)	Approx. constant	Variable		Soft clay c=20-29 kPa	Vautrain (1977)	Rousa, France
Test fill on group of columns (fast loading)	7.6	26	2.6-3.4 to 4.0-5.0	Increase			Very soft clay e=9-12 kPa	Munfakh et al (1984)	Jourdan Road Terminal, New Orleans
Field tests of a large group columns	6.4	35	3 (initial) to 2.6 (final)	Decreasing			Soft silt and clay with sand e=10 - 15 kPa	Goughnor & Bayuk (1979b)	Hampton, Virginia
Lab. model test on group of 5 columns(undrained loading)	0.45	46	4 - 8 (initial) to 3.2 - 6.7 (final)	Decreasing	Increasing		Clay	Aboshi (1979)	Japanes Sand Compaction Piles (SCP) study
Lab. model tests on single and 1 to 2 rows of columns	Variable	7-40	1.5-5.0	Constant to slightly increasing		Increasing	Kaolin clay	Bachus & Barksdale (1983)	Georgia Tech.
Embankment on a group of columns (semi rigid loading)	Variable	24-32		Increasing				Greenwood (1991)	Humber bridge, England
Field tests on strip footing(fast loading)	Variable							Greenwood (1991)	Canvey Island
Lab. triaxial tests on a single column (drained loading)	0.1			Increasing to peak and dropping			Kaolin clay	Ishizaki et al (1989)	Japanese SCP study
Lab. model tests	0.1&0.15	10-30	1.0-5.0	Increasing		Increasing	Kaolin clay	The Author	Glasgow University

Table 7.3: Some observations of stress concentration ratio in stone column reinforced foundations

References

Aboshi, H., Mizuno, Y., and Kuwabara, M. (1991), "Present state of sand compaction pile in Japan", Deep Foundation Improvements: Design, Construction, and Testing, ASTM - STP 1089 132-46.

Aboshi, H., Ichimoto, E., Enoki, M. and Harada, K. (1979), "The 'Compozer' - a method to improve characteristics of soft clays by inclusion of large diameter sand columns", Proceedings of the International Conference on Soil Reinforcement, Paris, pp 211-216.

Al-Tabbaa (1987), A. "Permeability and stress-strain response of speswhite kaolin", Ph.D. thesis, Cambridge University.

Almeida, M. S. S (1984) "Stage construction embankments on soft clays" Ph.D thesis, Cambridge University

Amaniampong, G and Pande, G.N. (1993) "Class a prediction of the behaviour of stone column reinforced foundation", Dept. of Civil Engineering, Report CR/789/93, Univ. College of Swansea

Asaoka, A., Matsuo, M., and Kokaka, T. (1994a), "Bearing capacity of clay improved with sand compaction piles", 13th ICSMFE 1994.

Asaoka, A, Kodaka, T. and Nozu, M (1994b), "Undrained shear strength of clay improved with sand compacted piles" Soils and Foundations, Vol. 34, No 4, pp23-32

Bachus, R.C. and Barksdale, R.D. (1984), "The behaviour of foundations supported by clay stabilised by stone columns", Eighth European Conference on Soil Mechanics and Foundation Engineering, Helsinki, pp 199-204.

Bachus, R.C. and Barksdale, R.D. (1985), "Vertical and lateral behaviour of model stone columns", International Conference in In-situ Soil and Rock Reinforcement, Paris, 99-104.

Balaam, N.P. and Booker, J.R. (1981), "Analysis of rigid rafts supported by granular piles", International Journal, Numerical and Analytical Methods in Geomechanics (5), pp. 379-403.

Balaam, N.P. and Booker, J.R. (1985), "Effect of stone column yield on settlement of rigid foundations in stabilised clay" International Journal, Numerical and Analytical Methods in Geomechanics (9), pp. 331-351.

Balaam, N. P. (1978), "Load-settlement behaviour of granular piles" PH. D. thesis, University of Sydney.

Balaam, N.P. and Poulos, H.G. (1978), "Methods of analysis of single stone columns", Proceedings of the Symposium on Soil Reinforcing and Stabilising Techniques, Sydney

Balaam, N.P. and Poulos, H.G. (1983), "The behaviour of foundations supported by clay stabilised by stone columns", Proceedings of the Eighth European Conference on Soil Mechanics and Foundation Engineering, Helsinki, Vol. 1, pp. 199-204.

Balaam, N.P., Poulos, H.G. and Brown, P.T. (1977), "Settlement analysis of soft clays reinforced with granular piles". Proceedings of the Fifth South East Asian Conference on Soil Engineering, Bangkok, Thailand, pp. 81-92.

Balaam, N.P. and Booker, J.R. (1985), "Effect of stone column yield on settlement of rigid foundations in stabilised clay", *Int. Jou. Num. Analyt. Meth. Geomech.*, Vol. 9, No. 4.

Barksdale, R.D. and Goughnour, R.R. (1984), "Settlement performance of stone columns in the U.S.", *In-situ Soil and Rock Reinforcement Conference*, Paris, 105-110.

Barksdale, R.D. and Bachus, R.C. (1983), "Design and construction of stone columns, Volume 1", Report No. FHWA/RD-83/026, Federal Highway Administration, U.S.A.

Baumann, V. and Bauer, G.E.A. (1974), "The performance of foundations on various soils stabilised by the vibro-compaction method. *Canadian Geotechnical Journal* 2, pp. 509-530.

Bell, A.L. (1915), "The lateral pressure and resistance of clay and the supporting power of clay foundations. *Proc. ICE*, 199, 233.

Belkheir, K.(1993) "Yielding and stress-strain behaviour of sand", M.Sc thesis, Glasgow University.

Bergado, D.T., Rantucci, G. and Widodo, S. (1984), "Full scale load test of granular piles and sand drains in soft Bangkok clay", *International Conference in In-situ Soil and Rock Reinforcement Conference*, Paris, 111-118.

Besancon, G., Iorio, J.P. and Soyés, B. (1984), "Analyse des parametres de calcul intervenant dans le dimensionnement des collonnes ballastees", *International Conference in In-situ Soil and Rock Reinforcement*, Paris, 119-126.

Bhandari, R.K.M. (1983), "Behaviour of a tank founded on soil reinforced with stone columns", *Proceedings of the Eighth European Conference on Soil Mechanics and Foundation Engineering*, Helsinki, Vol. 1, pp. 209-212.

Biot, M.A. (1941), "General theory of three-dimensional consolidation", *Journal. of Applied Physics*, Vol. 12, No. 2, pp. 155-164.

Bjerrum, L. (1972). "Embankments on soft ground". *Proc. ASCE Specialty Conference on Performance of Earth and Earth Supported Structure*, Purdue University, Lafayette, IN, Vol. I(1), pp1-54.

Brauns, J. (1978), "Initial bearing capacity of stone columns and sand piles", *Proceedings of the Symposium on Soil Reinforcing and Stabilising Techniques*, Sydney, pp. 477-496.

Brons, K.F. and Dekruiff, H. (1985), "The performance of sand compaction piles", *Eleventh International Conference on Soil Mechanics and Foundation Engineering*, San Francisco, 1683-1686.

Britto, A.M. (1983), *Anuser's guild to the soils Strain calculating porgram*, Internal Report, CUED, Engineering Dept., University of Cambridge.

Burland, J.B. and Roscoe, K.H. (1969), "Local strains and pore pressures in a normally consolidation clay layer during one-dimensional consolidation", *Geotechnique* Vol. 19, No. 3, 335-356.

Burland, J.B., McKenna, J.M. and Tomlinson, M.J. (1975), *Preface to Symposium on ground treatment by deep compaction*, *Geotechnique* 25, No.1, pp 1-2.

- Burland (1976), "Discussion, ground treatment by deep compaction", Institution of Civil Engineers, London, 142.
- Cairncross A.M, (1973) "Deformations around model tunnels in stiff clay", Ph.D Thesis, University of Cambridge.
- Castelli, R.J., Sarkar, S.K. and Mungakh, G.A. (1983), "Ground treatment in the design and construction of a wharf structure", Proc. ICE Conf. on Advances in Piling and Ground Treatment for Foundations, pp. 275-281.
- Charles, J.A. and Watts, K.S. (1983), "Compressibility of soft clay reinforced with granular columns", Proceedings of the Eighth European Conference on Soil Mechanics and Foundation Engineering, Helsinki, Vol. 1, pp. 347-352.
- Colleselli, F., Mazzucato, A., Previatello, P., and Spalatro, A. (1983), "Improvement of soil foundation by vibratory methods", Eighth European Conference on Soil Mechanics and Foundation Engineering, Helsinki, 223-228.
- Cox, A.D. (1962) "Axially symmetric plastic deformation in the soils" International Journal of Mechanical Science, Vol 4, pp 371-380
- Cox, A.D., Easton, G. and Hopkins, H.G. (1962) "Axially symmetrical deformation in soils", Philosophy Transaction of Royal Society Series A Vol. 254, pp1-45
- Davis, E.H. and Poulos, H.G. (1972), "Rate of settlement under two- and three-dimensional conditions", Geotechnique 22, No. 1, pp. 95-114.
- Davis, M. C. R. (1981), "Centrifugal modelling of embankments on clay foundation". Ph. D. Thesis, Cambridge University.
- Engelhardt, K. and Golding, H.C. (1975), "Field testing to evaluate stone column performance in a seismic area", Geotechnique, (25), 1.
- Gambin, M. P. (1984), "Puits Ballastes a La Seyne - sur-Mer", In-situ Soil and rock reinforcement Conference, Paris, pp139-144.
- Gerrard, C.M., Pande, G.N. and Schweiger, H.F. (1984), "Modelling behaviour of soft clay reinforced with stone columns", In-situ Soil and Rock Reinforcement Conference, Paris, 145-150.
- Goughnour, R.R. and Bayuk, A.A. (1979a), "Analysis of stone column-soil matrix interaction under vertical load", Proceedings of the International Conference on Soil Reinforcement, Paris, pp. 271-277.
- Goughnour, R.R. and Bayuk, A.A. (1979b), "A field study of long-term settlements of loads supported by stone column in soft ground", Proceedings of the International Conference on Soil Reinforcement, Paris, pp. 279-285.
- Goughnour, R.R. (1983), "Settlement of vertically loaded stone columns in soft ground", Proceedings of the Eighth European Conference on Soil Mechanics and Foundation Engineering, Helsinki, Vol. 1, pp. 235-240.
- Goughnour, R.R. and Barksdale, R.D. (1984), "Performance of a stone column supported embankment", Proc. of Inter. Conf. on Case Histories In Geotechnical Eng. Editor Shamasher Prakash, University of Missouri-Rolla, May 6-11, 1984, Vol. II, pp735-741.

Goughnour, R.R (1994), Personal communication

Greenwood, D.A. (1970), "Mechanical improvement of soils below ground surface", Proceedings of the Ground engineering Conference, ICE, pp. 9-20.

Greenwood, D.A. (1975), "Vibroflotation: Rationale for design and practice", Ch. 11 of Methods of treatment of unstable ground, Ed. F.G. Bell, Newnes-Butterworth, pp. 189-209.

Greenwood, D.A. and Kirsch, K. (1983), "Specialist ground treatment by vibratory and dynamic methods", Proceedings of the International Conference on Advances in Piling and Ground Treatment for Foundations, ICE, pp. 17-45.

Greenwood, D.A. (1970), "Mechanical improvement of soil below ground surface", Ground Engineering, June, 11-22.

Greenwood, D.A. and Kirsch, K. (1984), "Specialist ground treatment by vibratory and dynamic methods", State of the art Report, Piling and Ground Treatment, Thomas Telford Ltd., London, pp17-45.

Greenwood, .D.A. (1990), Load tests on stone columns in deep foundation improvements: design, construction, and testing", ASTM-STP 1089.pp. 148-171

Greenwood, .D.A. (1994), Personal communication

Greenwood, .D.A. (1995), Personal communication

Holtz, R.D., and Lindskog, G. (1972), "Soil movements below a test embankment", Proc. ASCE Speciality Conference on Performance of Earth and Earth Supported Structure, Purdue University, Lafayette, IN, Vol. I (1), pp273-284.

Houlsby, G.T. (1981), "Theoretical analysis of the fall cone test" Soil Mechanics Report No. SMO16/BRE/81 (O.U.E.L. Report No. 1360/81) Dept. of Civil Eng., University of Oxford.

Houlsby, G.T and Worth, C.P. (1982), "Direct solution of plasticity problems in soils by the method of characteristics" Soil Mechanics Report No.21/BRE/82 (O.U.E.L. Report No. 1395/82) Dept. of Civil Eng., University of Oxford.

Hu, W. (1993) "Analysis of regular inhomogeneous soils: Application to stone column reinforced foundation", First year research report, Civil Engineering Department, Glasgow University.

Hughes, J.M.O. and Withers, N.J. (1974), "Reinforcing of soft cohesive soils with stone columns", Ground Engineering, May, pp. 42-49.

Hughes, J.M.O., Withers, N.J. and Greenwood, D.A. (1975), "A field trial of the reinforcing effect of a stone column in soil", Geotechnique 25, 1, pp. 31-44.

Hunt, R.J. (1986), "The design of granular piles in soft compressible soils", M.Sc. Thesis, Imperial College, University of London.

Ishizaki, H., Matsuoka, H and Nakai, T. (1989) "Stress-deformation characteristics of clay improved by sand column under triaxial stress condition" Proc. of Japanese Civil Engineering Society, No 406/III-11, (In Japanese)

Ishizaki, H. (1989) "Deformation analysis of composite ground under undrained condition", Proc. of Japanese Civil Engineering Society, No 448/III-19, pp53-62 (In Japanese)

Jebe, W. and Bartels, K. (1983), "The development of compaction methods with vibrators from 1976 to 1982", Eighth European Conference on Soil Mechanics and Foundation Engineering, A.A. Balkema, Helsinki.

James R.G. (1973), "Determination of strains in soils by radiography" Internal Report CUED/C-SOIL/LN1 (a), Cambridge University

Janbu, N. (1963), "Soil compressibility as determined by Oedometer and Triaxial tests", European Conference of Soil Mechanics and Foundation Engineering, Wiesbaden, Germany, Vol.1.

James. R.G. (1973). "Determination of strains in soils by radiography", CUED/C, SOILS LN1(a), Dept. of Engineering, University of Cambridge.

Kaffezakis, G.J. (1983) " A model test investigation of the behaviour of stone columns", Special Research Problem, Georgia Institute of Technology, Atlanta. USA April 1983.

Kirkpatrick, W.M. (1954), " The behaviour of sands under three dimensional stress systems". Ph.D. Thesis, University of Glasgow.

Kirkpatrick, W.M. (1961), Discussion, Proc. 5th ICSMFE Vol 3 pp 131-133.

Kolbuszewski, J. J. (1948), "An experimental study of the maximum and minimum properties of sand", Proc. Midland SMFE Society, Vol. 4, pp 107-123

Kolbuszewski J. J. and Jones, R.H. (1961), "The preparation of sand samples for laboratory testing", Proc. 2nd ICSMFE (Rotterdam), Vol.1, pp. 158-165

Lade, P.V. (1988) "Double hardening constitutive model for soils, parameter determination and predictions for two sands", Constitutive Equations for Granular Non-cohesive Soils, pp 367-378

Lee J.S. and Pande G.N. (1994) " Analysis of stone column reinforced foundations" Departmental Research Report CR/835/94, University College of Swansea.

Leroueil, S., Tavenas, F., Mieussens, C., and Peignaud, M. (1978), "Construction pore pressure in clay foundations under embankments, Part I & II. Canadian Geotechnical Journal, 15, pp54-82

Liausu, P. (1984), "Reinforcement de Couches de Sol Compressibles par Substitution Dynamique", In-situ Soil and rock reinforcement Conference, Paris, pp151-155

Love, J.P. (1984), "Model testing of geogrids in unpowered roads", Ph.D. Thesis, Oxford University.

Maghav, M.R., Iyengar, N.G.R., Vitkar, P.P. and Nandia, A. (1979), "Increased bearing capacity and reduced settlements due to inclusions in soil", Proceedings of the International conference on Soil Reinforcement, Paris, pp. 329-333.

Maghav, M.R. and Vitkar, P.P. (1978), "Strip footing on weak clay stabilised with a granular trench or pile", Canadian Geotechnical Journal, pp. 605-609.

Mair R.J. (1979) "Centrifuge modelling of tunnel construction in soft clay" Ph. D. Thesis, Cambridge university.

- Majorana, C., Mazzalai, P. and Odorizzi, S (1983), "Prediction of the settlement of steel petroleum tanks resting on stone columns reinforced soil", Proceedings of the Eighth European Conference on Soil Mechanics and Foundation Engineering, Helsinki, Vol. 1, pp. 271-274.
- Mattes, N.S. and Poulos, H.G. (1969), "Settlement of a single compressible pile", Journal of Soil Mechanics and Foundations Division, ASCE, SMI, January.
- McKenna, J.M., Eyre, W.A., and Wolstenholme, D.R. (1975), "Performance of an embankment supported by stone columns", Geotechnique 25, 1, pp. 51-60.
- McCarron, W.O. and Chen, W.F. (1988), "An elastic-plastic two-surface model for non-cohesive soils", Constitutive Equations for Granular Non-cohesive Soils, pp 427-445
- Mesdary, M.S.(1969) "The shearing behaviour of granular material under a general stress system", Ph.D. thesis, Glasgow University.
- Meyerhof, G.G. (1983), "Closing address to the International Conference on advances in piling and ground treatment for Foundations", ICE.
- Mitchell, J.K. and Huber, T.R. (1985), "Performance of a stone column foundation", Jour. of Geotech. Eng. ASCE Vol. 111, No. 2, Feb. 1985, 205-223.
- Mitchell, J.K. (1981), "Soil improvement - state of the art report", Proceedings of the Tenth International Conference on Soil Mechanics and Foundation Engineering, Stockholm, Vol. 4, pp. 509-565.
- Mitchell, J K and Huber, T R (1985) "Performance of a stone column foundation" J. Geotech. Eng. ASCE 111, pp 205-223
- Mitchell, J K (1994), Private communication
- Miura, N. Murata, H. and Yasufuku, N (1984), "Stress-deformation and strength characteristics of sand in a partial crushing region", Soils and Foundations Vol 24(1), pp 77-89
- Miura, S. and Toki, S. (1982), "A sample preparation method and its effect on static and cyclic deformation-strength properties of the sand", Soils and Foundations Vol. 22(1), pp 61-77
- Moreau, Neil and Mary (1835). "Foundations - emploi du sable", Annales des Ponts and Chaussees, Memoirs, No. 224, pp. 171-214.
- Mulilis, J.P., Seed, H.B., Chan, C.K., Mitchell, J.K., and Arulanandan, K. (1977), "Effect of sample preparation on sand liquefaction", Proc. ASCE., Journal of Geotechnical Engineering Division Vol 103 (GT2), pp 91-108
- Munfakh, G.A., Sarkar, S.K. and Castelli, R.C. (1984), "Performance of a test embankment founded on stone columns", Piling and Ground Treatment, Thomas Telford Ltd., London.
- Munfakh, G.A. (1984), "Soil reinforcement by stone columns - varied case applications", International conference on In-situ soil and rock reinforcement, Paris, 157-162.
- Munfakh, G.A. (1994) Personal communication
- Ovesen, N.K (1979), Discussion on ""The use of physical models in design" 7th ECSMFE, Brighton, Vol(5). pp 319-323.

Pande, G.N., Wood, D.M. and Stewart, W.M (1992) "Analysis of regularly inhomogeneous soils: Application to stone column reinforced foundations". Proposal for the SERC research project, Grant NoGR/H15950.

Pander, G.N. (1994) "Analysis of regularly inhomogeneous soils: Application to stone column reinforced foundations" Final Report to EPSRC Grant No: GR/H/17299, Dept. of Civil Engineering, CR/835/94, Univ. College of Swansea

Ponniah, D.A.(1984) "Behaviour of plate anchors in cohesive soils under static and cyclic loads", Ph.D thesis, Glasgow University.

Poulos, H.G. and Davis, E.H. (1968), "The settlement behaviour of single axially-loaded piles and piers, *Geotechnique* 18, 351 -

Priebe, H. (1976), "Abschätzung des Setzungsverhaltens eines durch Stopfverdichtung verbesserten Baugrundes", *Die Bautechnik*, H.5., pp. 160-162.

Priebe. H. (1991) "Vibro Replacement -Design Criteria and quality control ", Deep foundation improvements: Design, construction and testing STP 1089, ASTM 1991

Priebe. H. (1993) "Design criteria for ground improvement by stone columns" Fourth National conf. ground improvement, January 18-19 1993, Lahore Pakistan

Rosco K.H. and Burland J.B. (1969) "Local strains and pore pressures in a normally consolidated clay layer during one-dimensional consolidation" *Geotechnique* 1969 Vol 19, No 3, pp 335-356

Schlosser, F and Juran, I (1979), "Design parameters for artificially improved soils" - General Report 7th European . Conference of Soil Mech. and Foundation Engineering. Brighton 1979 Vol. 5 pp 207-209

Schweiger, H.F. and Pande, G.N. (1986), "Numerical analysis of stone column supported foundations", *Computers & Geotechnics*, Vol. 2, pp. 347-372.

Schweiger, H.F. and Pande, G.N. (1986), "Modelling behaviour of stone column reinforced soft clays", *Proc. 2nd Int. Symp. Num. Models in Geomechanics*, Ghent, M. Jackson & Son, Publishers Ltd., pp 171-77.

Schweiger, H.F. and Pande, G.N. (1988), "Numerical analysis of road embankment constructed on soft clay stabilised with stone columns", *Proc. Num. Methods in Geomechanics*, A.A. Balkema, Rotterdam, pp. 1329-1333.

Steinfeld, K. (1953), "Über den raumlichen Erdwiderstand", *Mitteilungen der Nannoverschen Versuchsanstalt für Grundbau und Wasserbau*, Heft 3, S. 51ff.

Stewart, W. M. (1988), " Plate anchors in sand under static and cyclic loads" Ph.D Thesis, Glasgow University.

Stone, K.J.L. and Wood, D.M. (1989), "Model studies on soil deformations over a moving basement" *Engineering geology of underground movement*, eds: F.G. Bell, Culshaw, M.G., Cripps, J.C. and Lovell, M.A. Geological Society Engineering geology Special Publication 5, pp 159-165.

Stewart, W.M. and Hu, W. (1993), "Analysis of regular inhomogeneous soils-report on pilot tests", Departmental Research Report CE-GE93-27, Glasgow University.

Tavenas, F.A., Mieussens, C., and Bourges, F. (1979) "Lateral displacements in clay foundations under embankments". *Canadian Geotechnical Journal* 1979 Vol. 16., pp532-550

- Taylor, D.W. (1948) "Foundation of Soil Mechanics" Wiley International Edition, John Wiley
- Taylor, R.N. (1984), "Ground movements associated with tunnels and trenches", Ph. D. thesis, Cambridge University.
- Terashi, M., Kitazume, M. and Minagawa, S. (1991), "Bearing capacity of improved ground by sand compaction construction and testing", ASTM - STP 1089 47-61.
- Terashi, M and Kitazume, M (1990) "The bearing capacity of the clay ground improved by sand compact pile of low replacement area ratio" Report of the Port and Harbour Research Institute, VBoI 29, No. 2 (In Japanese)
- Thorburn, S. (1975), "Building structures supported by stabilised ground", Geotechnique 25, No. 1, pp. 83-94.
- Thorburn, S. and Macvicar, R.S.L. (1968), "Soil stabilisation employing surface and depth vibrators", The Structural Engineer, 46, No. 10, pp. 309-316.
- Van Impe, W. and De Beer, E (1983), "Improvement of settlement behaviour of soft layers by means of stone columns", Proceedings of the Eighth European Conference on Soil Mechanics and Foundation Engineering, Helsinki, Vol. 1, pp. 309-312.
- Vaid, Y.P. , Chern, J.C. and Tumi, H. (1985), "Confining pressure, grain angularity and liquefaction", Pro. ASCE, journal of the Geotechnical Engineering Division Vol 111 (10) pp 1229-1235.
- Vautrain, J., (1977) "Reinforced earth wall on stone columns in soil", Inter. symposium on soft clay, Bangkok, July, 1977, pp 188-194
- Vesic, A.S. (1972), "Expansion of cavities in infinite soil mass", Proc. ASCE, SM3, PP 265.
- Wallays, M., Dalapierre, J. and Van Den Poel, J. (1983), "Load transfer mechanism in soil reinforced by stone or sand columns", Eighth European Conference on Soil Mechanics and Foundation Engineering, Helsinki, 313-317.
- Watt, A.J., De Boer, J.J. and Greenwood, D.A. (1967), "Loading tests on structures founded of soft cohesive soils strengthened by compacted granular columns", Proc. 3rd Asian Conf. SM&FE, Haifa, 1, pp. 248-251.
- Watts, K.S. and Charles, J.A. (1991), "The use, testing and performance of vibrated stone columns in the United Kingdom", Deep Foundation Improvements Design, Construction and Testing, ASTM - STP pp 212-223.
- Wood, D.M. (1974) "Some aspects of the mechanical behaviour of kaolin under truly triaxial conditions of stress and strain" Ph.D. thesis, Cambridge University.
- Wood, D. M. (1990) "Soil Behaviour and Critical State Soil Mechanics" Cambridge University Press
- Wood, D.M.(1994) "Localised shear deformation in sand" Private communication.
- Wroth, C.P., Randolph, M.F., Houlsby, G.T. and Fahey, M. (1979), "A review of the engineering properties of soil with particular reference to the shear modulus", Cambridge University Engineering Department, CUED/D-Soils TR75.

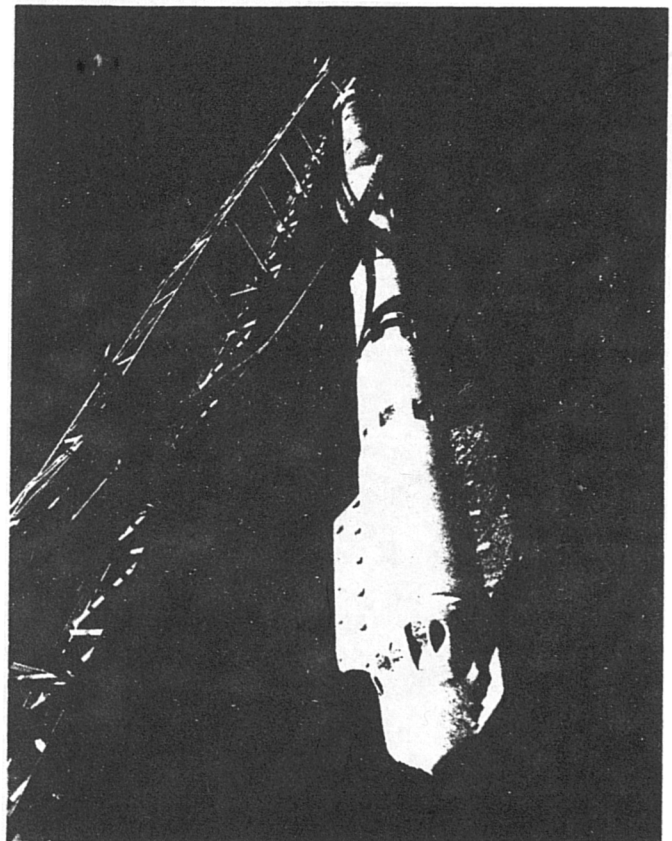
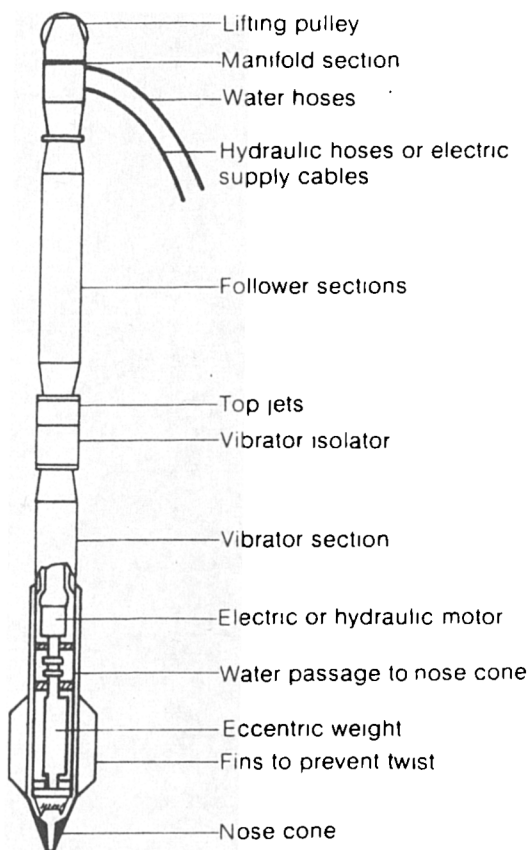
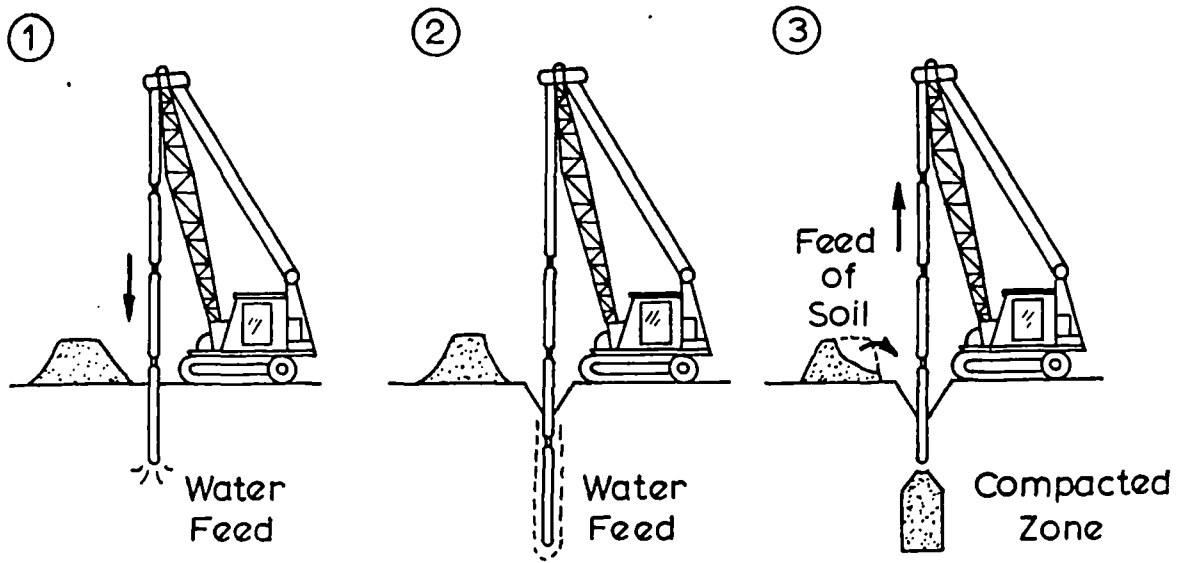
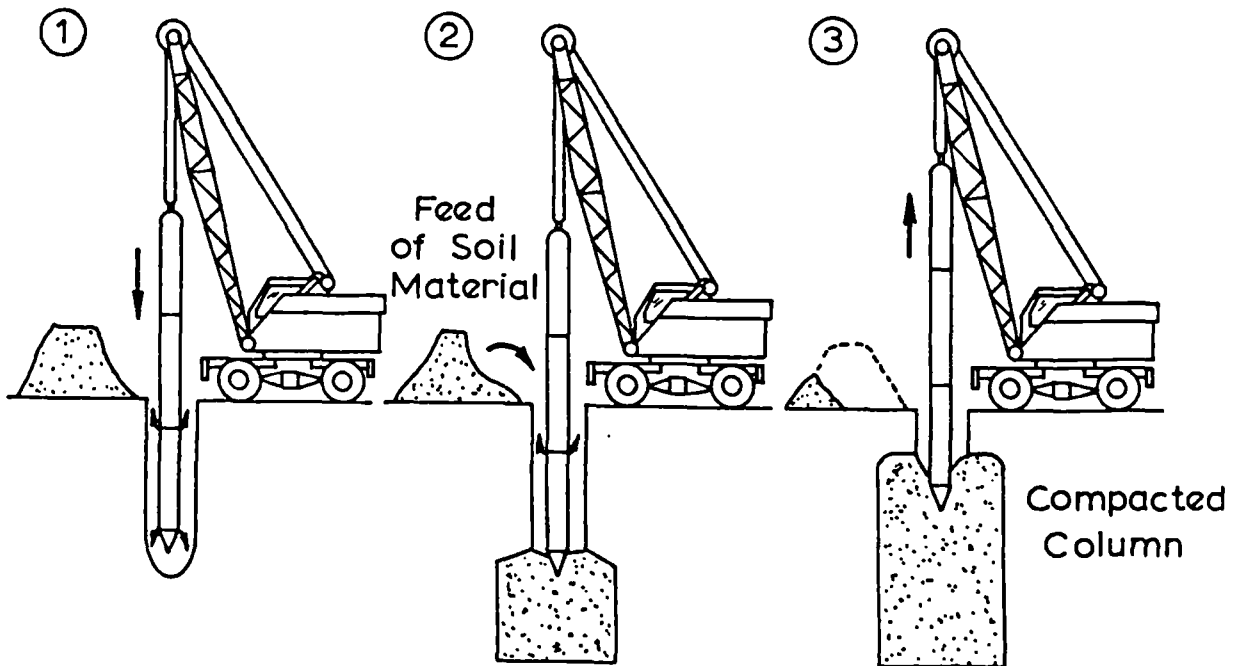


Fig 1.1: The poker (vibrator)



(a) The vibro-replacement method



(b) The vibro-displacement method

Fig 1.2: The vibro-flotation process (a) The vibro-replacement method; (b) The vibro-displacement method

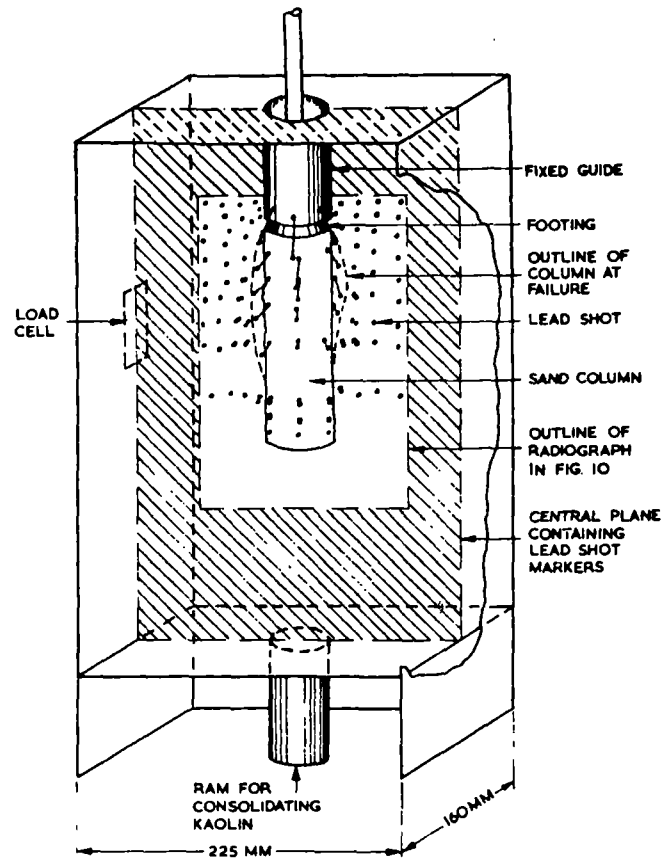


Fig 1.3: The single model stone column test set up (after Hughes & Withers 1974)

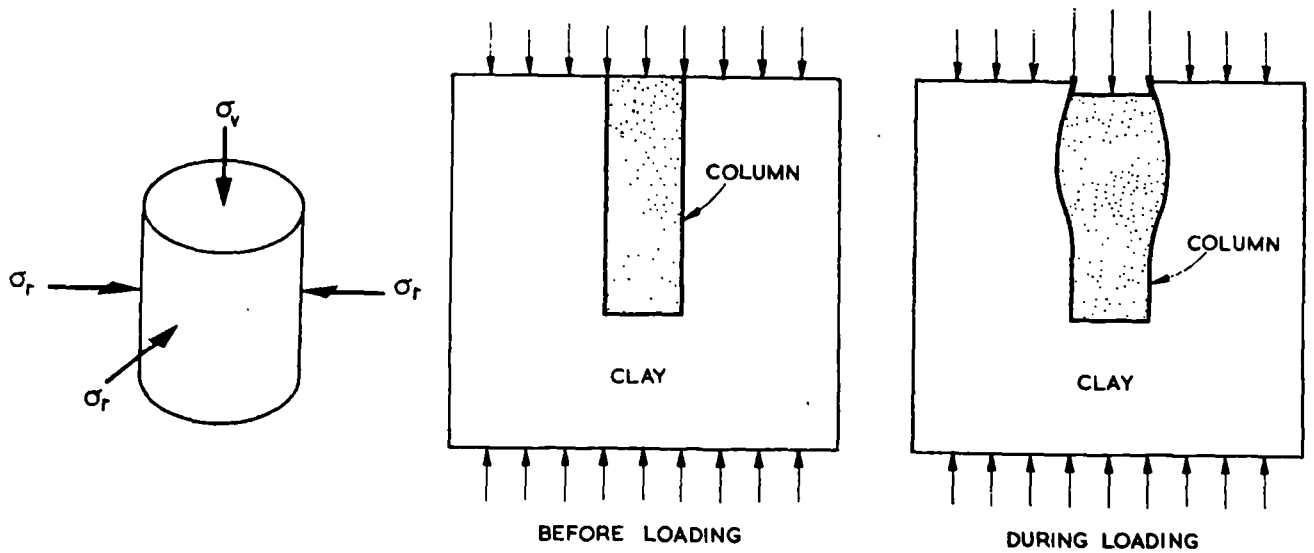


Fig 1.4: The load bearing mechanism of a single column (after Hughes & Withers 1974)

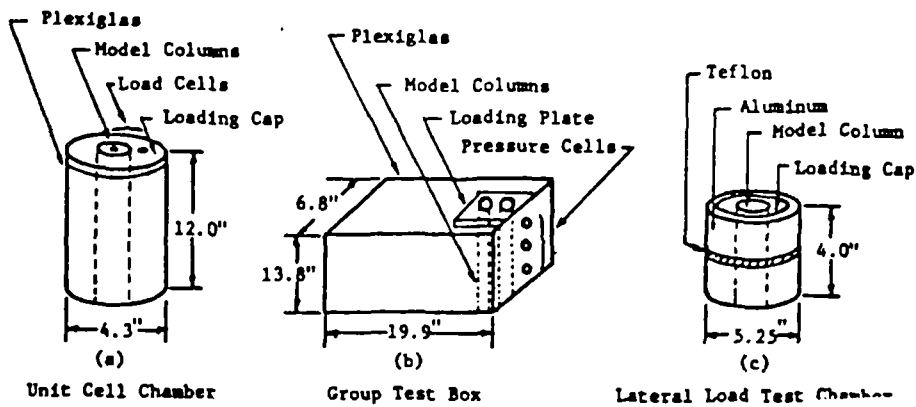


Fig 1.5: The experimental set up of model tests in Georgia Tech.(a) unit cell Chamber; (b) group test box; (c) lateral load test chamber. after Barksdale & Bachus 1989

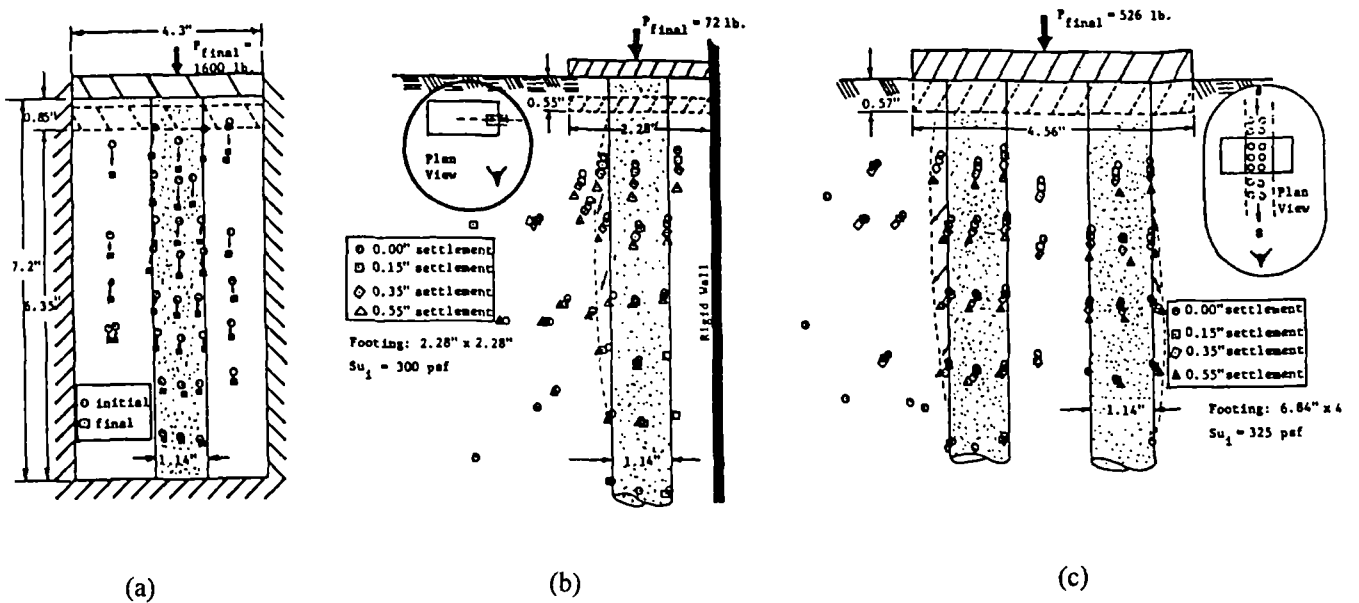


Fig 1.6: The displacement characteristic of model tests in Georgia Tech.(a) displacements in unit cell test; (b) displacements of single column (1x1P); (c) displacements of a group column (2x3), After Barksdale & Bachus 1989

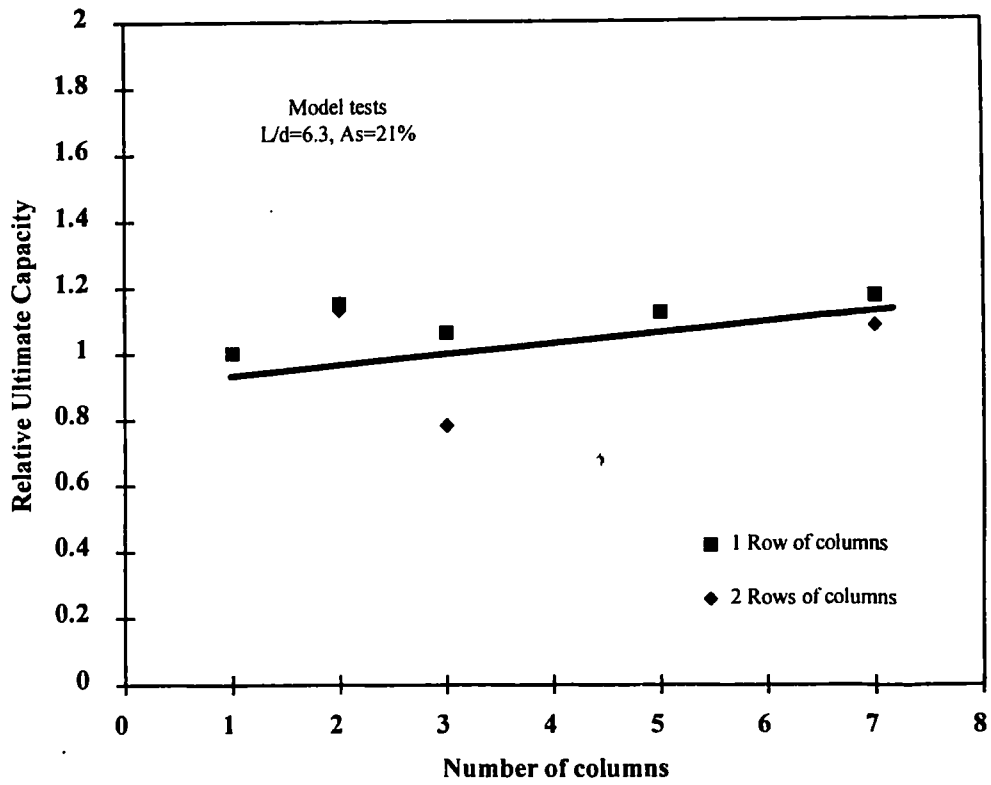


Fig 1.7: Increase in load bearing capacity per column with increase total number of columns (reproduced after Barksdale & Bachus 1983)

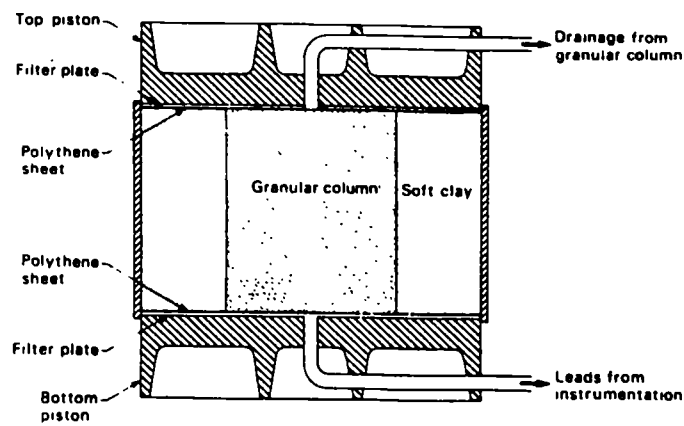
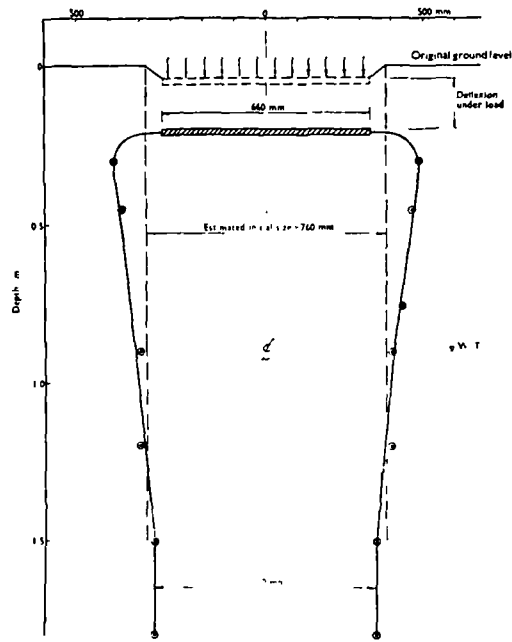
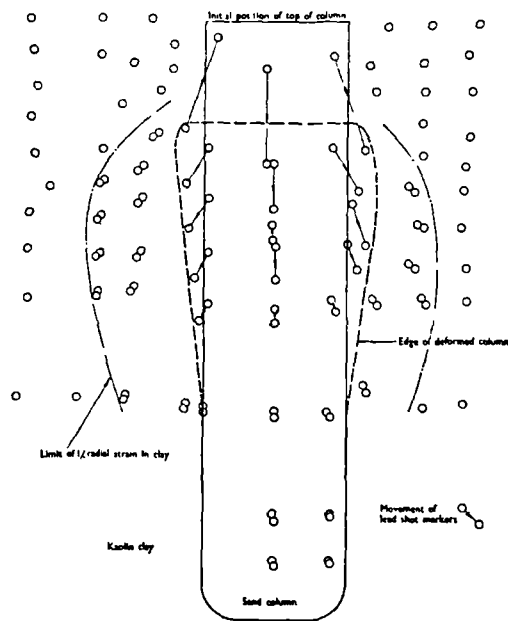


Fig 1.8: Large oedometer test on a single stone column (after Charles & Watts 1983)



(a)



(b)

Fig 1.9: Comparison of deformation behaviour of a single column under a rigid footing load (a) deformations in a field test (b) deformations in a laboratory model test, after Hughes et al 1975

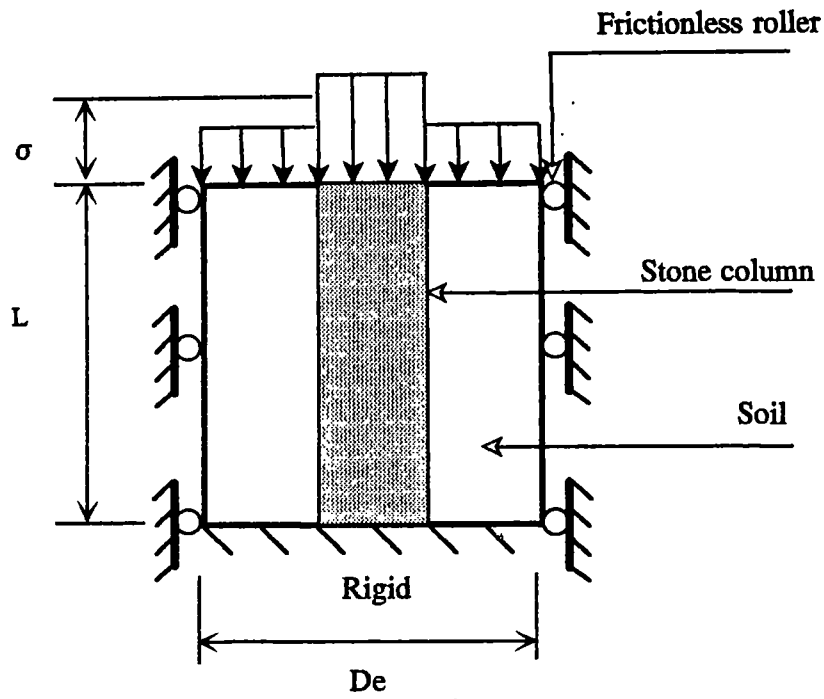


Fig 1.10: Unit cell approximation

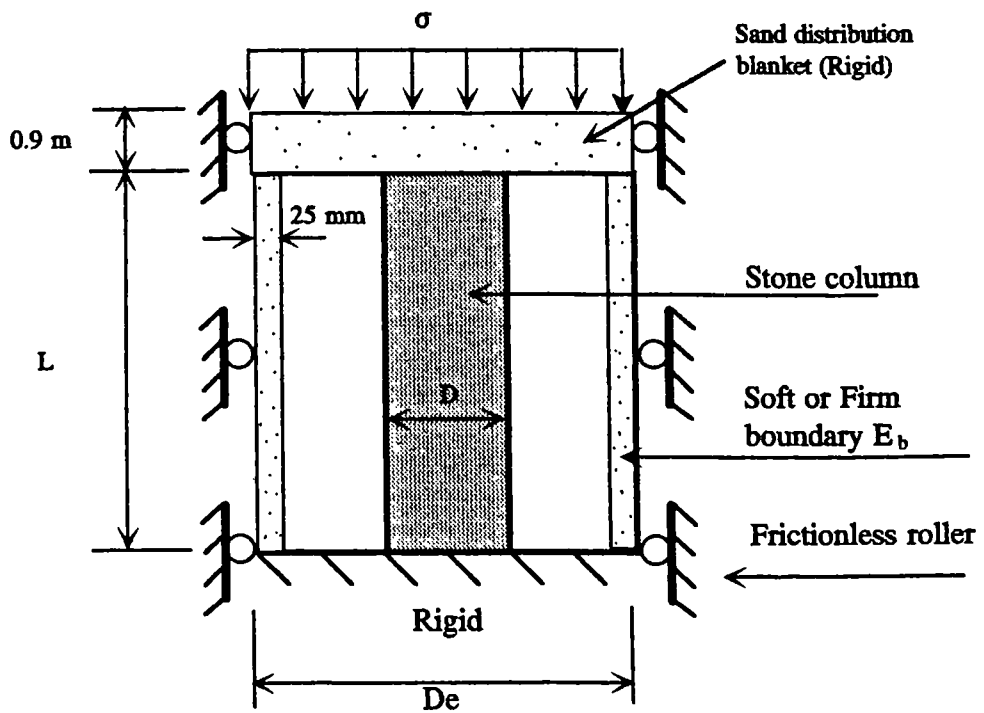


Fig 1.13: Modified unit cell approximation with soft boundaries (reproduced after Barksdale & Bachus 1983)

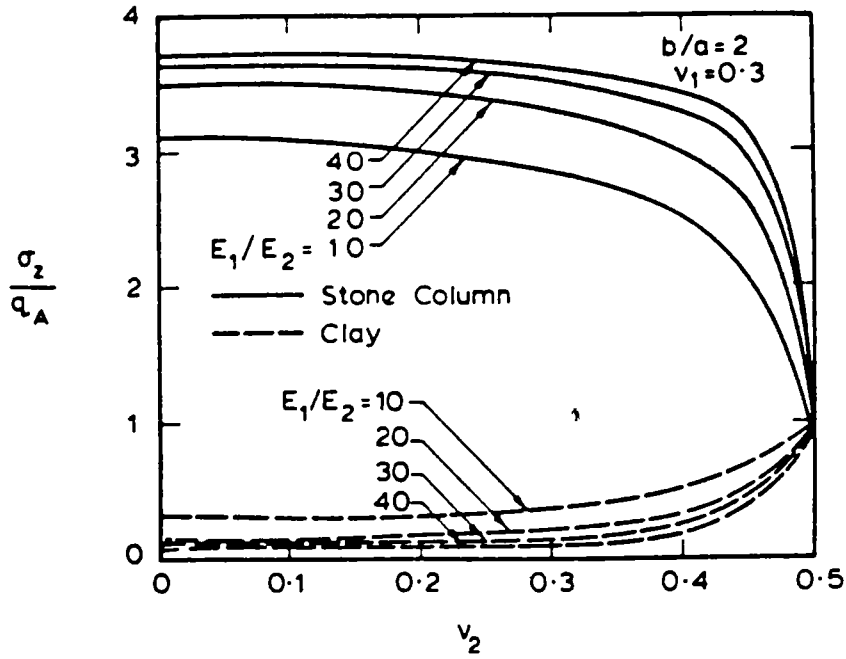


Fig 1.11: The stress distribution between column and clay (after Balaam 1978)

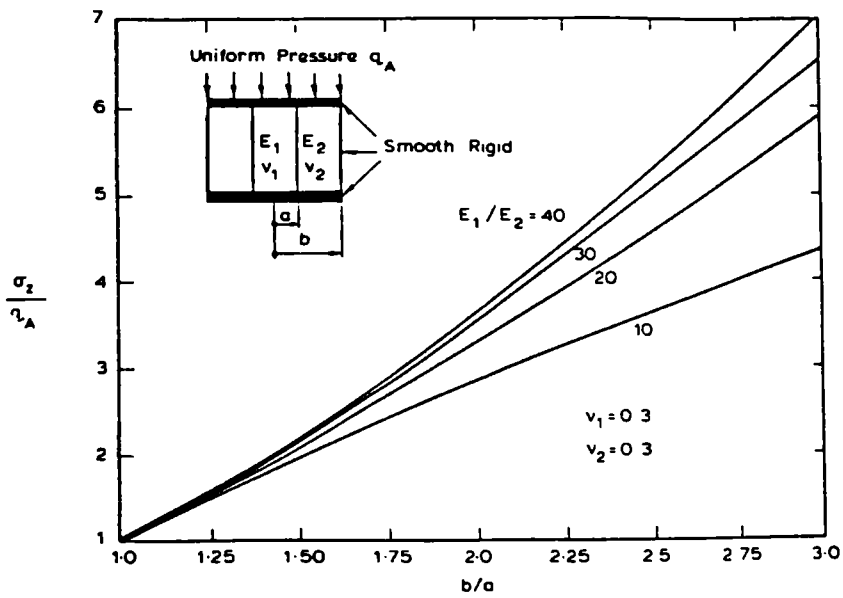
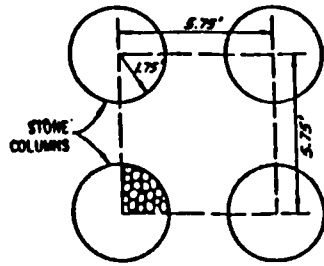


Fig 1.12: Variation of vertical stress in stone column with b/a (after Balaam 1978)

ACTUAL PLAN VIEW OF STONE COLUMNS

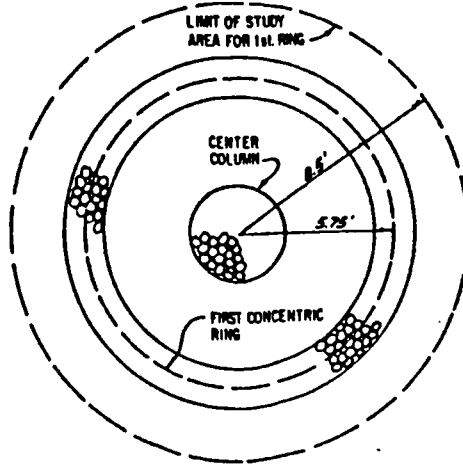


TOTAL SURFACE AREA IN PATTERN = $(5.75 \text{ ft})^2 = 33 \text{ sq. ft.}$

EXPOSED STONE COLUMN AREA = $\pi (1.75 \text{ ft})^2 = 9.6 \text{ sq. ft.}$

\therefore PERCENTAGE OF STONE COLUMN AREA TO TOTAL AREA = 29%

TRANSFORMED AXISYMMETRIC VIEW



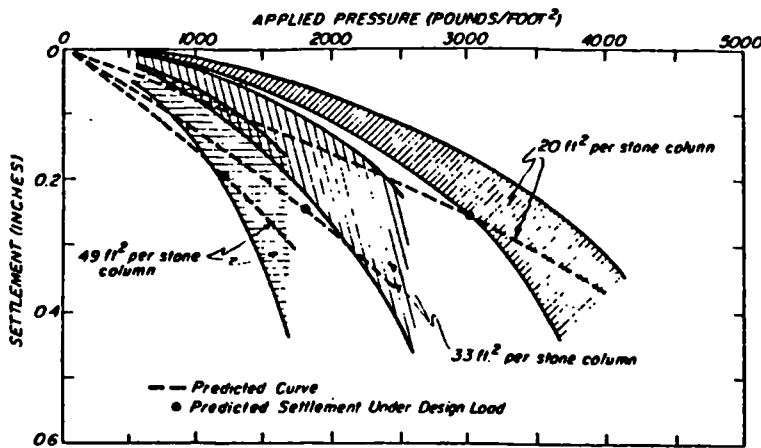
TOTAL STUDY AREA = $\pi (8.6 \text{ ft})^2 = 227.0 \text{ sq. ft.}$

REQUIRED SURFACE AREA OF STONE COLUMN MATERIAL = $0.29 (227.0) = 65.8 \text{ sq. ft.}$

REQUIRED RING AREA OF STONE COLUMN MATERIAL = $65.8 \text{ sq. ft.} - 9.6 \text{ sq. ft.} = 56.2 \text{ sq. ft.}$

REQUIRED RING THICKNESS = $\frac{56.2 \text{ sq. ft.}}{2 \pi (5.75 \text{ ft.})} = 1.5 \text{ ft.}$

(a)



(b)

Fig 1.14: Homogenisation analysis of stone column foundation (a) calculation of stone column material surface area, (b) comparison of measured and predicted load: settlement behaviour of single loaded stone column within a group, after Mitchell & Huber 1985

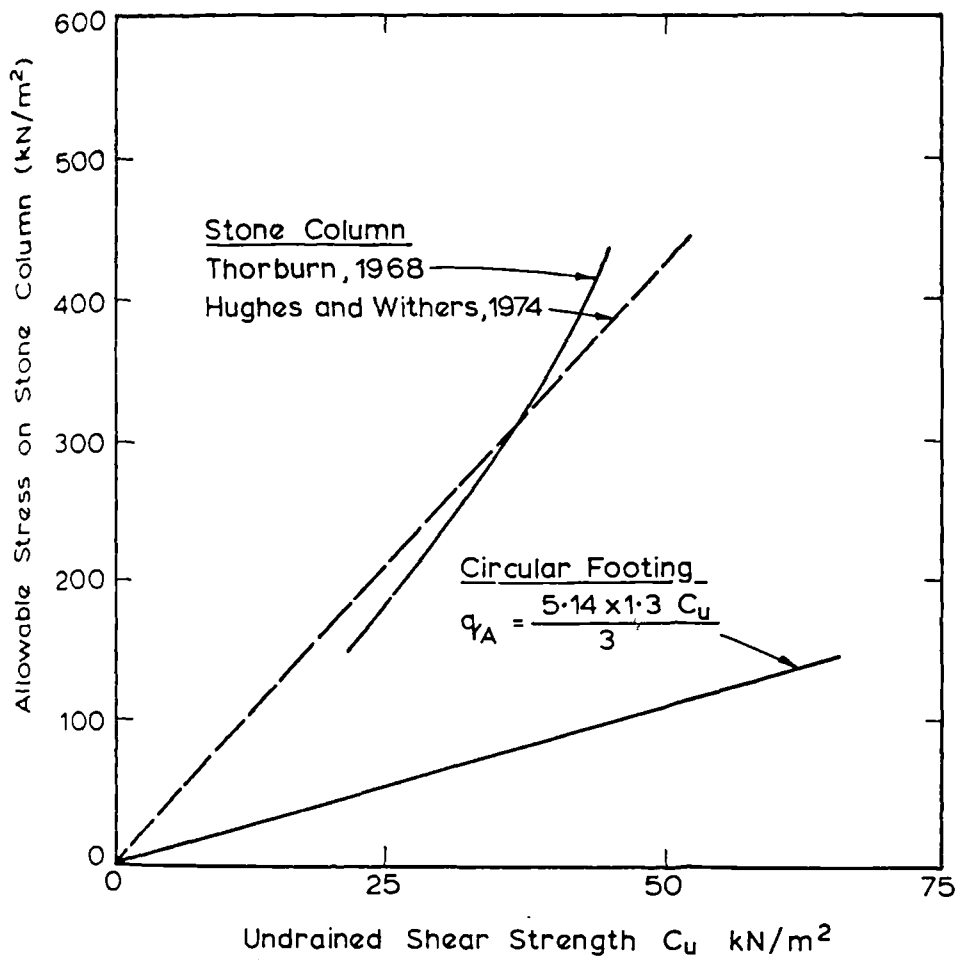


Fig 1.15: Allowable stress on stone column (after Balaam 1983)

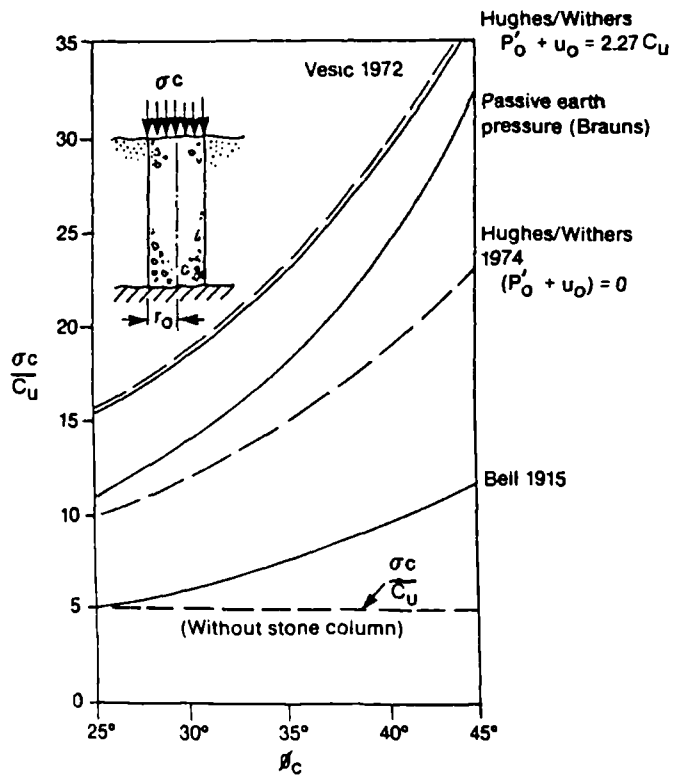


Fig 1.16: Ultimate capacity of a single stone column (after Greenwood & Kirsch 1983)

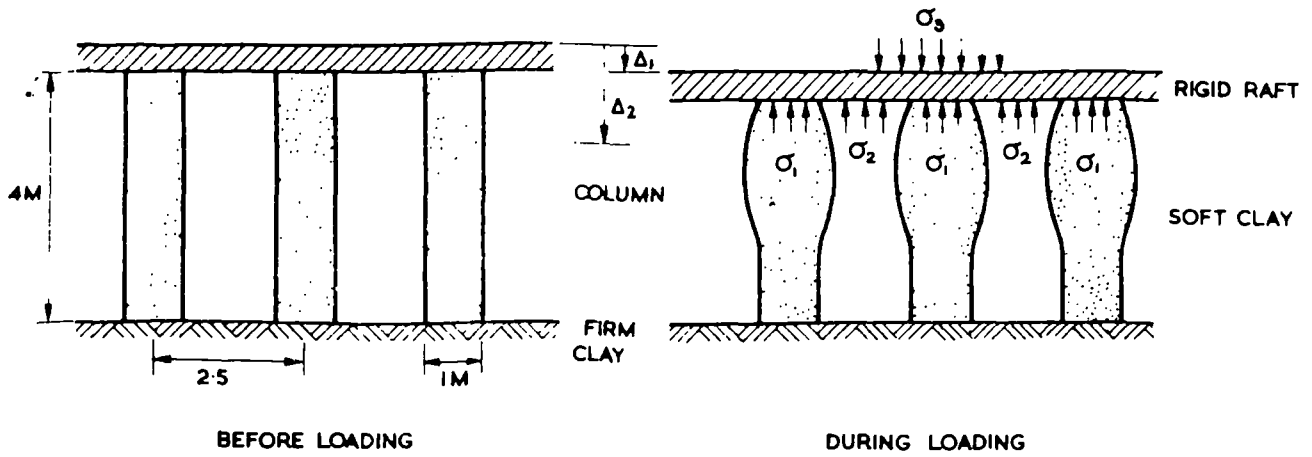


Fig 1.17: Assumed load bearing mechanism of a small group columns under a rigid footing load (after Hughes & Withers 1974).

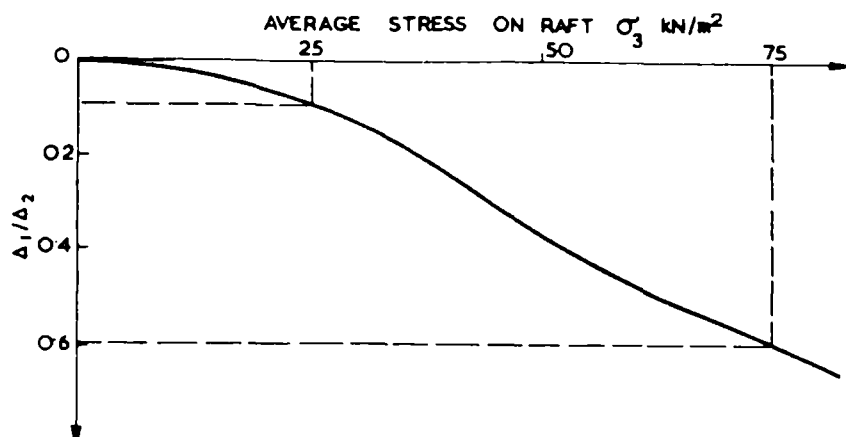
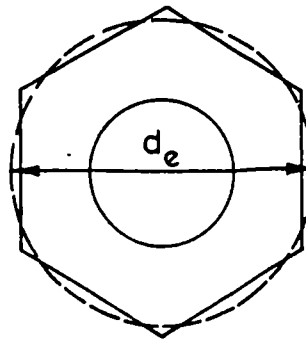
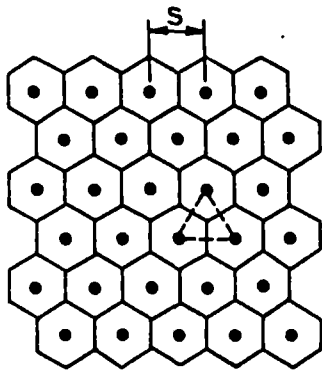


Fig 1.18: The load: settlement reduction relationship of a stone column reinforced foundation (after Hughes & Withers 1974)

Pile Spacing

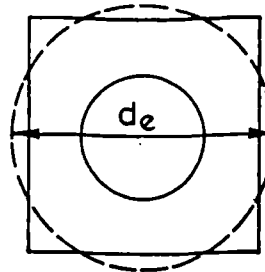
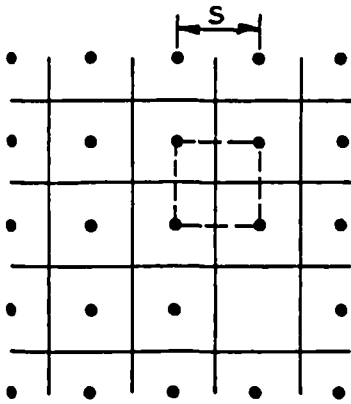


$$d_e = \left(\frac{12}{\pi^2} \right)^{1/4} s$$

$$= 1.05s$$

(a) Triangular Arrangement of Stone Columns

Pile Spacing

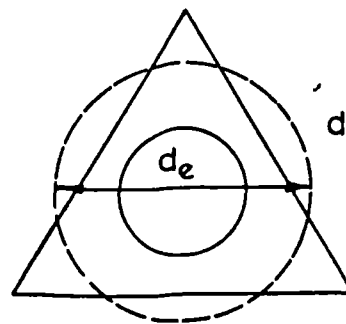
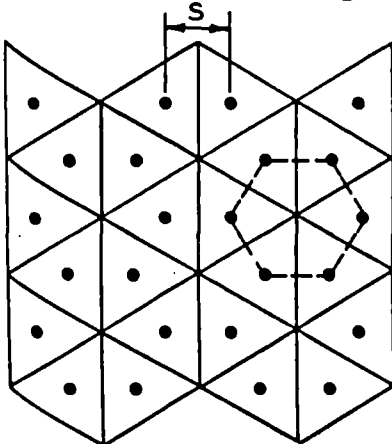


$$d_e = \left(\frac{16}{\pi^2} \right)^{1/4} s$$

$$= 1.13s$$

(b) Square Arrangement of Stone Columns

Pile Spacing



$$d_e = \left(\frac{27}{\pi^2} \right)^{1/4} s$$

$$= 1.29s$$

(c) Hexagonal Arrangement of Stone Columns

Fig 1.21: The equivalent unit cell (after Balaam 1983)

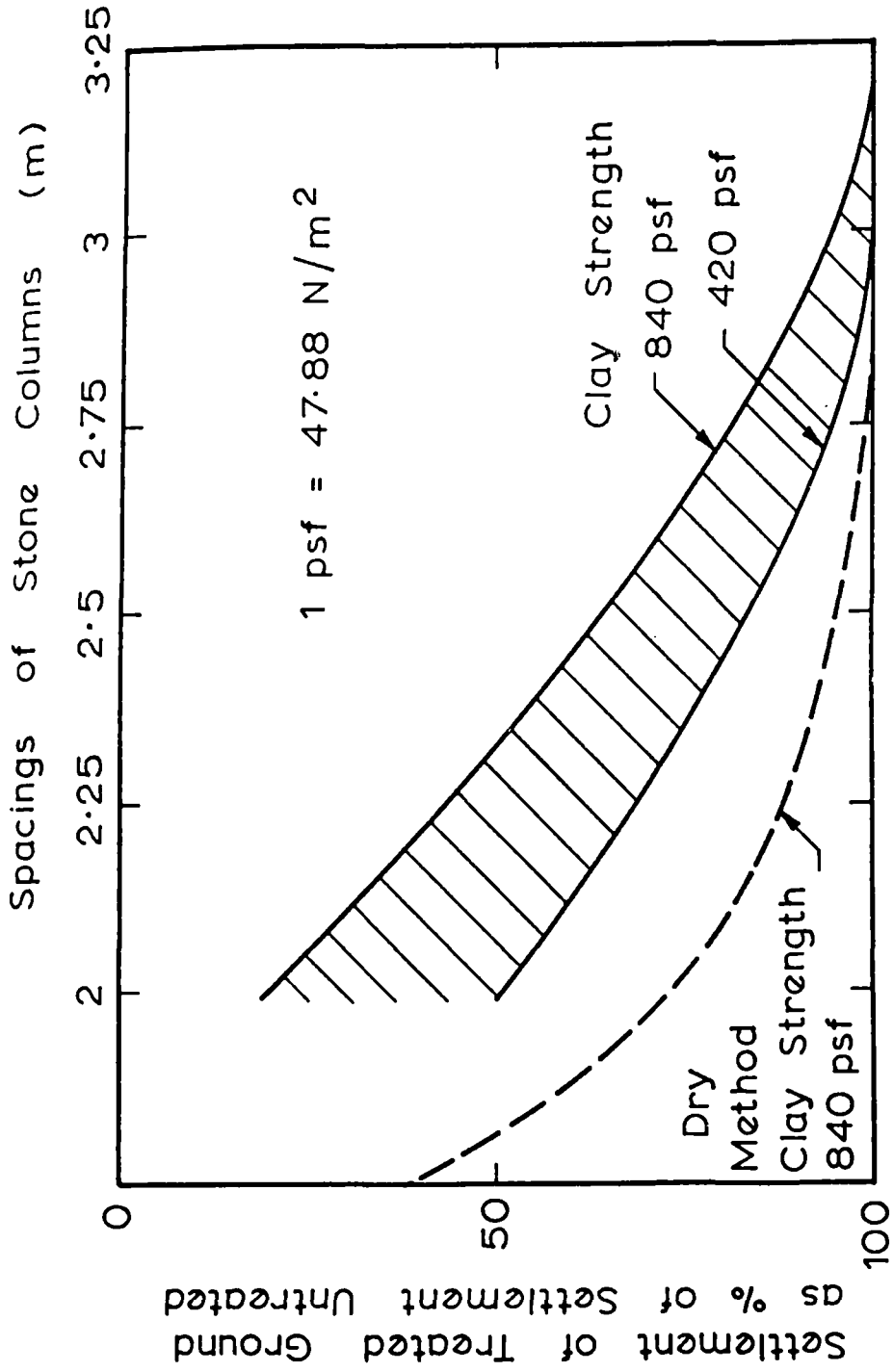
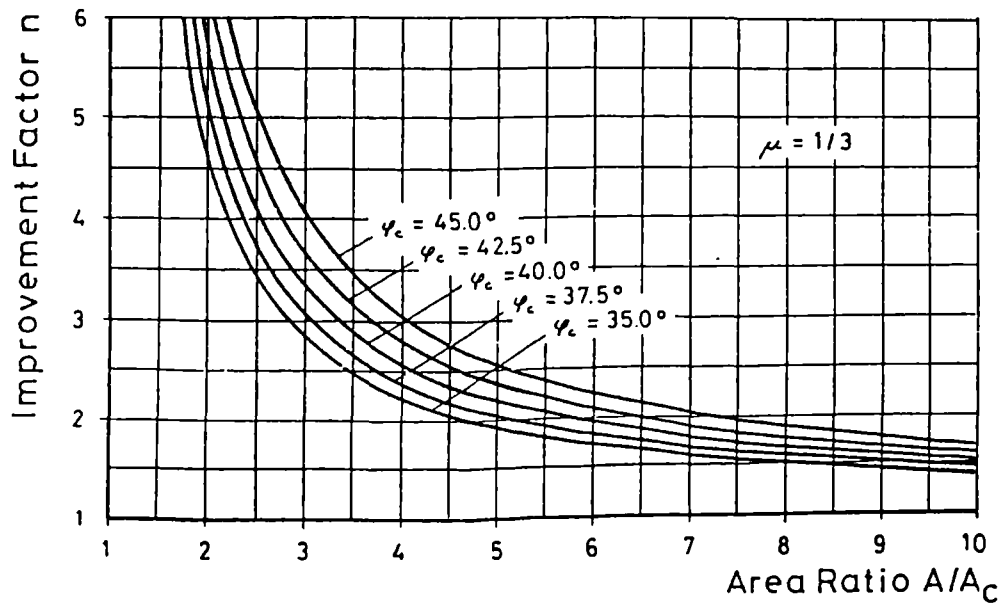
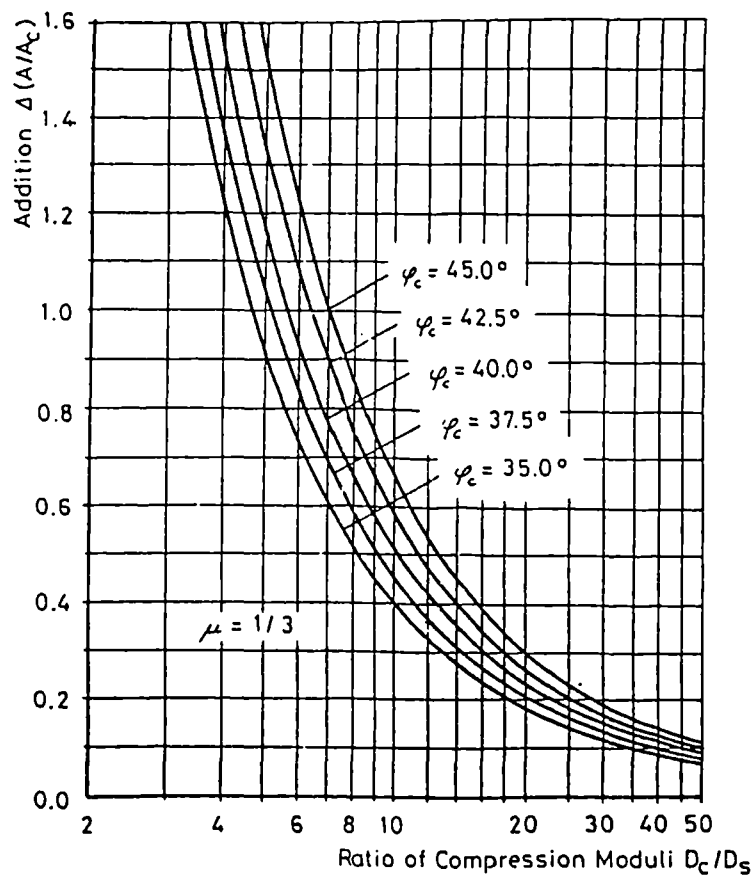


Fig 1.22: The relationship between column spacing and settlement reduction in a stone column reinforced foundation (after Greenwood 1970)

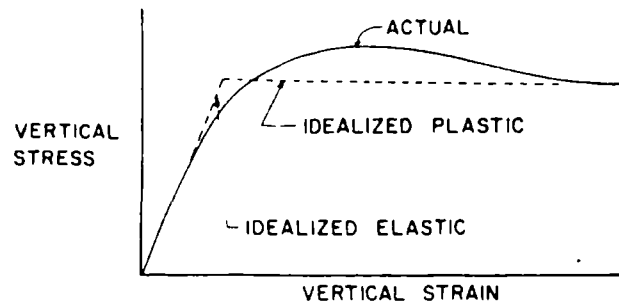


(a)

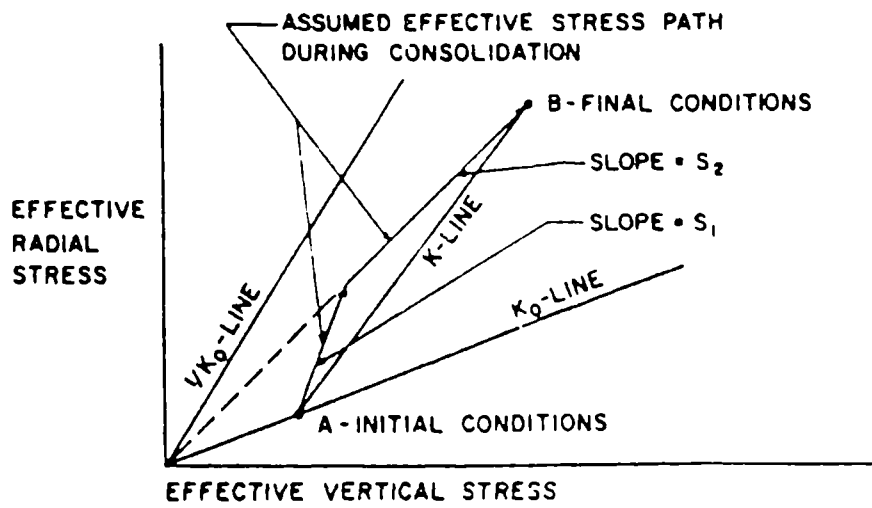


(b)

Fig 1.23: The basic diagrams used in Priebe's method (a) the influence of area ratio on the improvement factor; (b) the influence of the compressibility ratio between column and soil on the settlement reduction, after Priebe 1993



(a)



(b)

Fig 1.24: The basic diagrams used in Goughnour's method (a) The idealised stress-strain behaviour of the unit cell, (b) The assumed effective stress path in a unit cell during the loading, after Goughnour & Bayuk 1979a

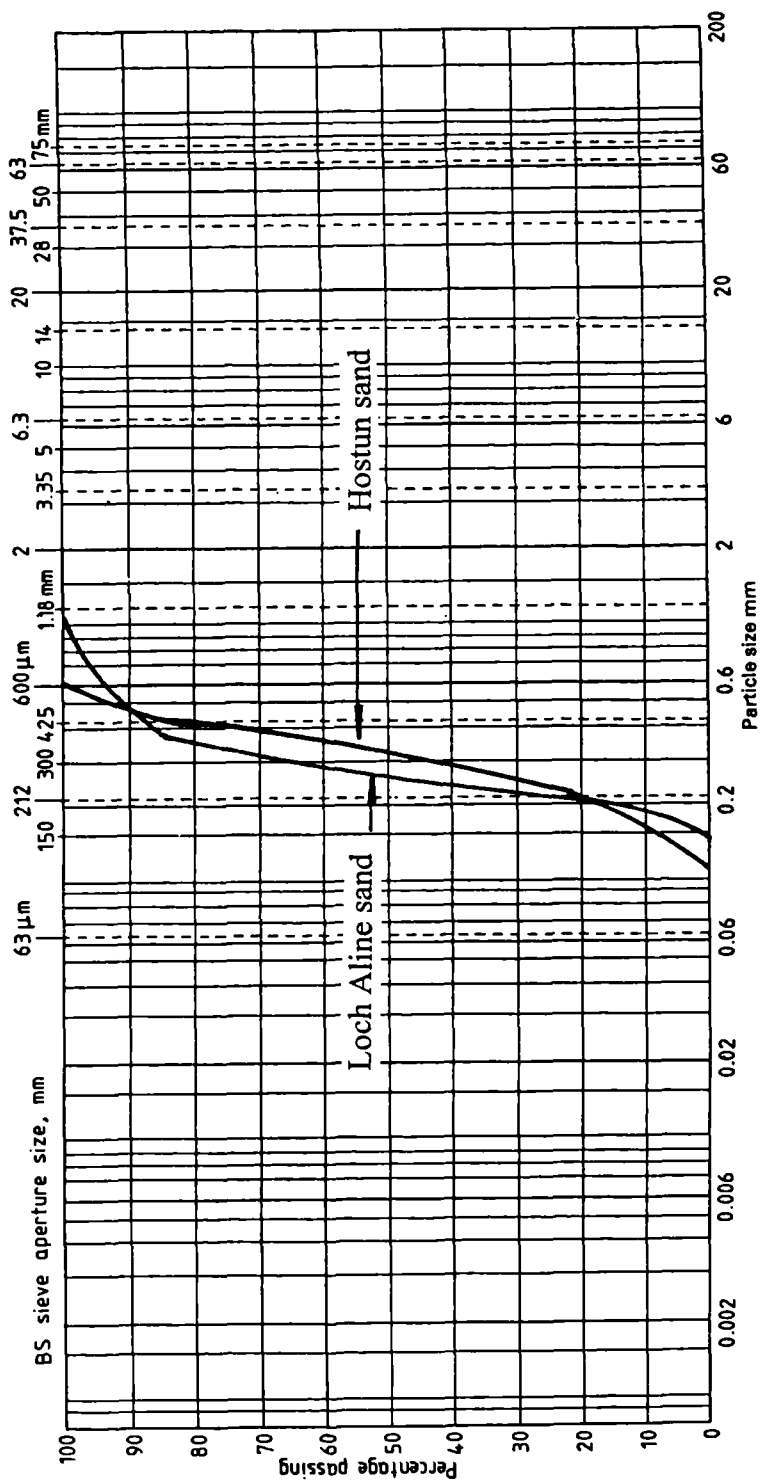


Fig 2.1: Particle size distribution

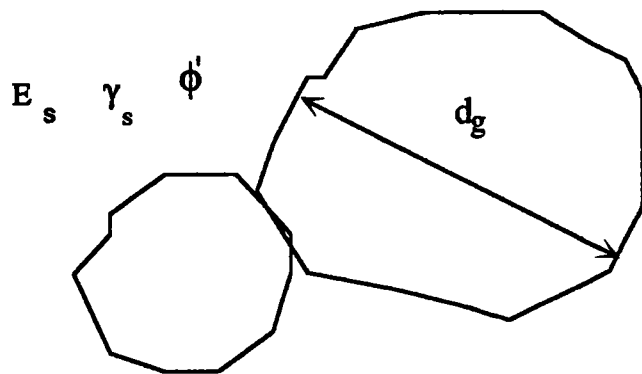
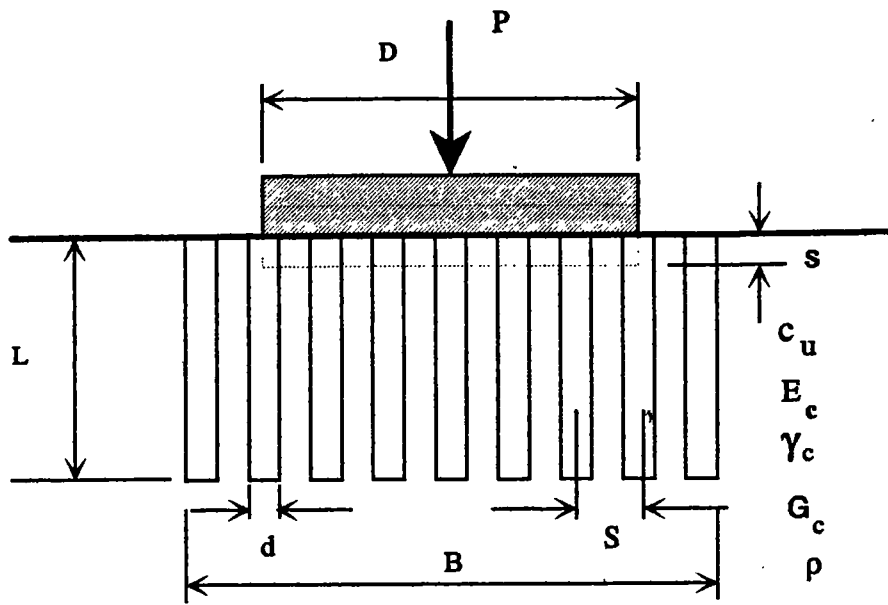


Fig 2.2: The setup of model stone column foundation

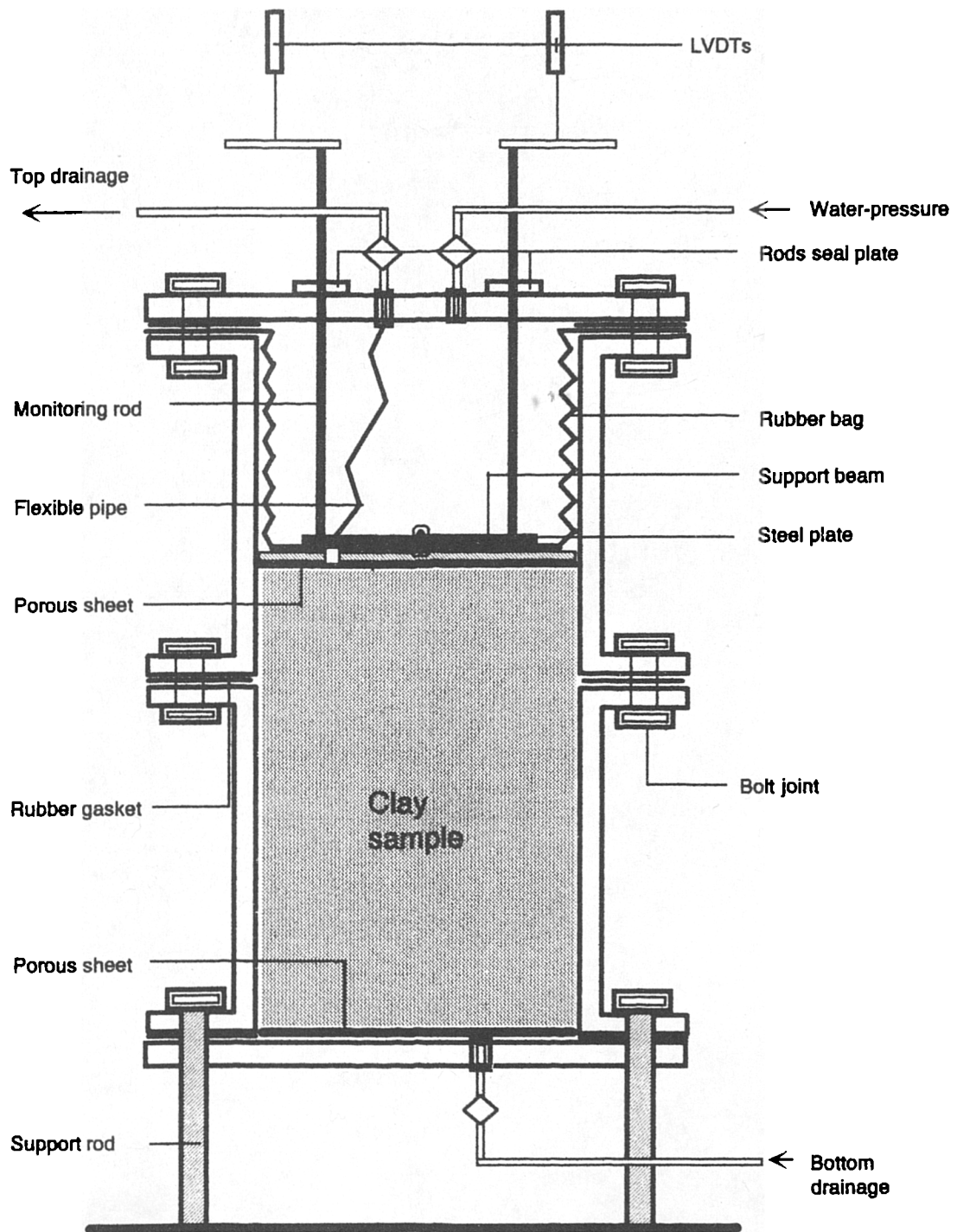


Fig 2.3: Consolidation tank (small tank, downwards)

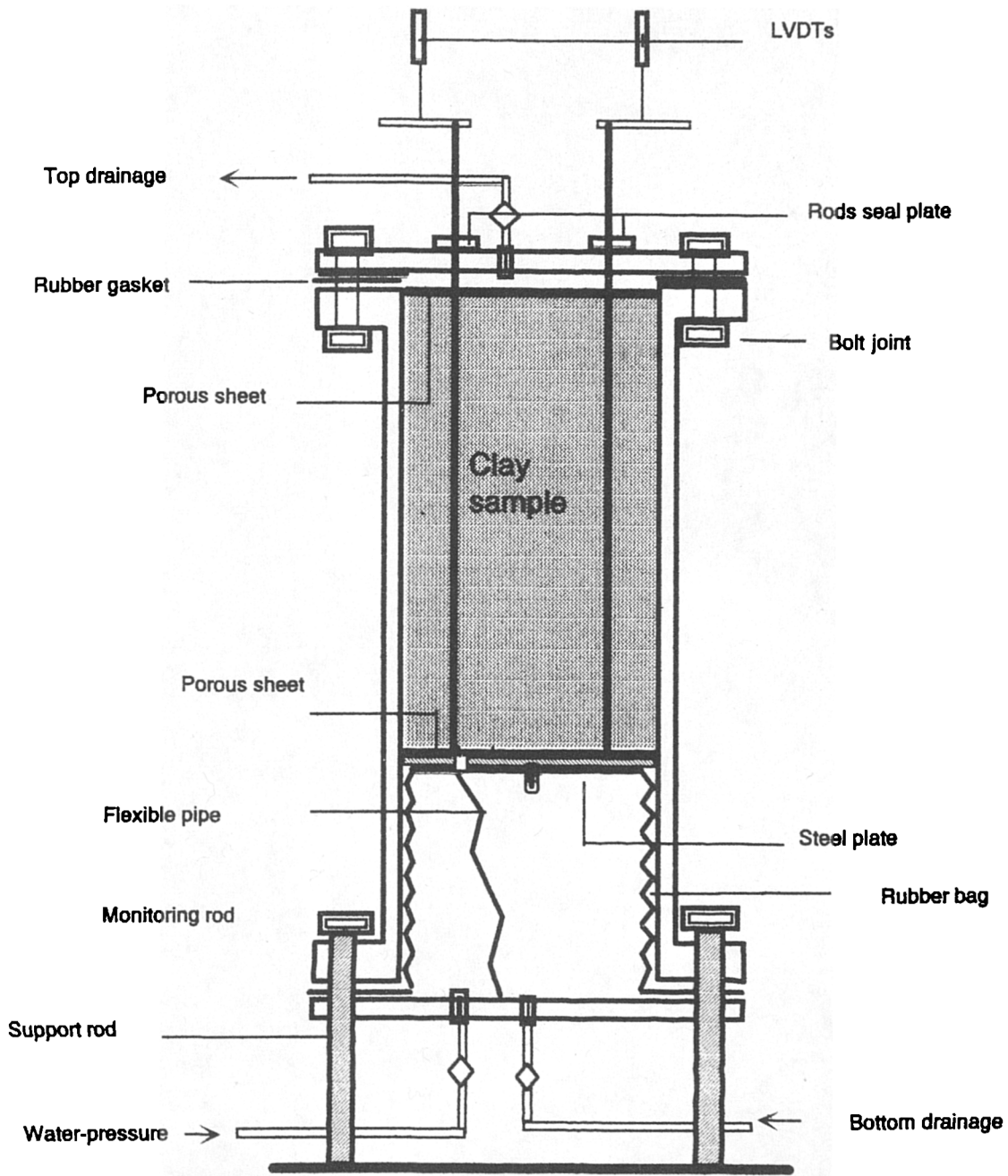
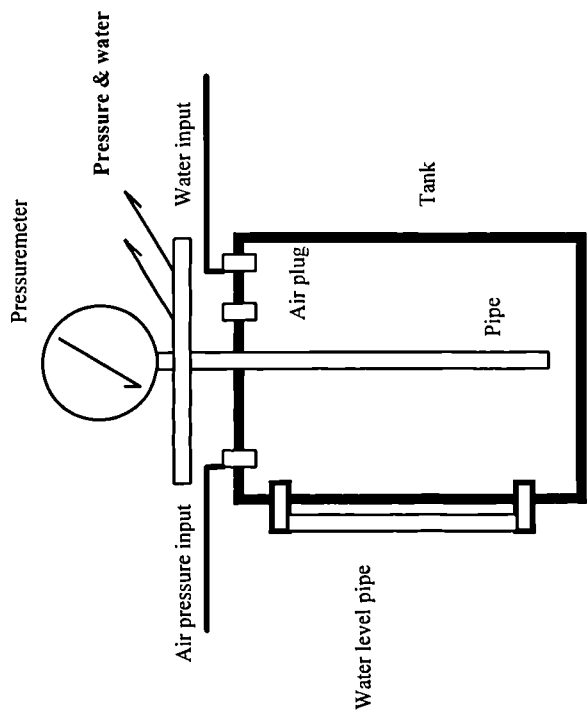
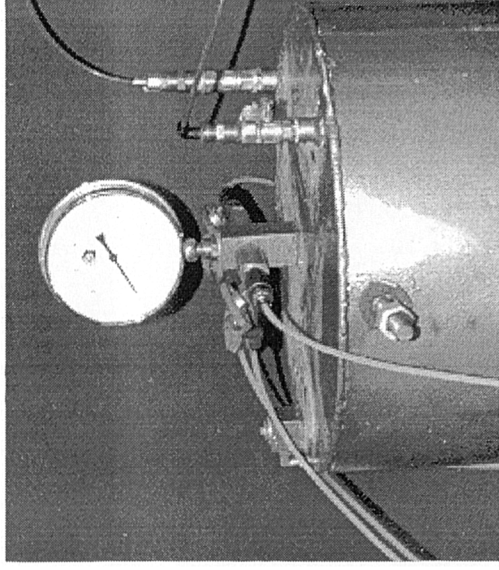


Fig 2.4: Consolidation tank (small & large tank, upwards)



(a)



(b)

Fig 2.5: The water and air-pressure interface tank (a) section (b) photograph of top of the interface tank

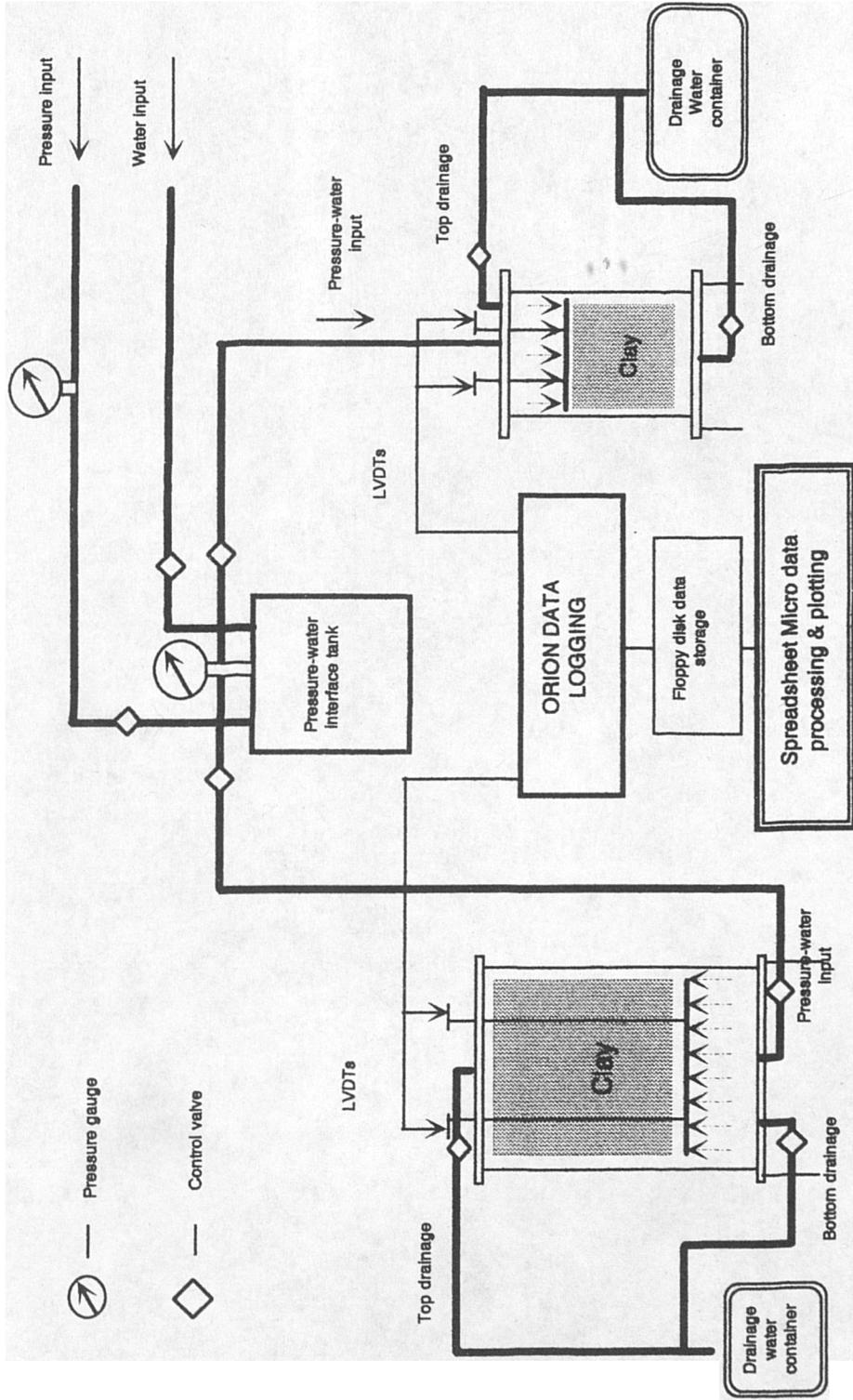


Fig 2.6: Schematic diagram of consolidation system

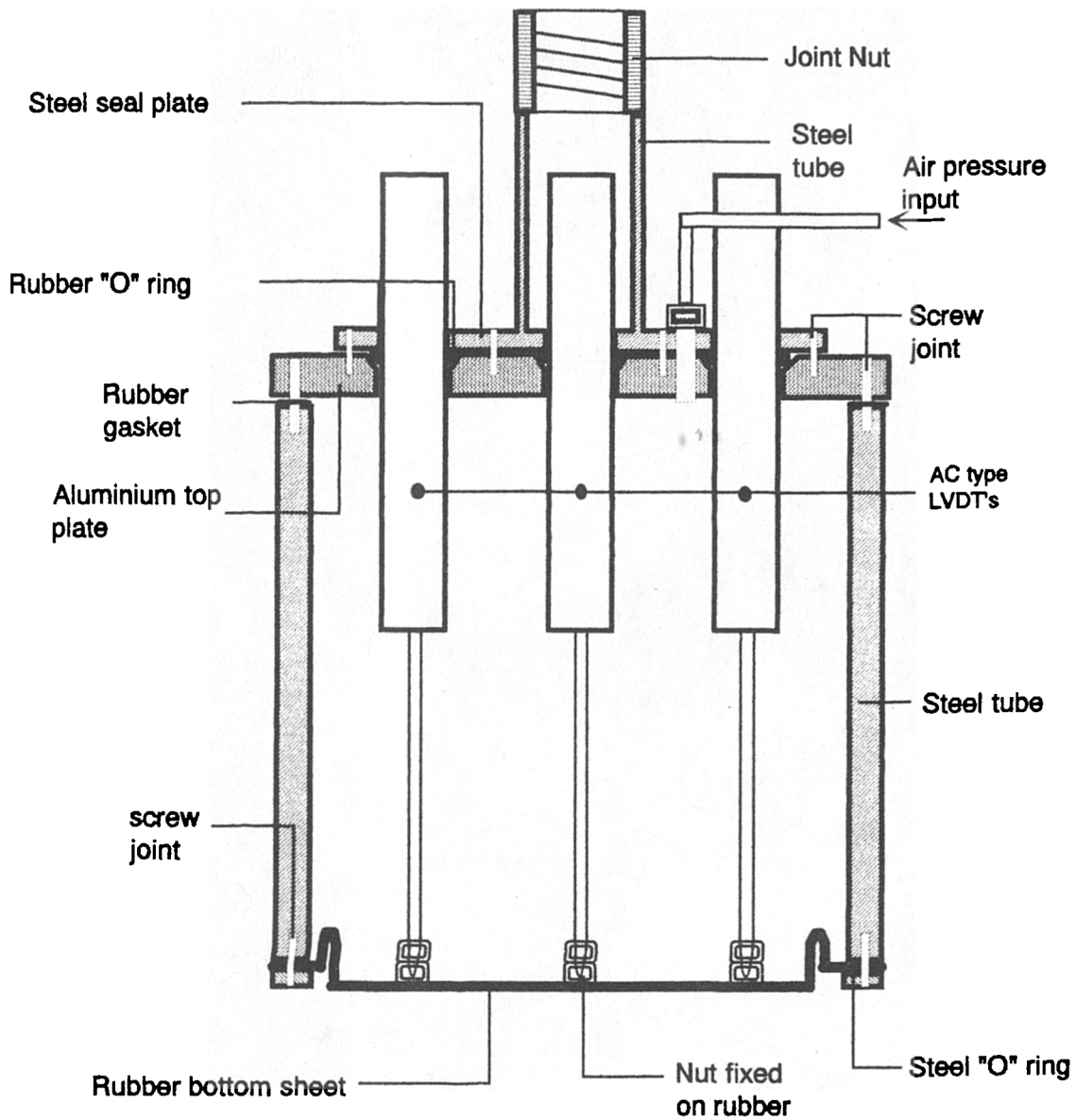


Fig 2.7: The flexible loading device

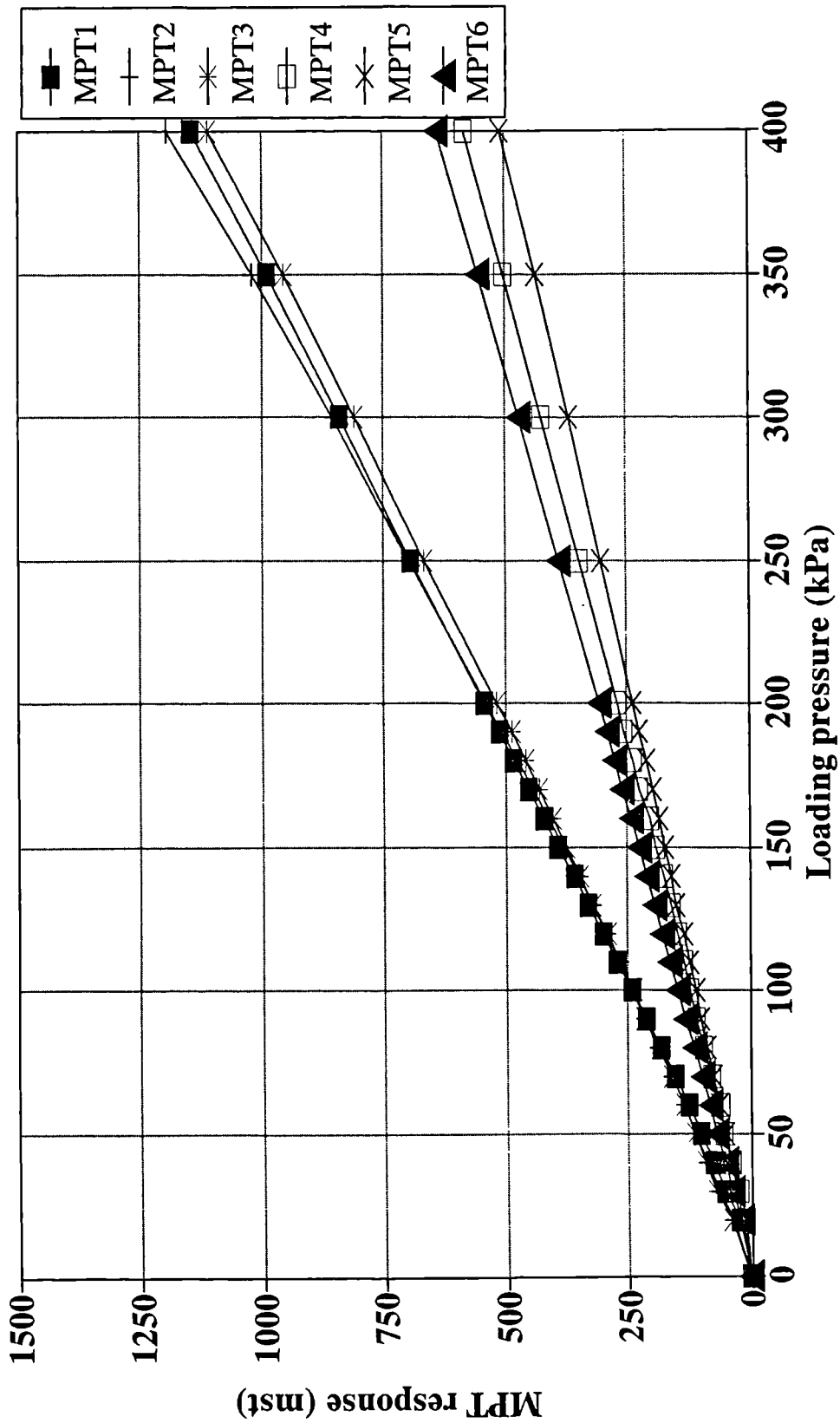


Fig 2.8: Response from miniature pressure transducers during calibration

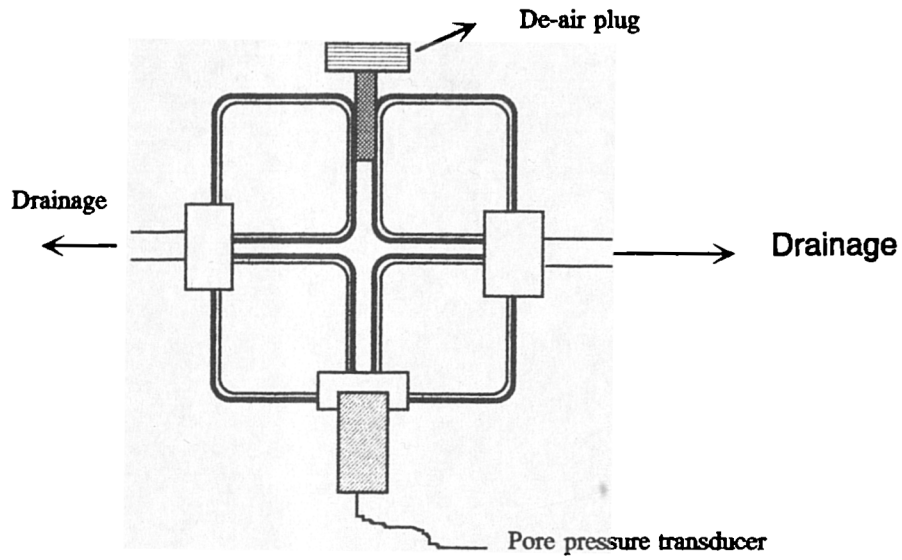


Fig 2.9: The pore pressure transducer and mounting block

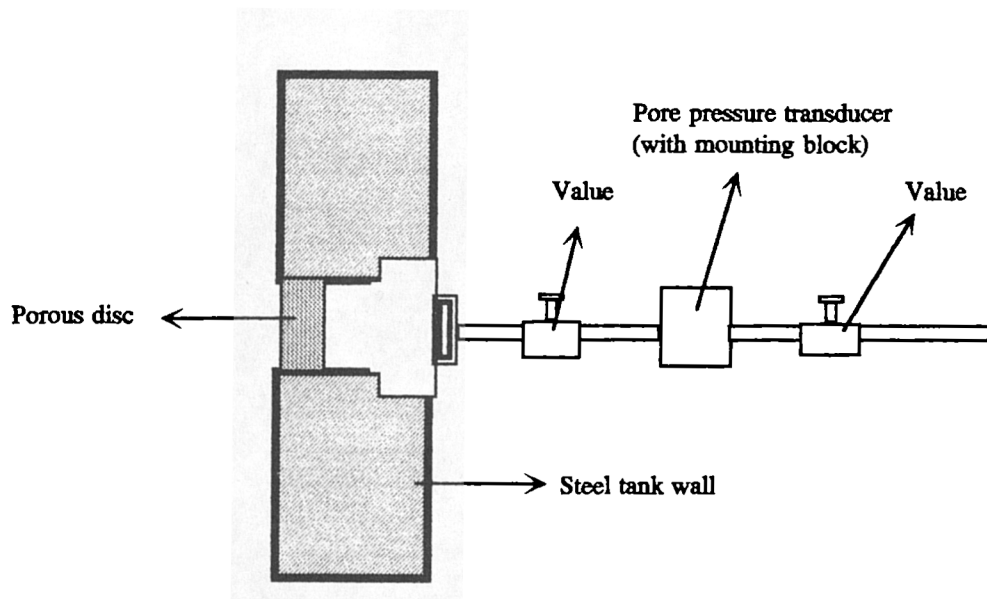
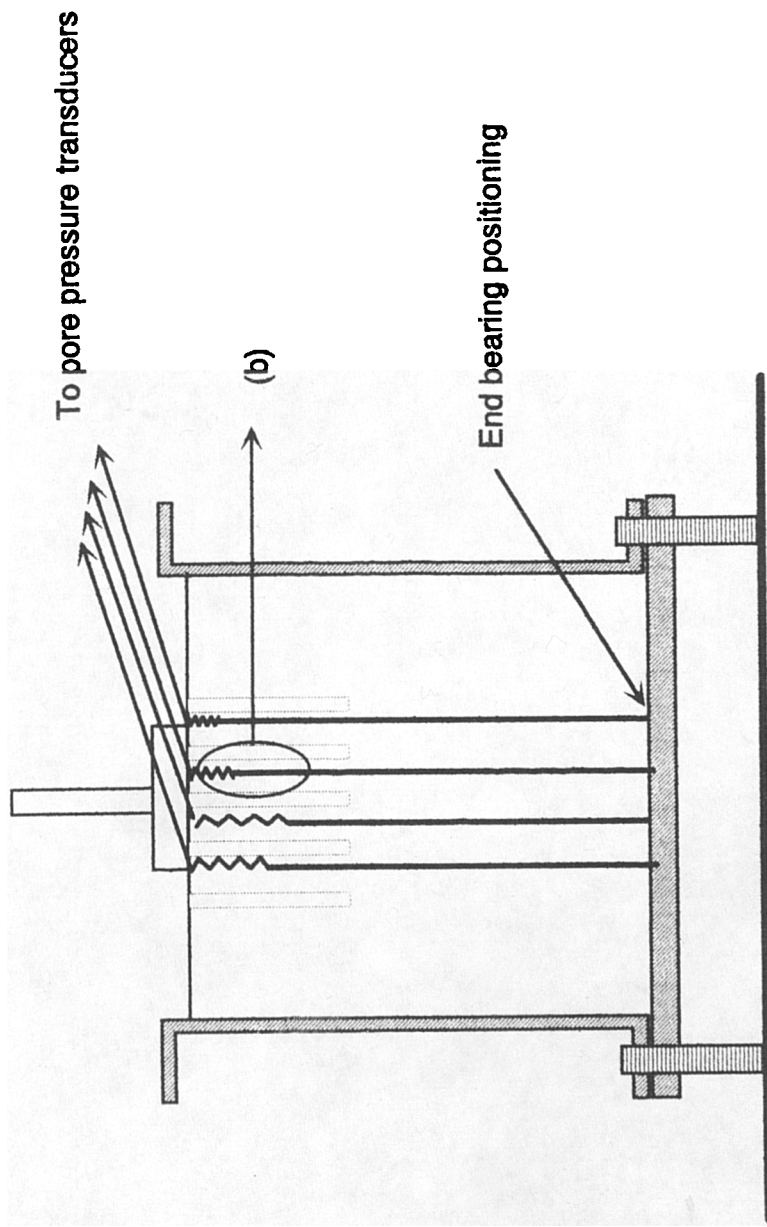
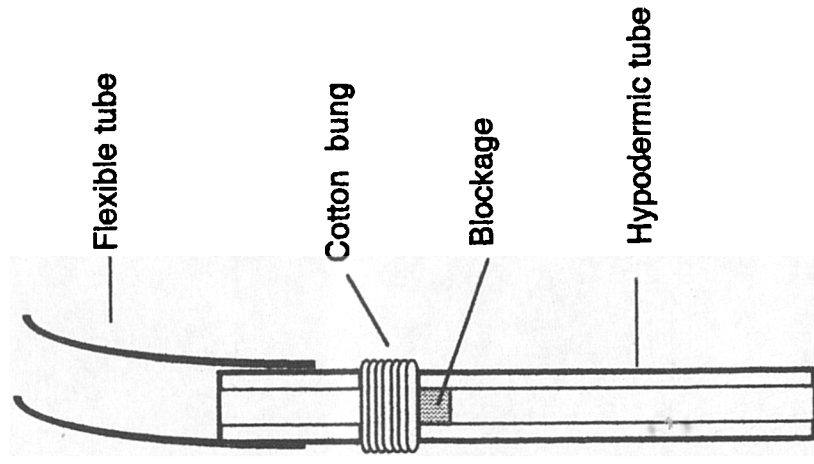


Fig 2.10: Mounting arrangement for pore pressure transducer in consolidation tank



(a)



(b)

Fig 2.11: Pore pressure measurement using hypodermic tube

(a): In-situ setup ; (b): The detail of the tube/clay interface

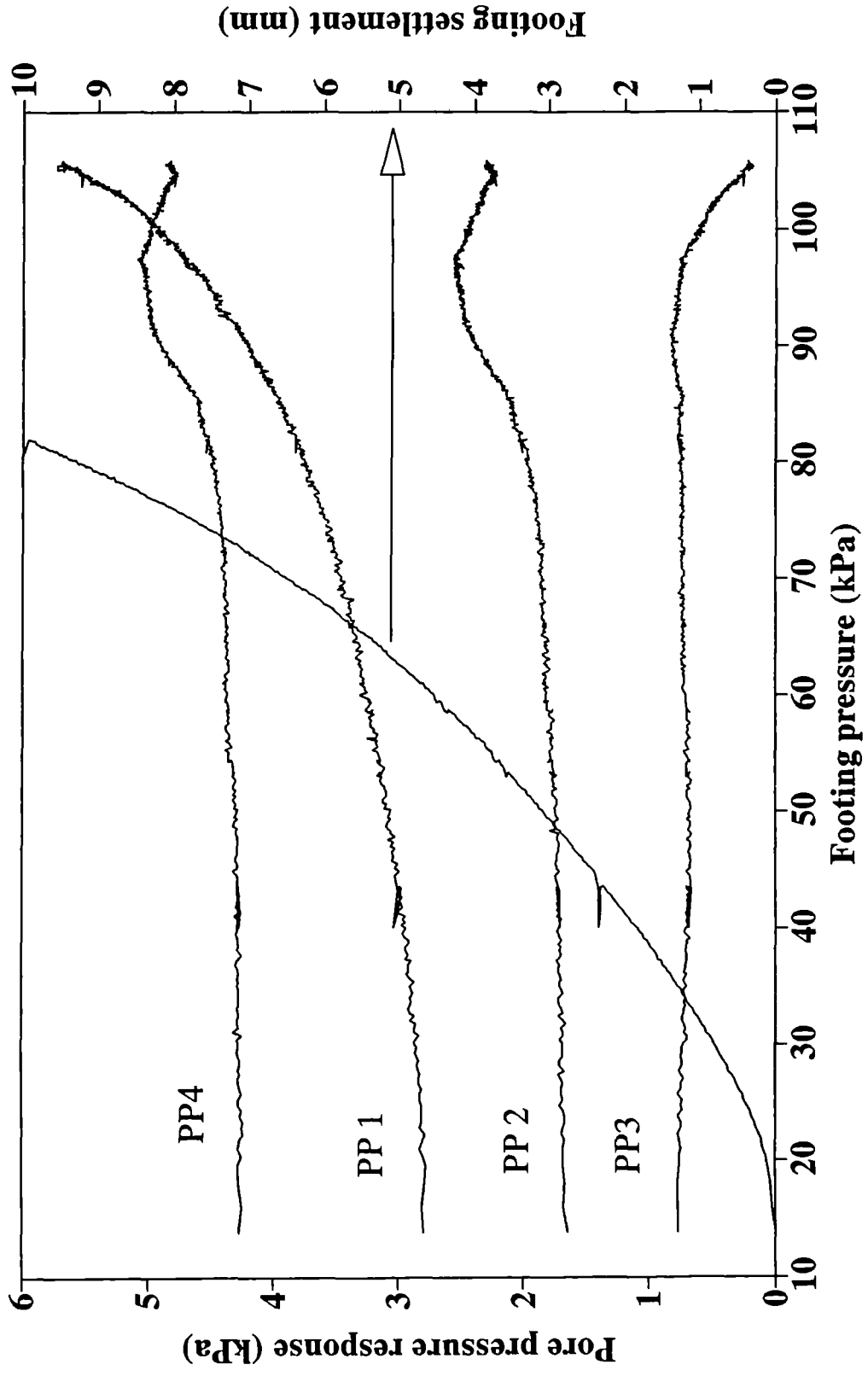
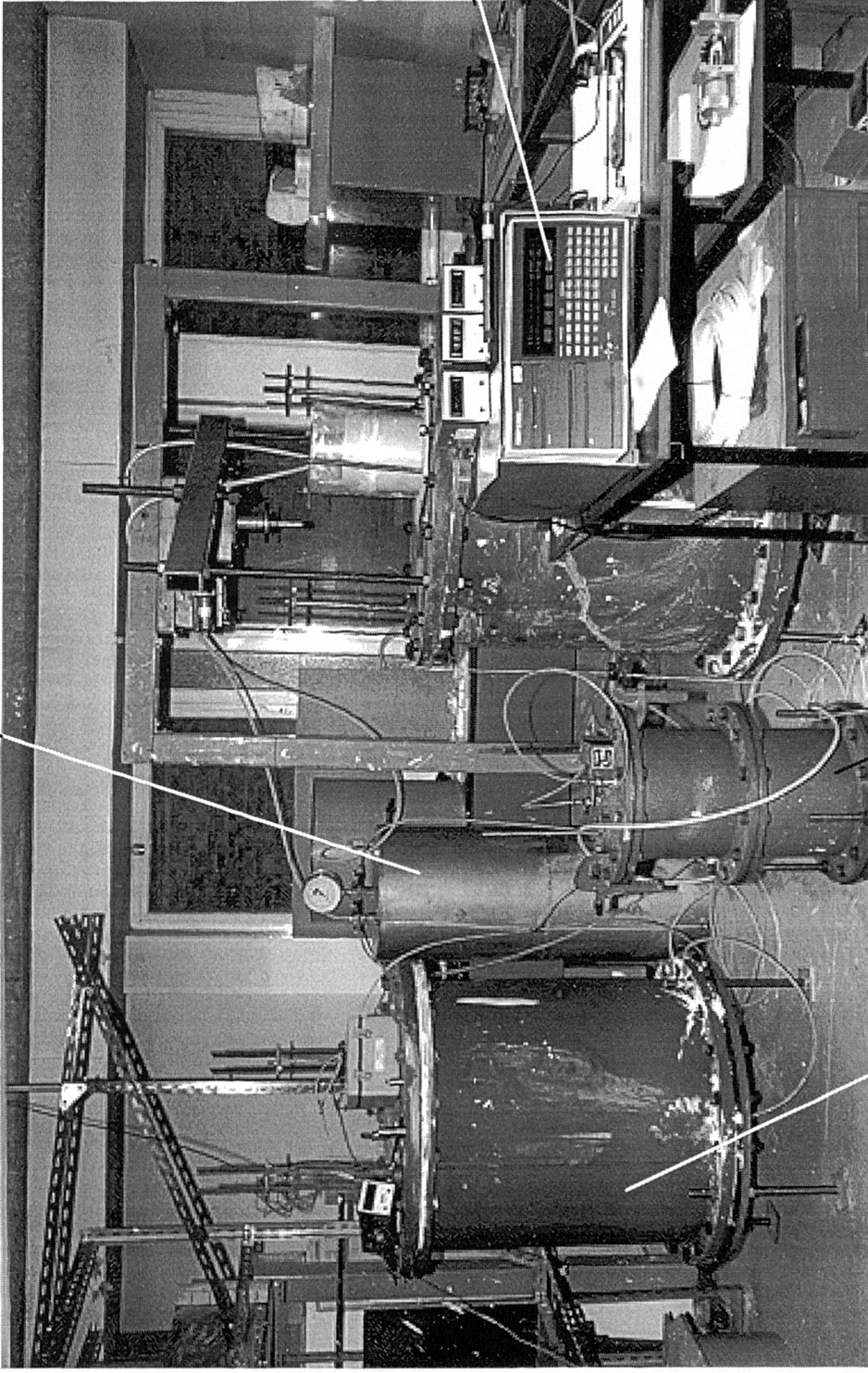


Fig 2.12: Pore pressure response from hypodermic tubes (test TS05)

Water pressure interface tank



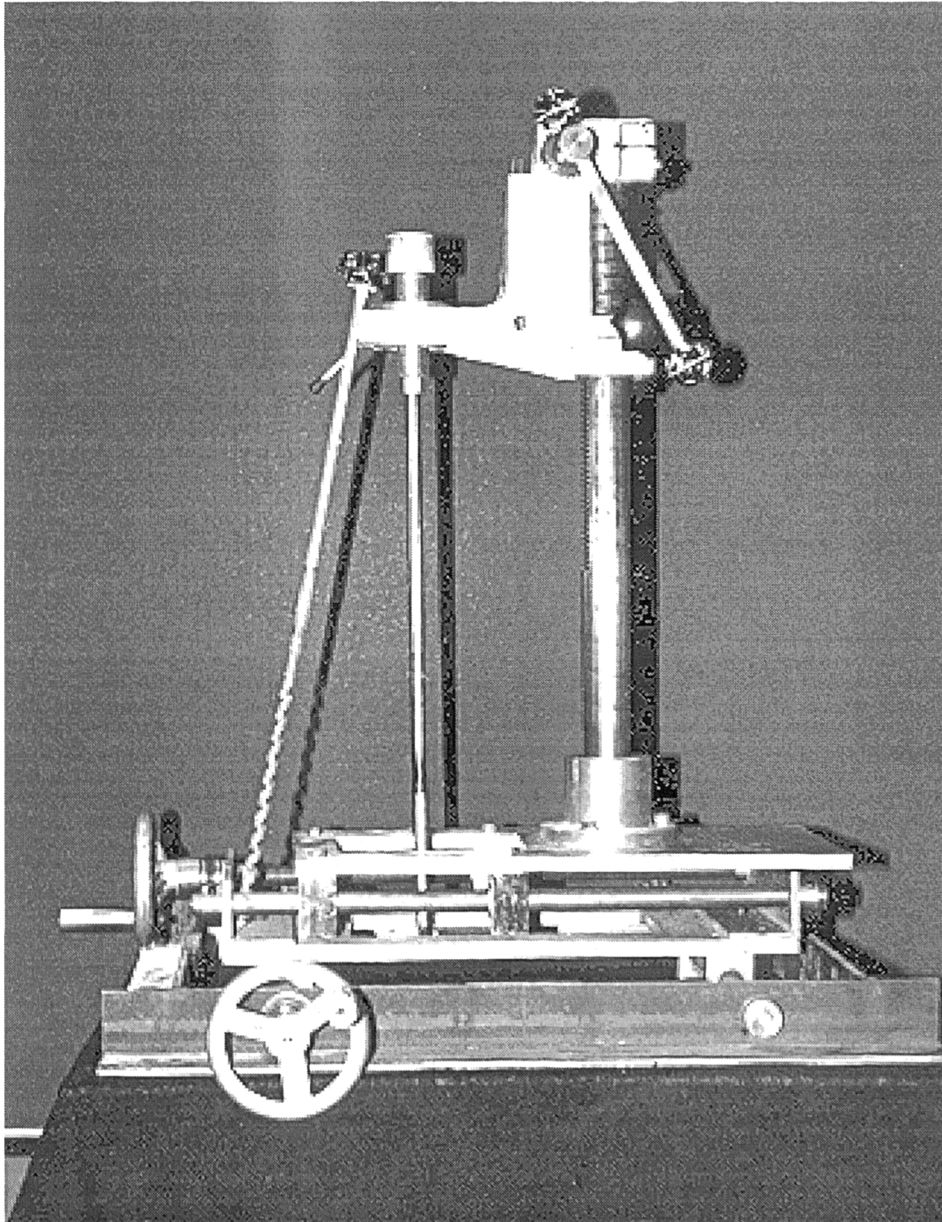
Data logging

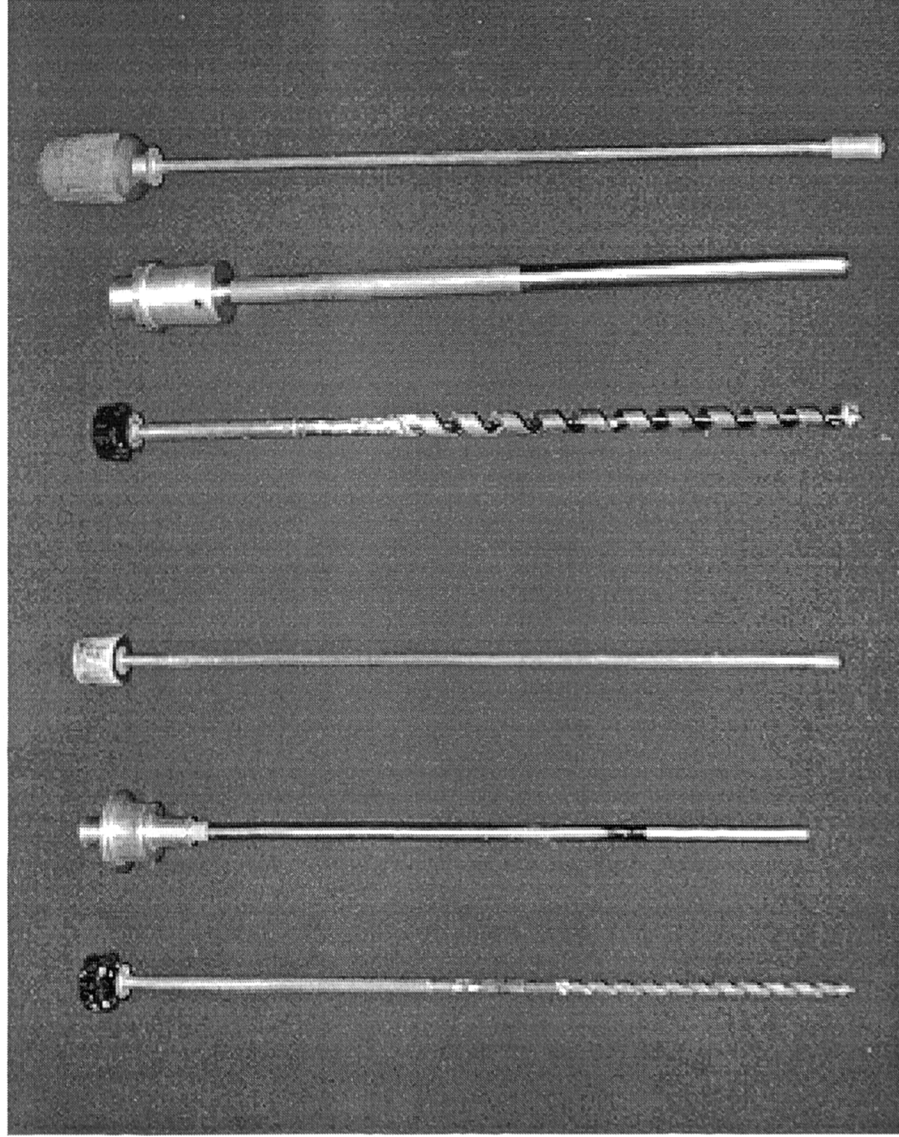
Large tank

Small tank

Plate 2.1: The consolidation system

Plate 2.2: The drilling rig and the frame





(a)

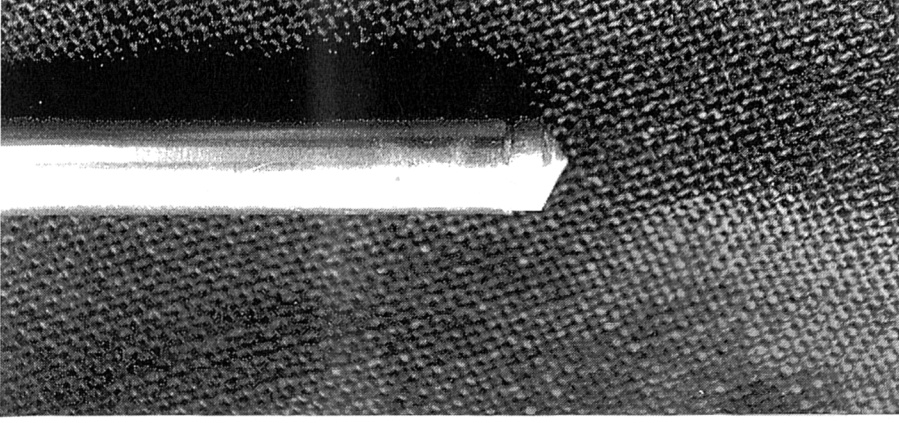
(b)

(c)

(a')

(b')

(c')



(d)

Plate 2.3: Tools used for column construction (a) & (a') auger; (b) & (b') stainless steel tube; (c) & (c') brass plug with conical tip; (d) tube and conical tip

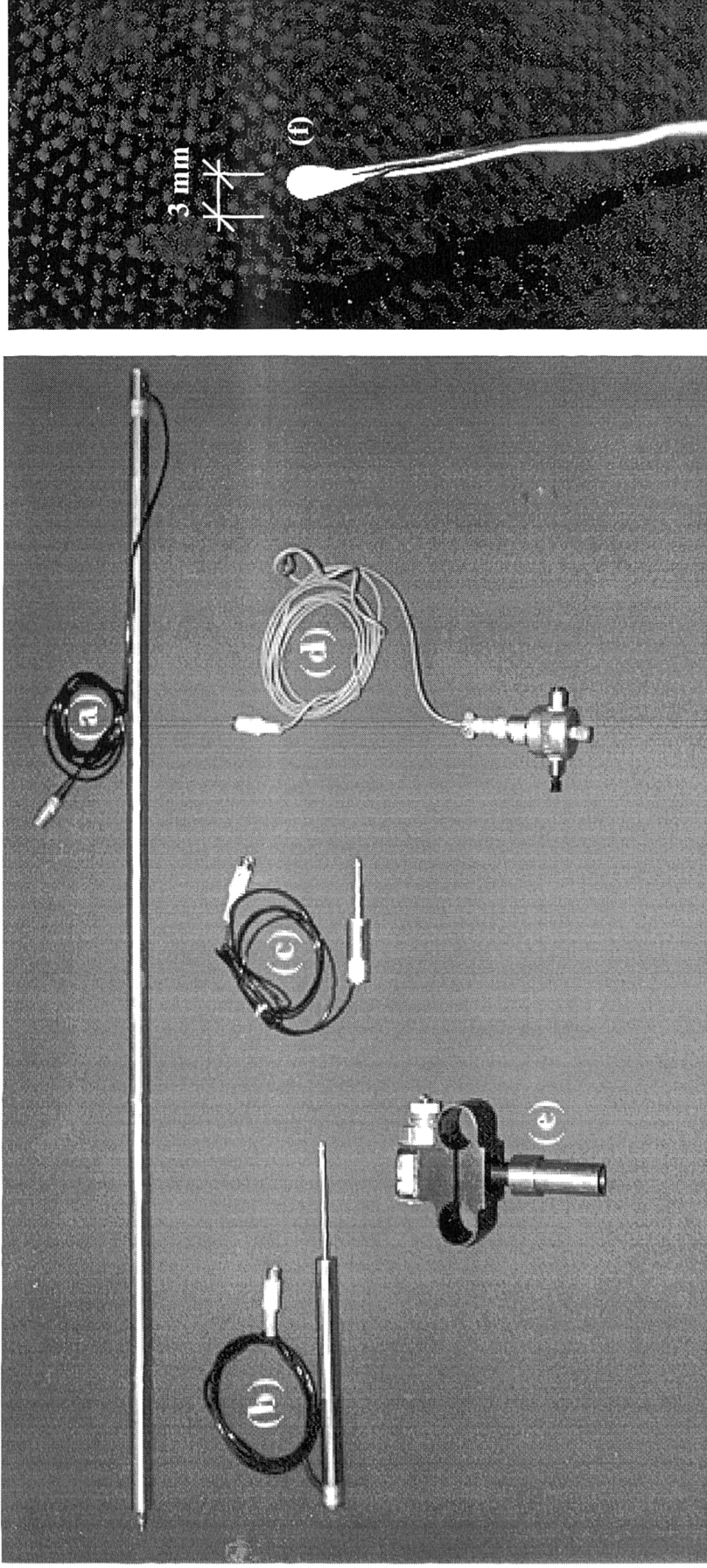
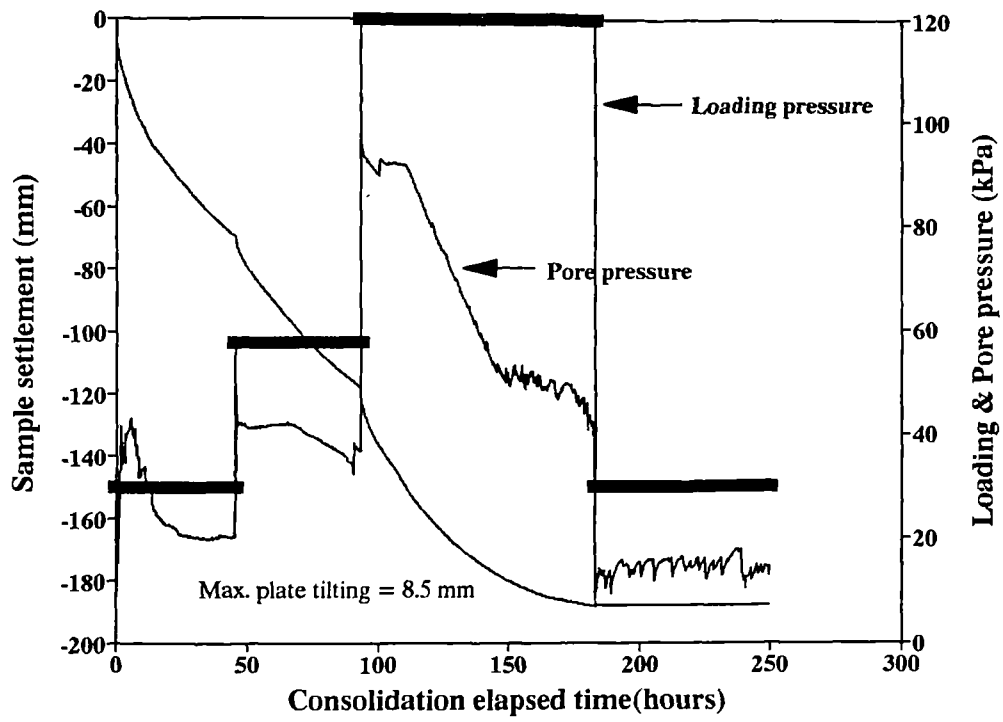
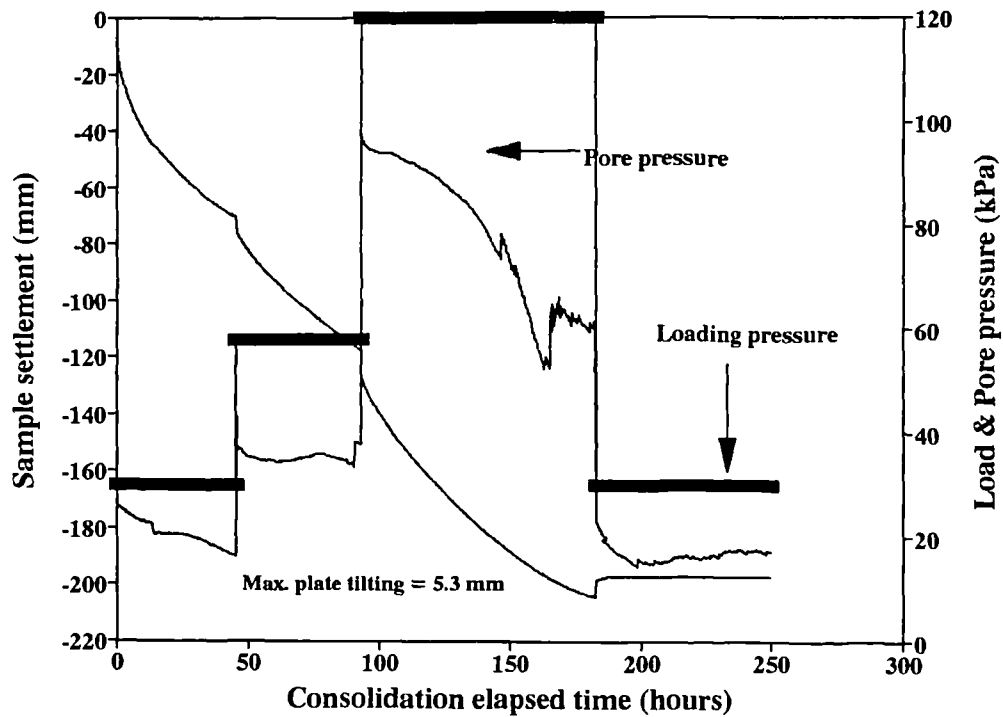


Plate 2.4: Transducers and load cells (a) LVDT 500 mm stroke; (b) LVDT 200 mm stroke; (c) LVDT 50 mm stroke; (d) pore pressure transducer with mounting block; (e) load cell; (f) miniature pressure transducer

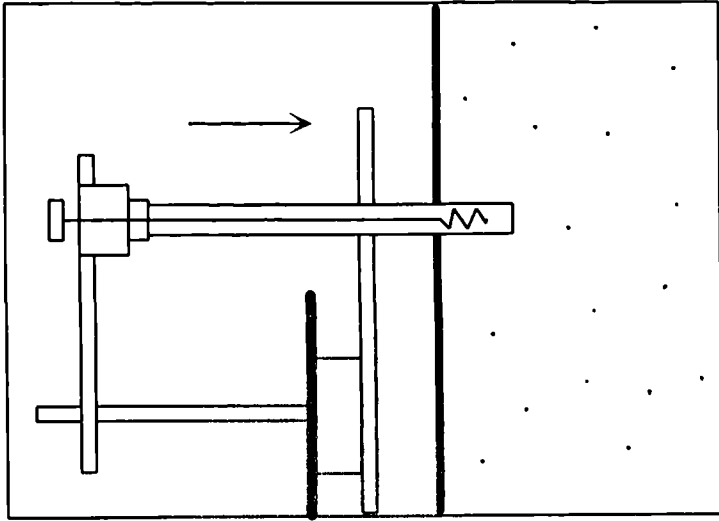


(a)

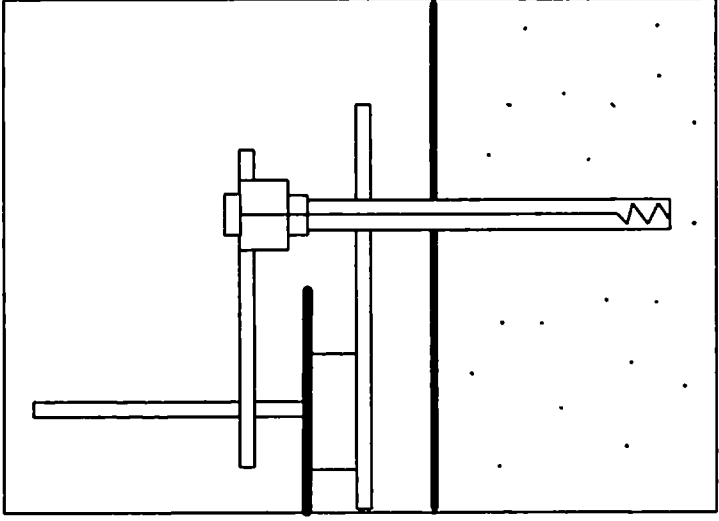


(b)

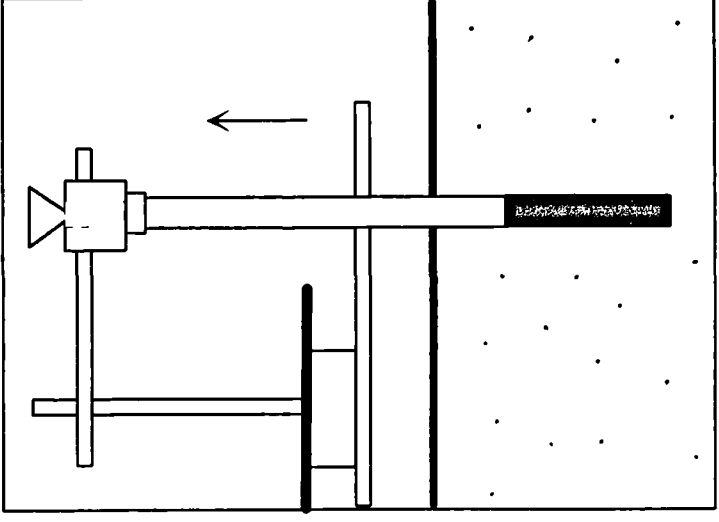
Fig 3.1: Typical load-time-settlement relationship during slurry consolidation
 (a): TS05 initial $c_u = 10.5$ kPa; (b): TS07 initial $c_u = 8$ kPa



(a): Insert tube and exhume the clay by an auger

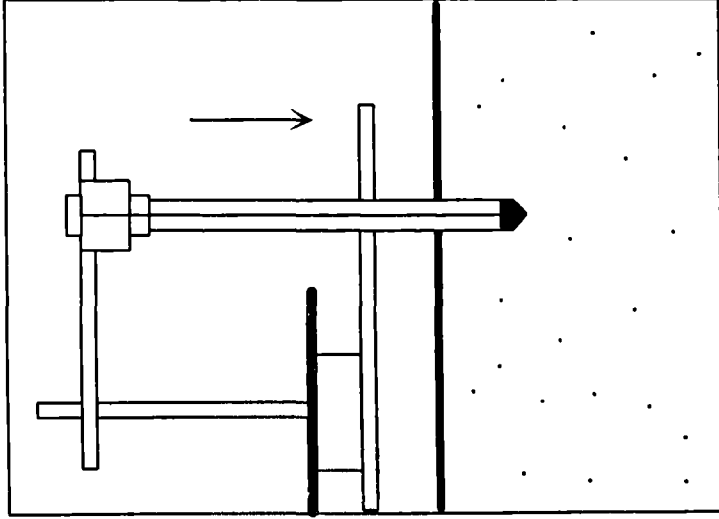


(b): Form a lined hole in the clay bed

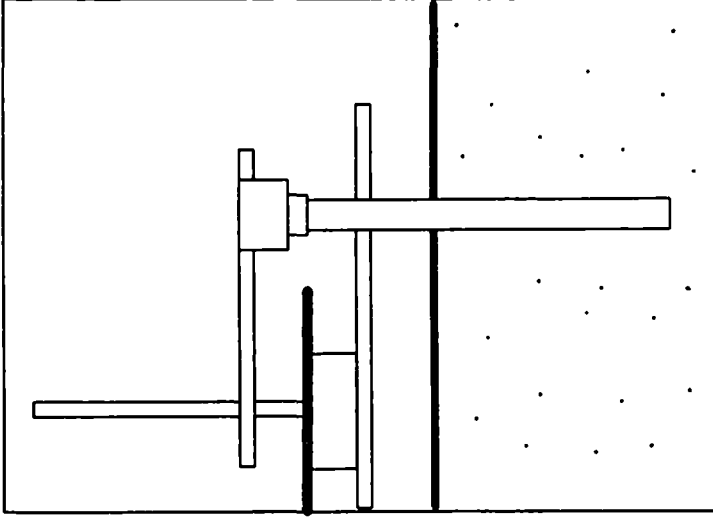


(c): Withdrawn the tube and freely fall the sand to form a column

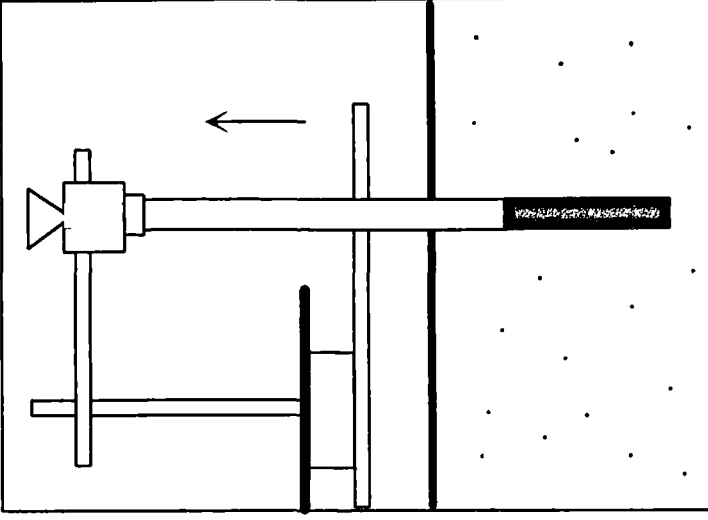
Fig 3.2: Installing a column using a replacement method.



(a): Insert tube together with a plug with a conical end into the clay bed



(b): Plug removed and left a lined hole in the clay bed



(c): Withdrawn the tube and freely fall the sand to form a column

Fig 3.3: Installing a column using a displacement method

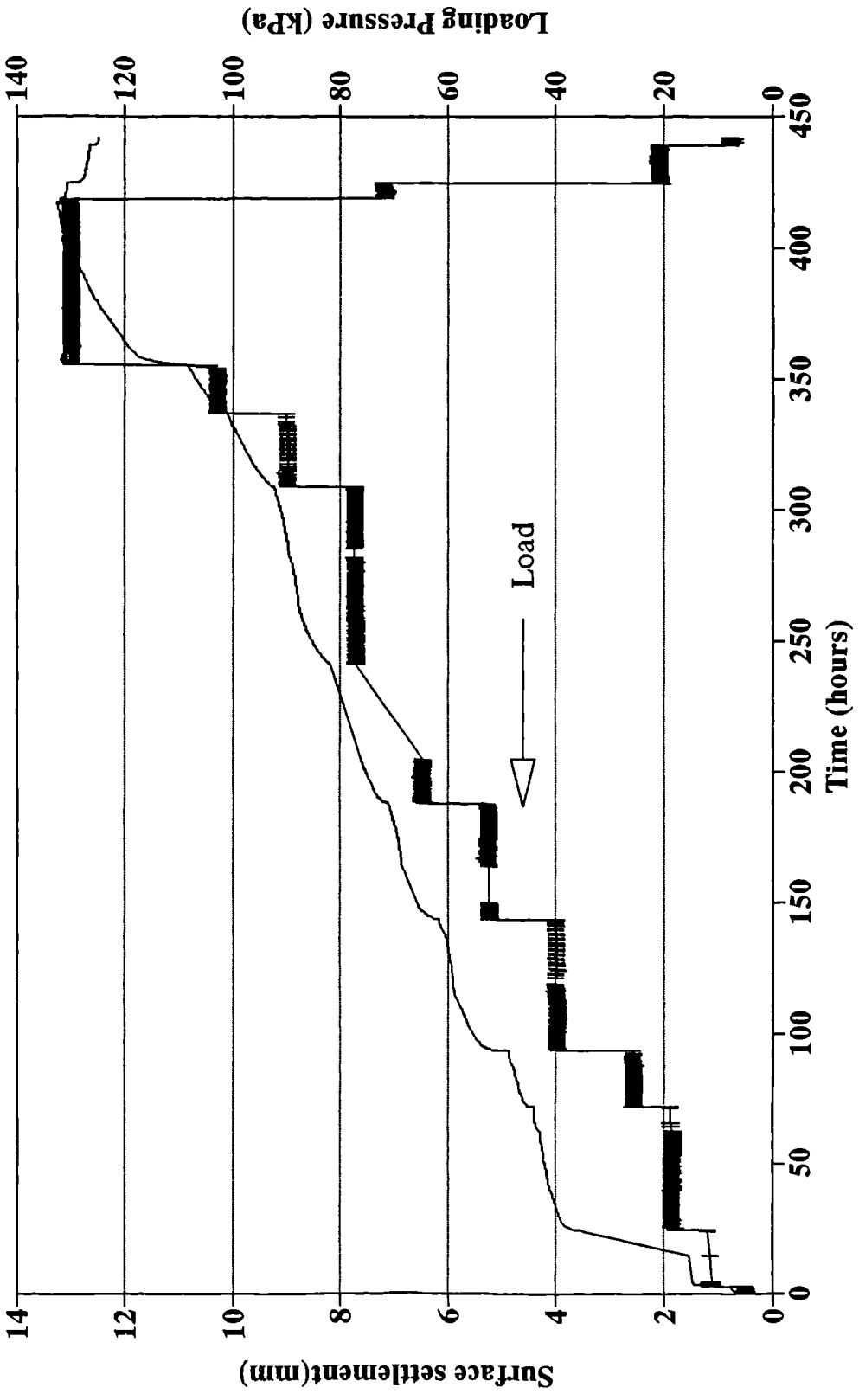


Fig 3.4 Load : time : settlement response from incremental loading test (pilot test TS01)

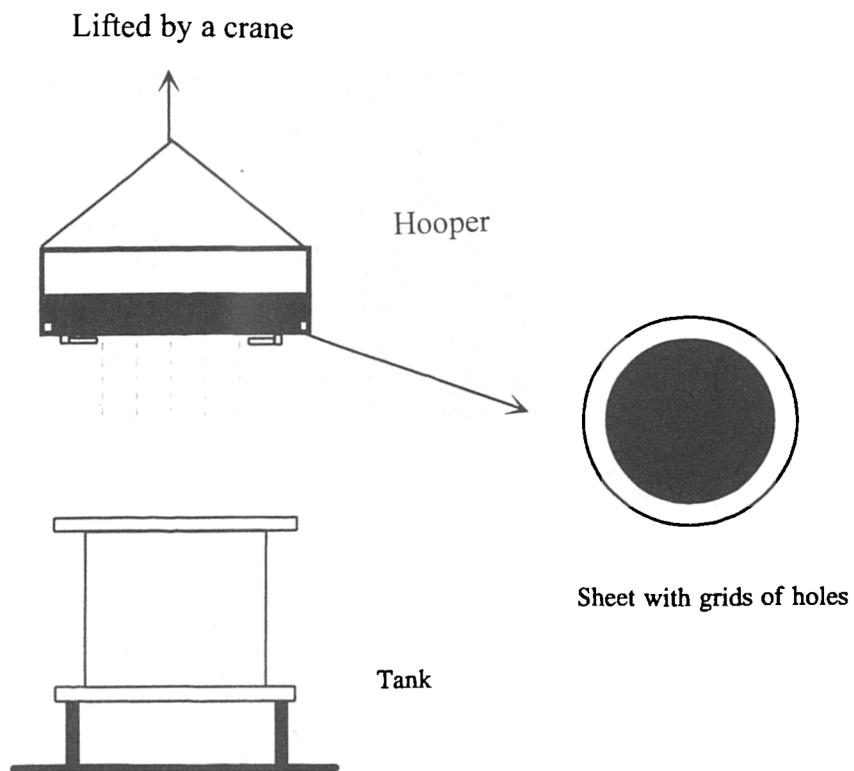


Fig 3.5: Sand raining system

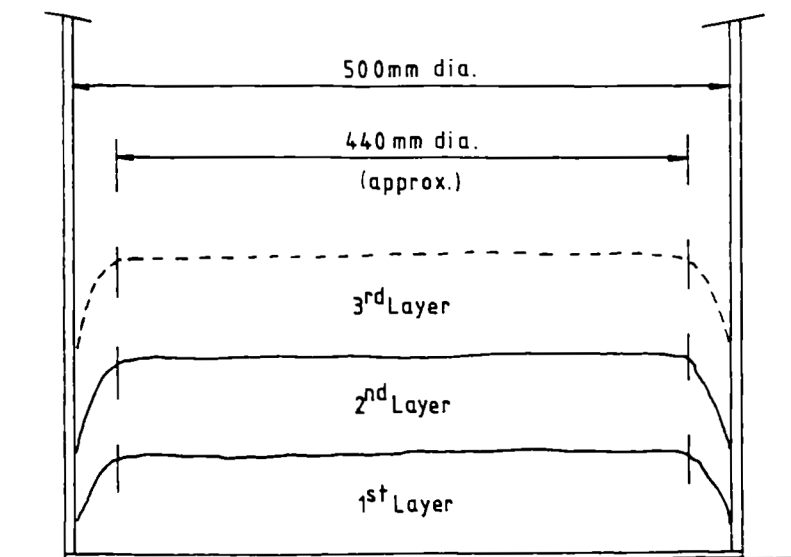


Fig 3.6: Shape of sand layers in medium dense sand bed (after Stewart 1988)

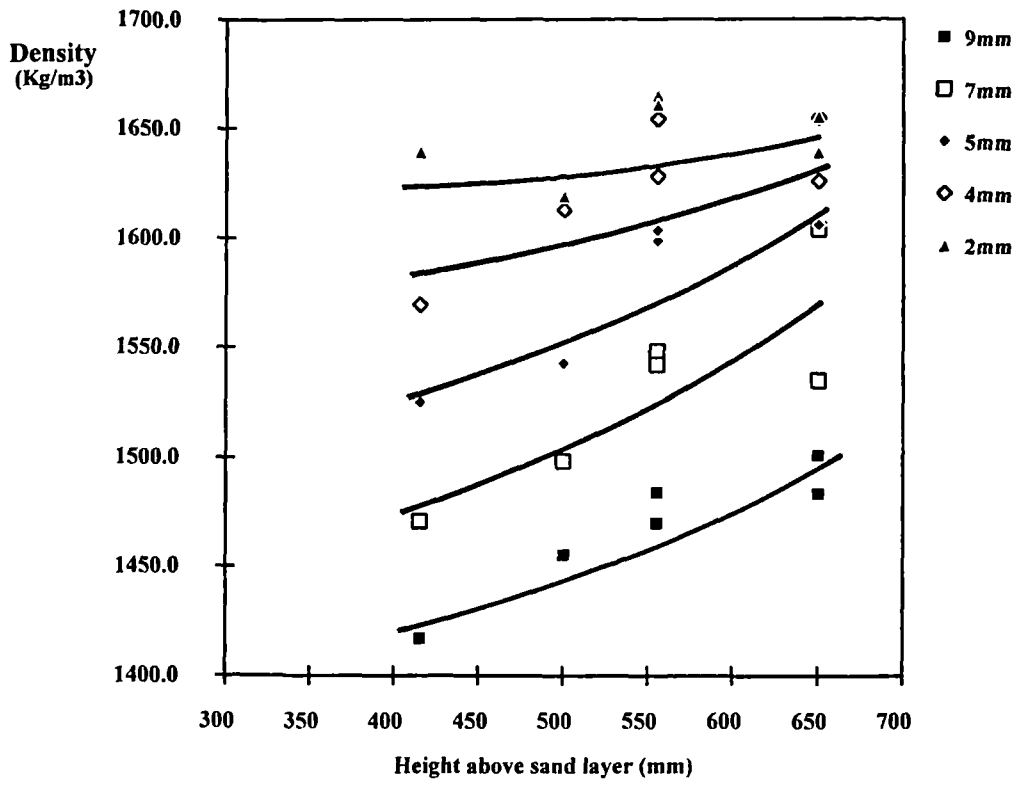


Fig 3.7: Effect of the grid diameter on the density of the sand beds

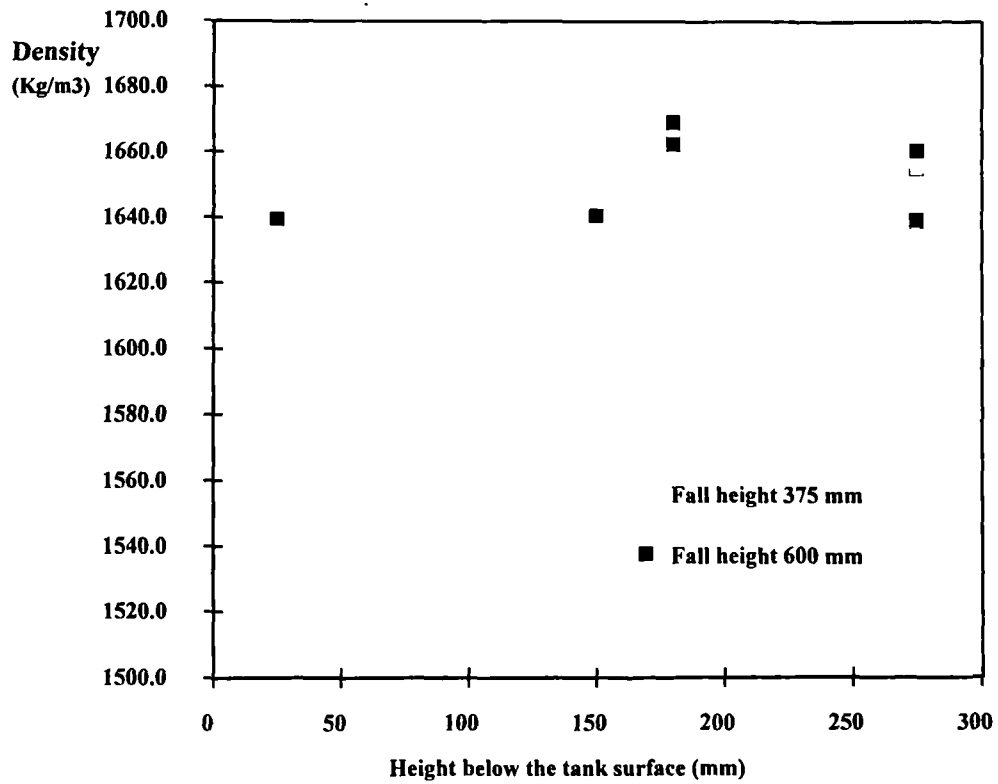
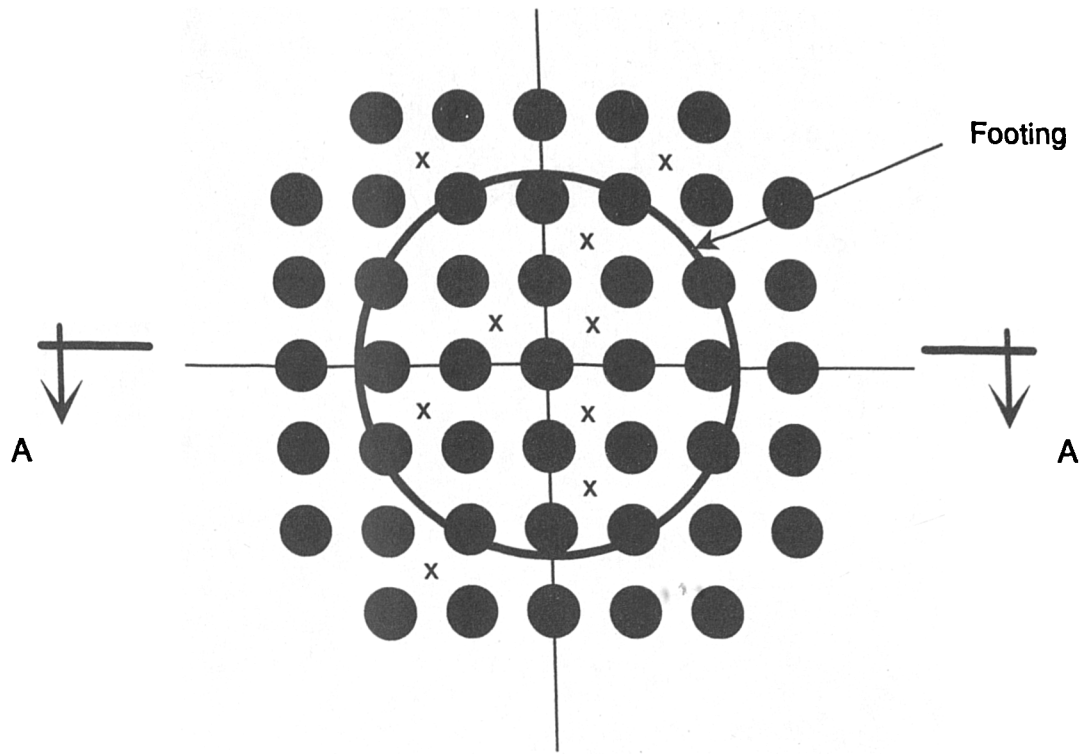
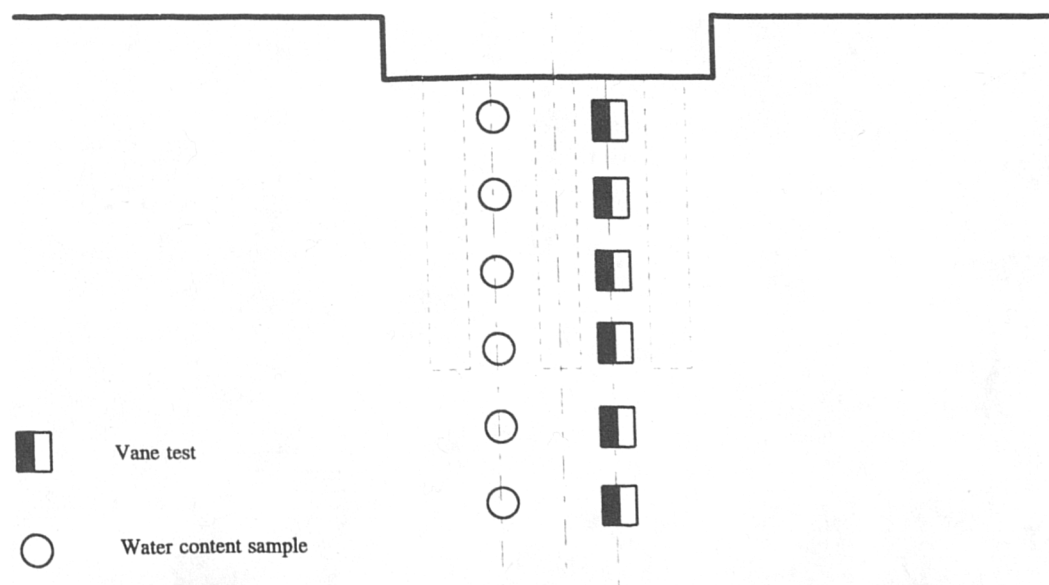


Fig 3.8: Effect of the fall height on the density of the sand beds



(a): Plan



(b): section A-A

Fig 3.9: The location of shear vane tests and water content samples

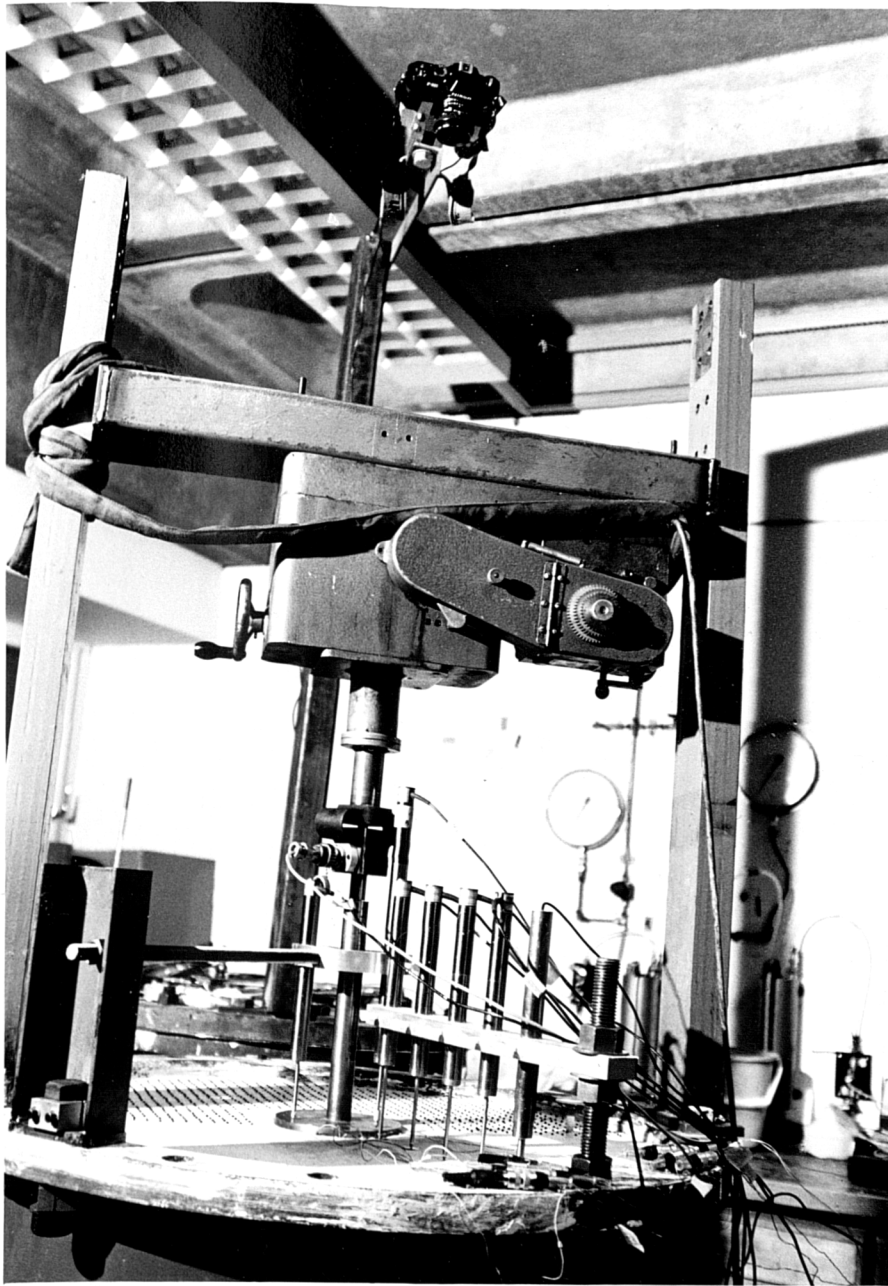


Plate 3.1 Set up of penetration test with a rigid footing

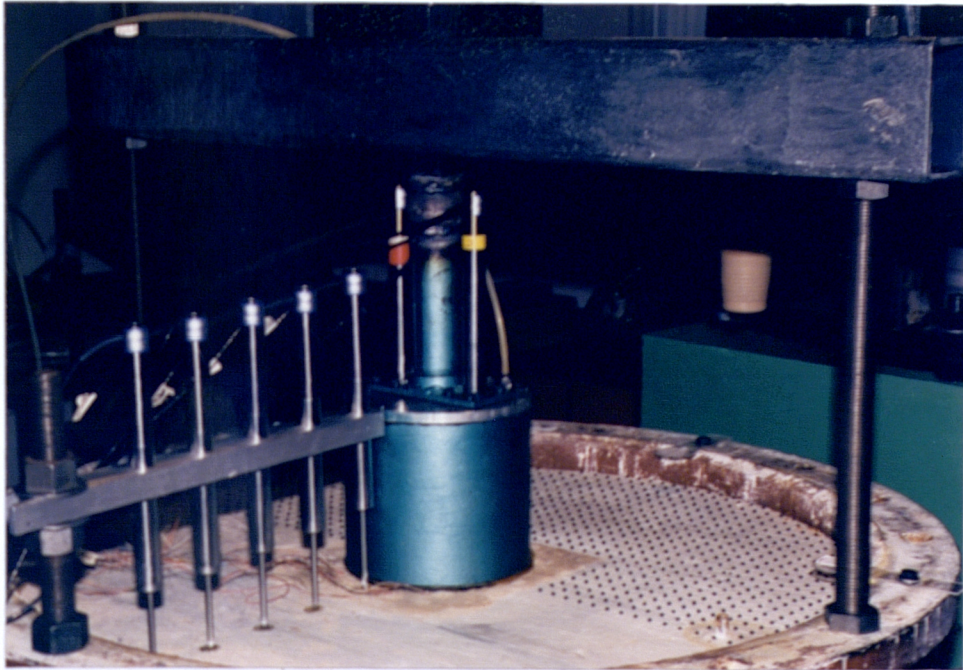


Plate 3.2: Set up of flexible loading test (TL01-1)

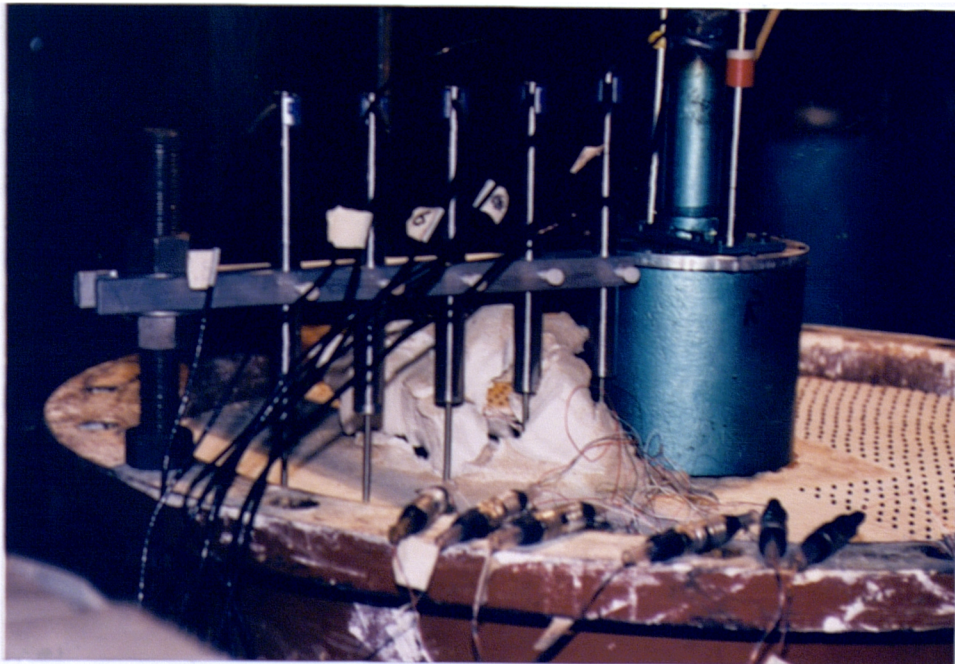


Plate 3.3: Flexible loading test TL01-1 after overall failure

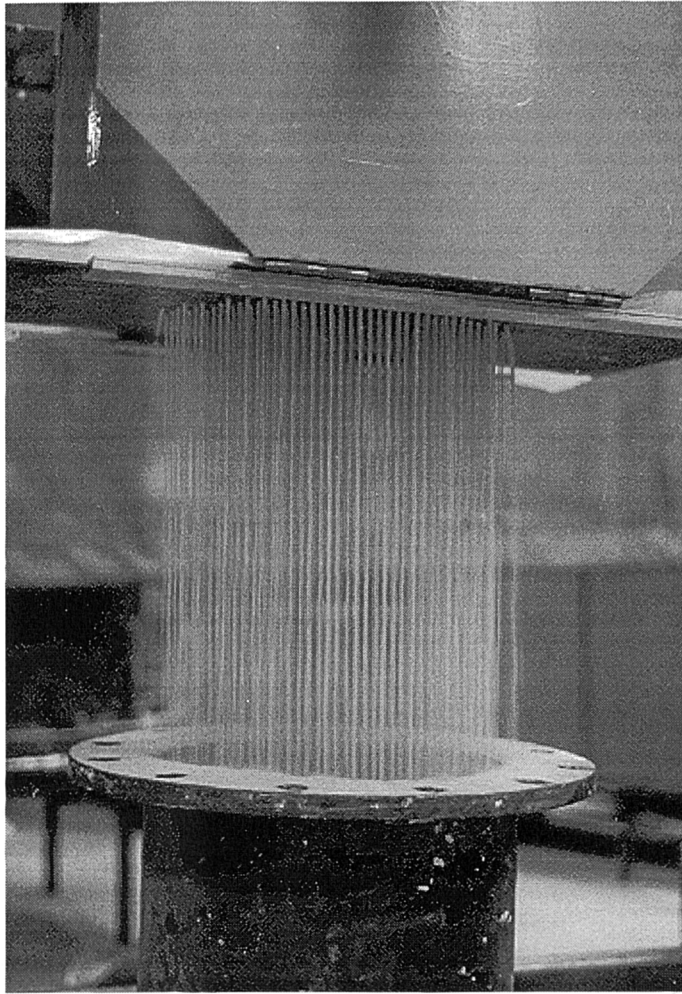


Plate 3.4: Sand raining

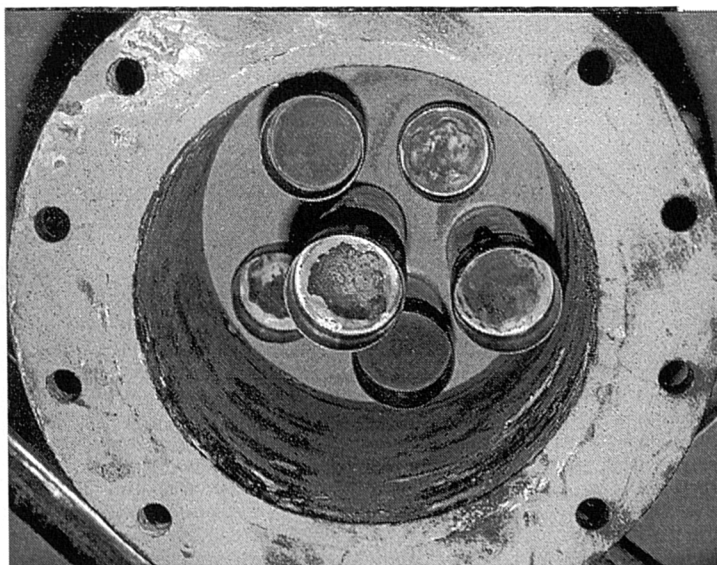


Plate 3.5: Arrangement of density pots

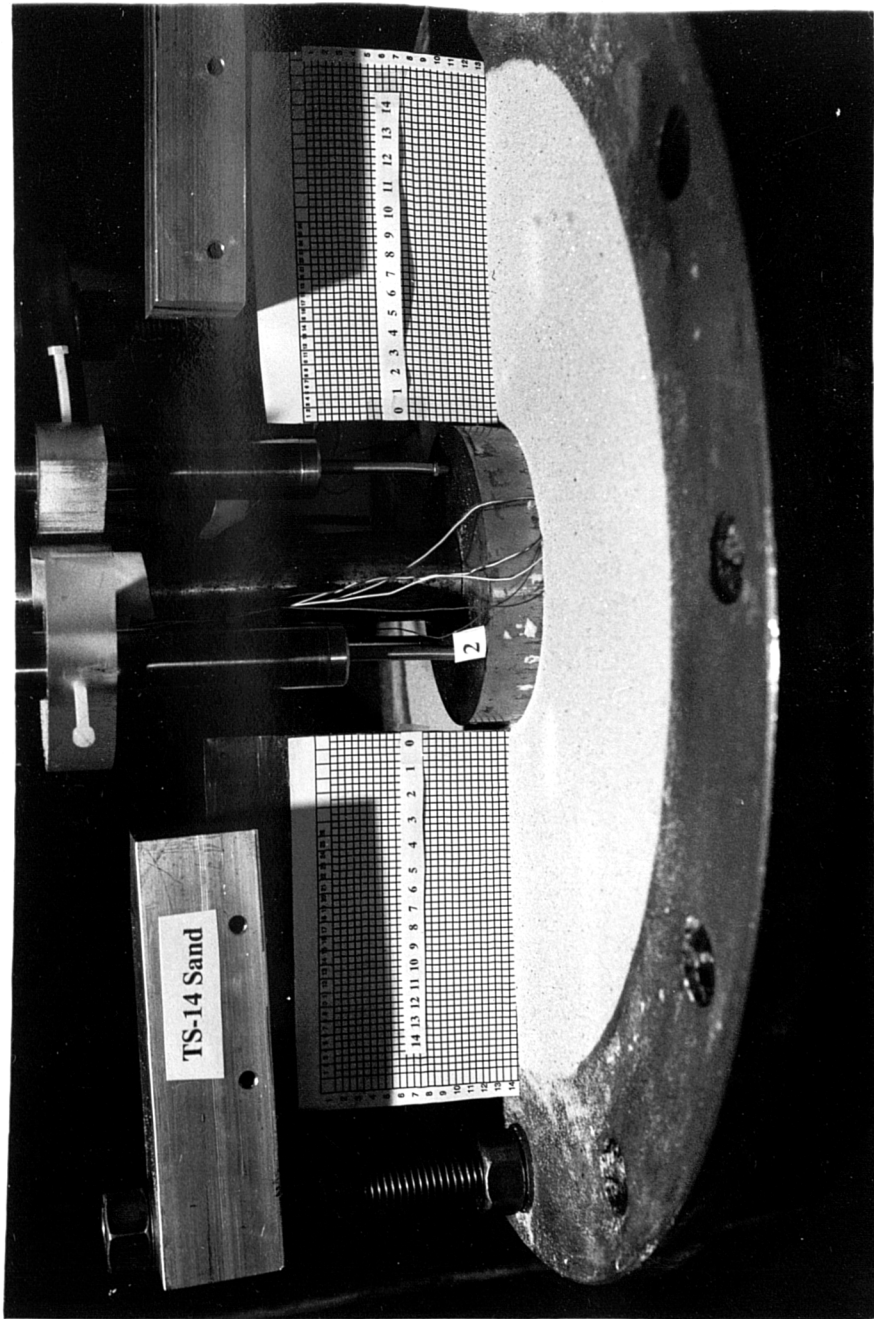


Plate 3.6: Surface heave recording at penetration test on sand bed

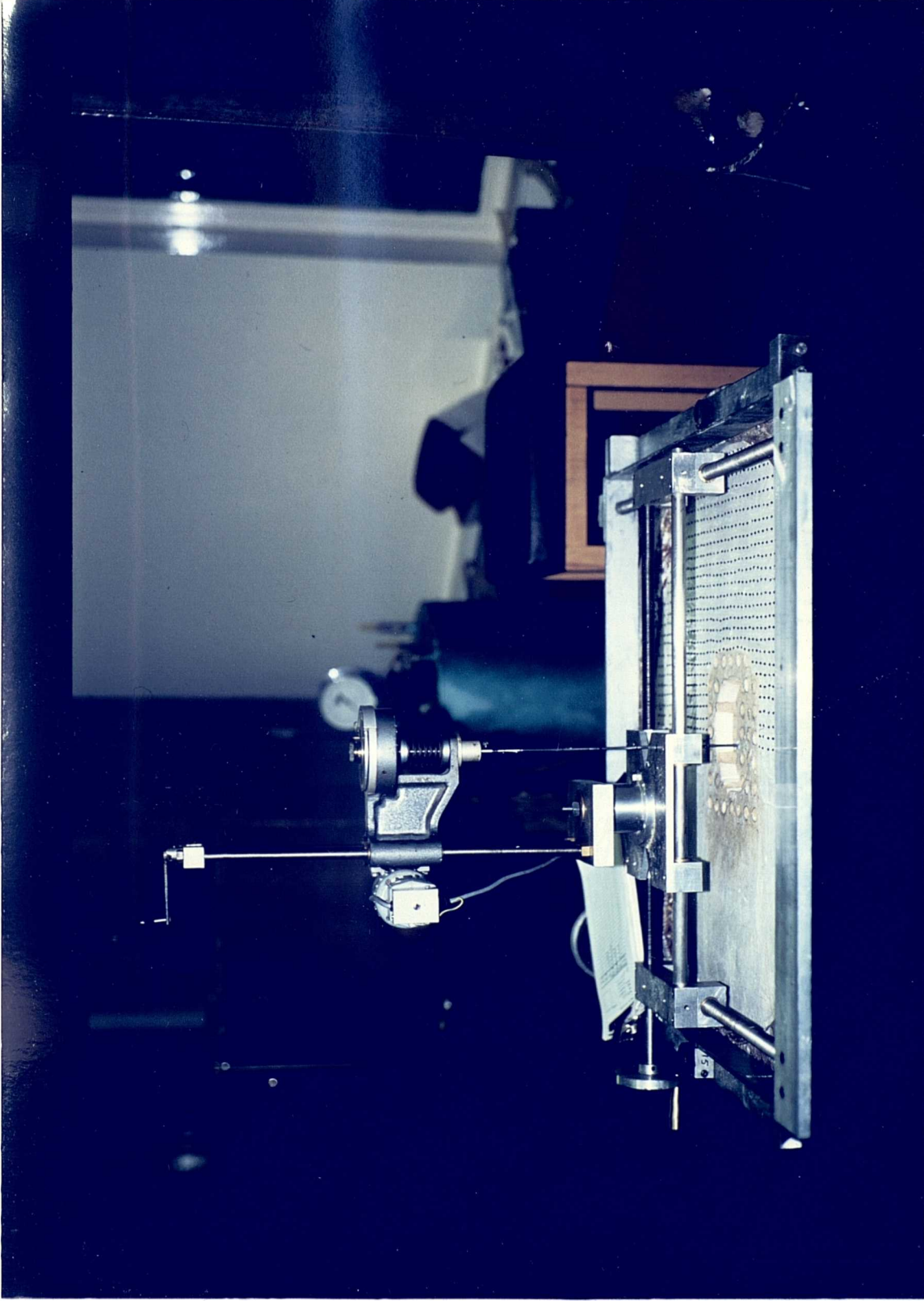


Plate 3.7: In-situ shear vane using a miniature laboratory vane

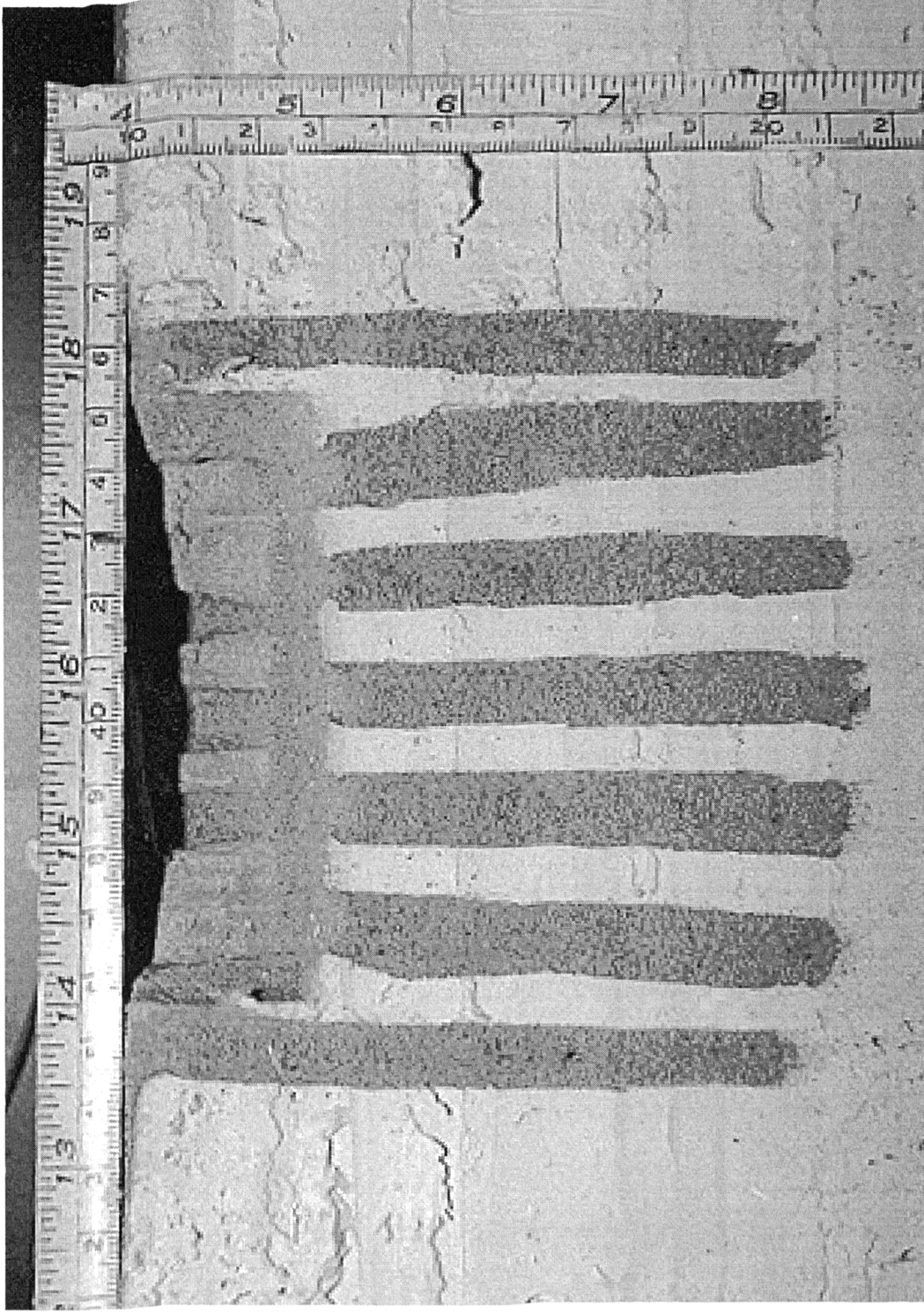


Plate 3.8: Sliced section of model TS05 using a wire cutter, after test



Plate 3.9: The plaster cast of a deformed model columns after penetration test (TS09)

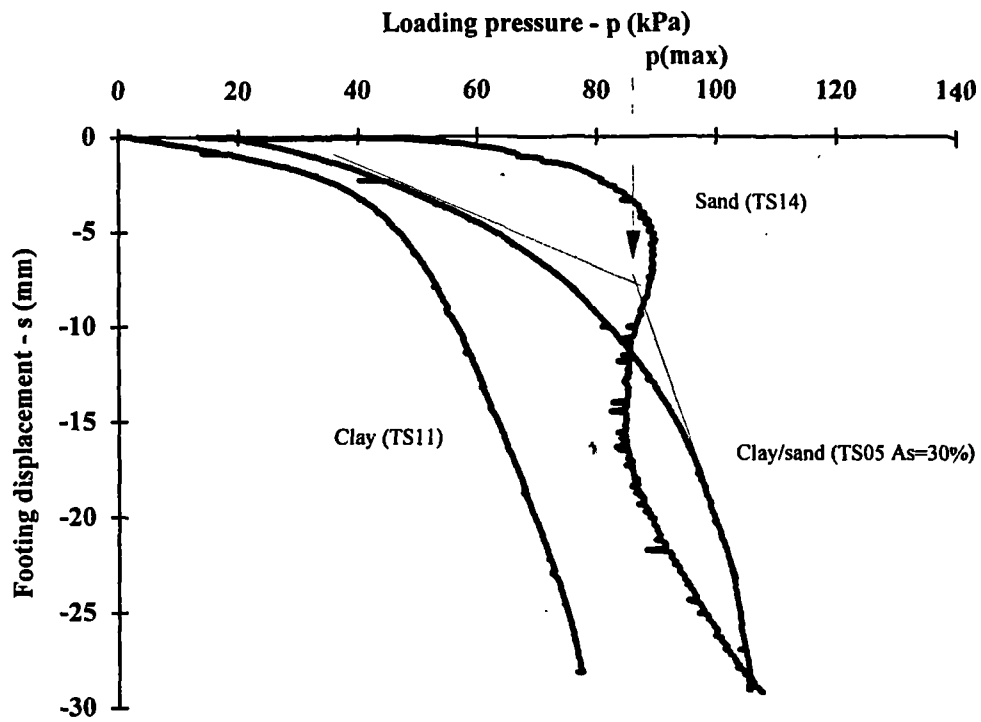


Fig 4.1: The load : displacement response on sand, reinforced clay and clay beds (tests TS14, TS05 & TS11)

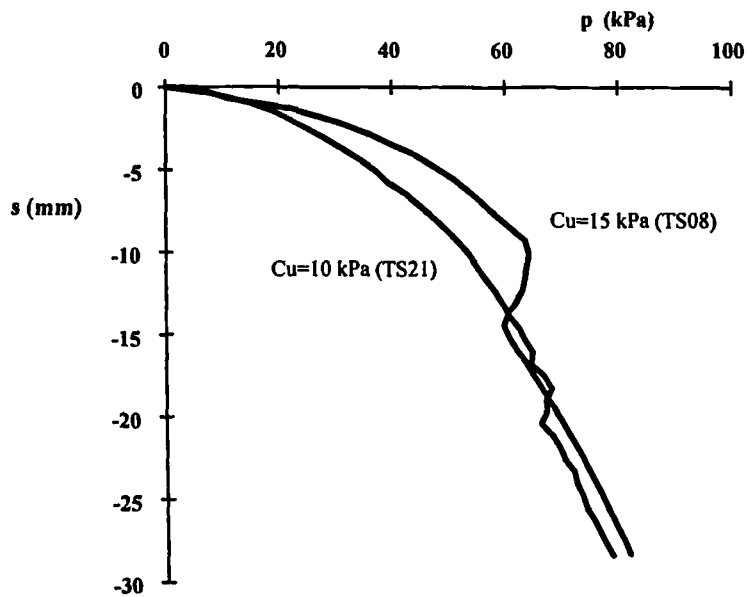


Fig 4.2: Influence of clay initial strength on the load : displacement response (TS08 & TS21)

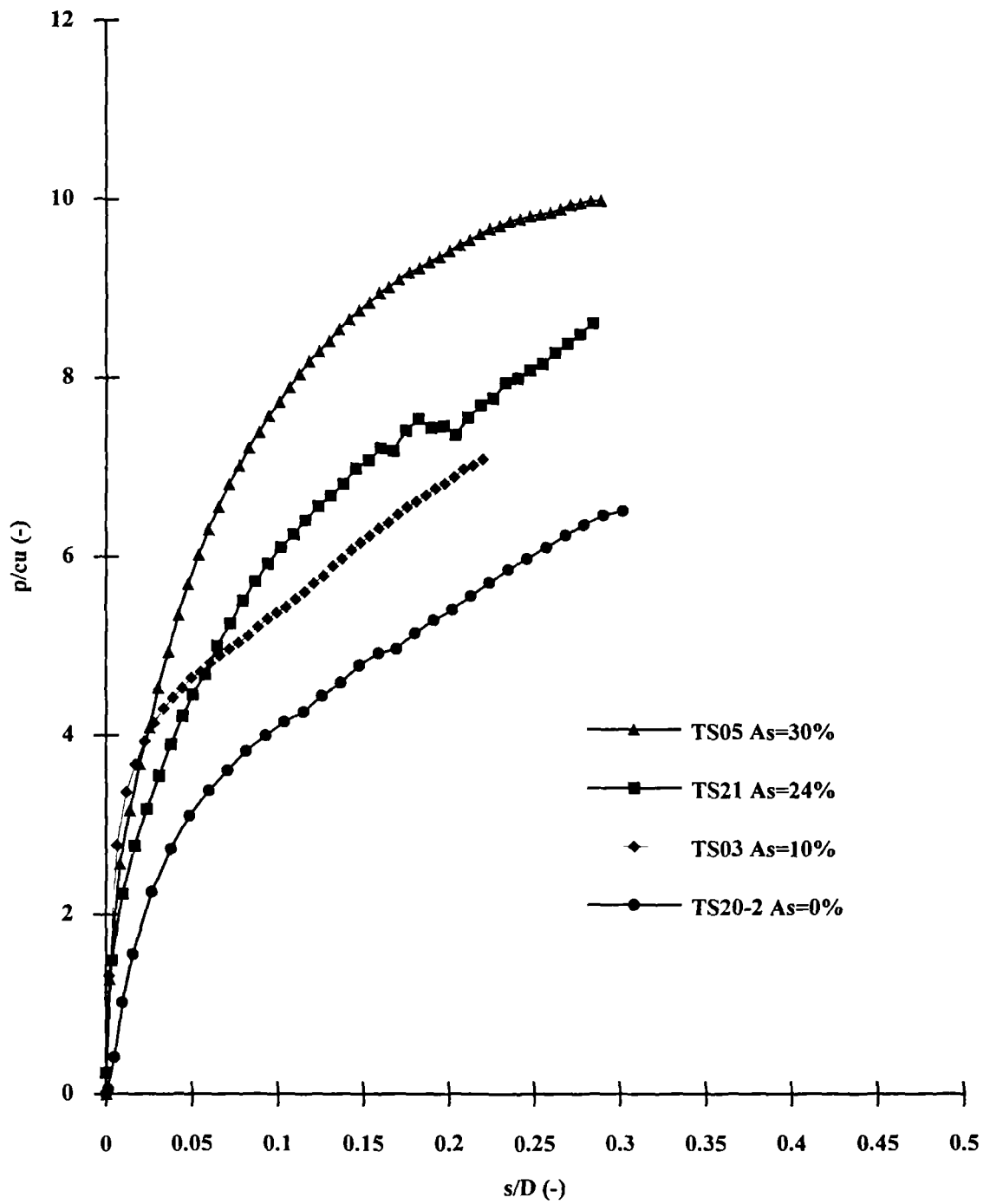


Fig 4.3: Effect of area ratio on the load : displacement response (short columns)

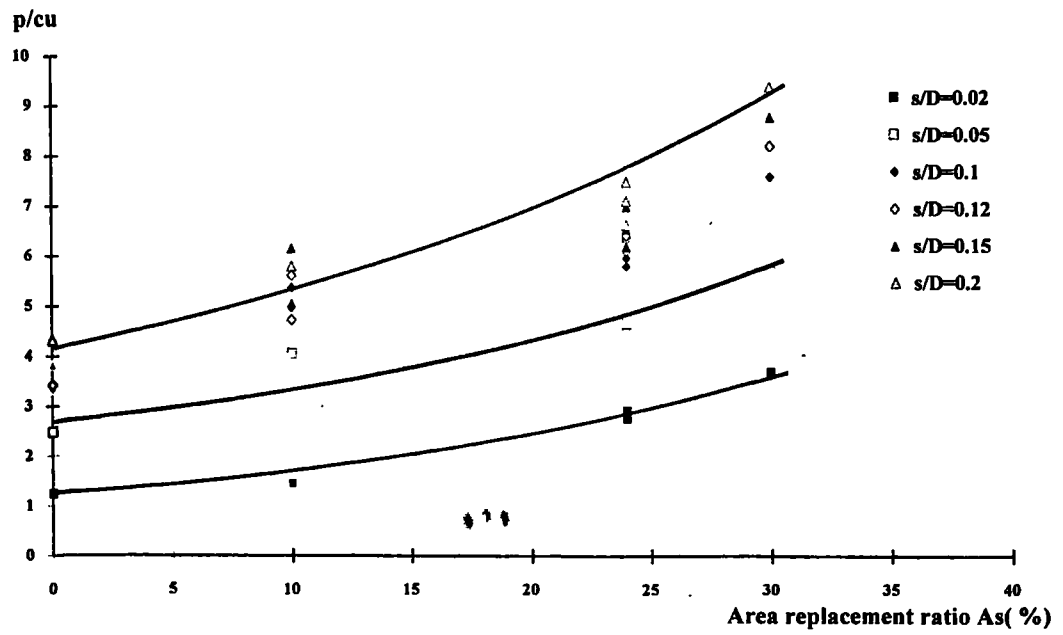


Fig 4.4: Relationship between area ratio and the load bearing capacity the composite ground

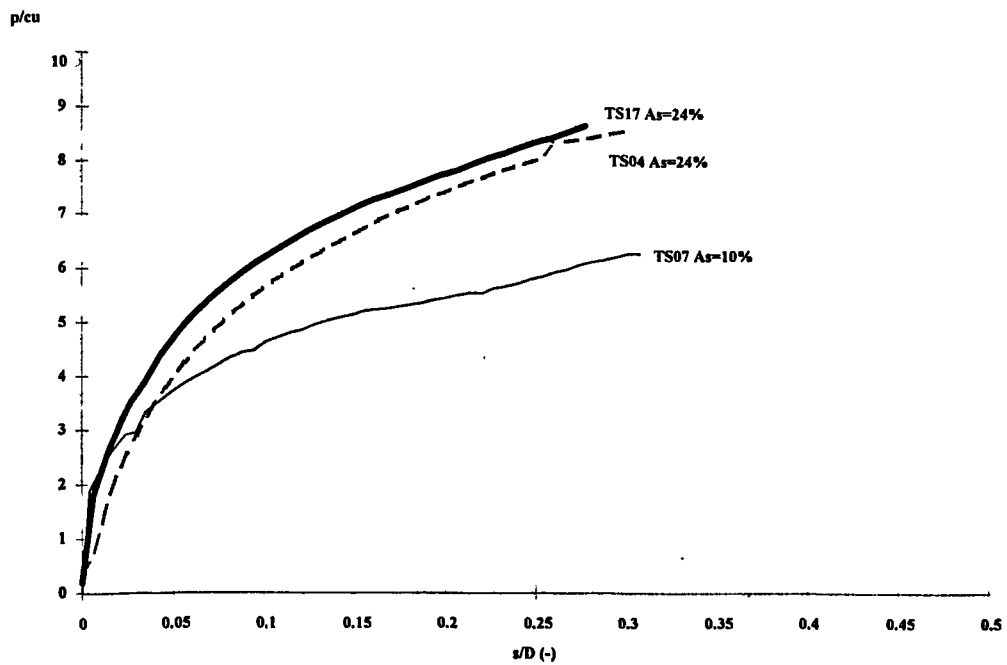


Fig 4.5: Effect of area ratio on load : displacement response (long columns)

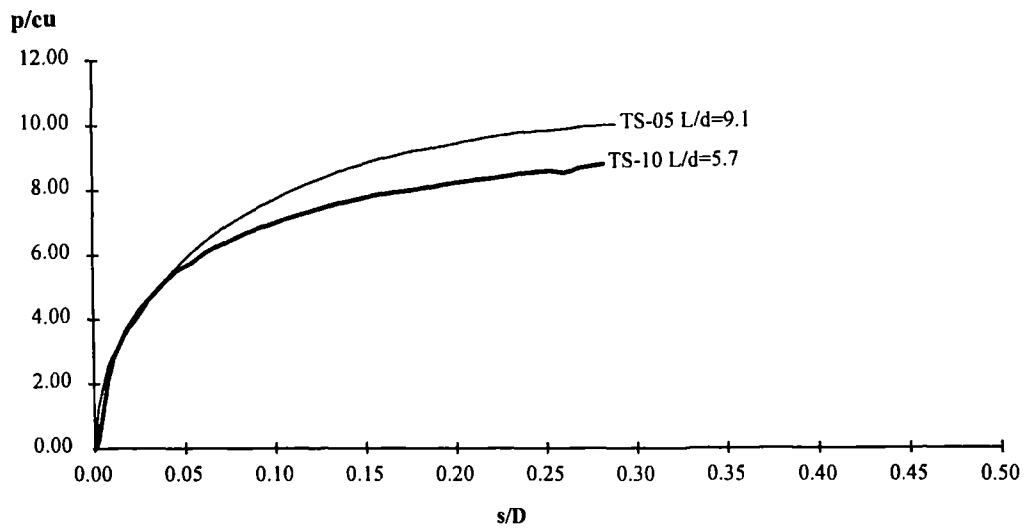


Fig 4.6: Effect of column length on load : settlement response (short columns)

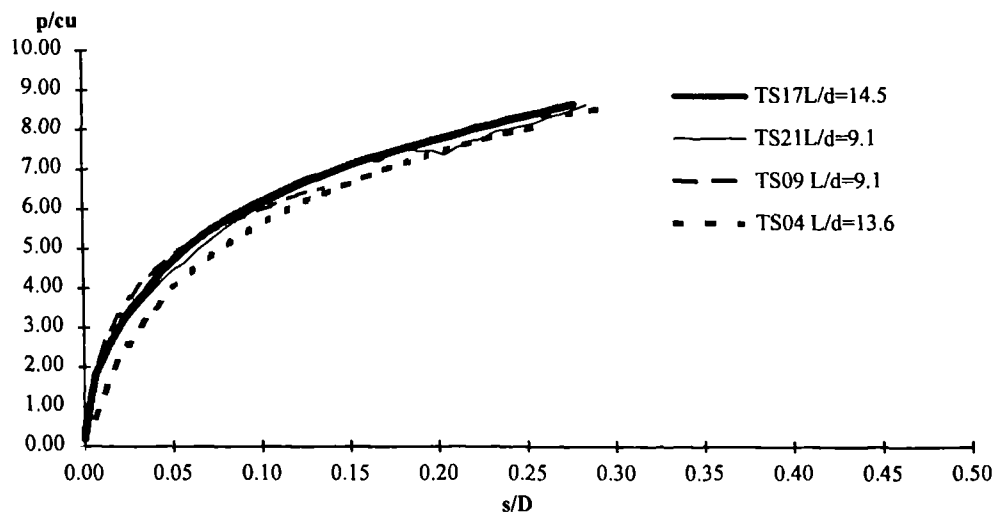


Fig 4.7: Effect of column length on load : settlement response (long columns)

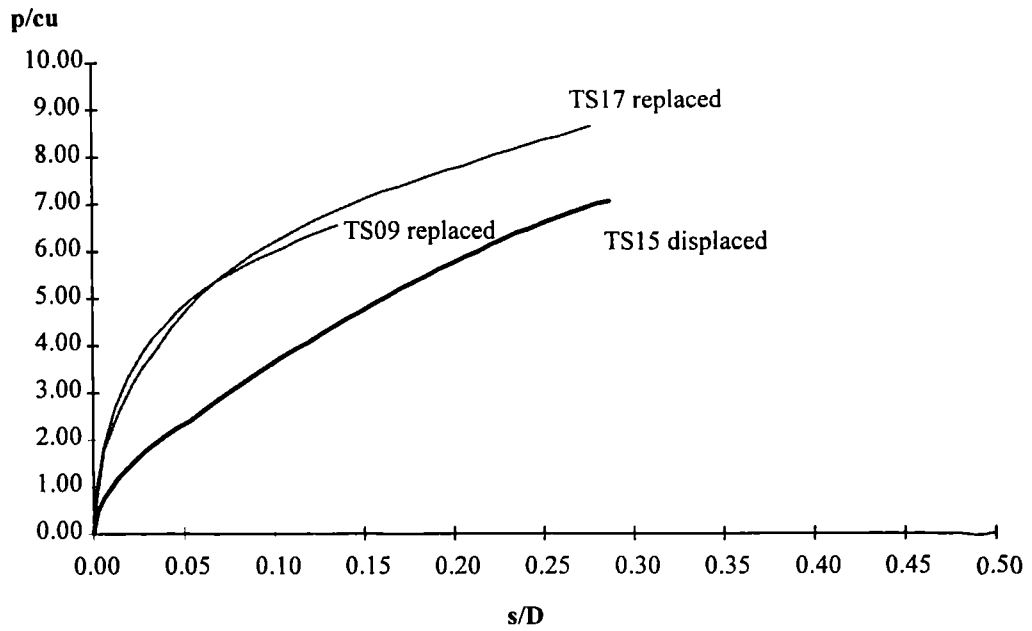


Fig 4.8: Effect of column installation method on load: settlement response ($A_s=24\%$)

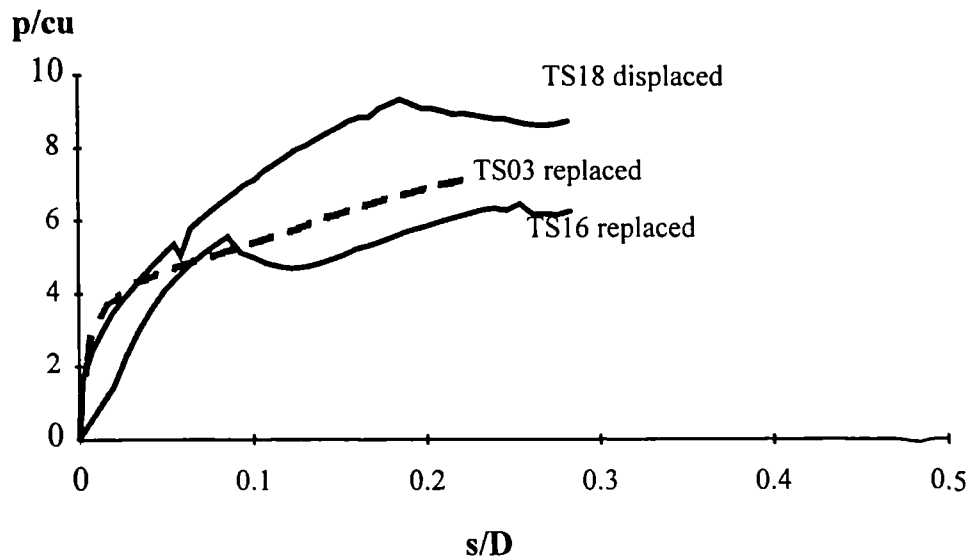


Fig 4.9: Effect of column installation method on load: settlement response ($A_s=10\%$)

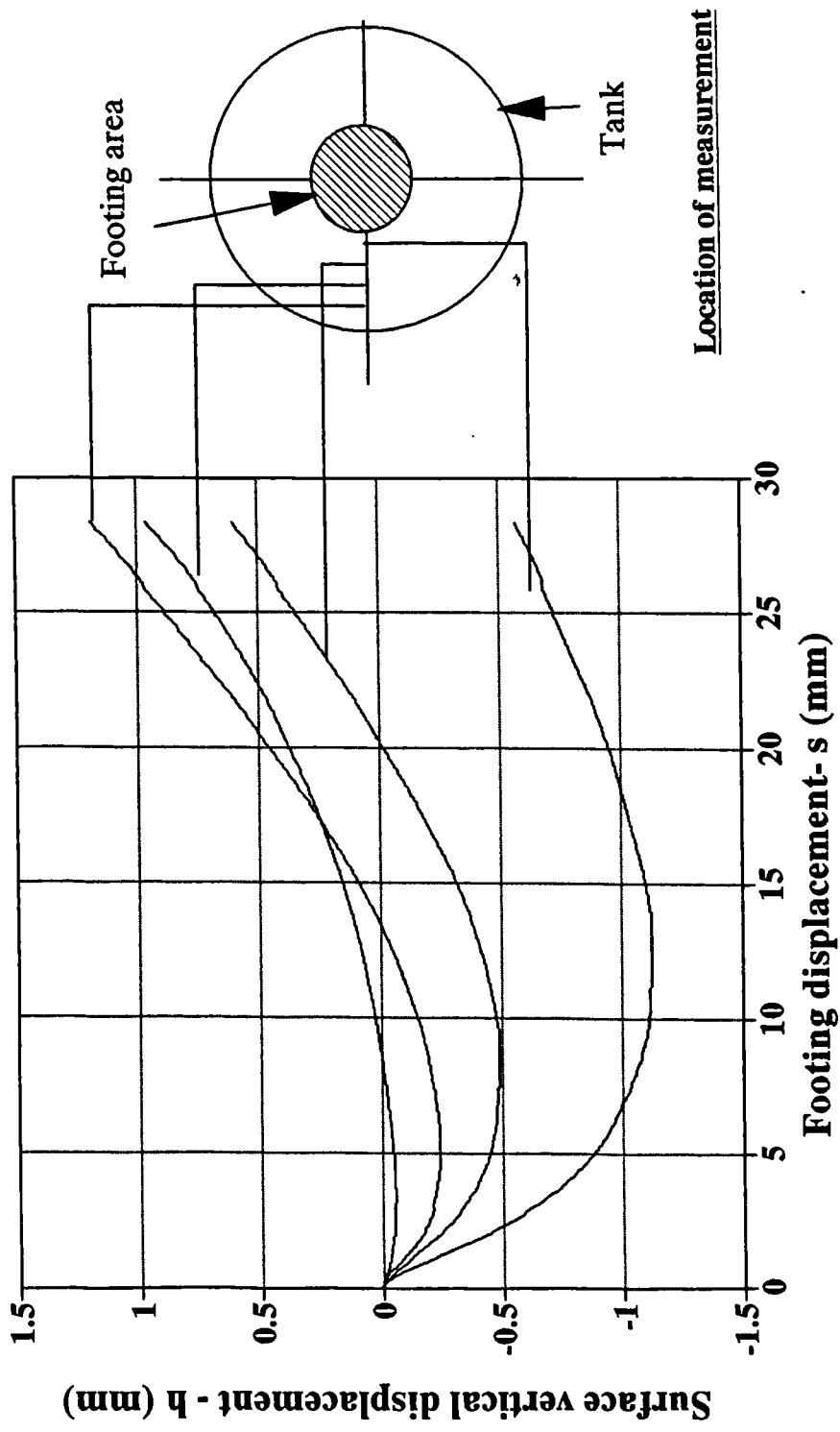


Fig 4.10: A typical surface vertical displacement : footing settlement response (TS10)

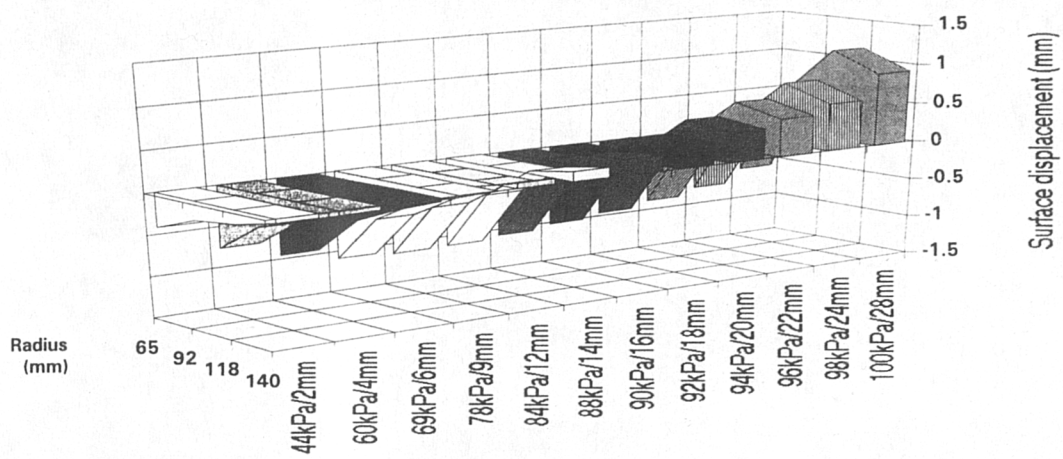


Fig 4.11: The 3-D view of the development of the surface vertical displacement Reinforced clay bed (TS10)

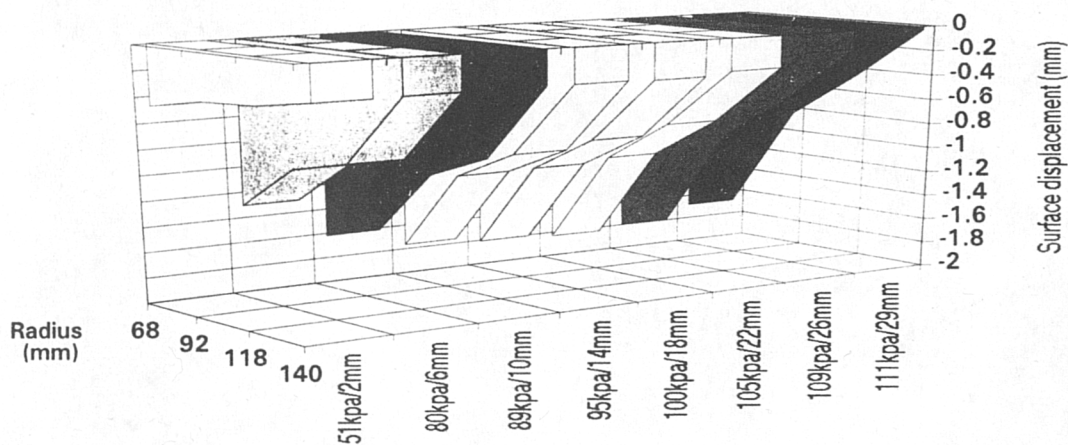


Fig 4.12: The 3-D view of the development of the surface vertical displacement Unreinforced clay bed (TS11)

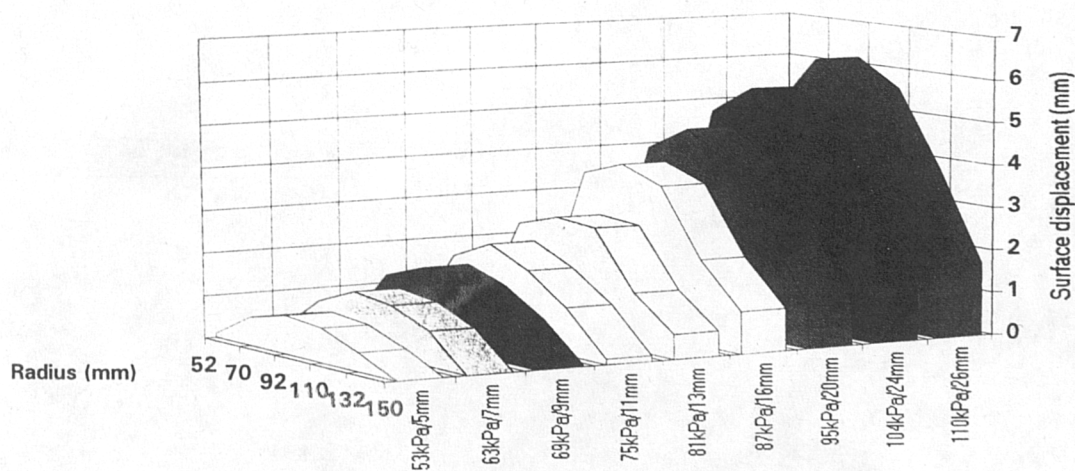
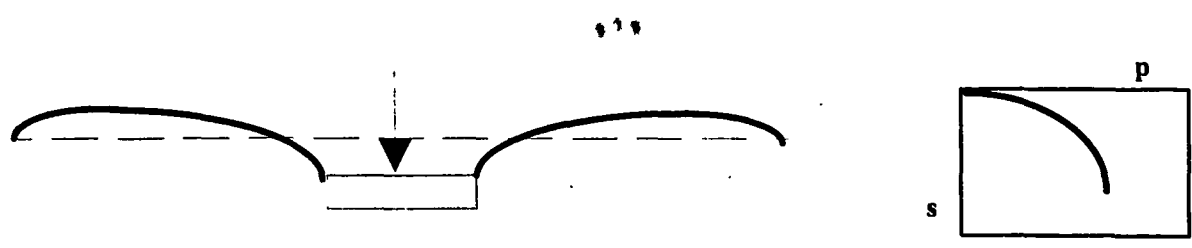


Fig 4.13: The 3-D view of the development of the surface vertical displacement Plain sand bed (TS14)



(a) unreinforced clay bed (TS11)



(b) reinforced clay bed (TS05)



(c) sand bed (TS14)

Fig 4.14: Relative surface heave profile and corresponding load-displacement curve
 (a) unreinforced clay bed; (b) reinforced clay bed; (c) sand bed

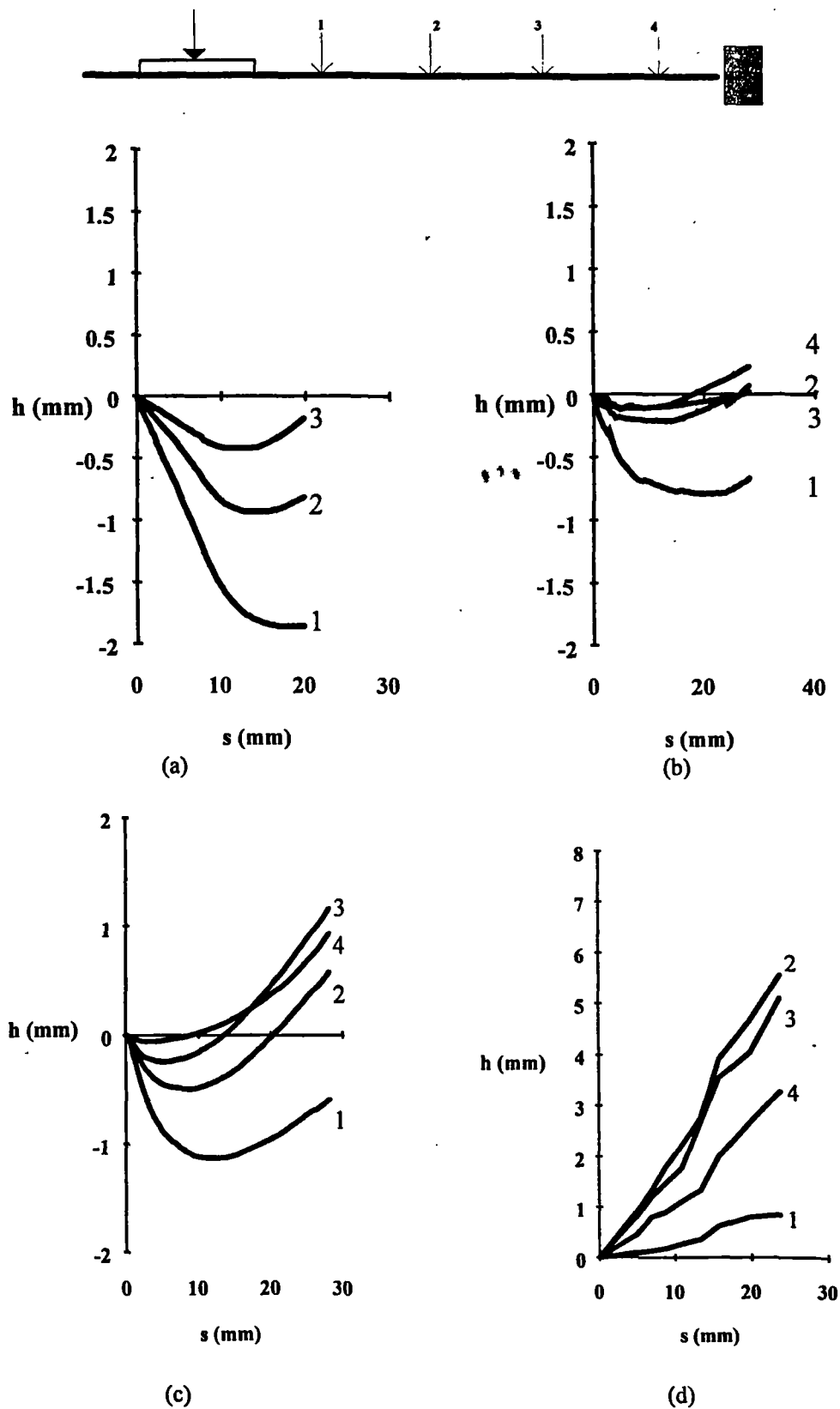


Fig 4.15: Effect of area ratio on the surface vertical displacement profile
 (a) test TS03 $A_s = 10\%$; (b) test TS17 $A_s = 24\%$; (c) test TS10 $A_s = 30\%$; (d) test TS14 plain sand

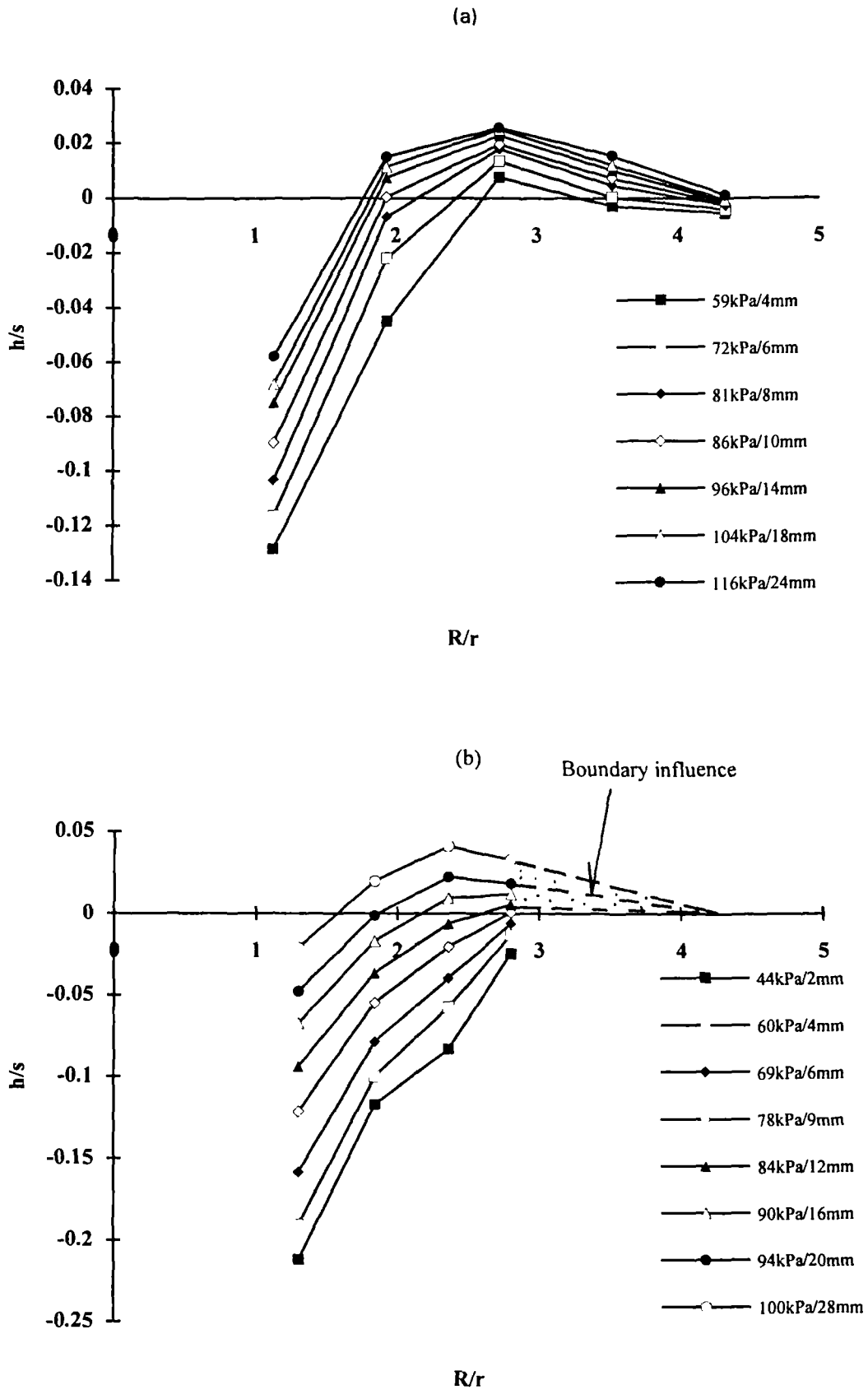


Fig 4.16: Effect of the size of the tank on the surface vertical displacement profiles
 (a) large tank - TL02; (b) small tank - TS10

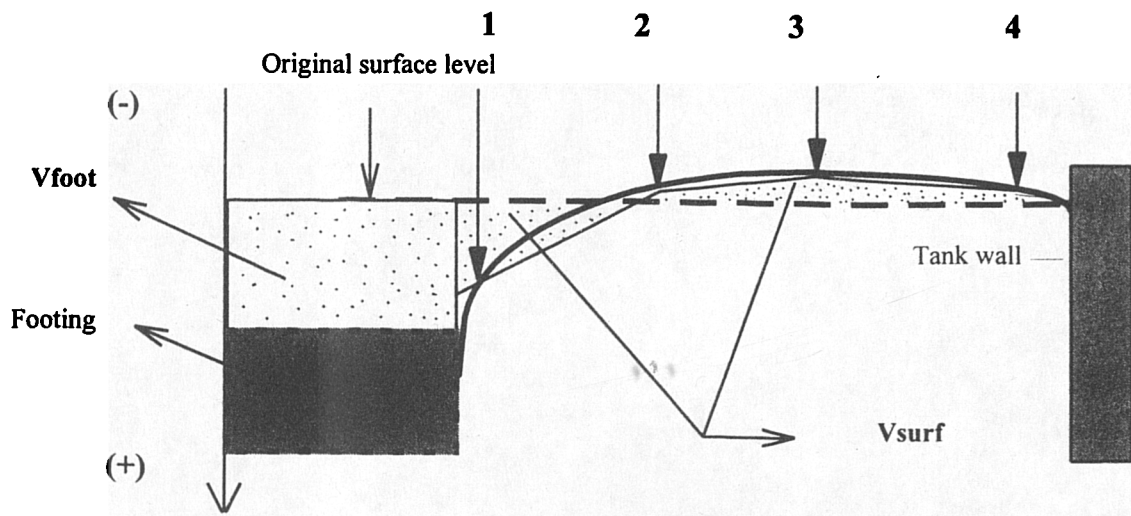


Fig 4.17: Calculation of the surface volume change

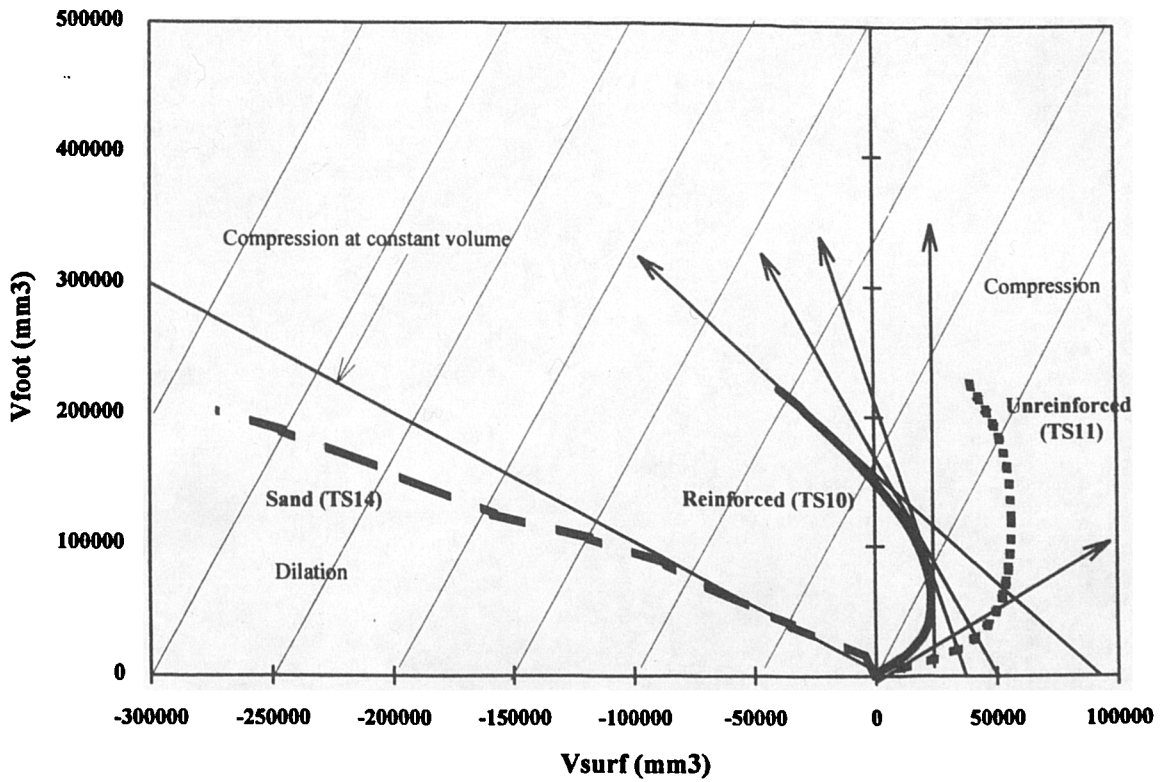


Fig 4.18: Surface volume change : footing penetration volume response (TS11, TS10 & TS14)

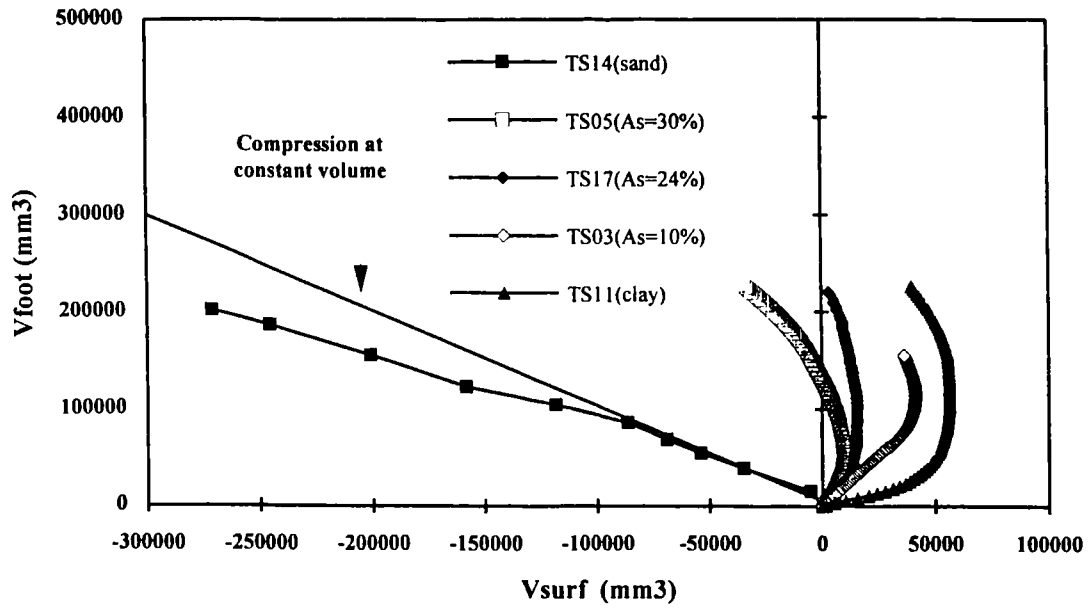


Fig 4.19: Effect of the area ratio on the surface volume change profiles

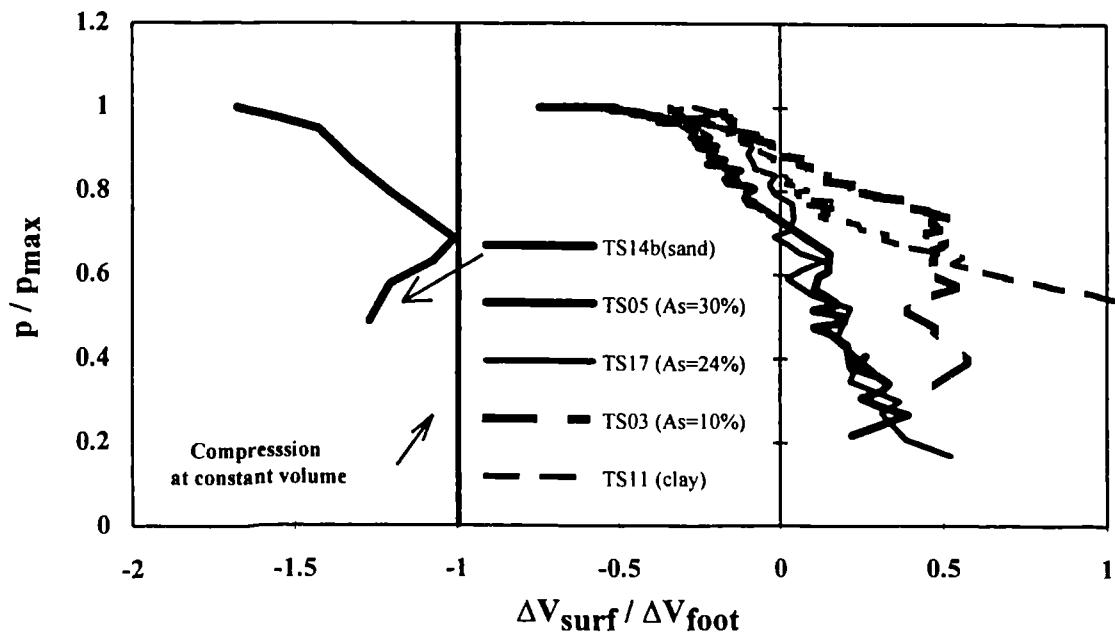


Fig 4.20: Effect of the area ratio on the rate of surface volume change profiles

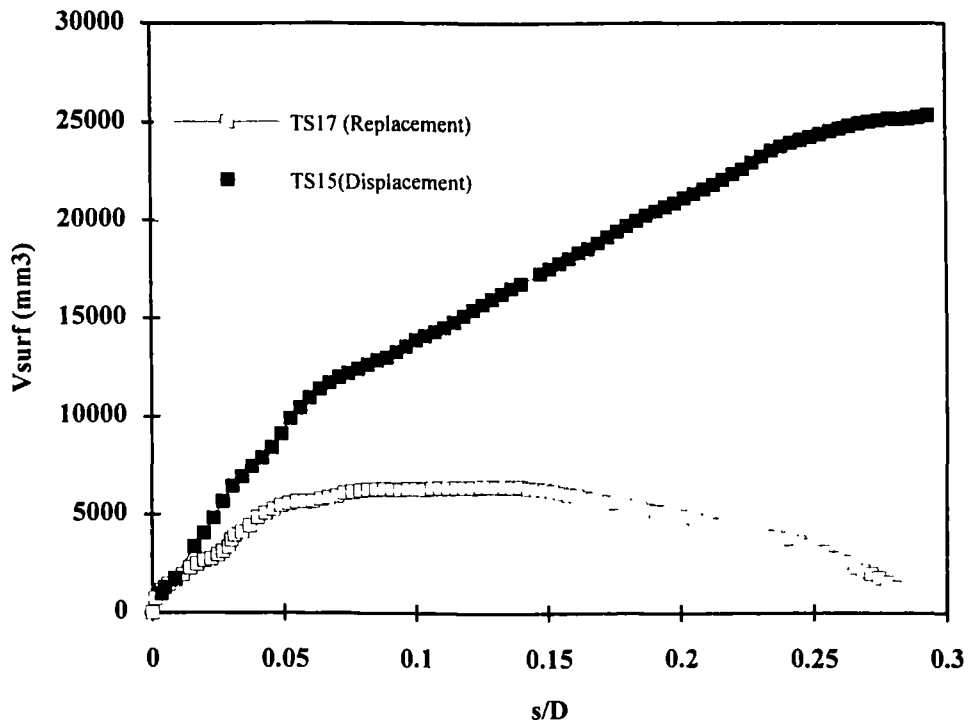


Fig 4.21: Effect of column installation method on the surface volume change profiles ($A_s=24\%$)

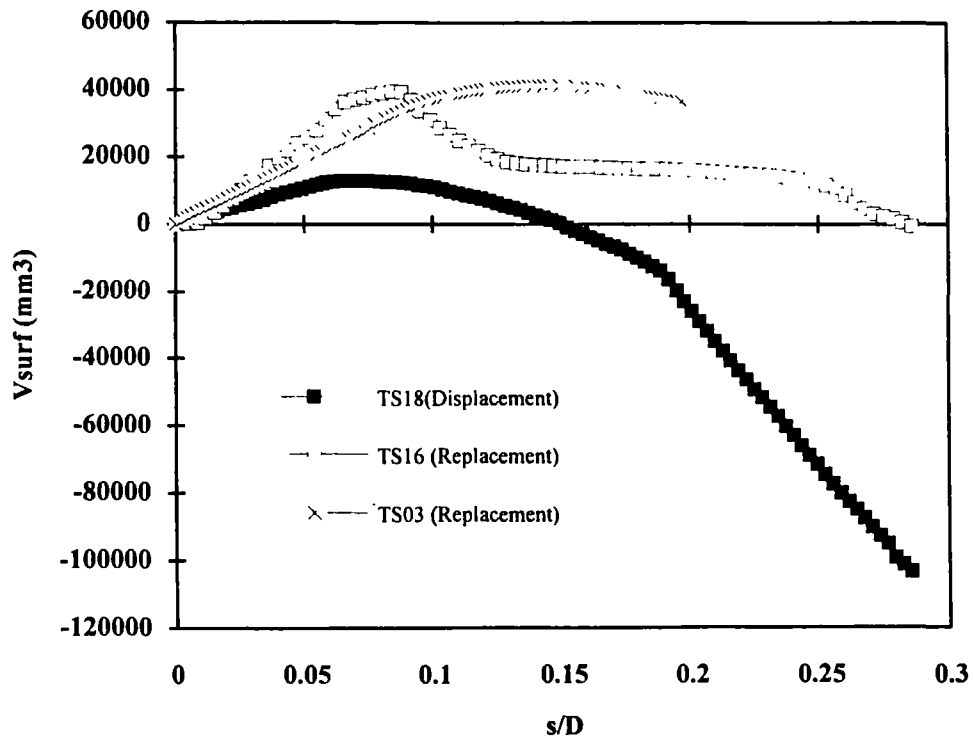


Fig 4.22: Effect of column installation method on the surface volume change profiles ($A_s=10\%$)

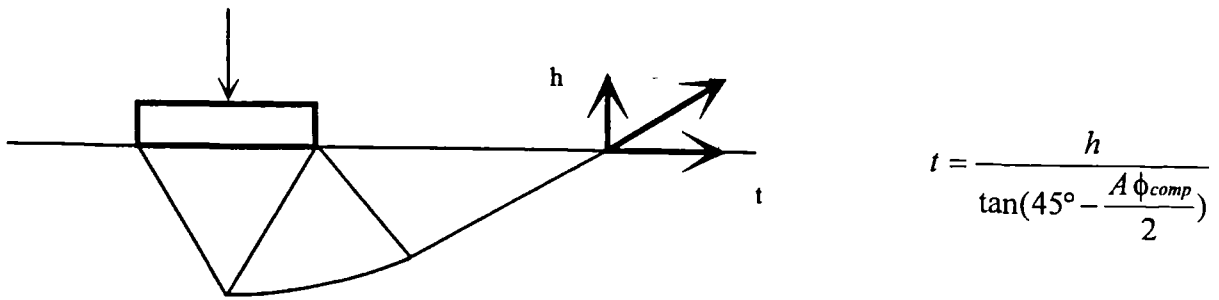


Fig 4.23: The approximate relationship between surface vertical displacement and surface horizontal displacement

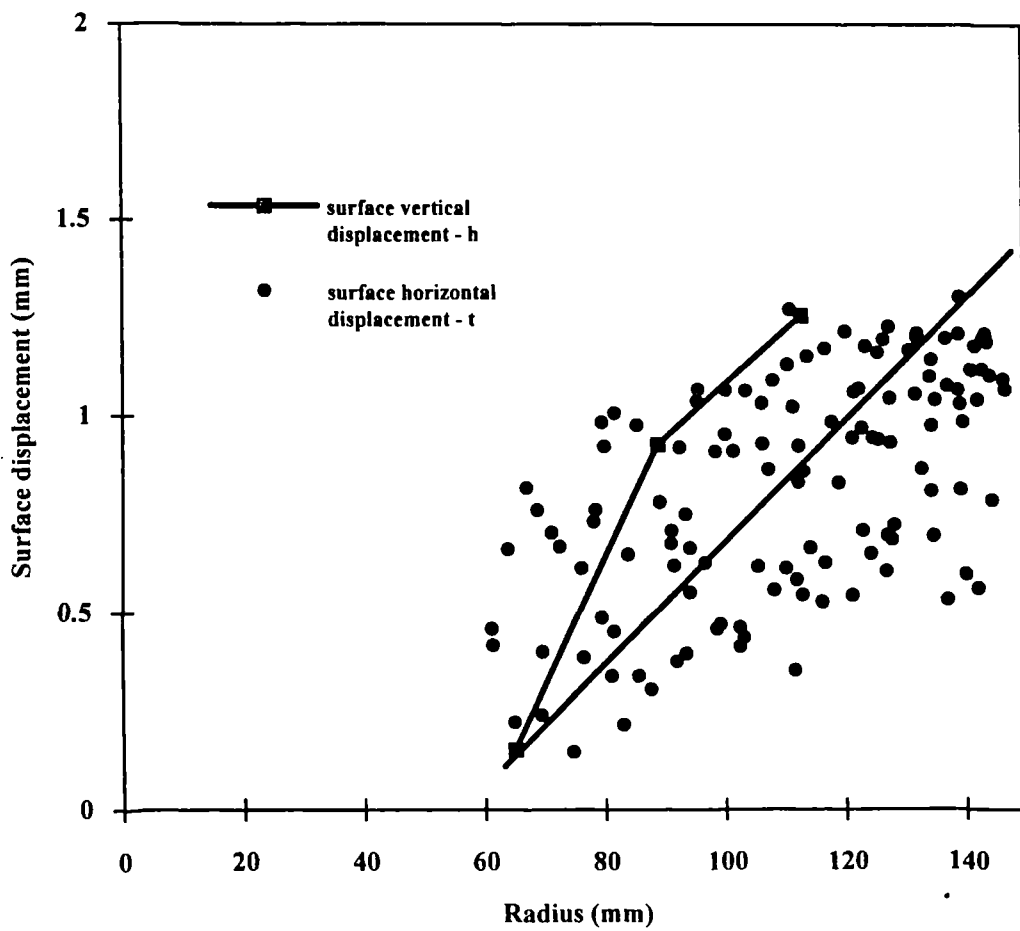


Fig 4.24: Observed surface movements in vertical and horizontal directions (TS05)

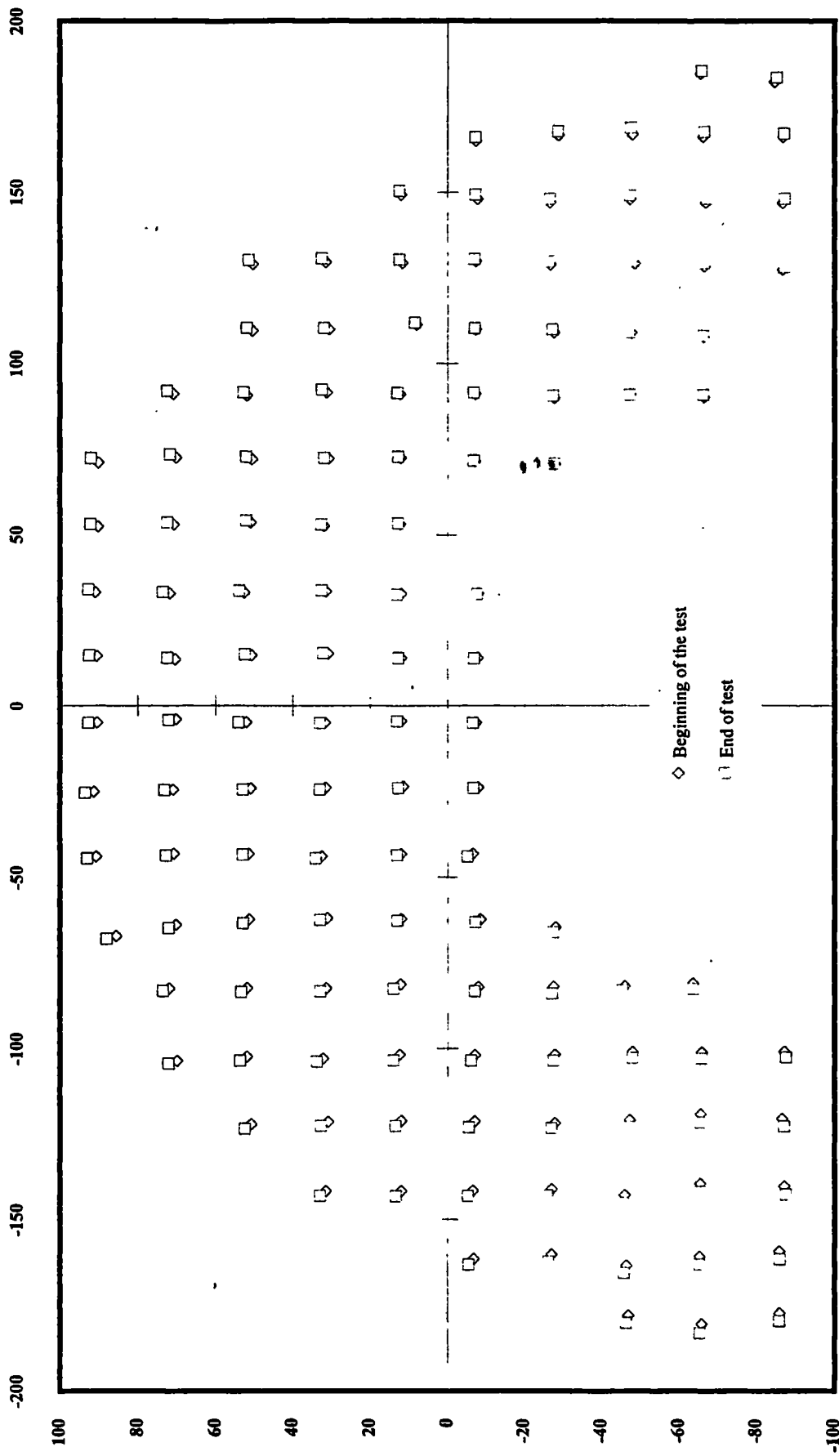


Fig 4.25: Profile of surface horizontal movement from Image Analysis (TS05 1 unit=0.77mm)

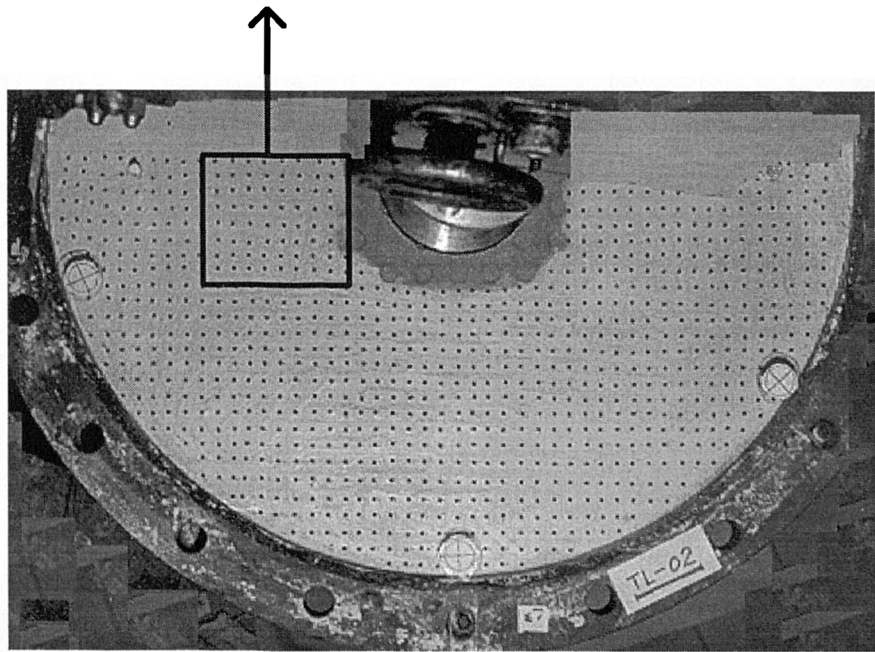
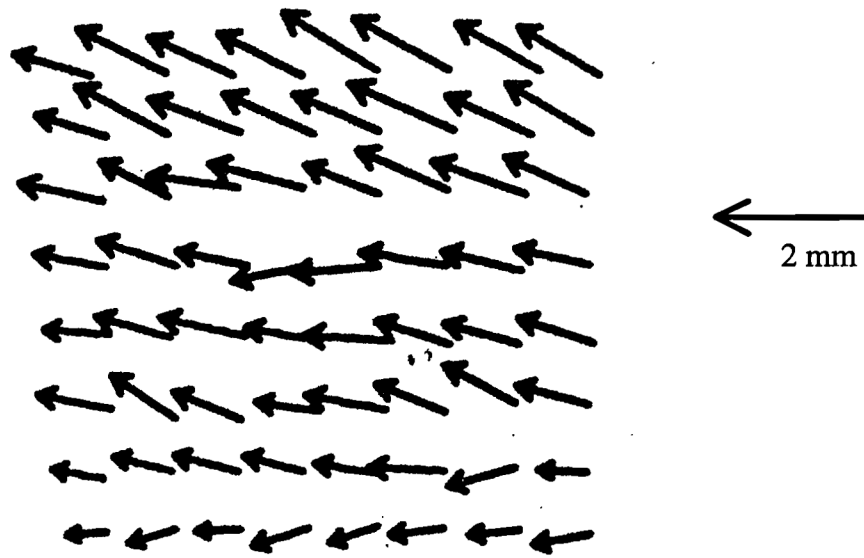
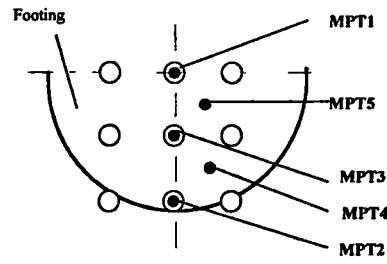


Fig 4.26: Surface horizontal displacement vectors from Film Measuring Machine (before and after test, a section of TL02)



Arrangement of the transducers

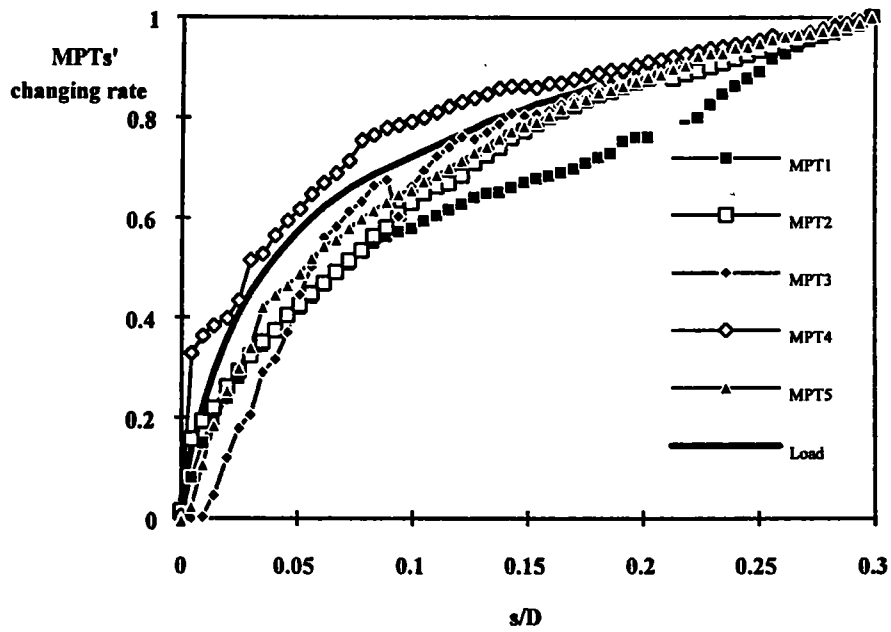


Fig 4.27: The rate of the stress increase measured from miniature pressure transducers : footing displacement response (test TS21)

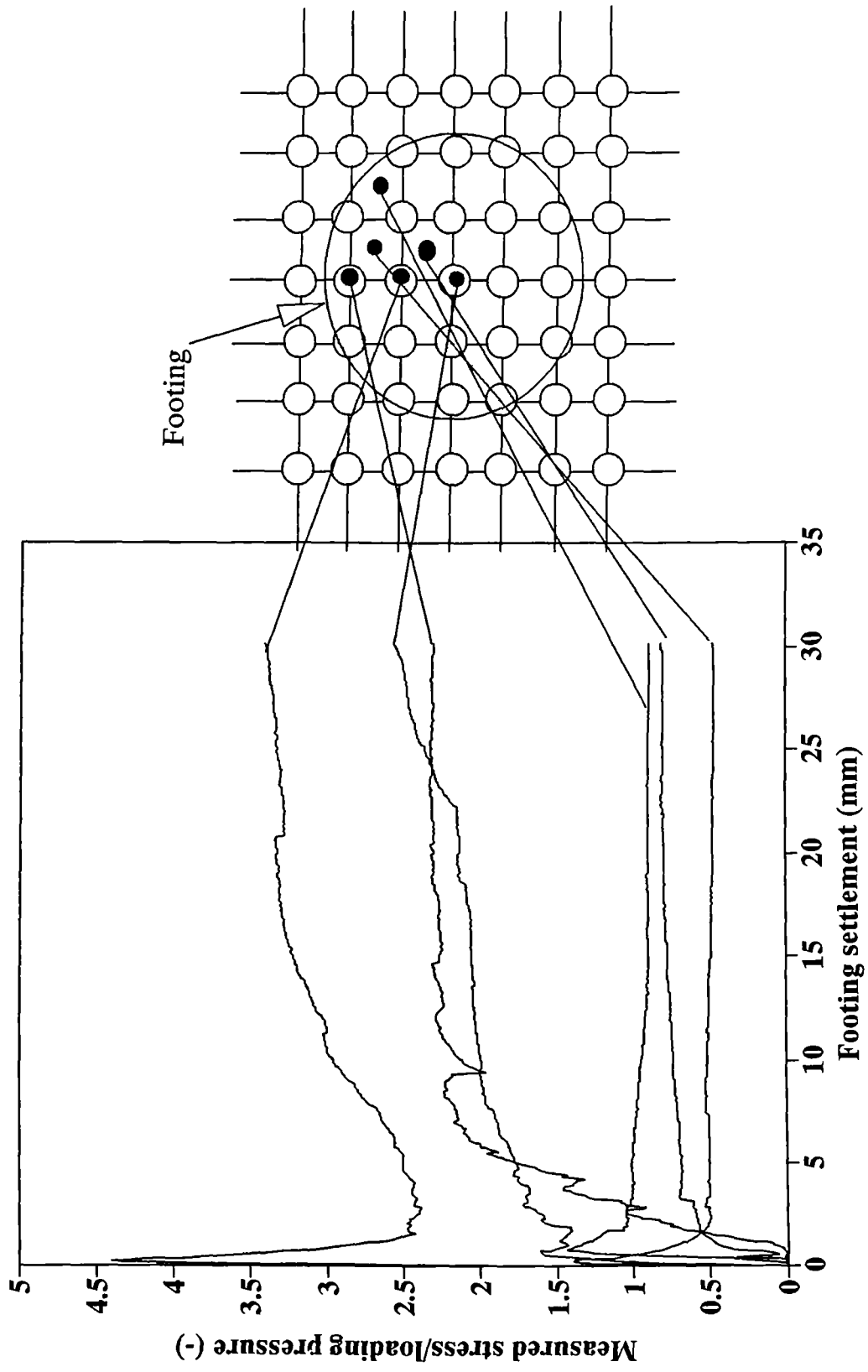
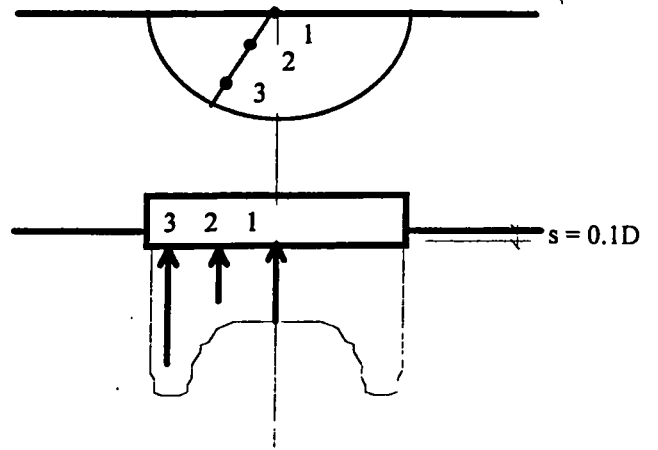
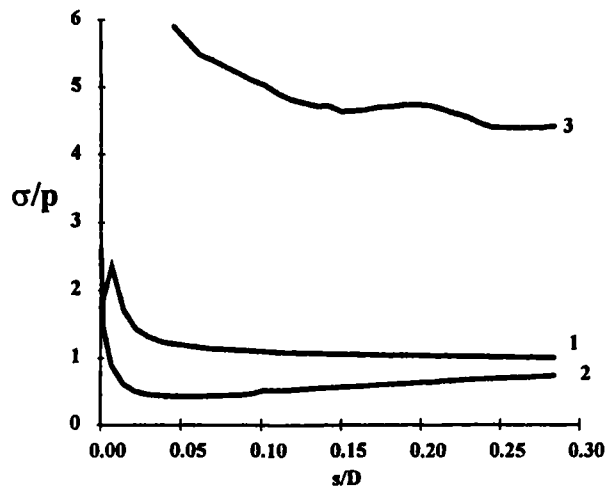
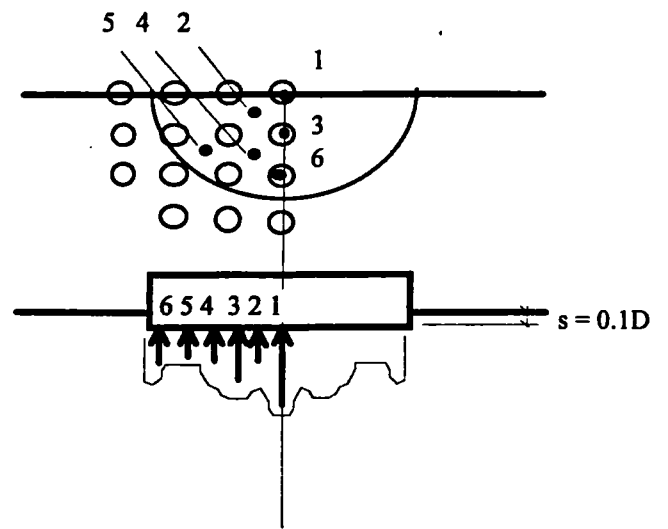
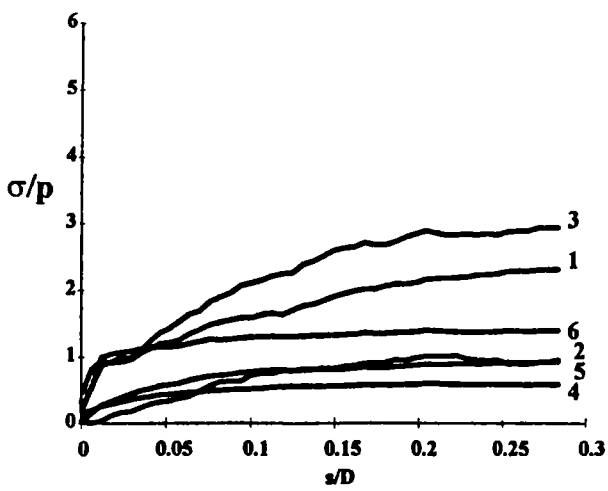


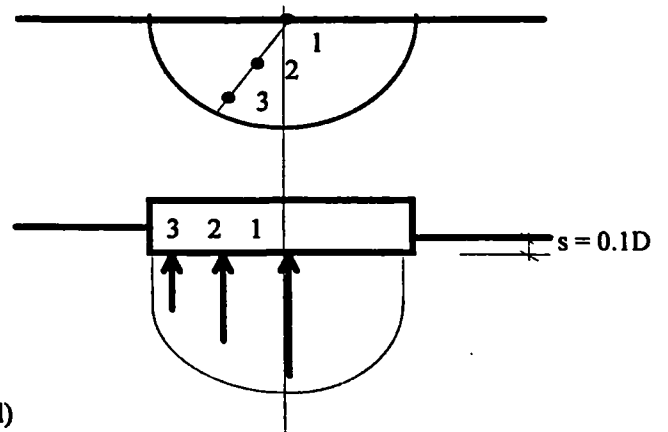
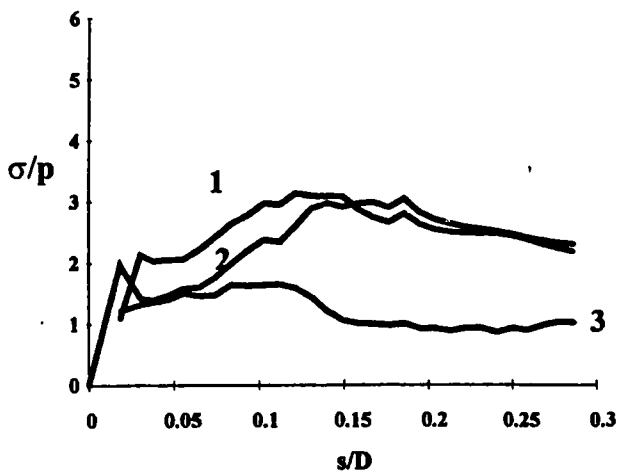
Fig 4.28 : A typical profile of distribution of contact stresses from miniature pressure transducers (TL-02)



(a): TS11 (clay)

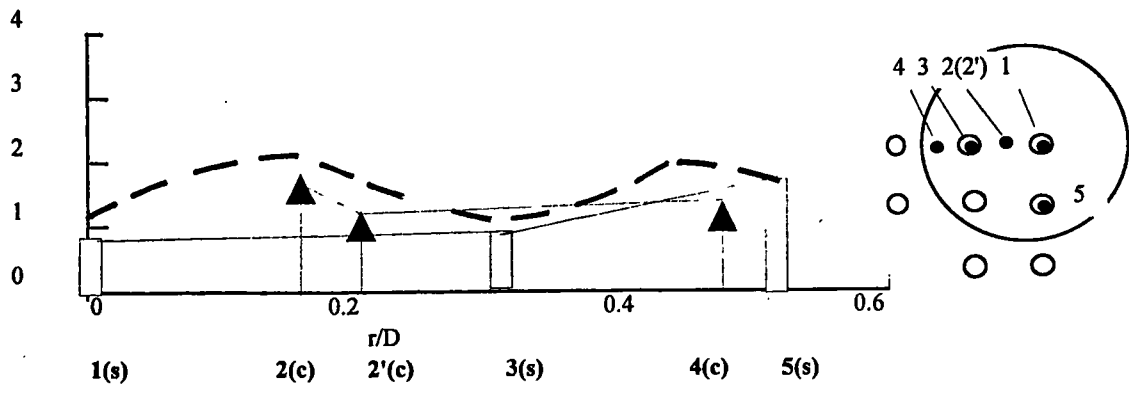


(b): TS21 ($A_s=24\%$)

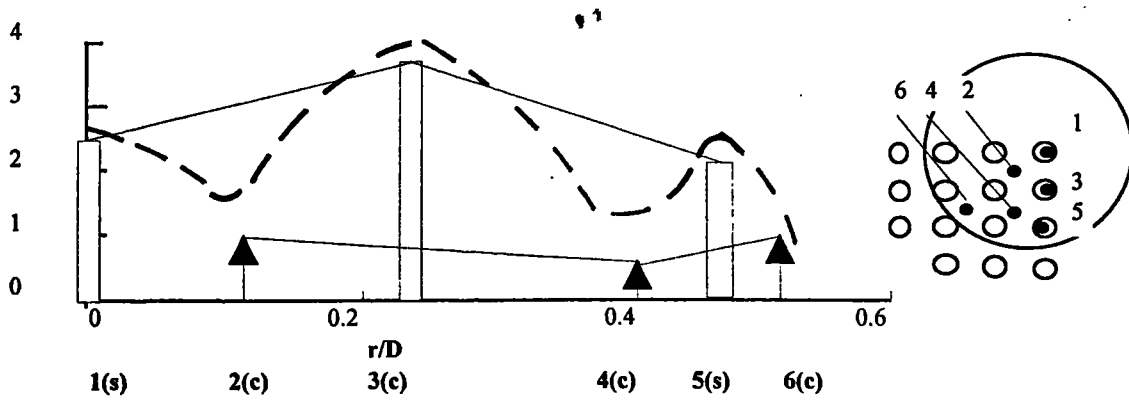


(c): TS14 (sand)

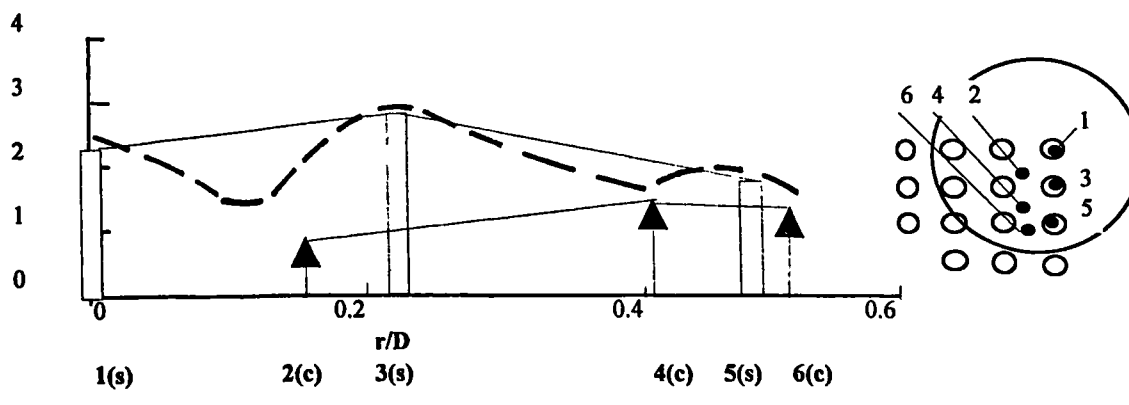
Fig 4.29: Comparison of the distribution of contact stresses in (a) clay TS11; (b) reinforced clay TS21, $A_s=24\%$; (c) sand bed TS14



(a): TS16 ($A_s=10\%$)



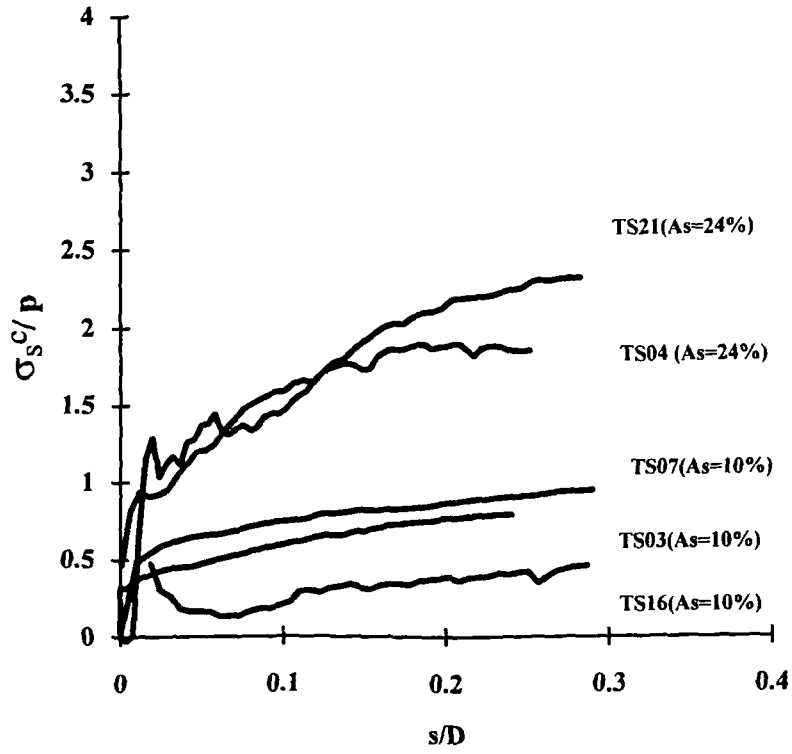
(b): TL02 ($A_s=24\%$)



(c): TS10 ($A_s=30\%$)

Fig 4.30: Effect of area ratio on the distribution of contact stresses across footing
 (a): TS16 ($A_s=10\%$); (b): TL01 ($A_s=24\%$); (c): TS10 ($A_s=30\%$)

(a) centre column



(b) middle column

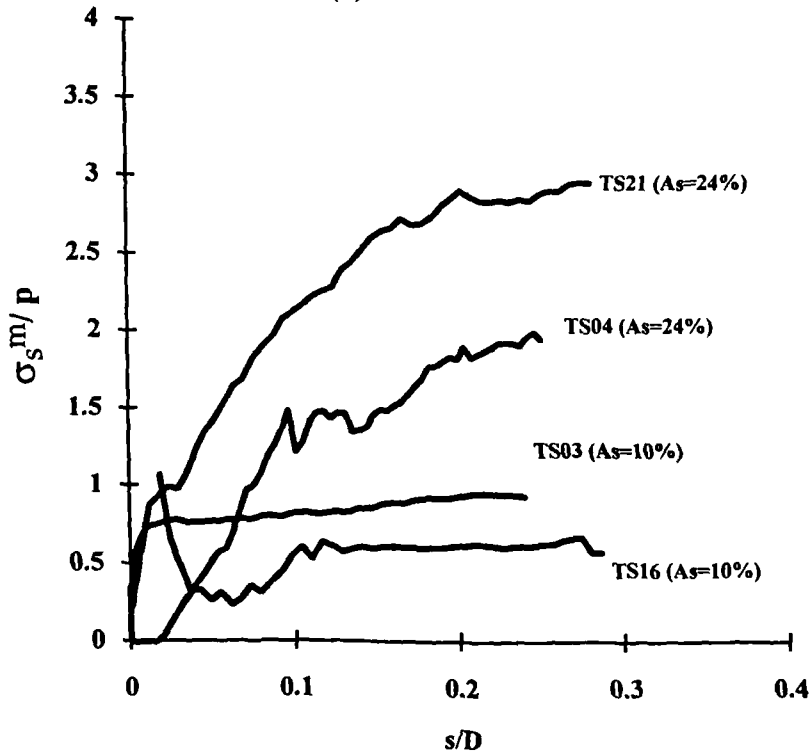


Fig 4.31: Effect of the area ratio on contact stress in column : displacement response
(a) centre column; (b) middle column

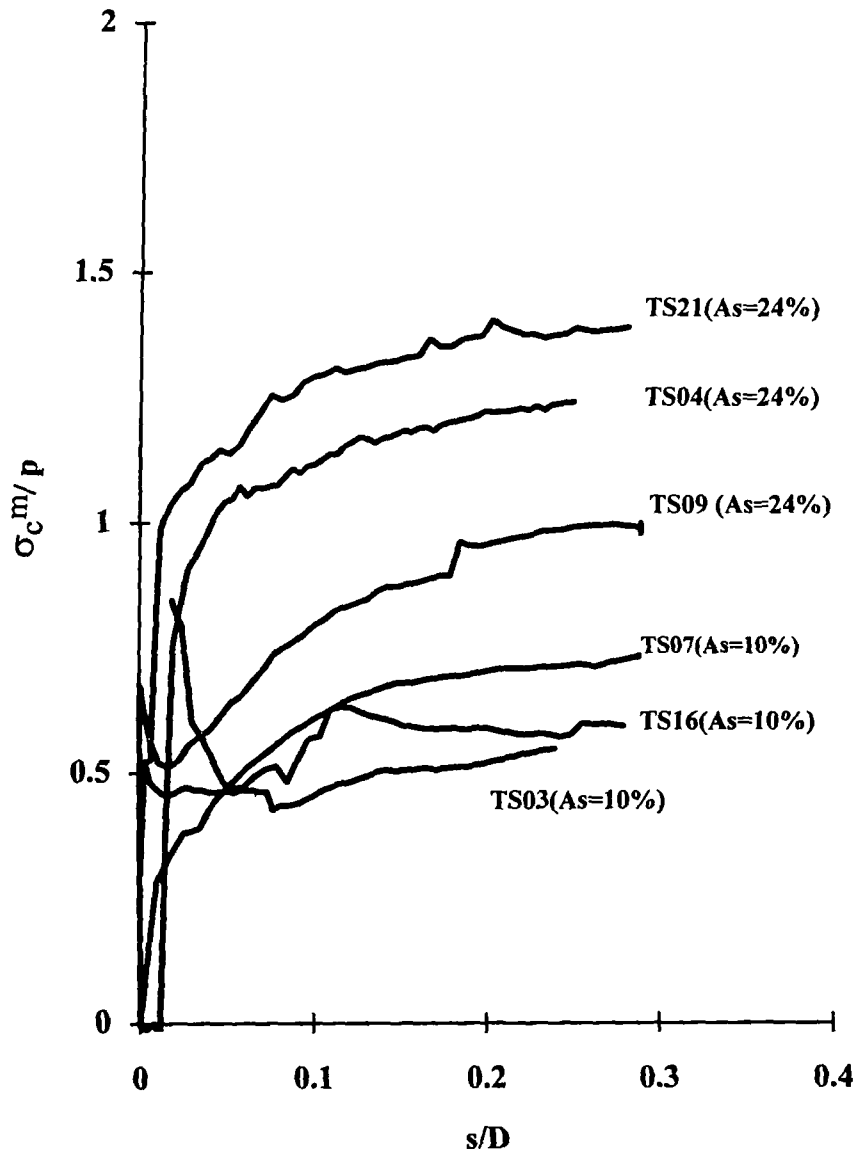


Fig 4.32: Effect of the area ratio on contact stress in clay : displacement response

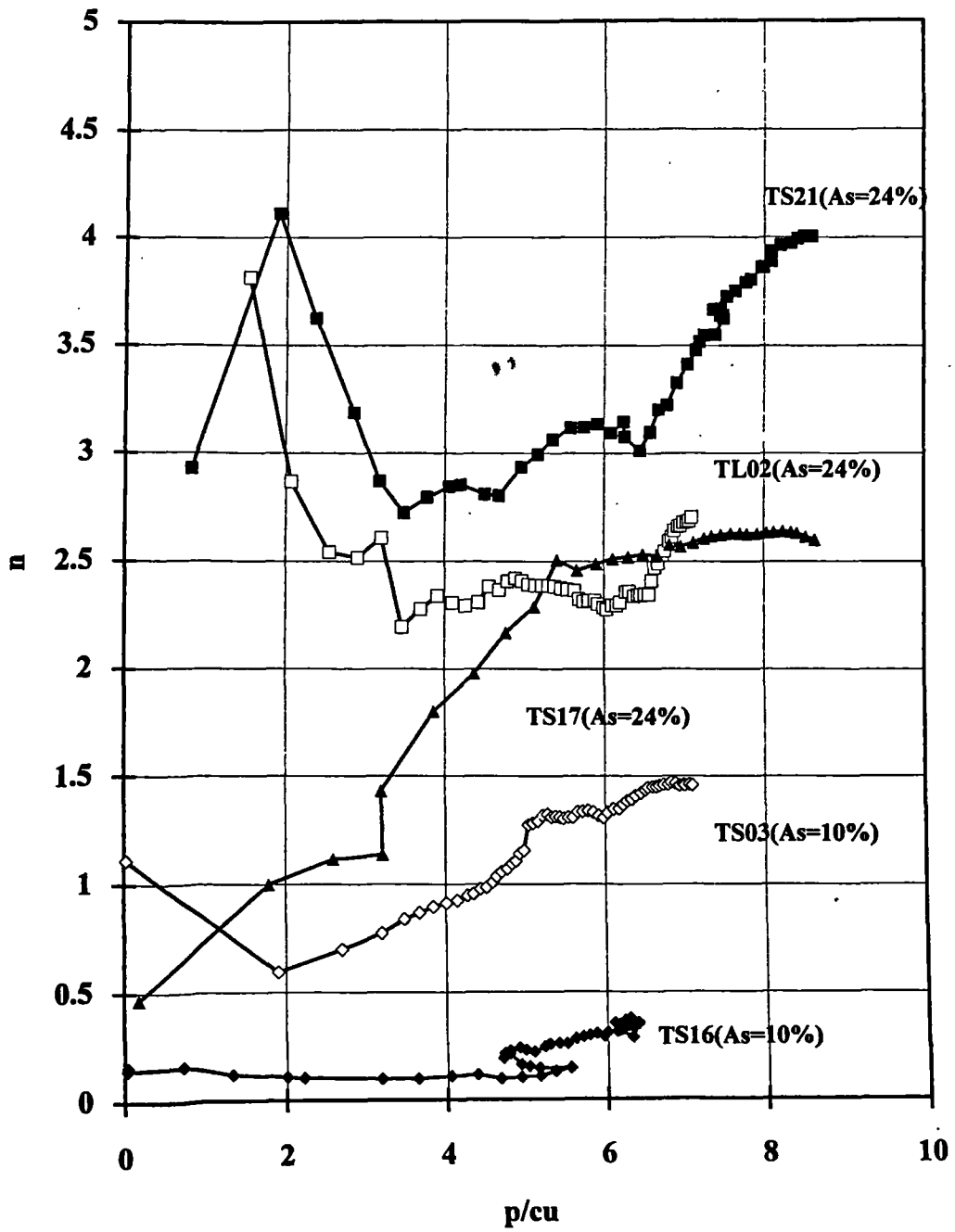


Fig 4.33: Effect of area ratio on the contact stress concentration ratio : load response (stress in centre column/stress in clay)

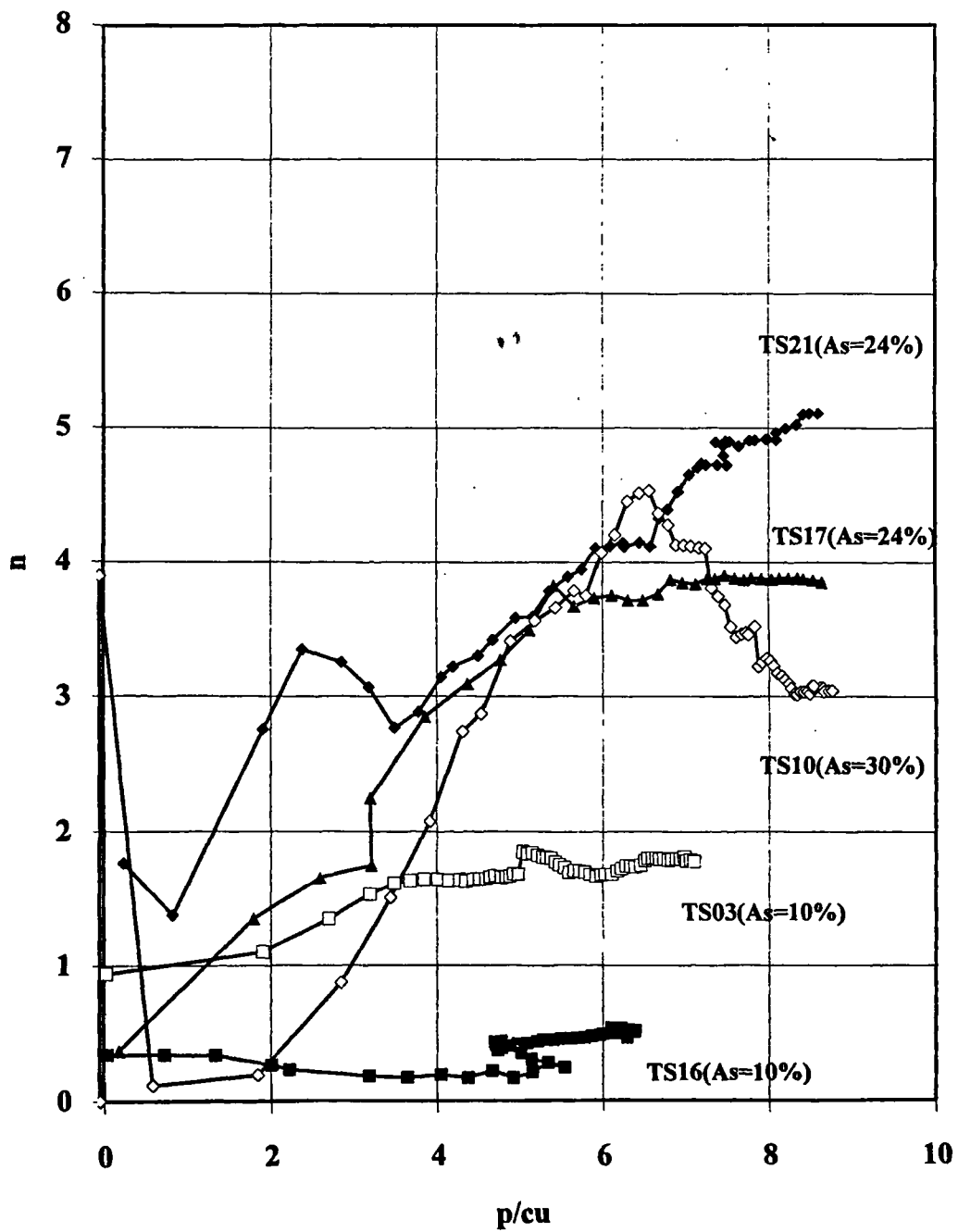
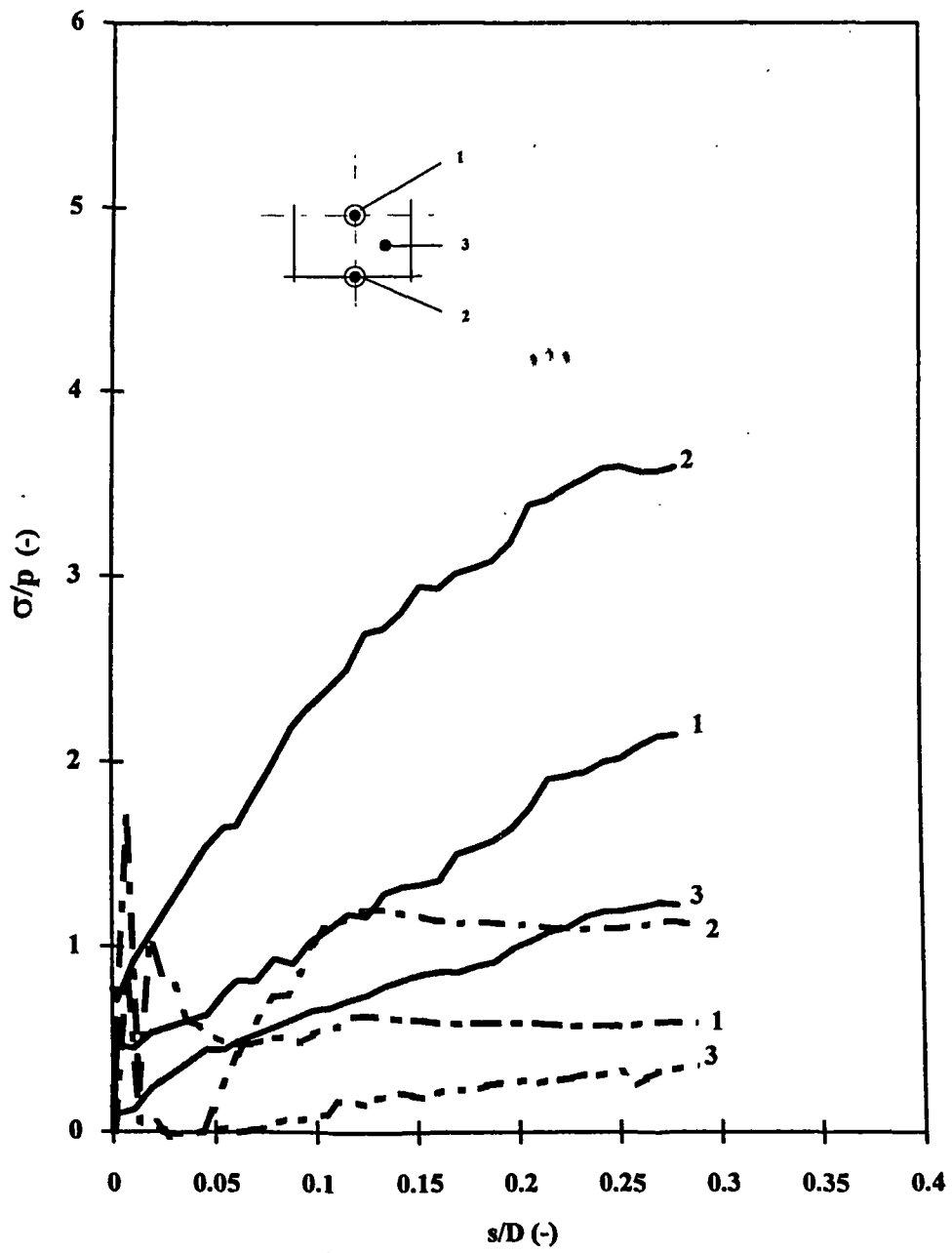


Fig 4.34: Effect of area ratio on the contact stress concentration ratio : load response (stress in middle column/stress in clay)



TS18 Displacement method ———
 TS16 Replacement method - - -

Fig 4.35: Effect of column installation method on the contact stresses : displacement response (TS18 & TS16)

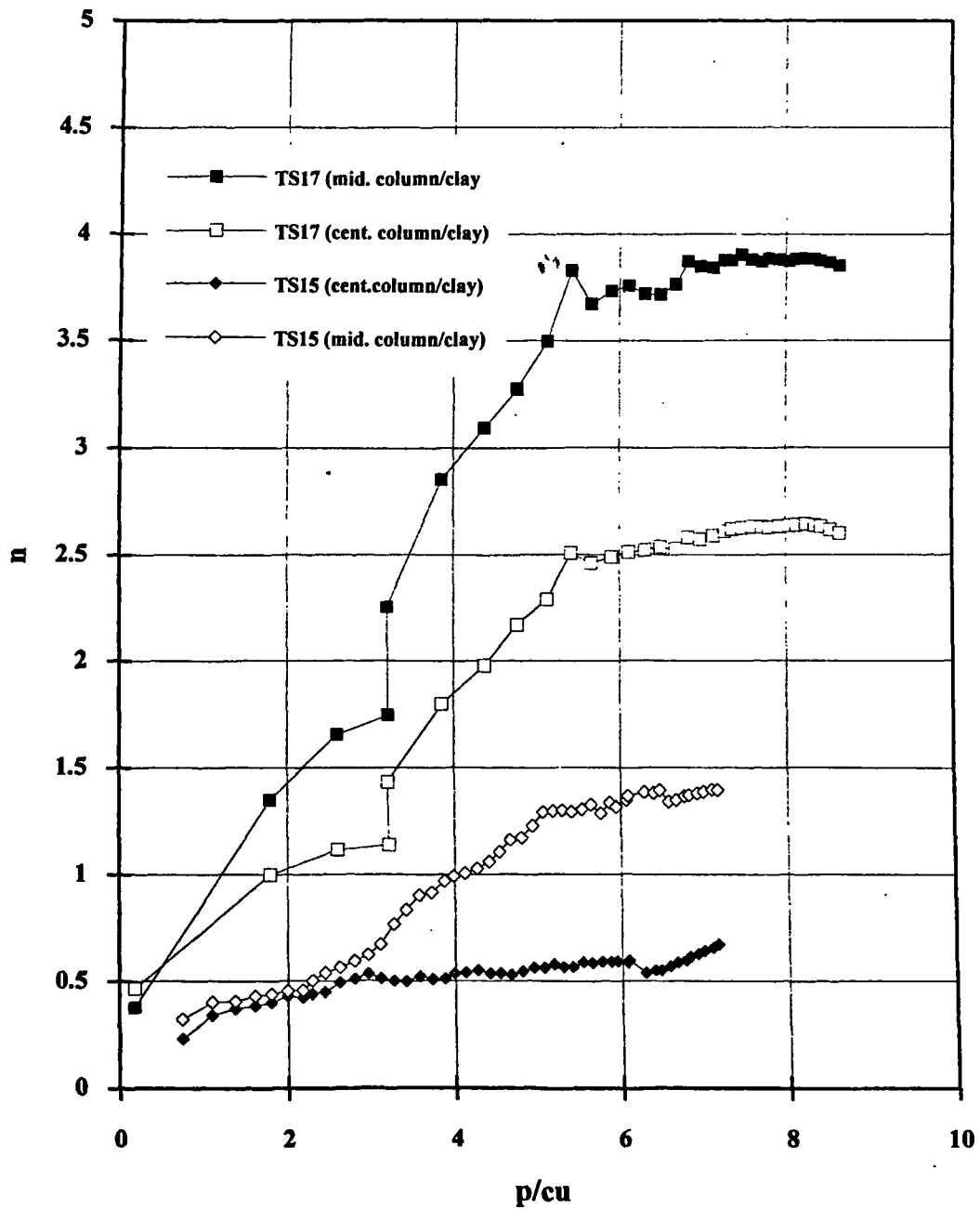


Fig 4.36: Effect of column installation method on the contact stress concentration ratio : load response ($A_s=24\%$, TS17 replacement method, TS15 displacement method)

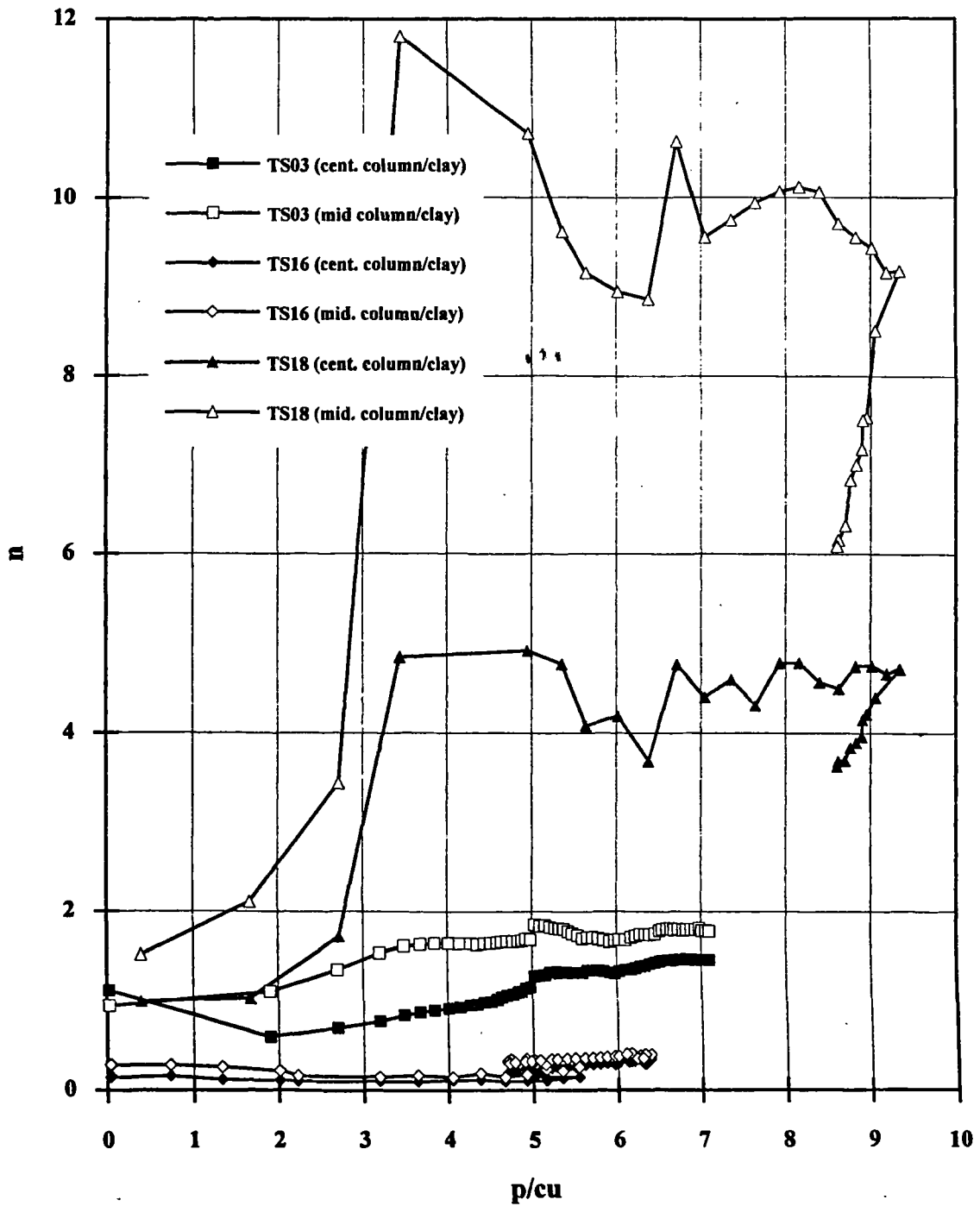
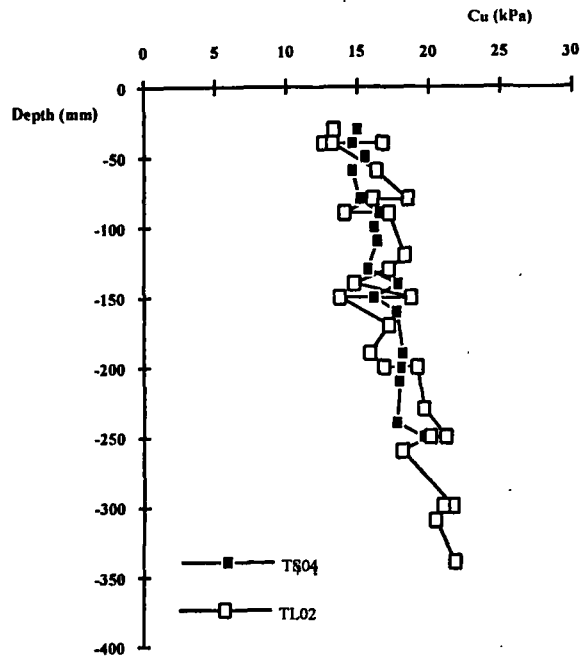
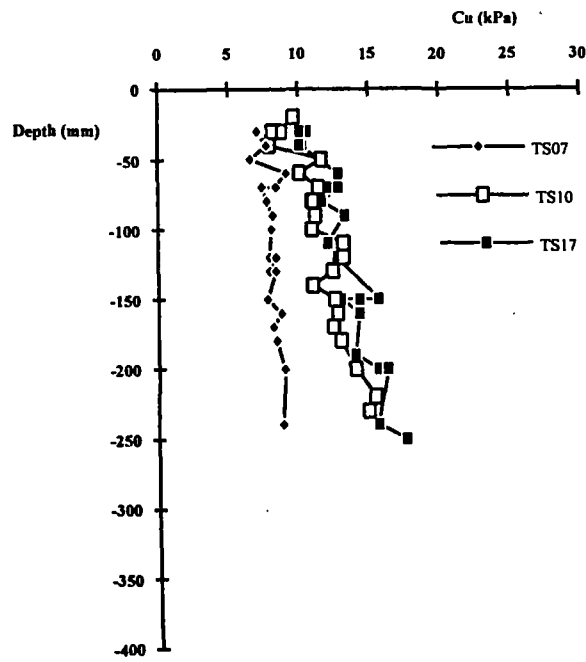


Fig 4.37: Effect of column installation method on the contact stress concentration ratio : load response ($A_s=10\%$, TS03 & TS16 replacement method, TS18 displacement method)



(a)



(b)

Fig 4.38: Typical profiles of undrained shear strength with depth (a) $p_{cmax} = 160$ kPa; (b) $p_{cmax} = 120$ kPa;

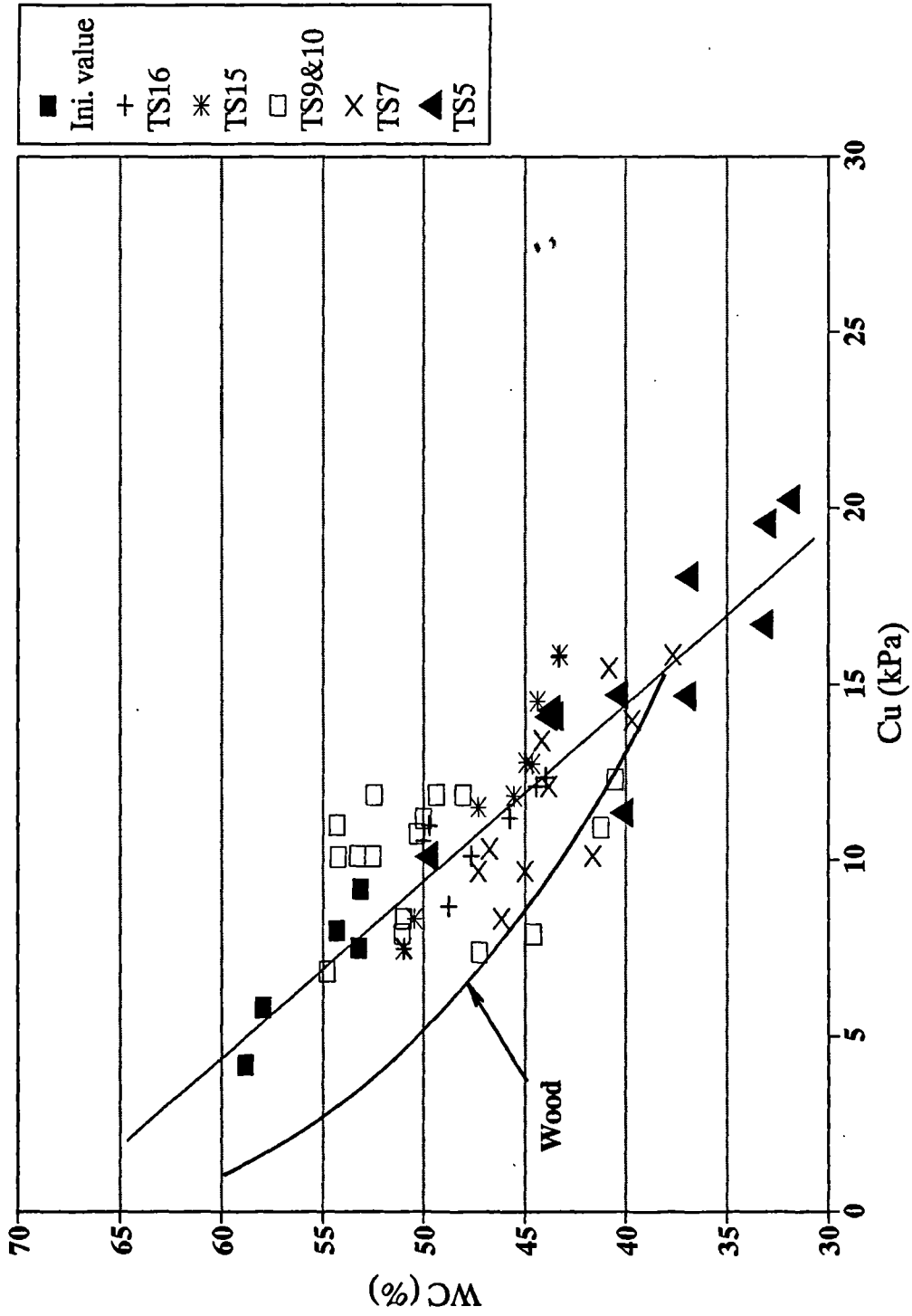
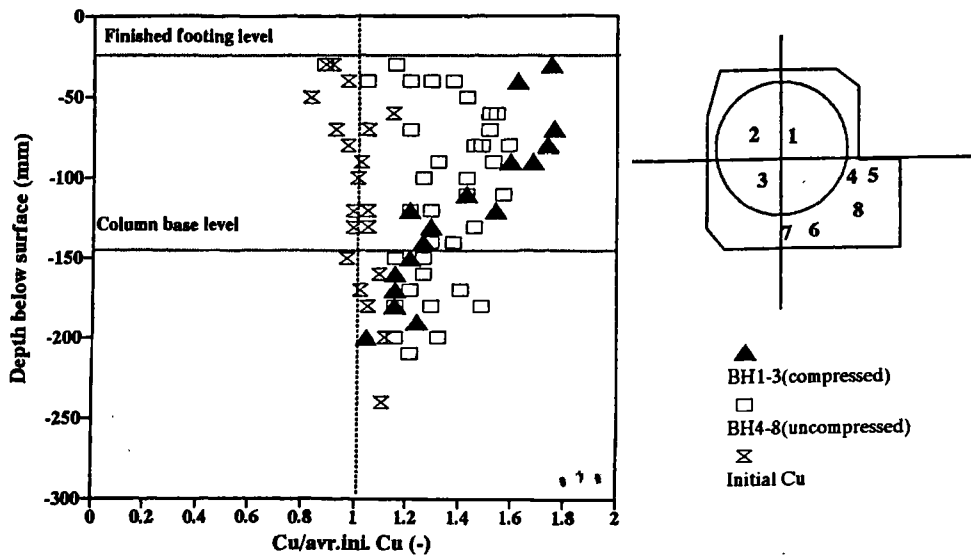
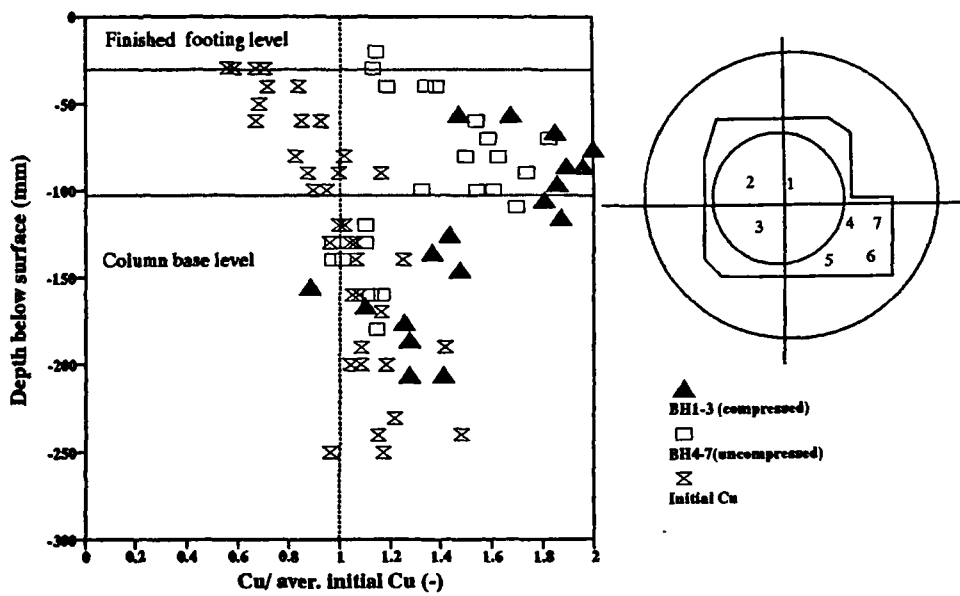


Fig 4.39: The relationship between water content and undrained shear strength for speswhite kaolin clay



(a)



(b)

Fig 4.40: Effect of the area ratio on the profile of undrained shear strength before and after test (a) $A_s=10\%$ -TS07; (b) $A_s=30\%$ -TS05

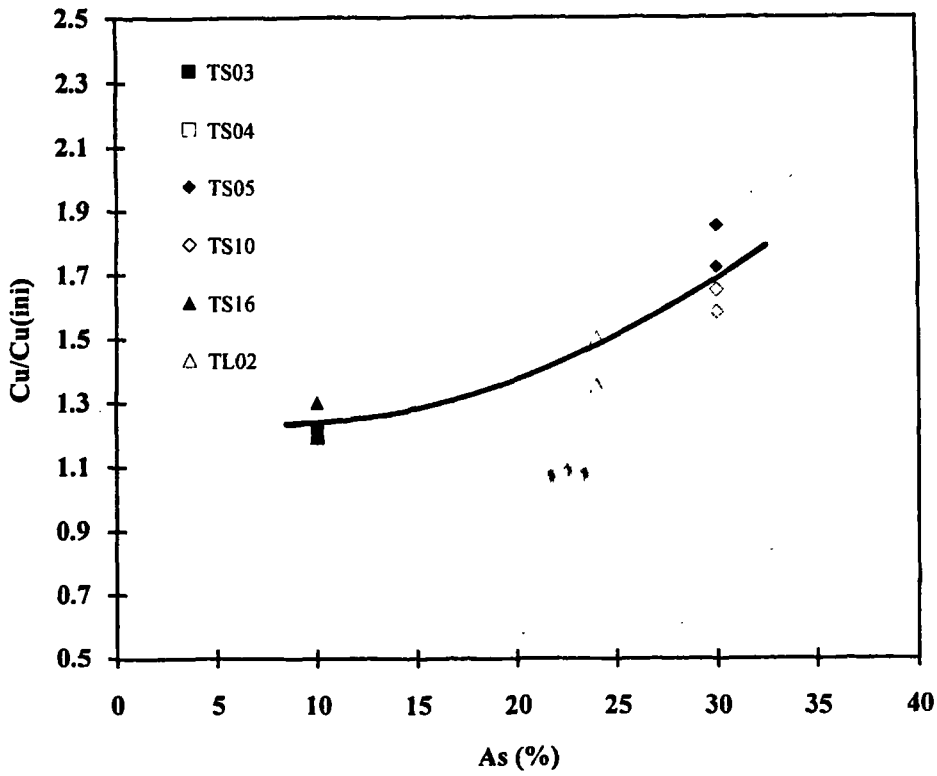


Fig 4.41: The relationship between area ratio and the ratio of undrained shear strength after test to initial undrained shear strength

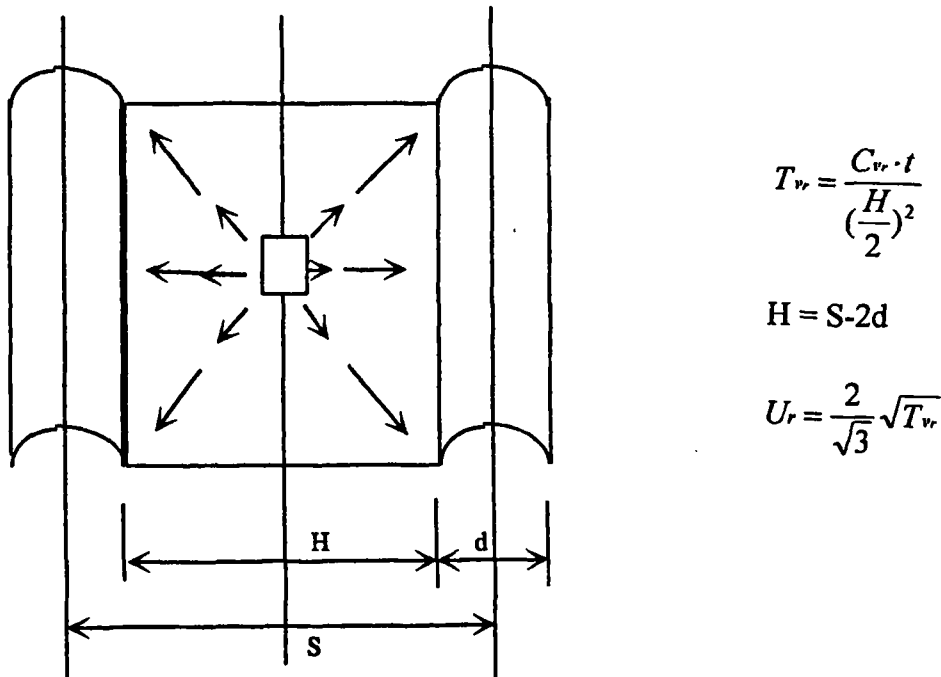
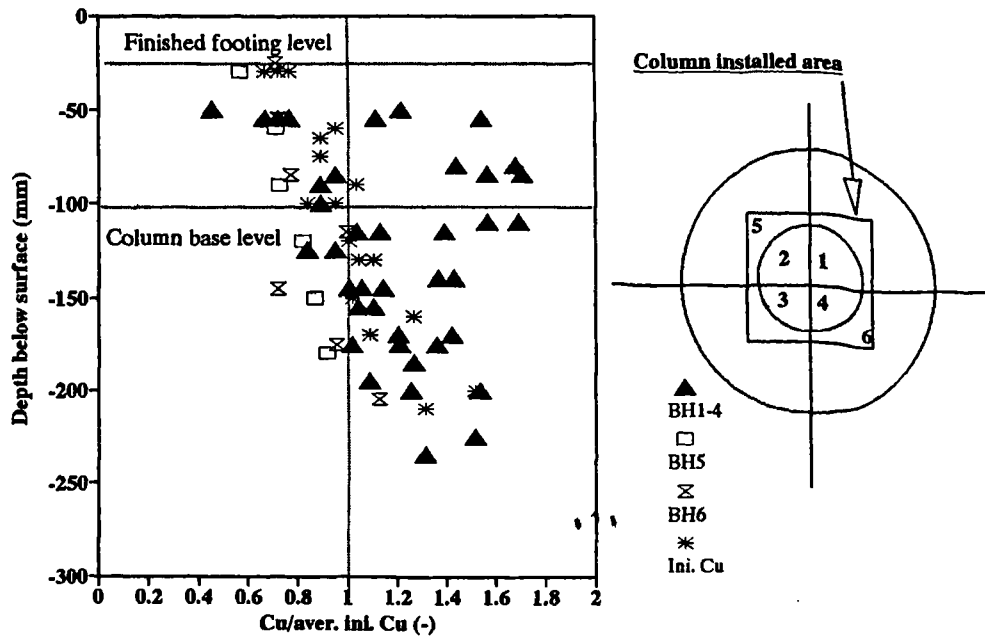
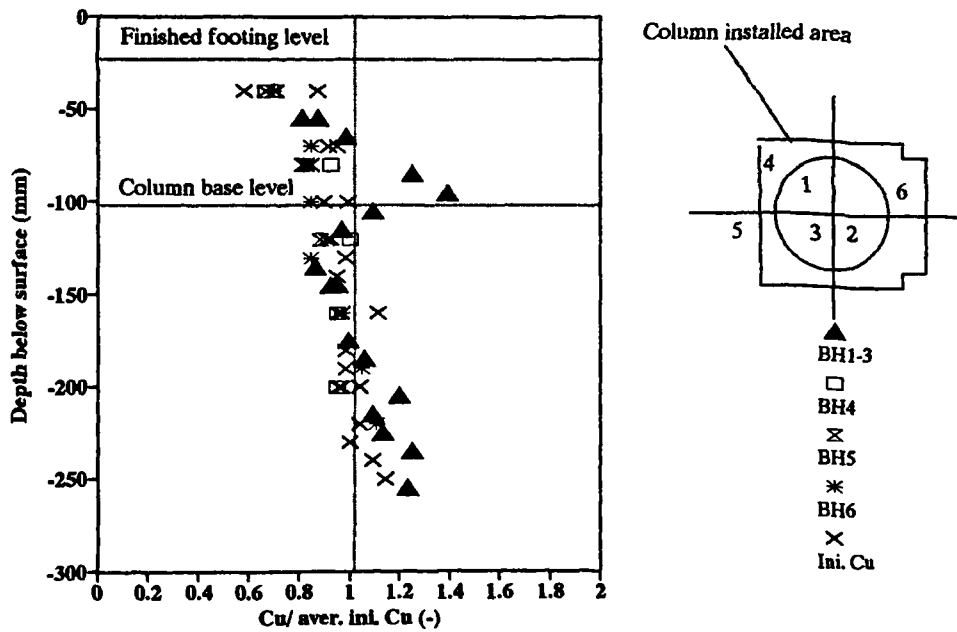


Fig 4.42: Notation of the radial consolidation analysis

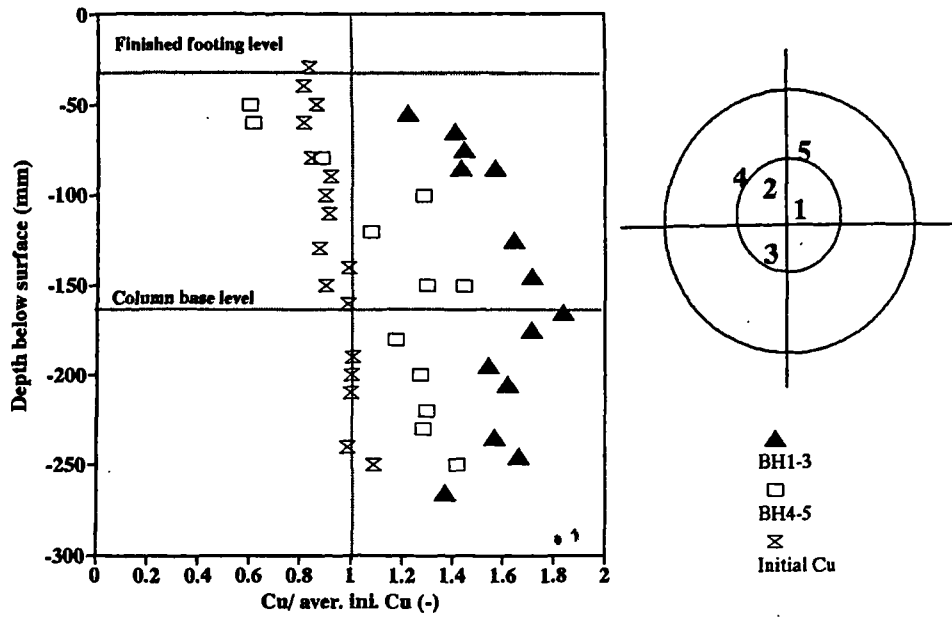


(a)

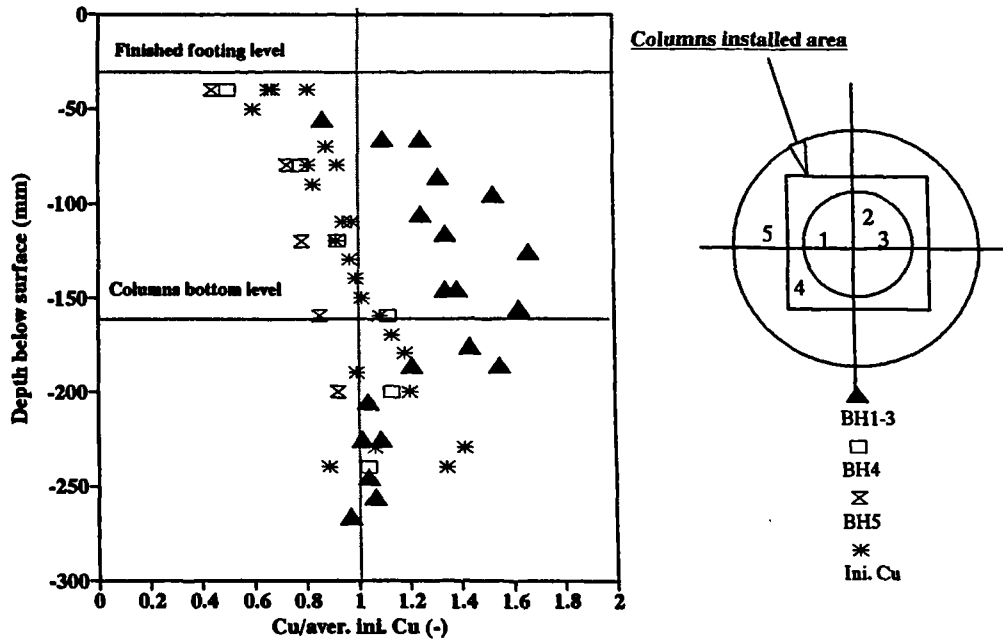


(b)

Fig 4.43: Effect of the column installation method on the profile of undrained shear strength before and after test ($A_s=10\%$) (a) displacement method -TS18; (b) replacement method -TS16



(a)



(b)

Fig 4.44: Effect of the column installation method on the changing of undrained shear strength before and after test ($A_s=24\%$) (a) displacement method -TS15; (b) replacement method -TS09

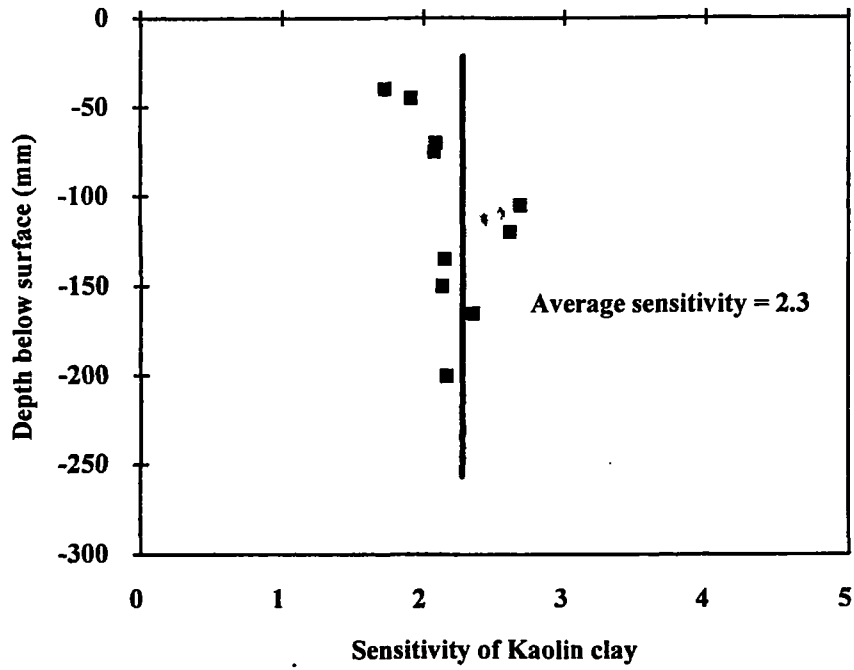
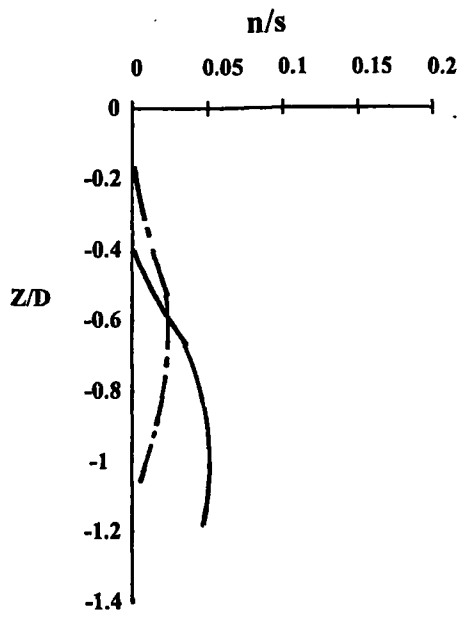
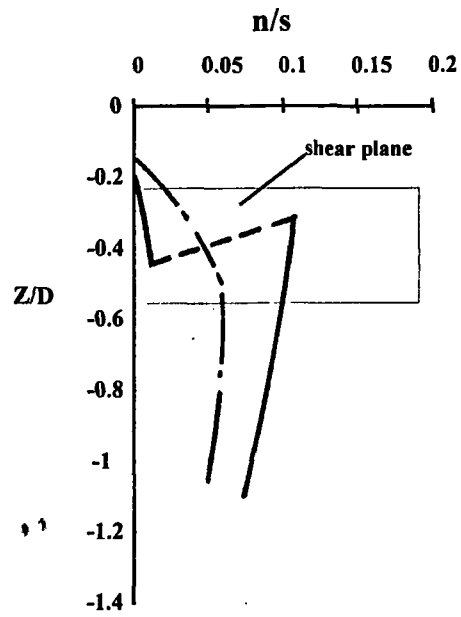


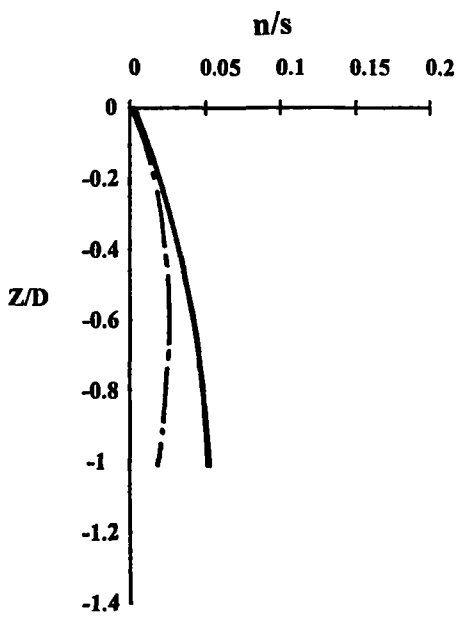
Fig 4.45: The profile of average sensitivity with depth (TS-19)



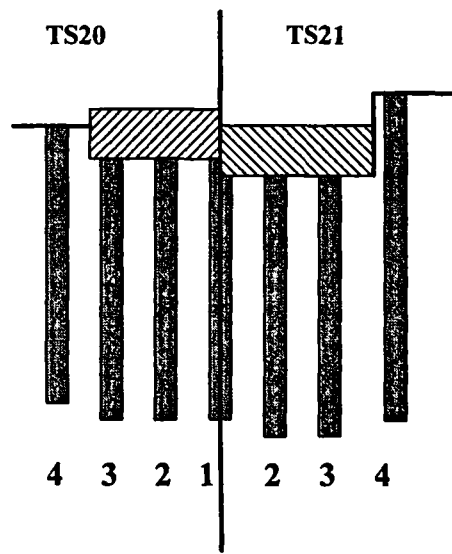
(a) middle column (2)



(b) edge column (3)



(c) out column (4)



(d) Location of columns

TS20: (15 mm of footing penetration)
 TS21 (30 mm of footing penetration)

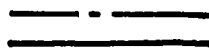
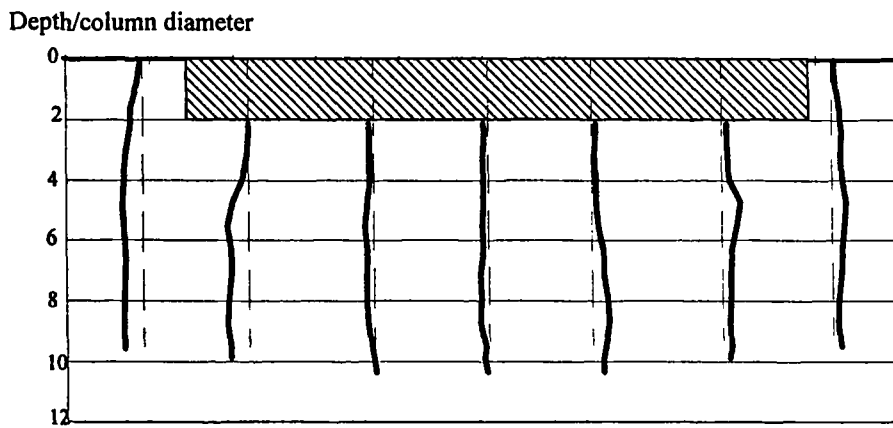
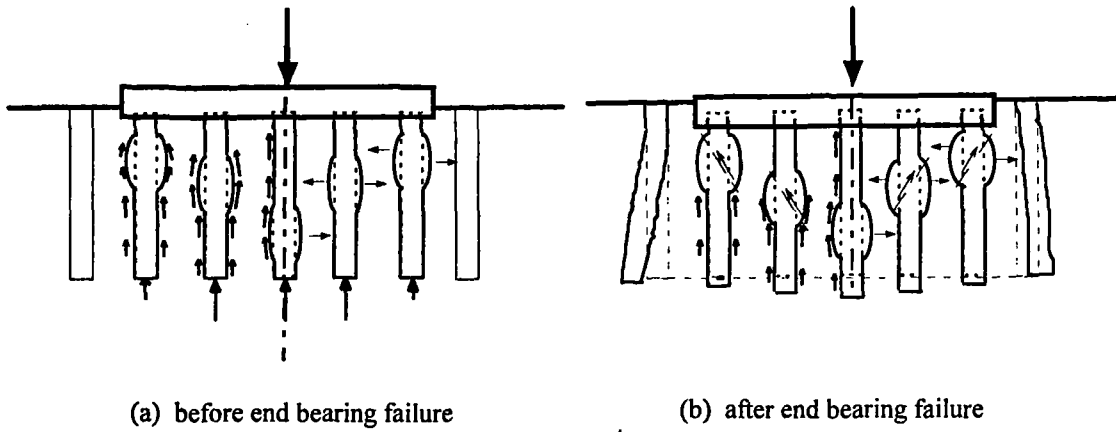
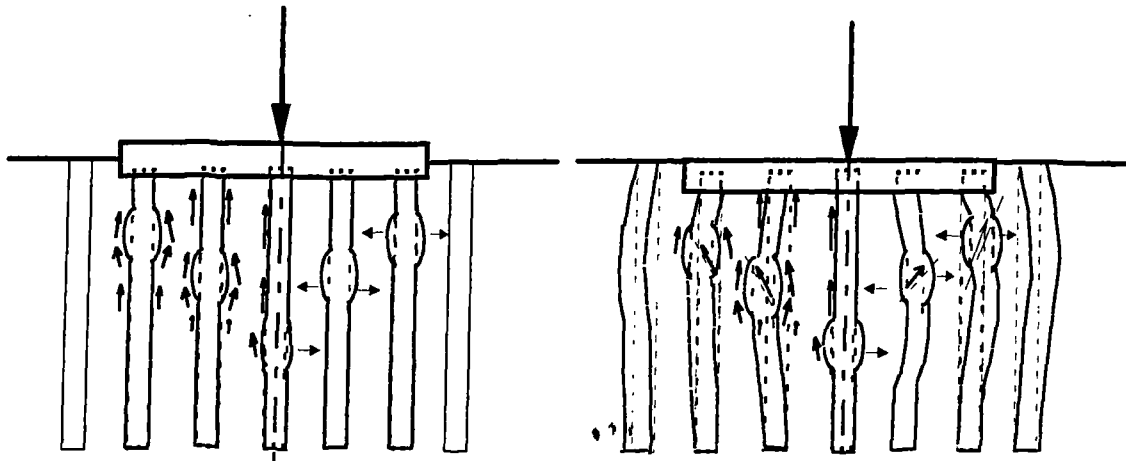


Fig 4.46: The progress of the lateral deformation deduced from centreline of columns



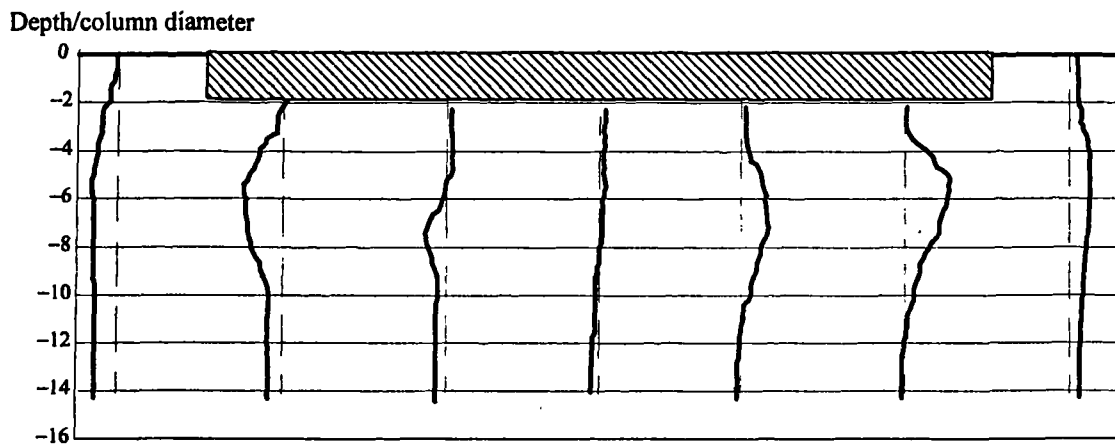
(c) horizontal movements deduced from centrelines of columns (TS-08)

Fig 4.47: Suggested mode of deformation for short columns (a) before end bearing failure; (b) after end bearing failure; (c) horizontal movements deduced from centrelines of columns (TS-08)



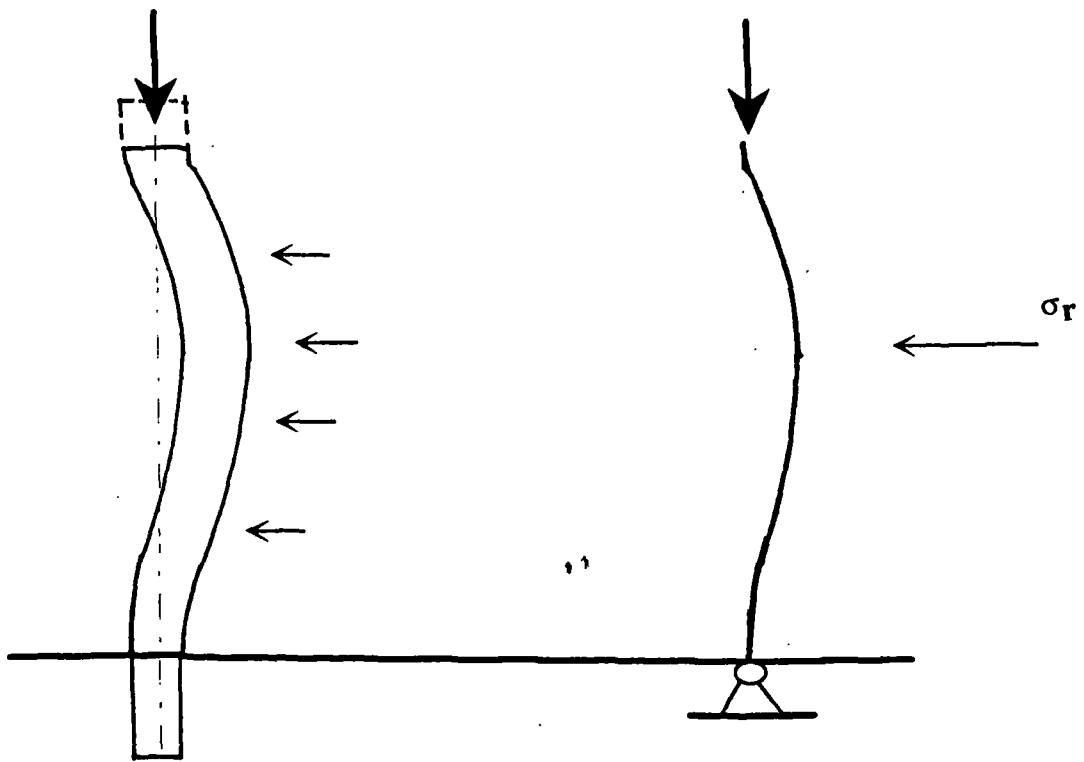
(a) before overall failure;

(b) after overall failure;

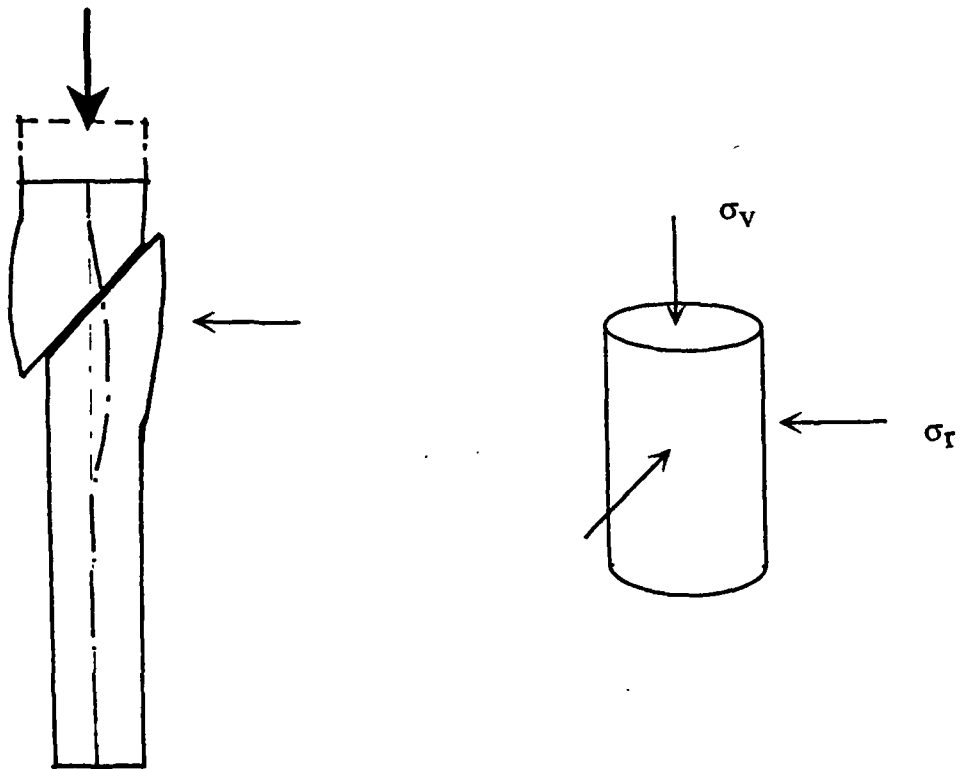


(c) horizontal movements deduced from centrelines of columns (TS-17)

Fig 4.49: Suggested mode of deformation for long columns (a) before overall failure; (b) after overall failure; (c) horizontal movements deduced from centrelines of columns (TS-17)



(a) buckling failure



(b) bulging failure

Fig 4.51: Suggested long column failure mode (a) buckling failure; (b) bulging failure

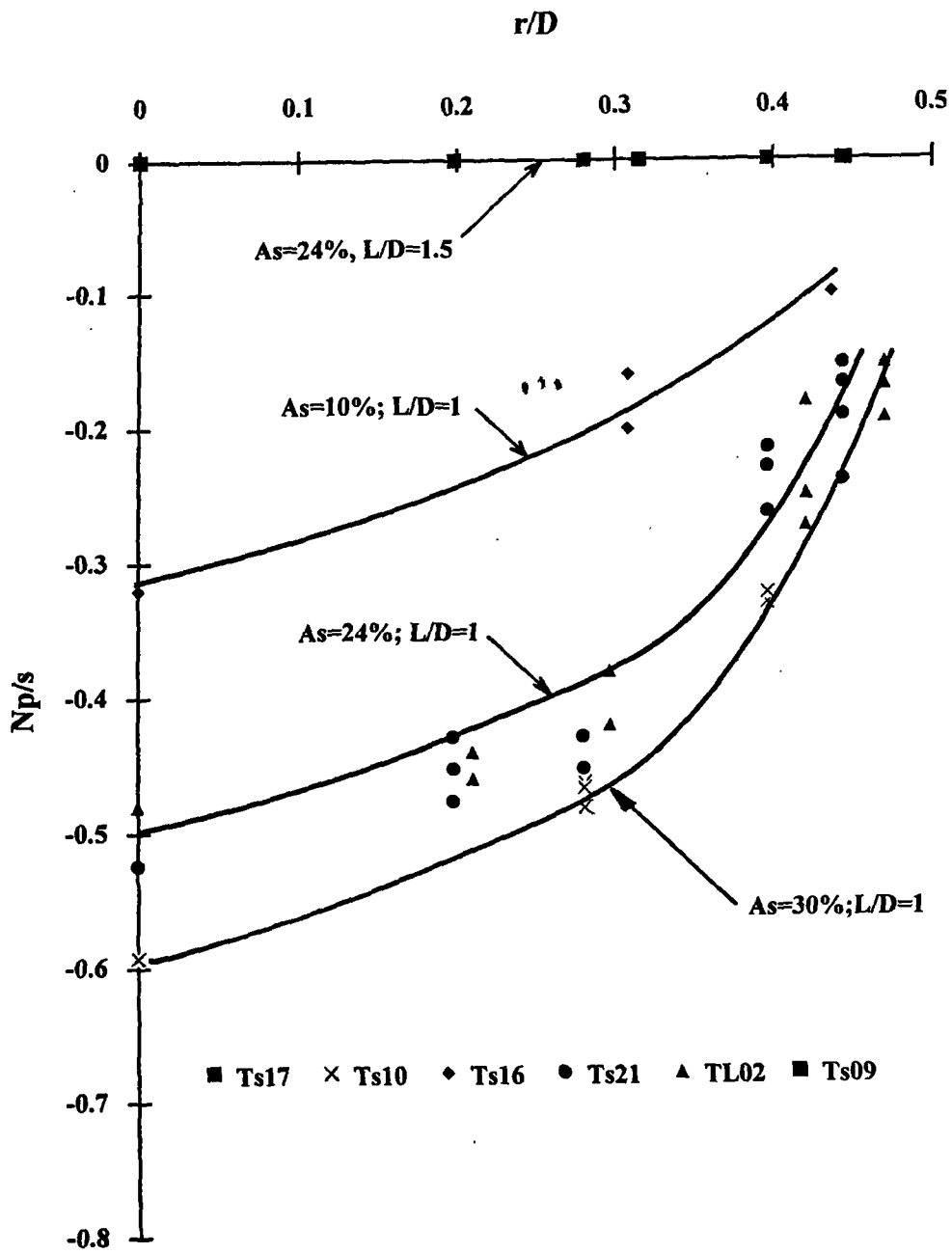


Fig 4.52: Effect of the area replacement ratio and column length on the profiles of column base penetration

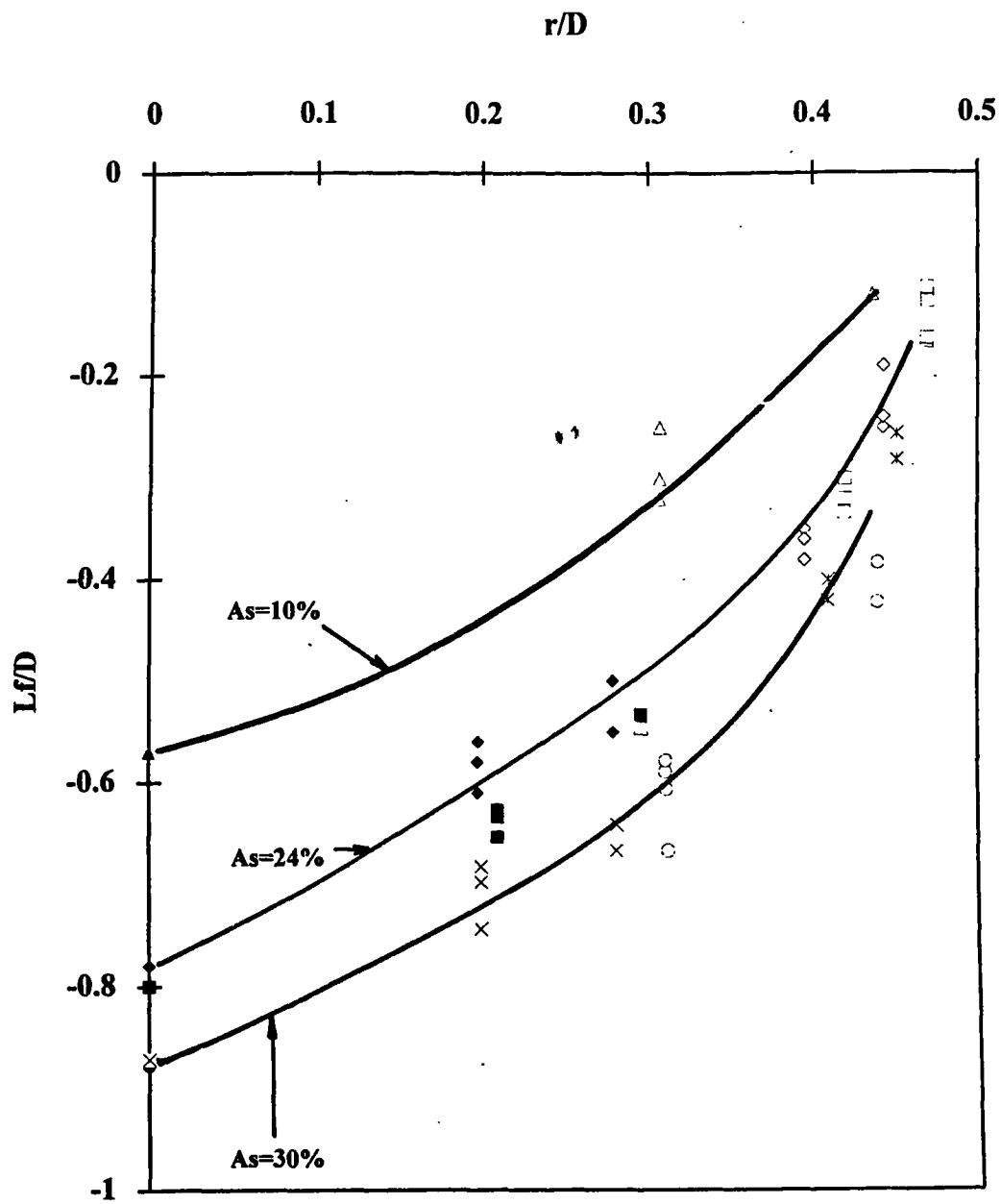
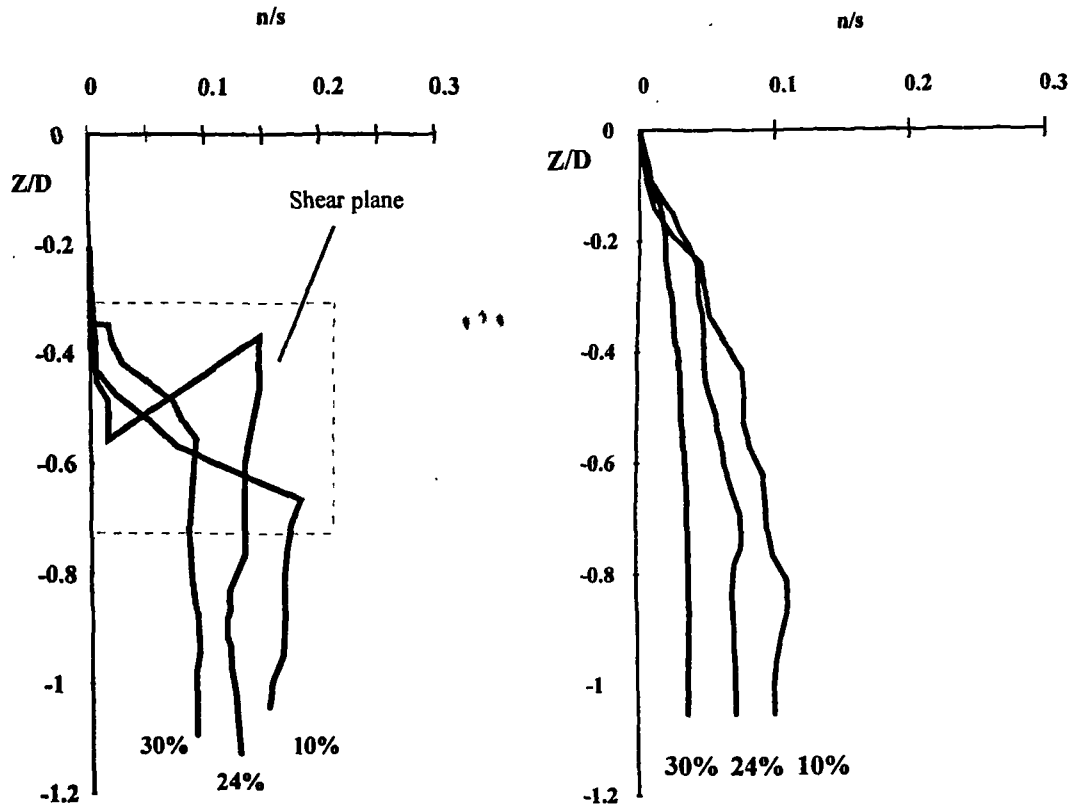


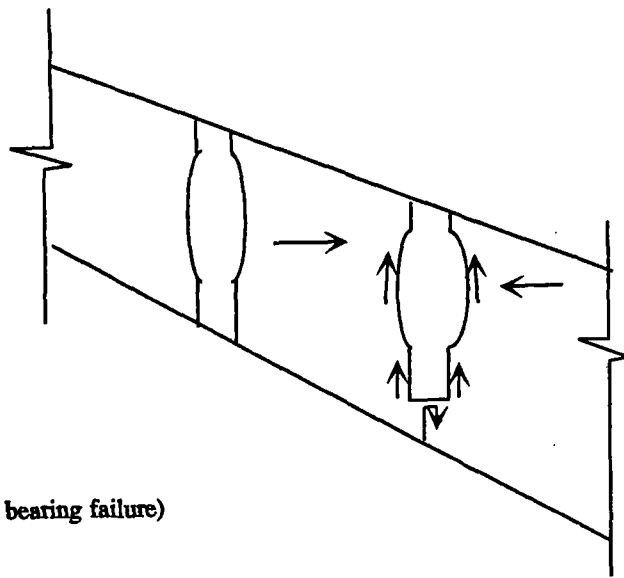
Fig 4.53: Effect of the area replacement ratio on the depth of maximum deformation in columns



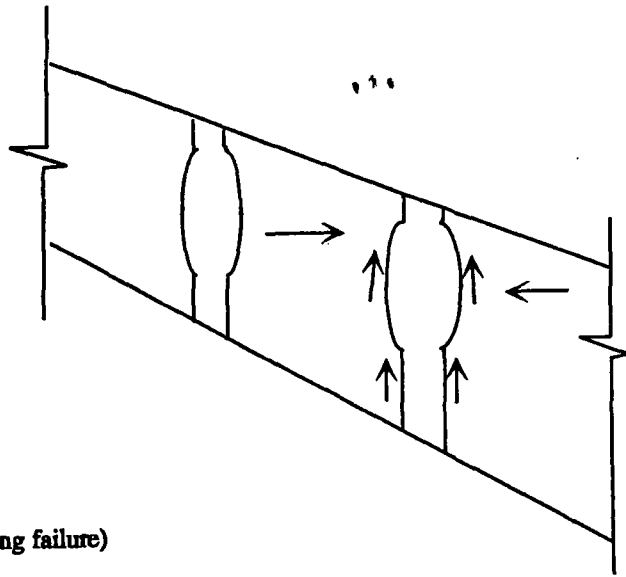
(a) edge column

(b) out column

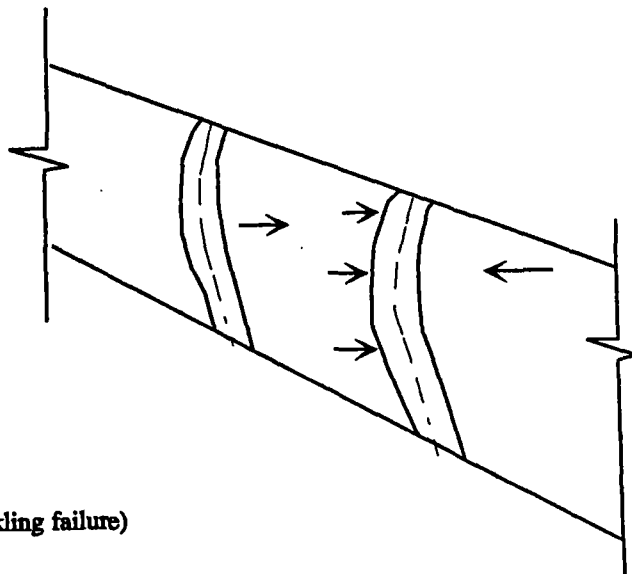
Fig 4.54: Effect of area ratio on horizontal displacement profile deduced from centreline of columns (10%=TS16, 24%=TS21, 30%=TS05)



(a) short column (end bearing failure)



(b) long column (bulging failure)



(c) long column (buckling failure)

Fig 4.56: Suggested failure mode of column within Zone II (a) short column - penetration; (b) long column - bulging; (c) long column - buckling

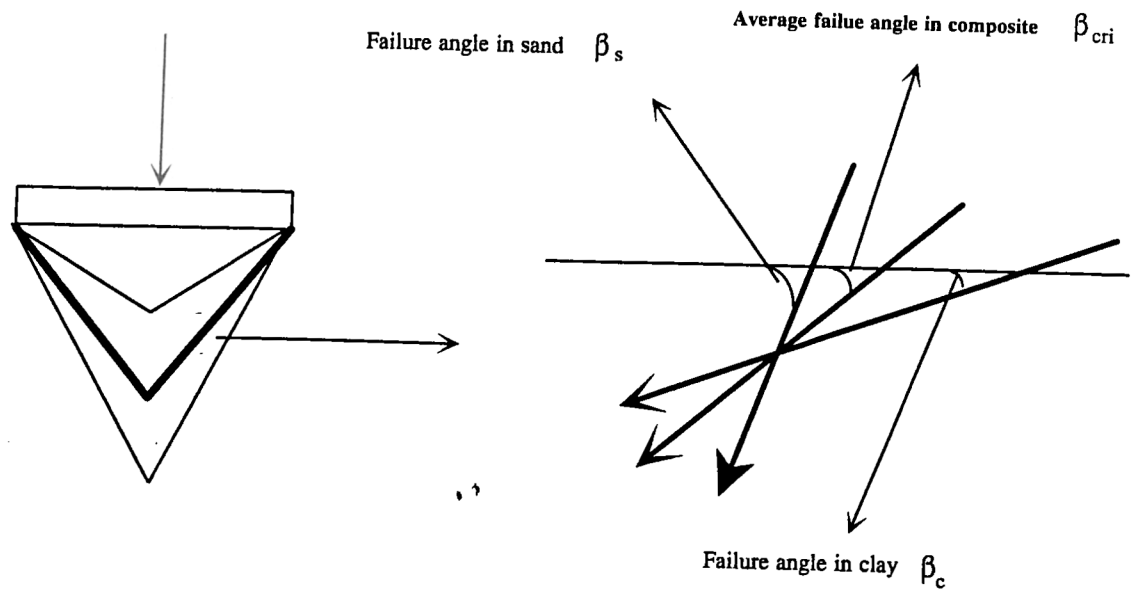


Fig 4.57: The failure angle β in the failure surface

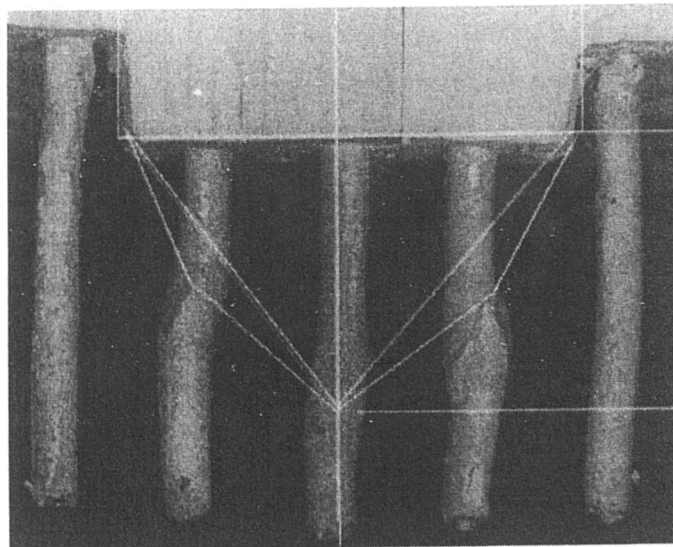


Fig 4.58: Estimation of failure surface from column cast (TS10)

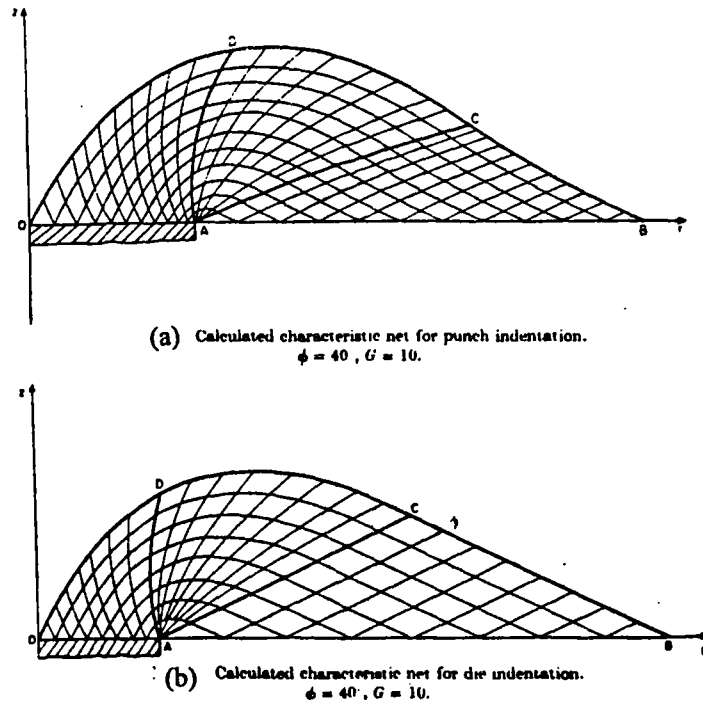


Fig 4.62: Calculated deformation characteristic net for (a) axial symmetry system; (b) plane strain system (after Cox 1962)

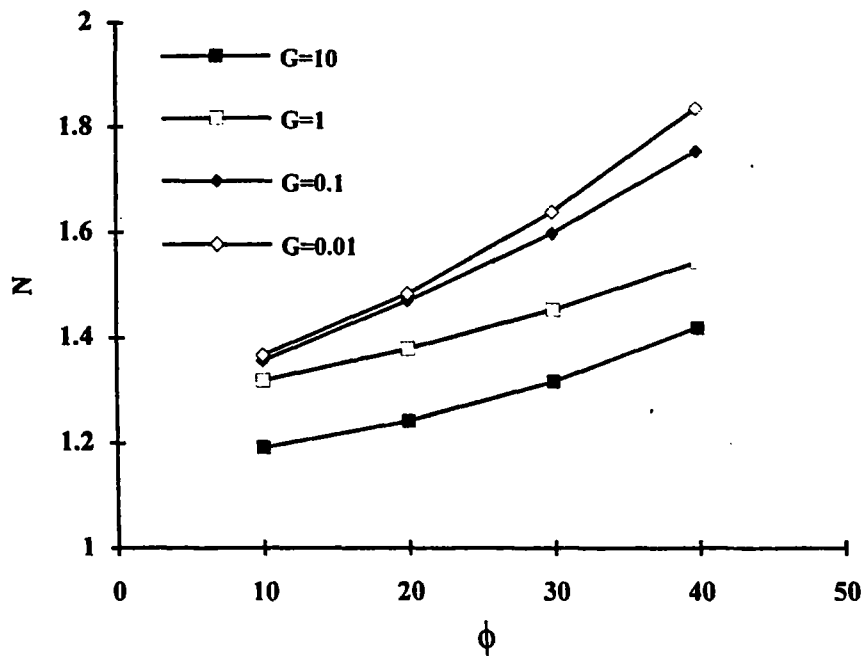
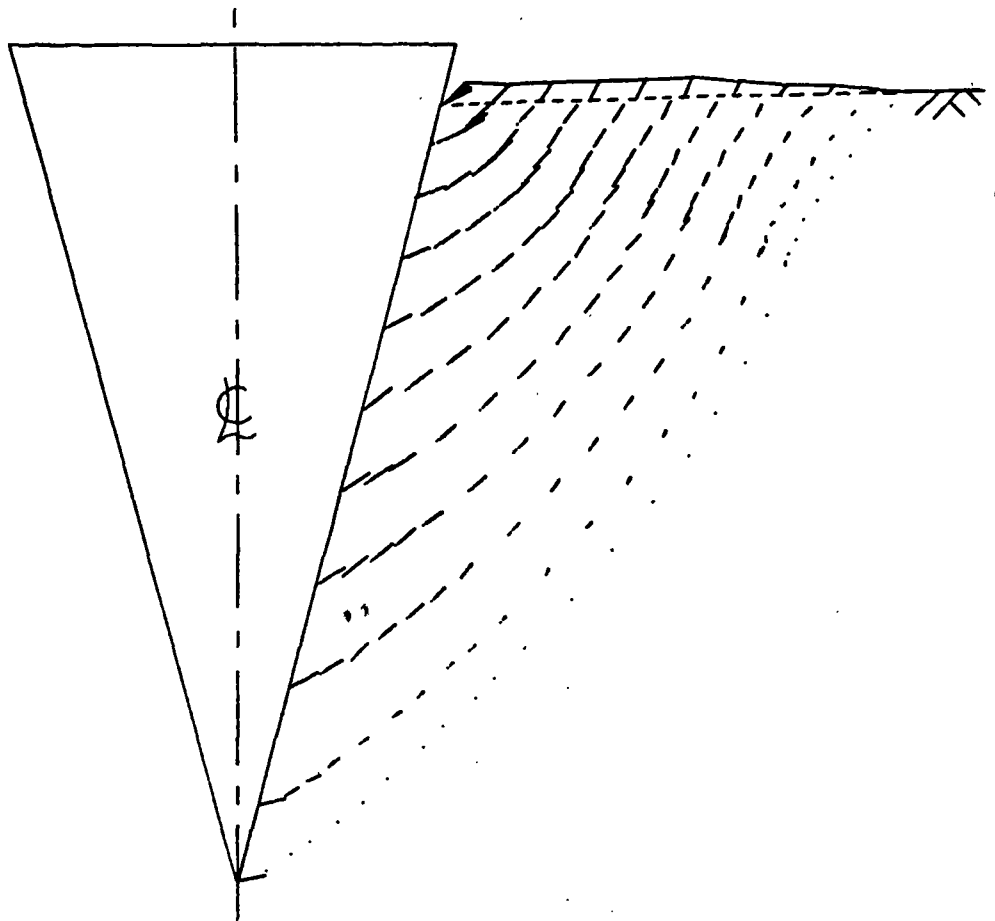
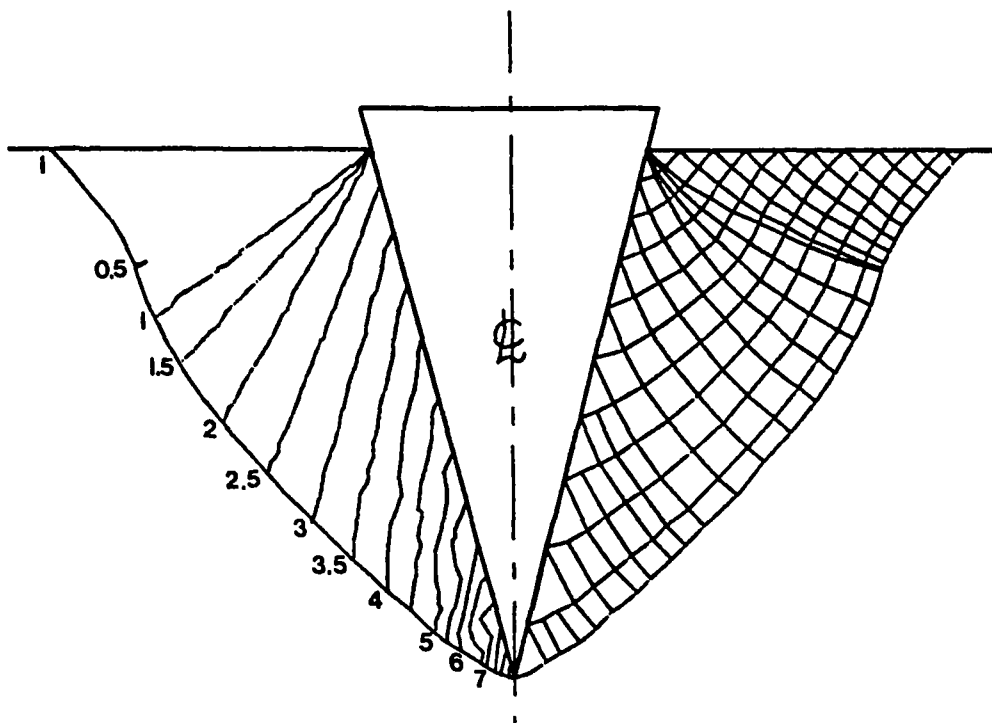


Fig 4.63: The relationship between axial symmetry influence parameter N and internal frictional angle of the soil (data from Cox 1962)

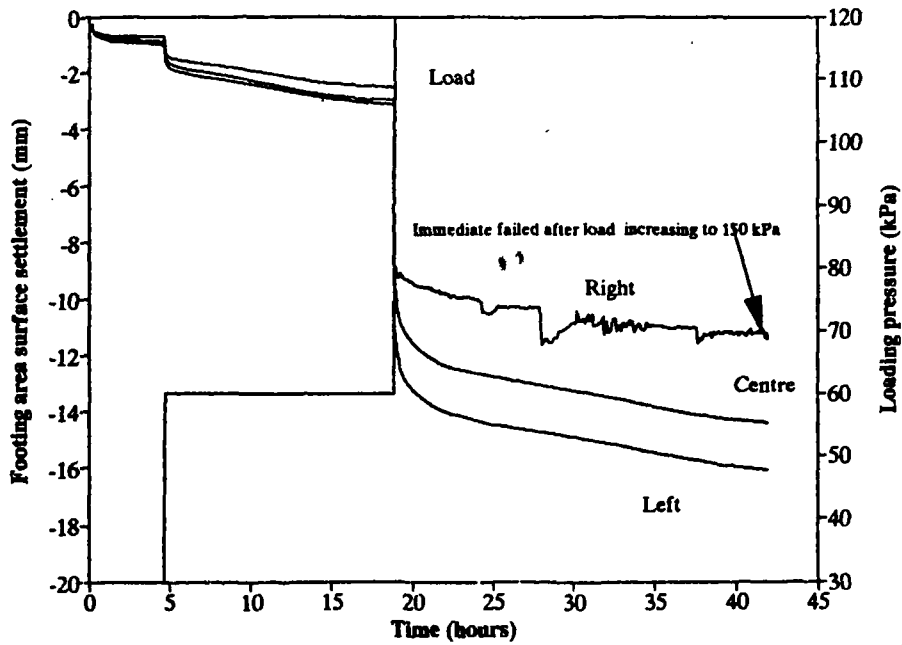
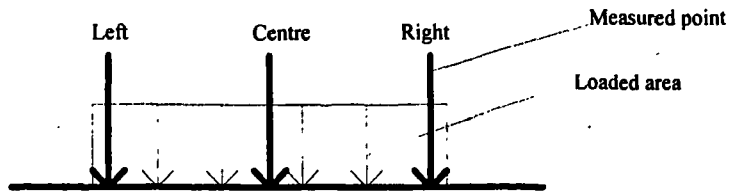


(a) Displacement field for cone penetration in a cohesive soil

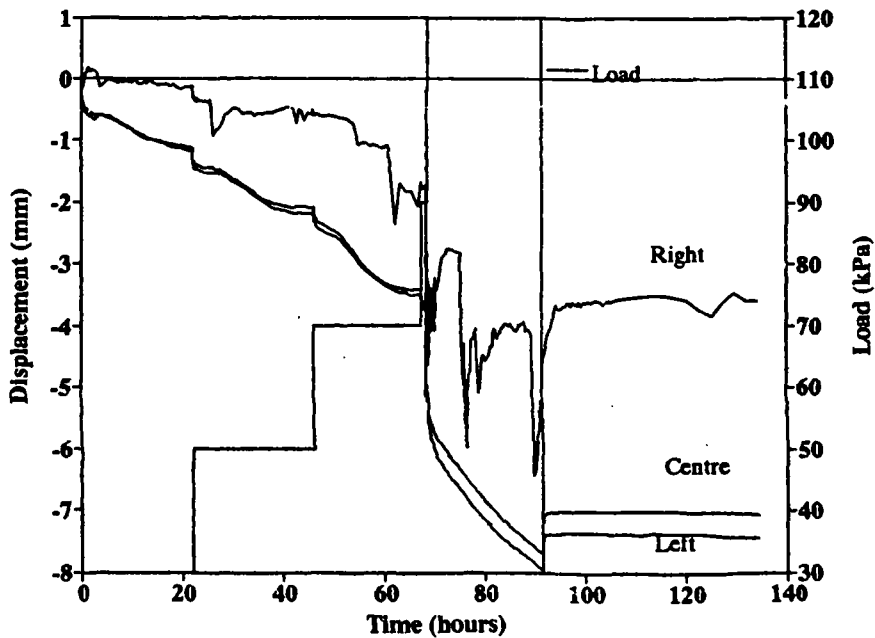


(b) Stress characteristics and contours of σ/c_u for cone penetration

Fig 4.64: Deformation characteristic of cone penetration test in a cohesive soil (a) displacement field; (b) stress characteristics and contours of σ/c_u (after Houlsby 1981)



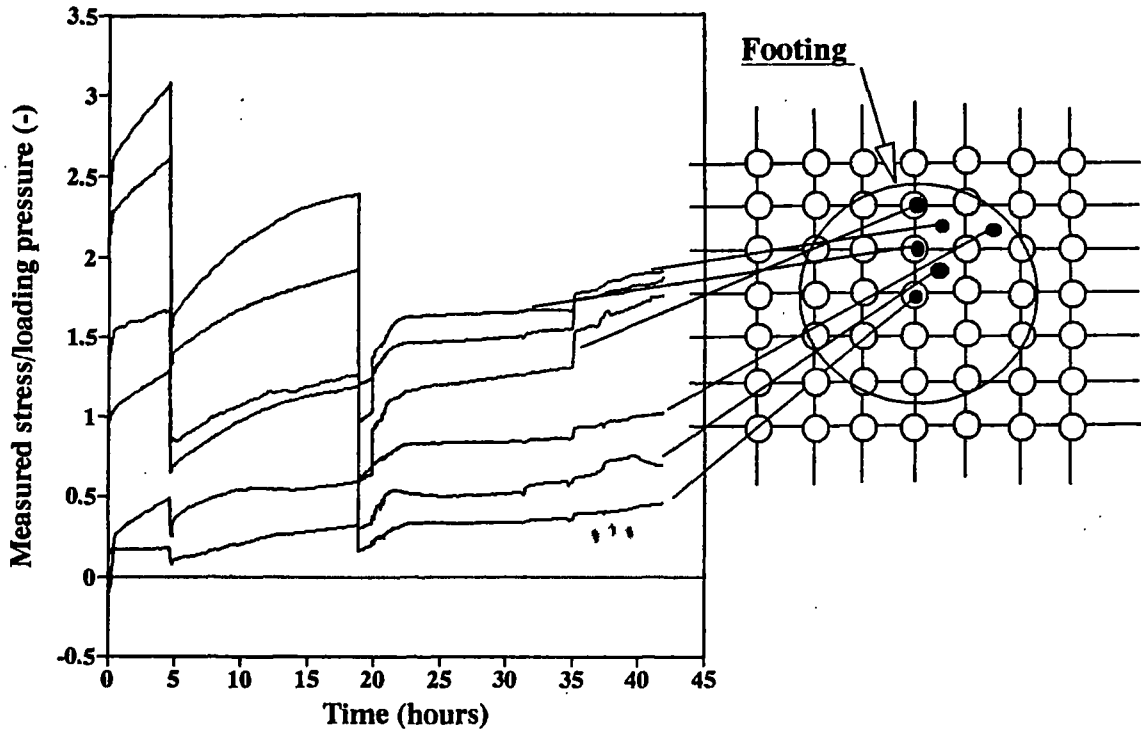
(a)



(b)

Fig 4. 65: Load : time : settlement relationship under flexible loading (a) fast loading test TL01-1; (b) Slow loading test TL01-2

(a) Fast loading test (TL01-1)



(b) Slow loading test (TL01-2)

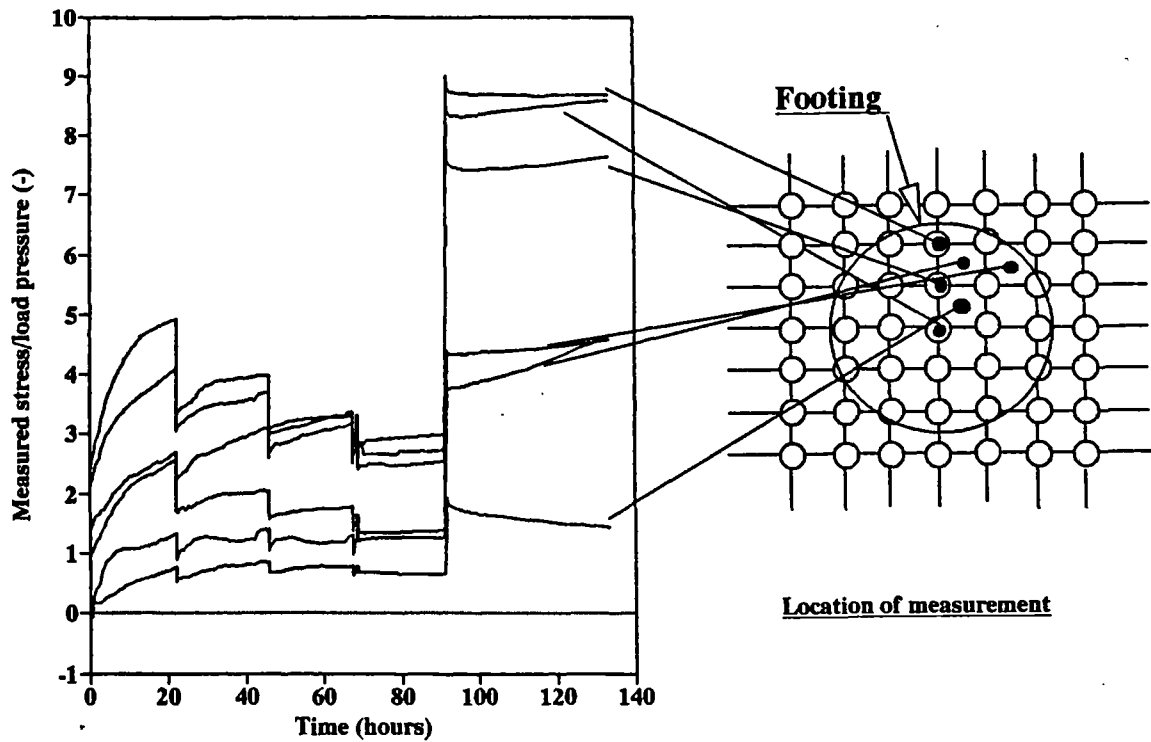
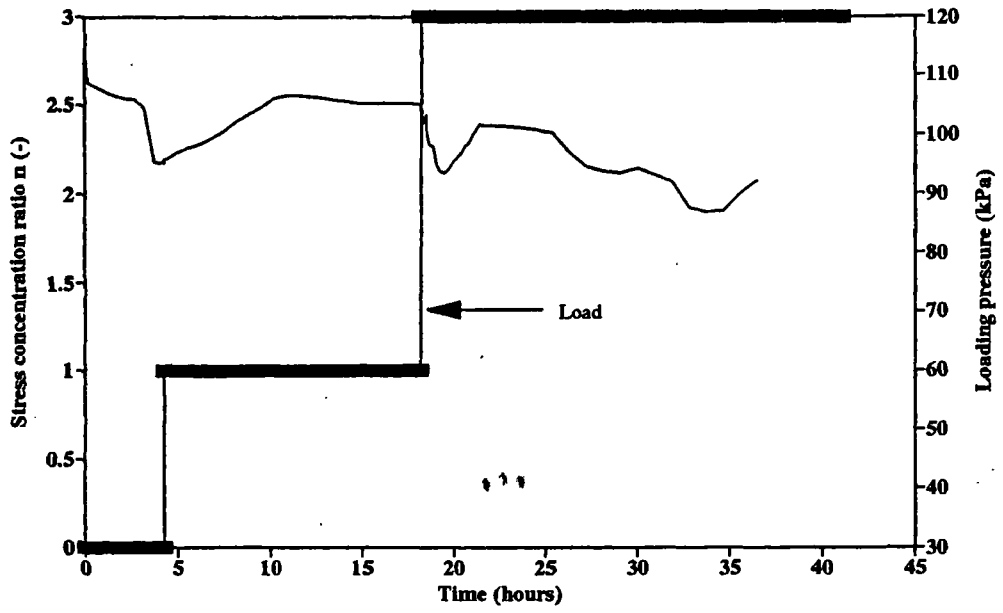
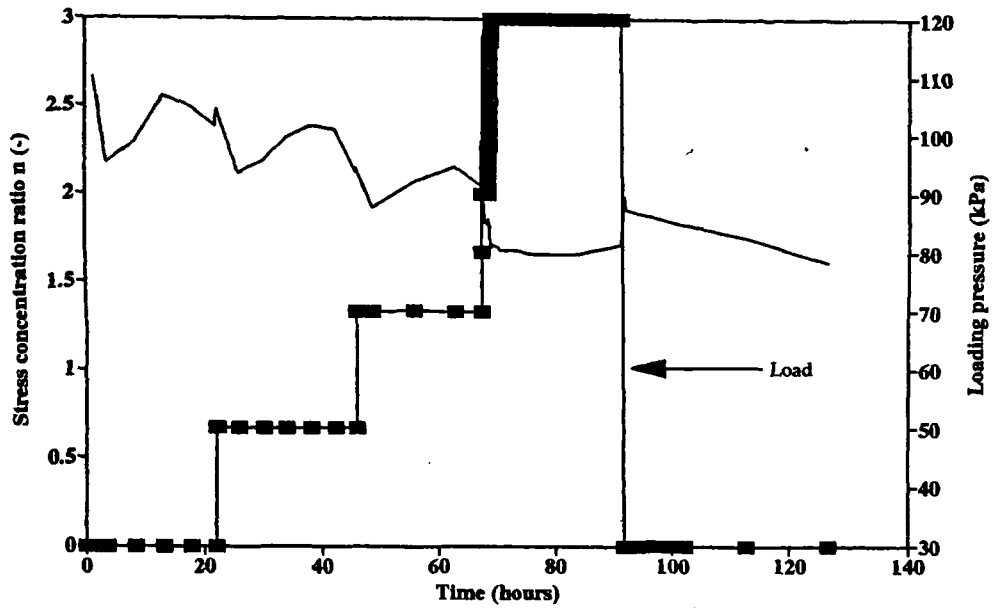


Fig 4.66: Distribution of contact stresses (a) fast loading TL01-1; (b) slow loading TL01-2



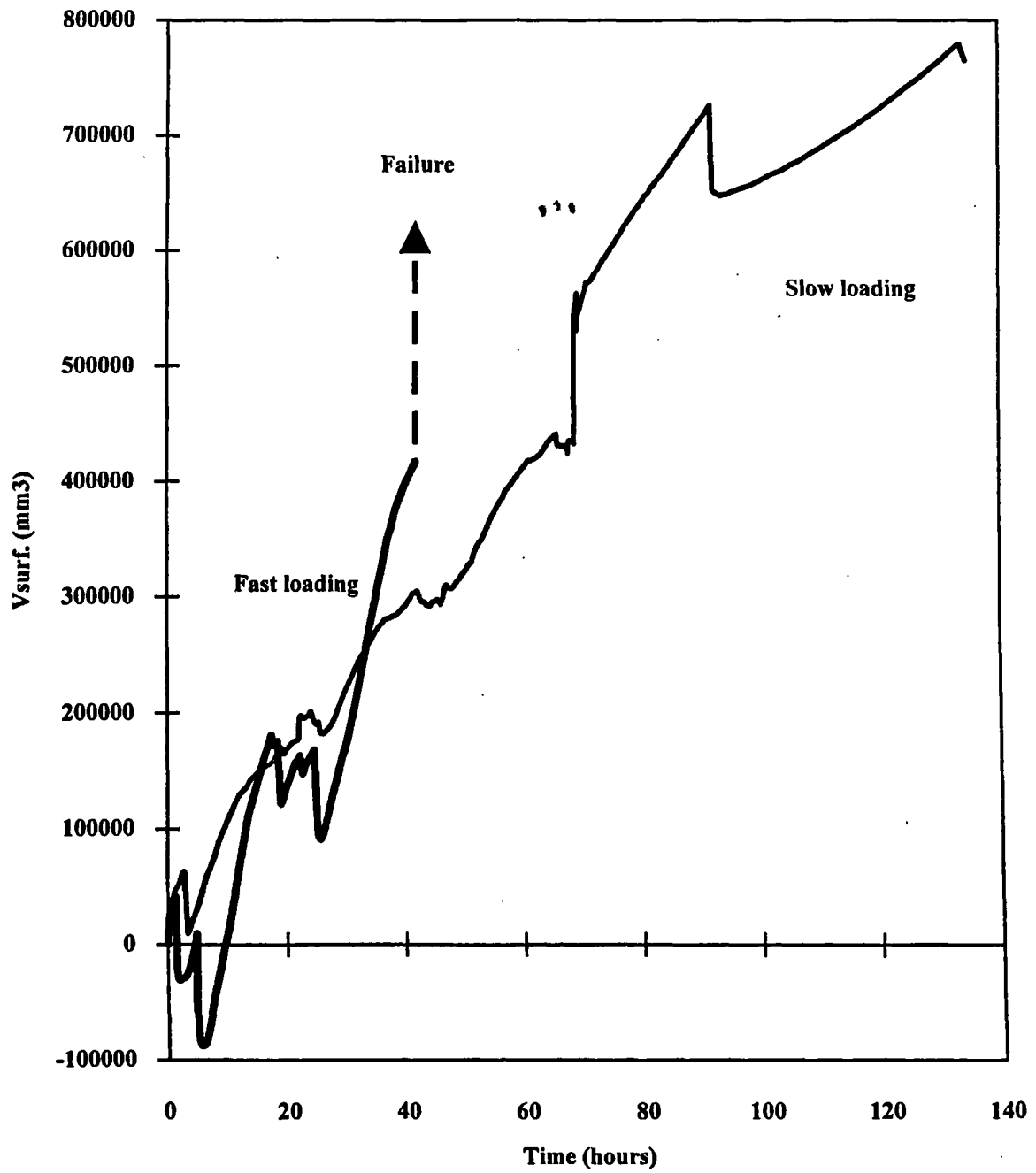
(a) Fast loading test TL01-1

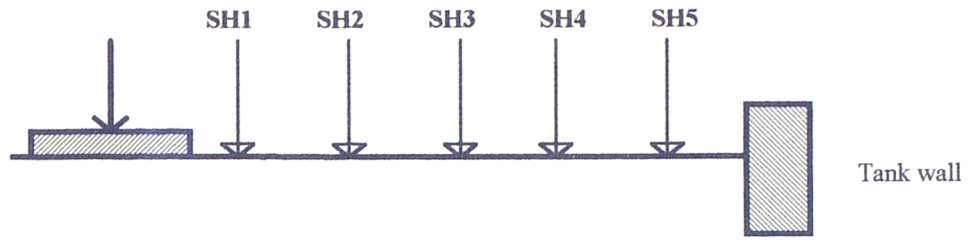


(b) Slow loading test TL01-2

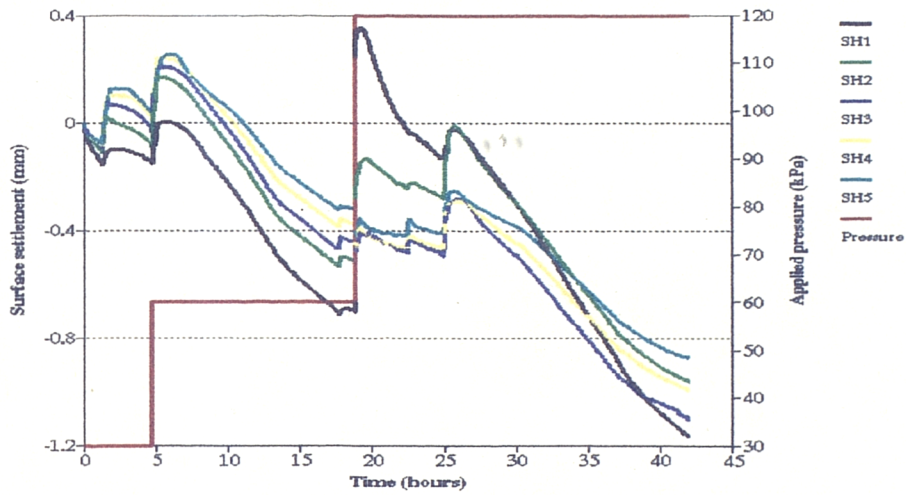
Fig 4.67: Stress concentration ratio : time : load response (a) fast loading TL01-1; (b) slow loading TL01-2

Fig 4.68: Surface volume change : time response under flexible loading

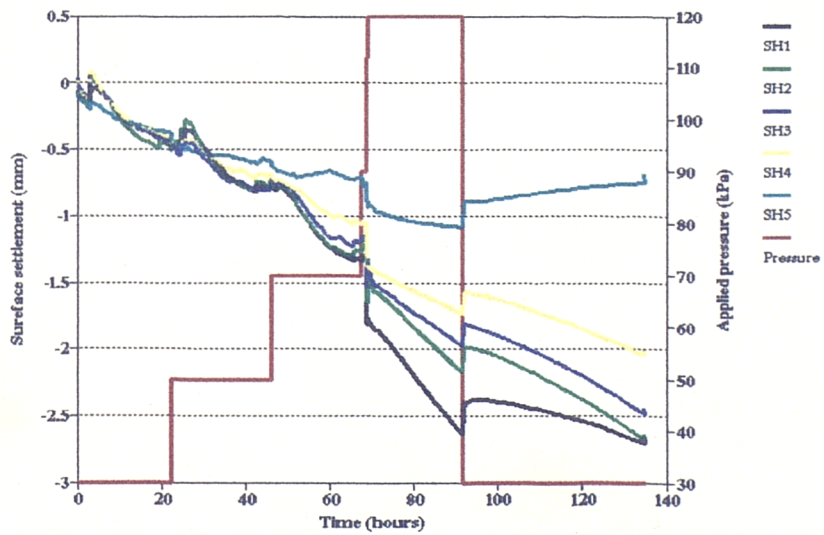




(a)



(b)



(c)

Fig 4.69 Surface settlement : time : load response under flexible loading
 (a) location of measurements; (b) fast loading test TL01-1; (c) slow loading test TL01-2

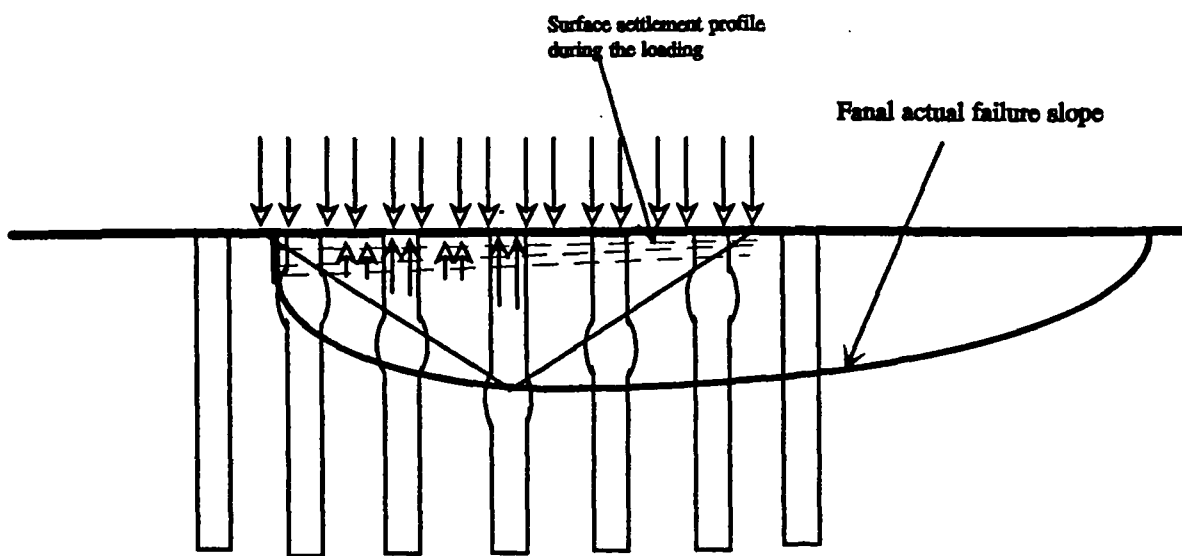
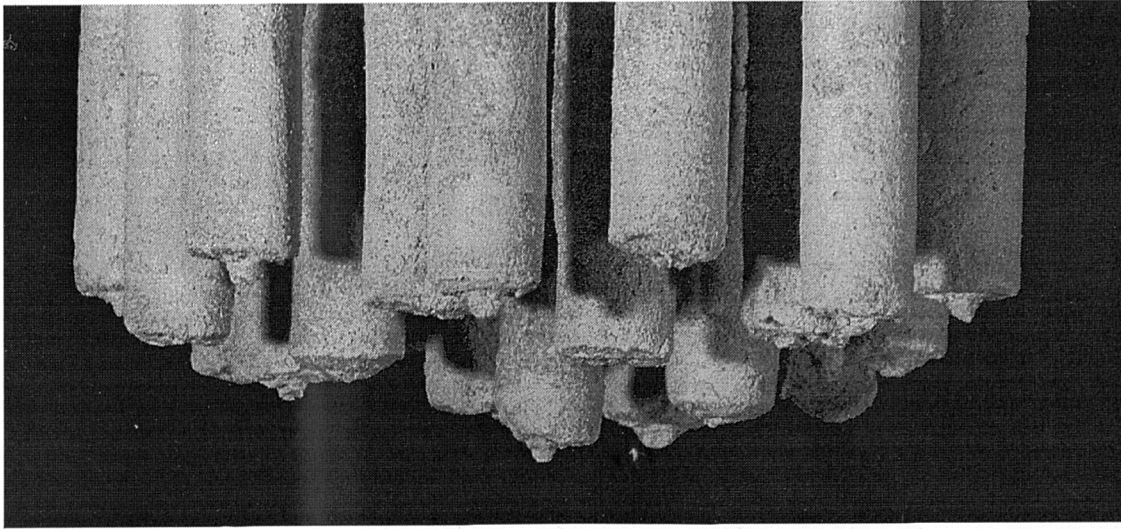
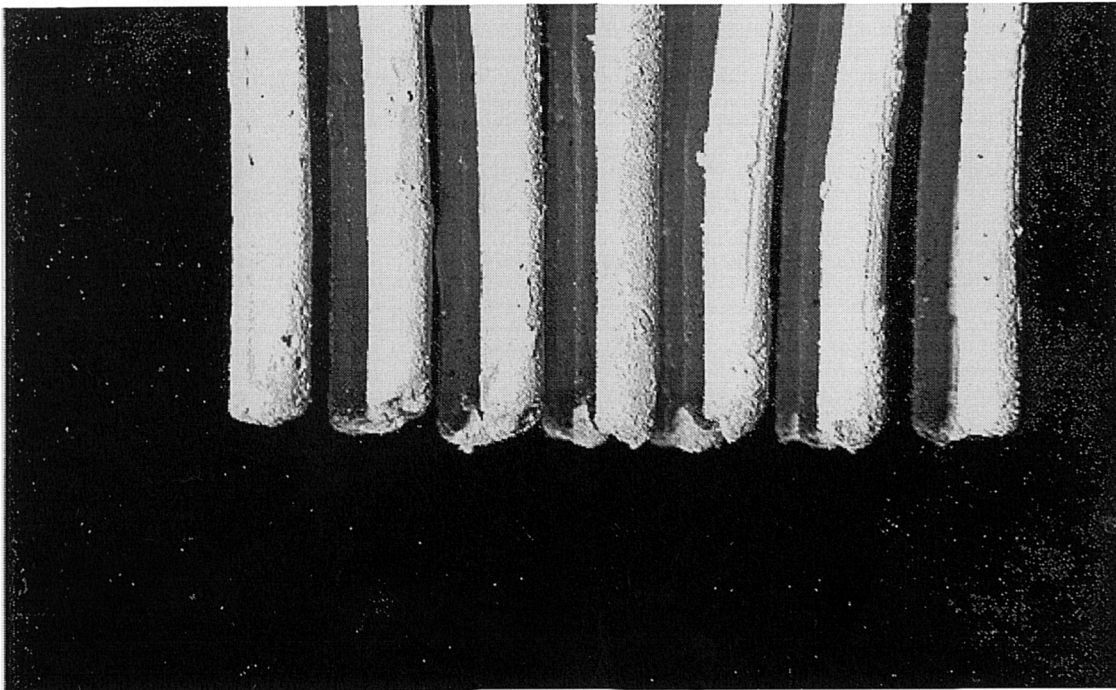


Fig 4.70: Suggested mode of deformation under flexible load (test TL01-1)



(a) short columns TS10



(b) long columns TS17

Plate 4.1: The column base after test (a) short columns TS10; (b) long columns TS17

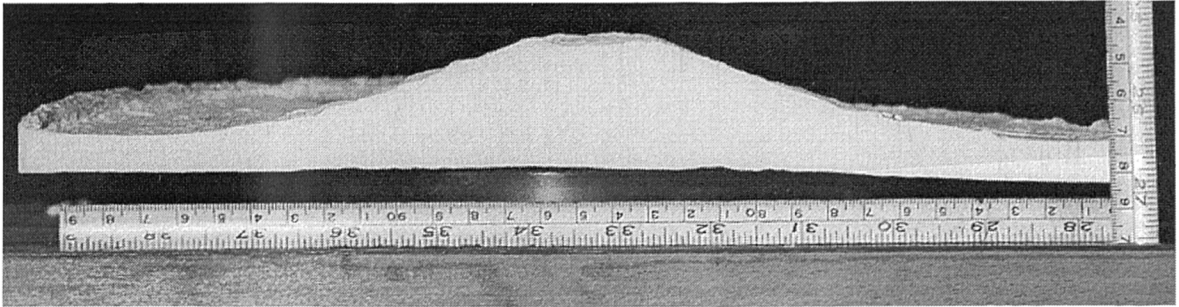


Plate 4.2: The shape of finished surface after column installation using displacement method (TS15)

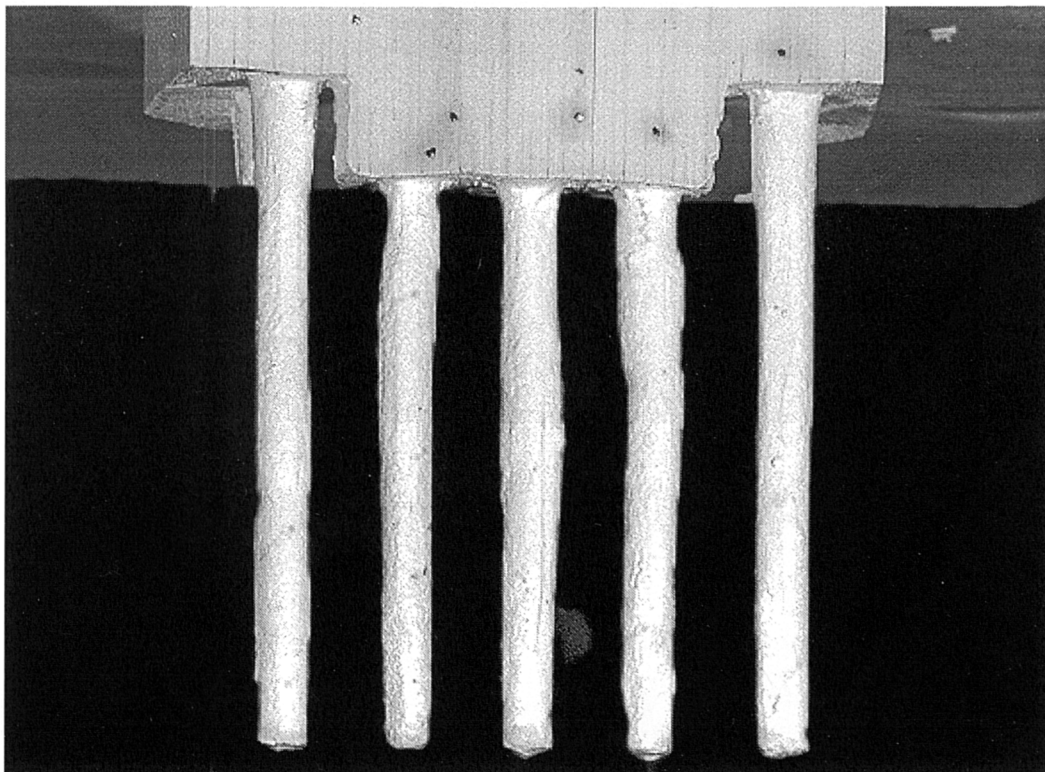


Plate 4.3: The shape of columns installed using a displacement method, after test (TS15)

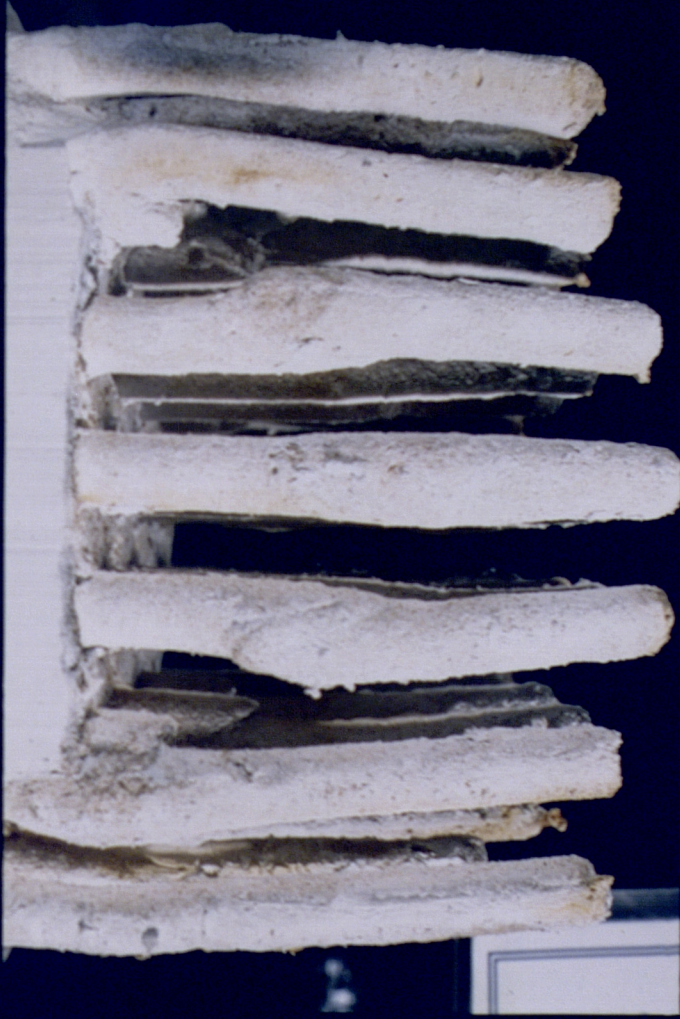


Plate 4.4: Central section of model stone columns after test (short columns TS08)

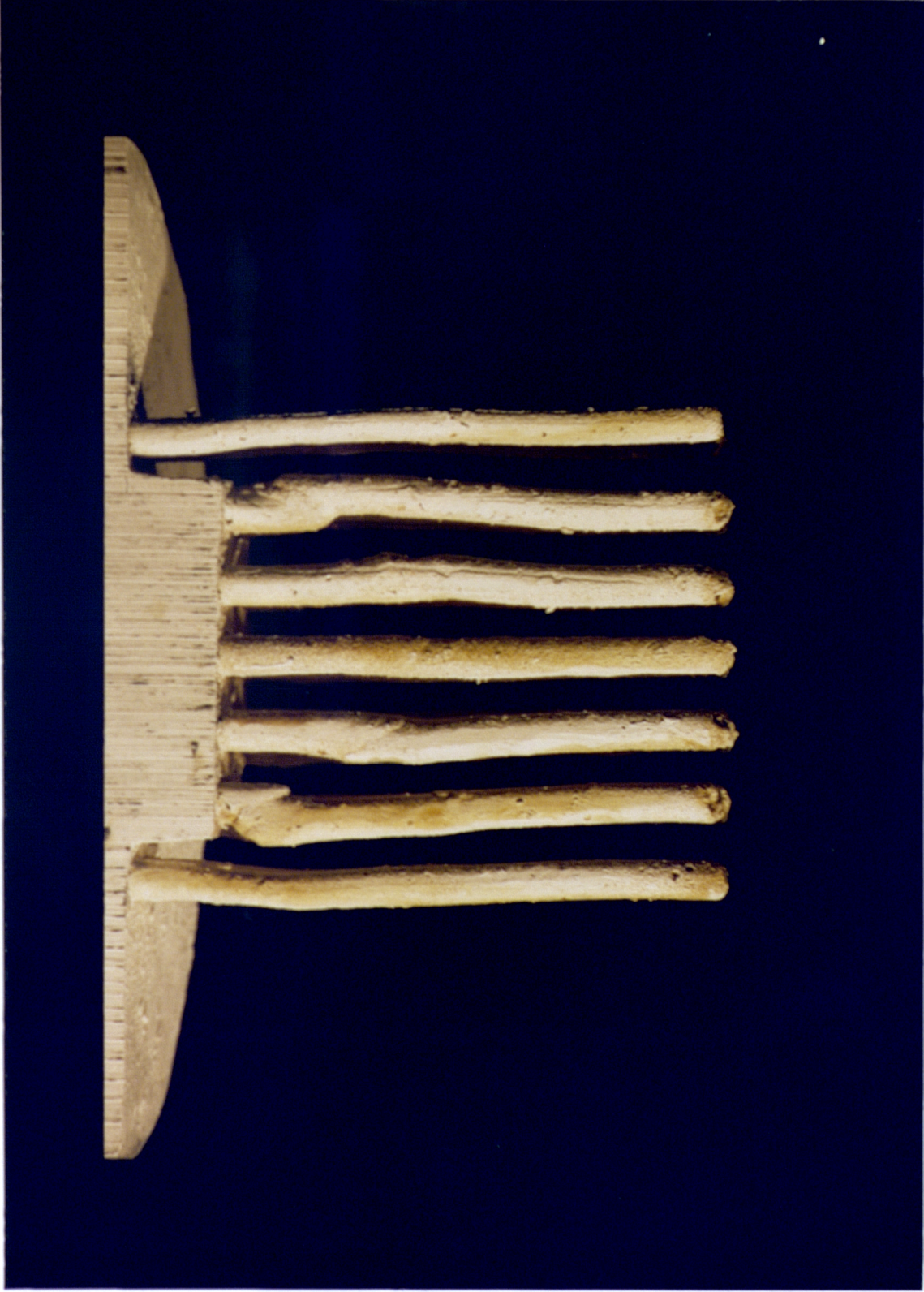
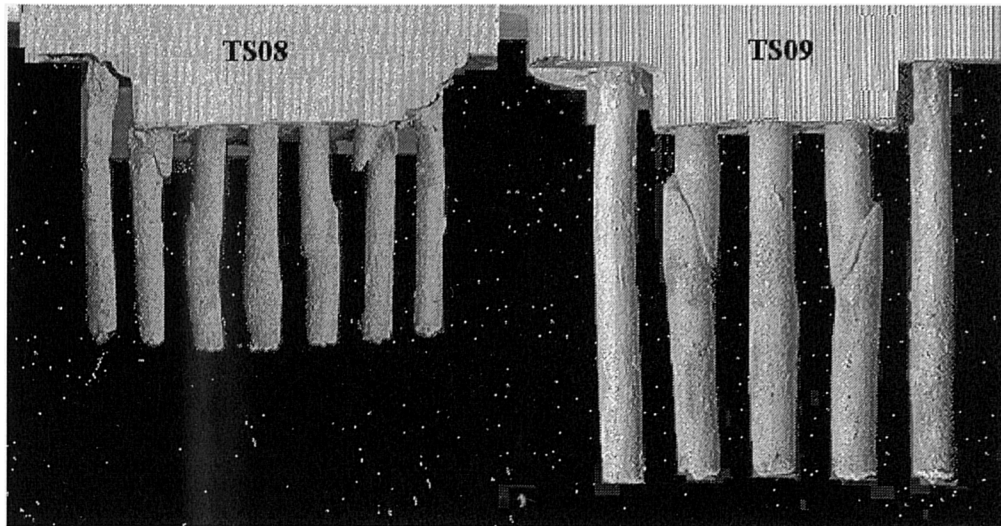
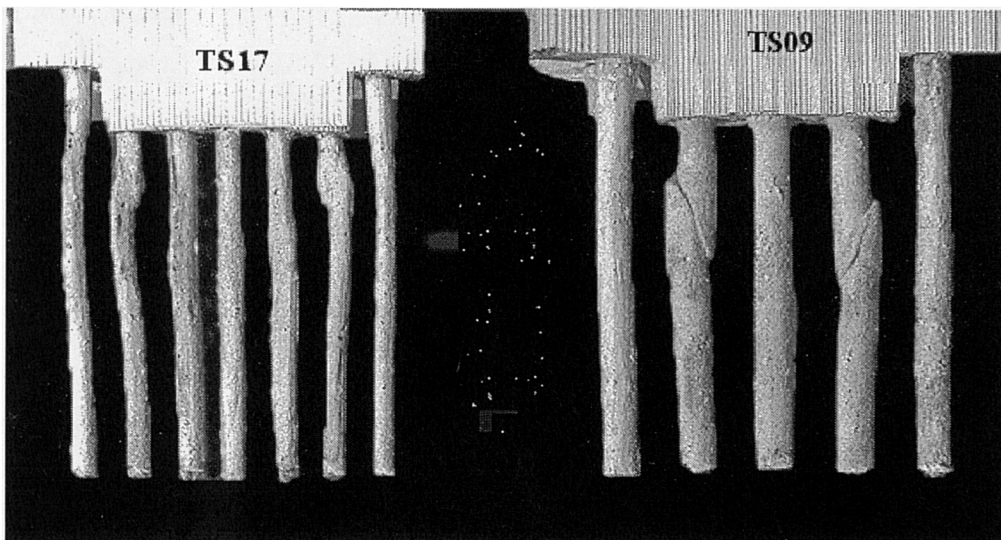


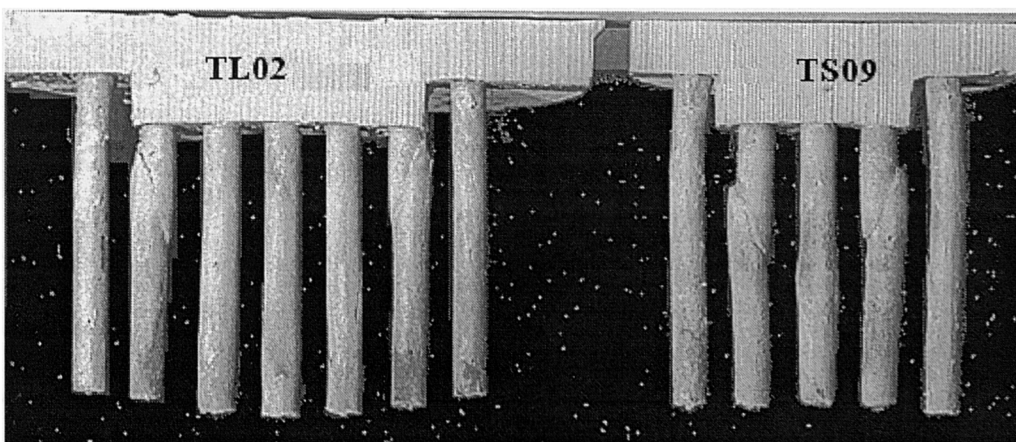
Plate 4.5: Central section of model stone columns after test (long columns TS17)



(a)



(b)



(c)

Plate 4.6: Comparison of the column deformation pattern
(a) TS09 & TS08; (b) TS09 & TS17; (c) TS09 & TL02

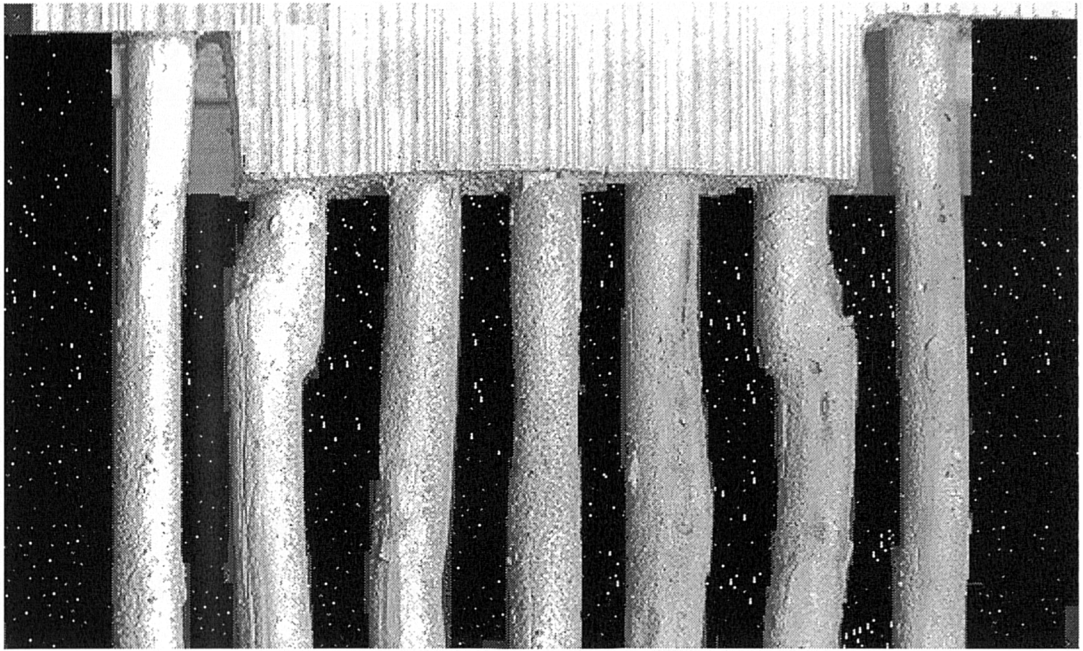
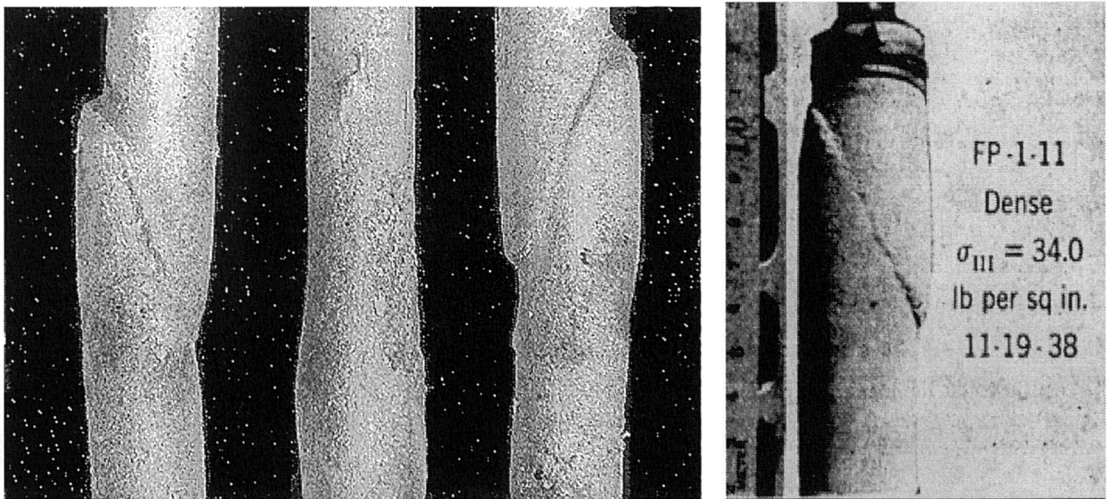


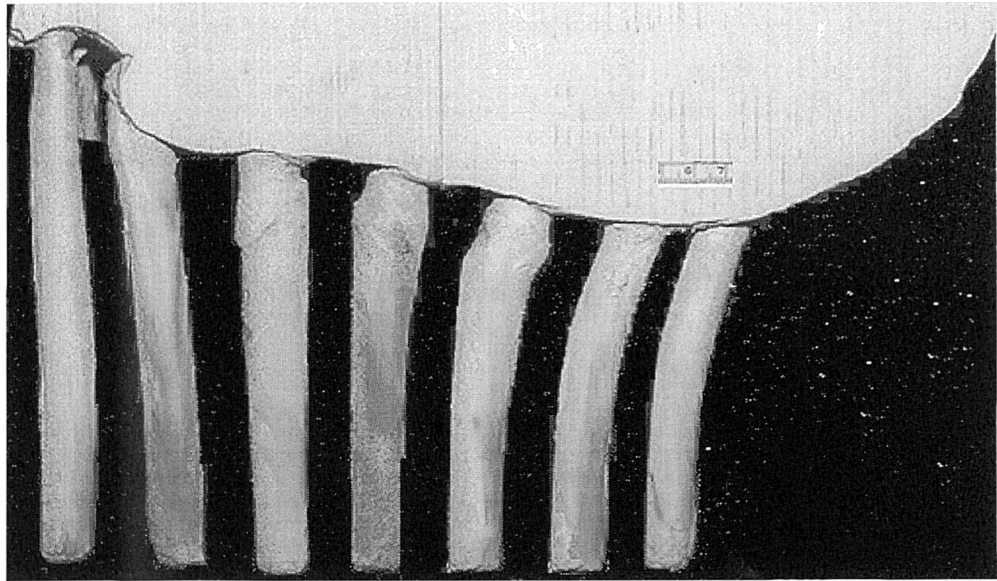
Plate 4.7: Deformed column shapes (long column, buckling failure TS17)



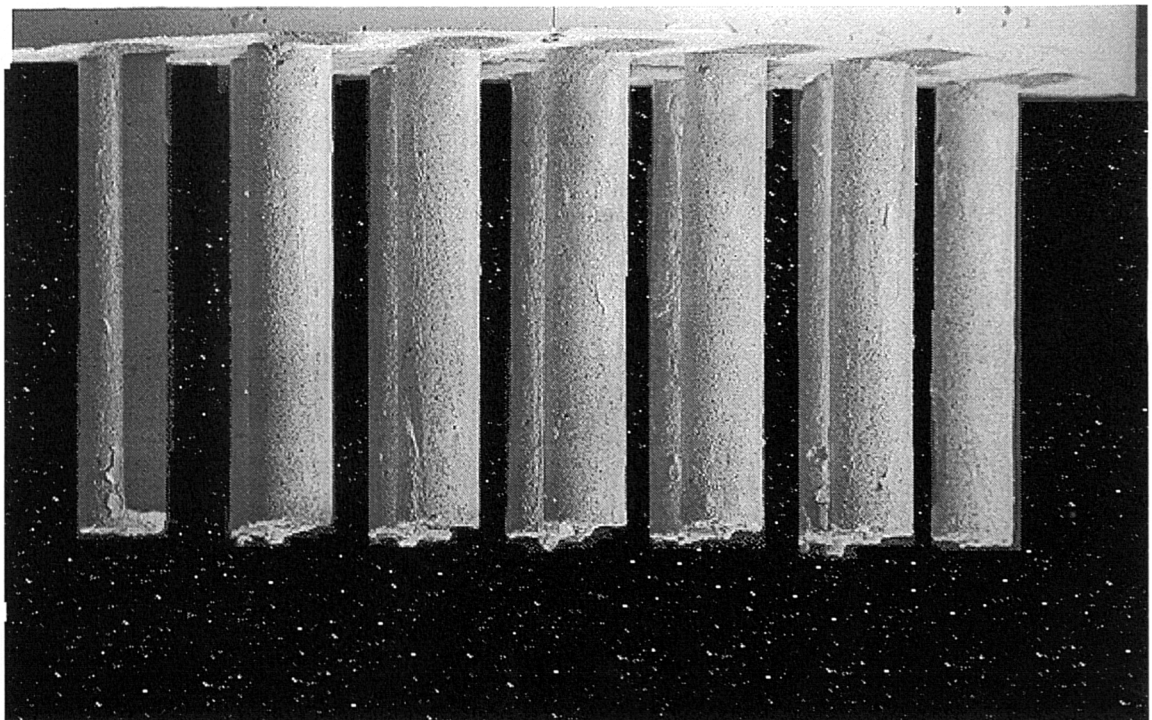
(a)

(b)

Plate 4.8: (a) Deformed model columns (short column, bulging failure TS09); (b) shape of failure sand specimen after triaxial test, after Taylor 1948



(a) fast loading test TL01-1



(b) slow loading test TL01-2

Plate 4.9: Central section of column casts after flexible loading test (a) fast loading test TL01-1; (b) slow loading test TL01-2

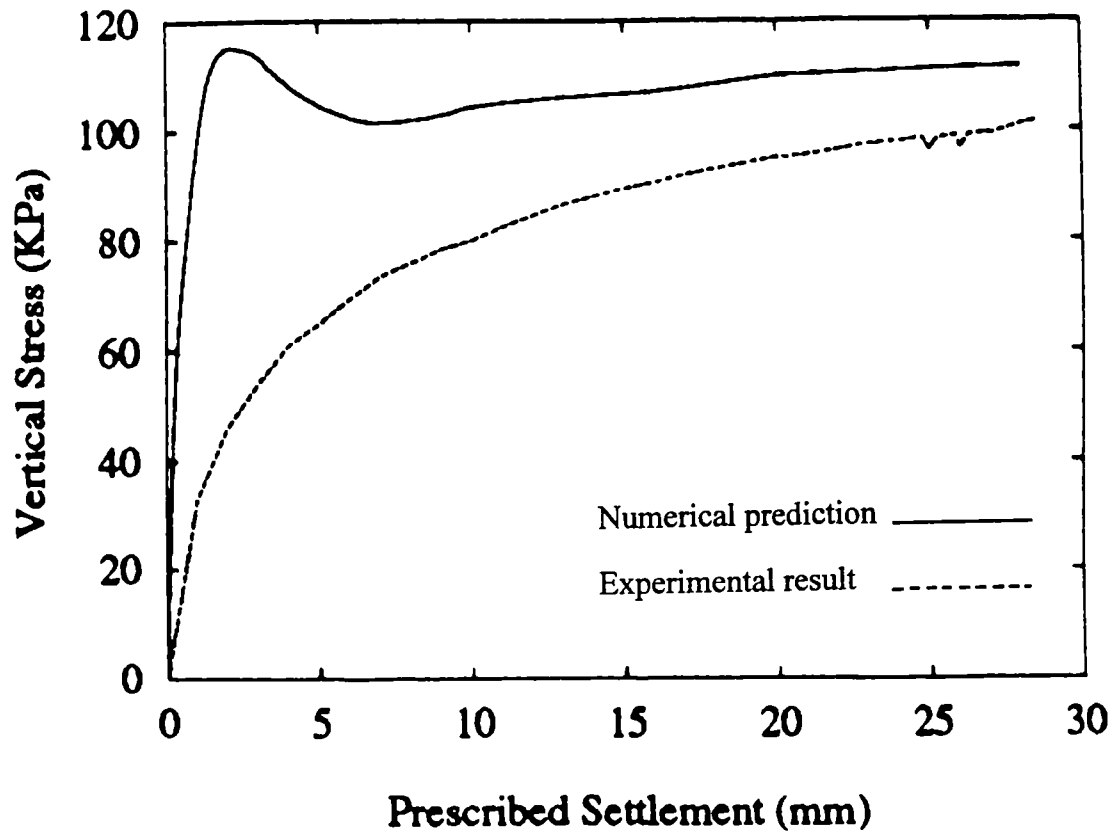
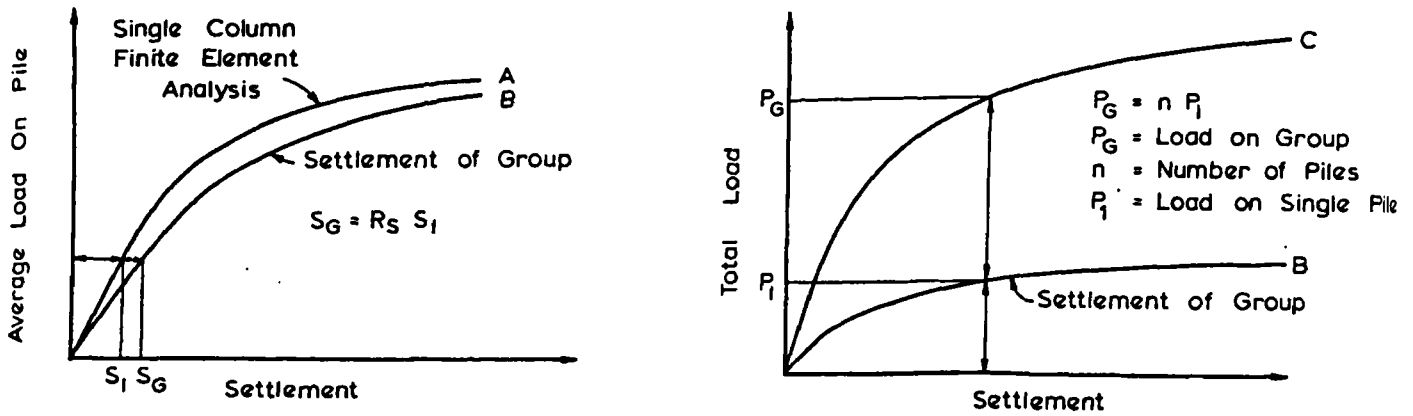


Fig 5.1: Comparison of load : displacement response between numerical prediction (Swansea homogenised analysis) and the Author's model test (test TS10)



(a) Average Load on Pile in Group VS Settlement (b) Load - Settlement Curve For Pile Group

Fig 5.2: Single column based bearing capacity analysis for a group of stone columns (a) average load on column in group vs. settlement; (b) load : settlement response for column group; after Balaam 1978

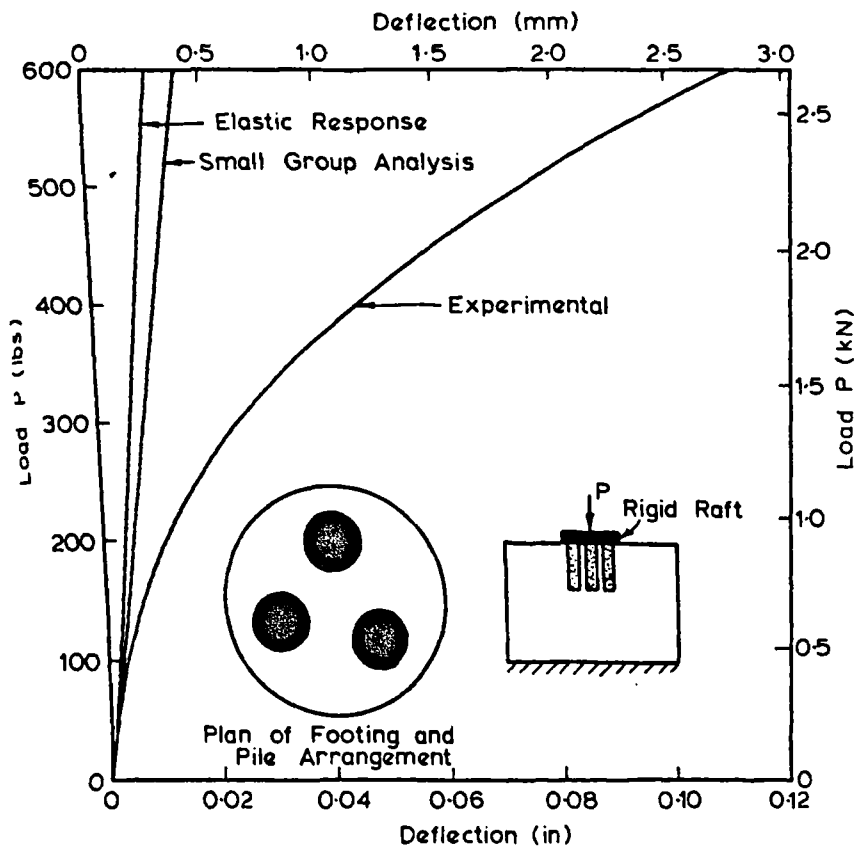
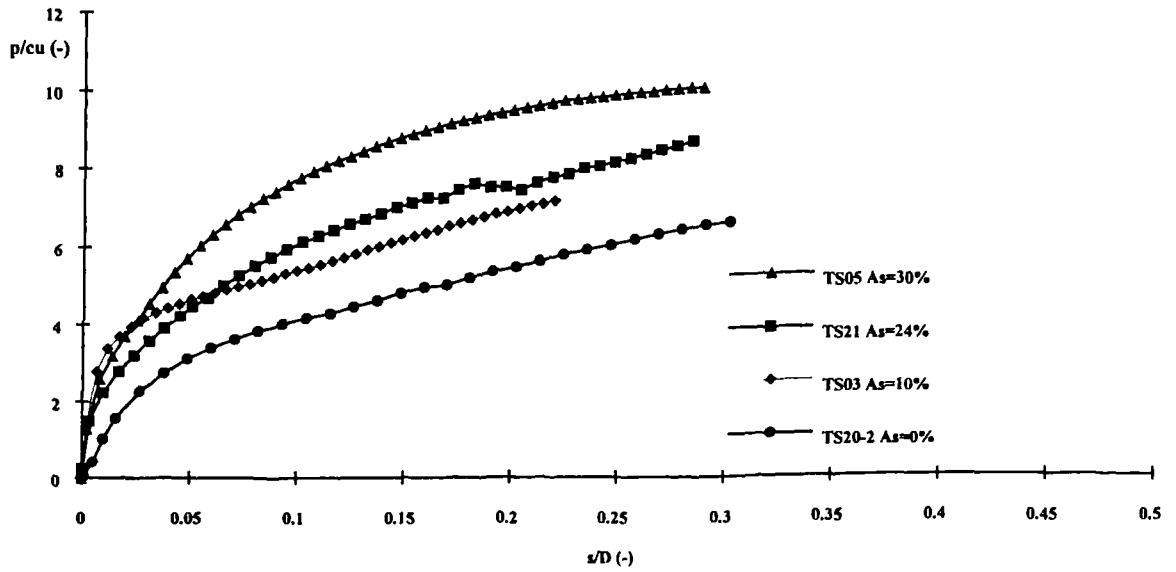
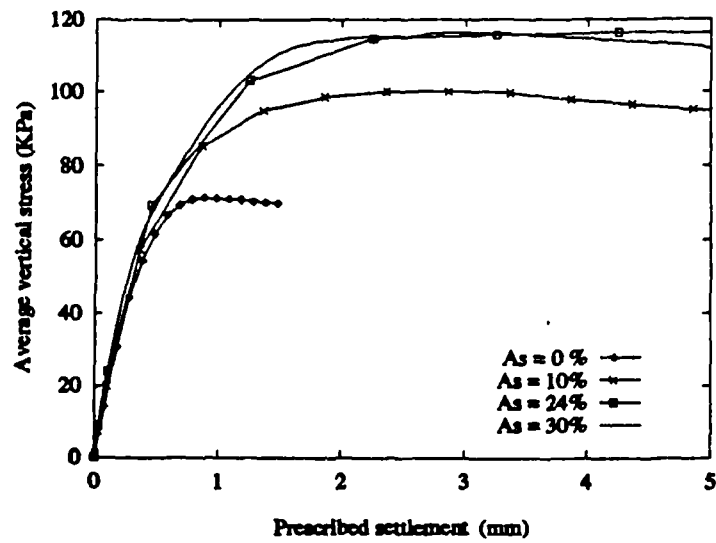


Fig 5.3: Comparison of load : displacement response of small group of stone columns between prediction based on single column analysis and model test result. (after Balaam 1978)



(a)



(b)

Fig 5.4: Effect of area ratio on the load : displacement response (a) result from the Author's model tests; (b) result from Swansea homogenised analyses, after Pande 1994

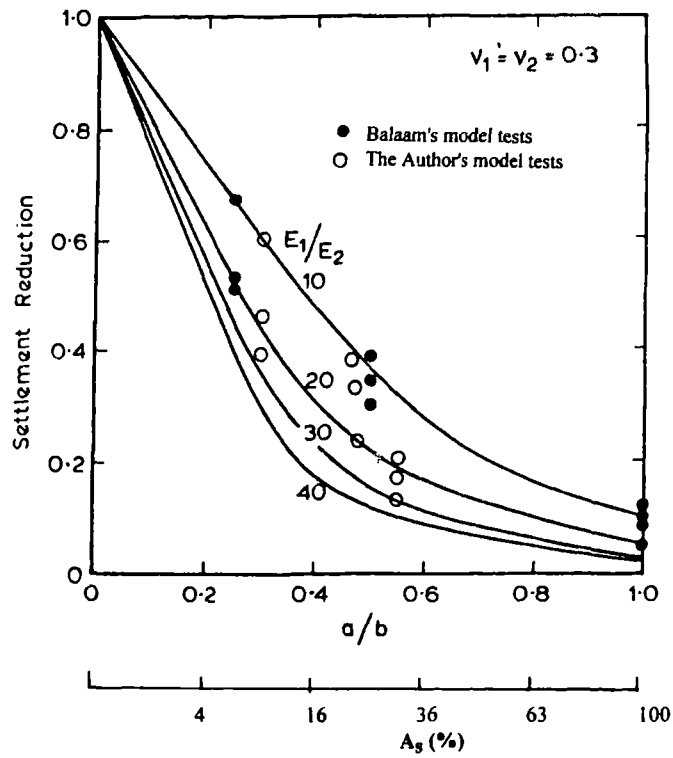


Fig 5.5: Comparison on the effect of area ratio on the settlement reduction between Balaam's unit cell analysis and the Author's model test results.

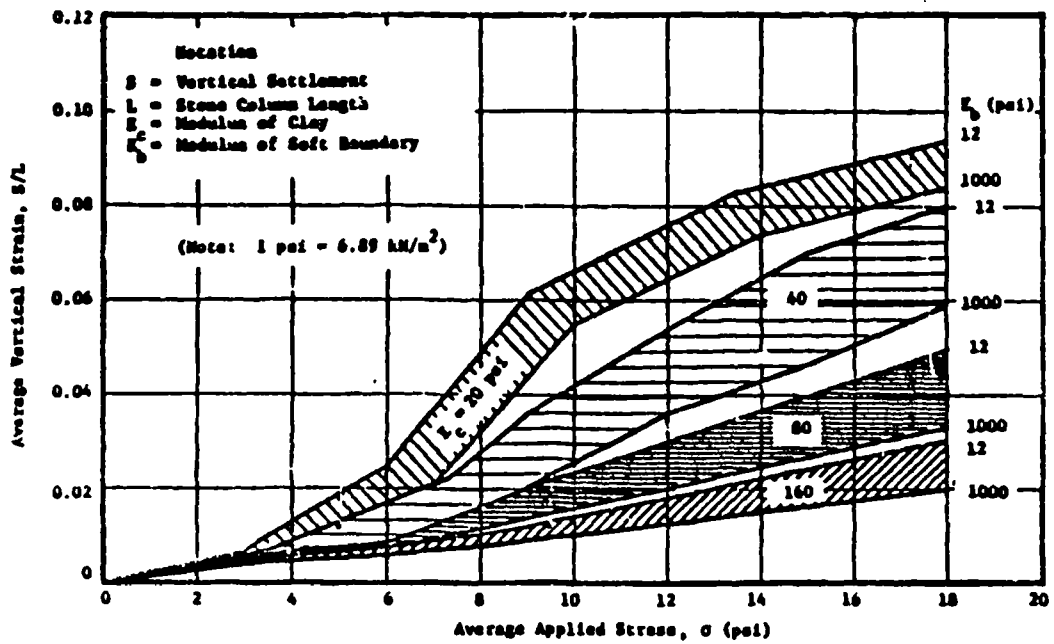
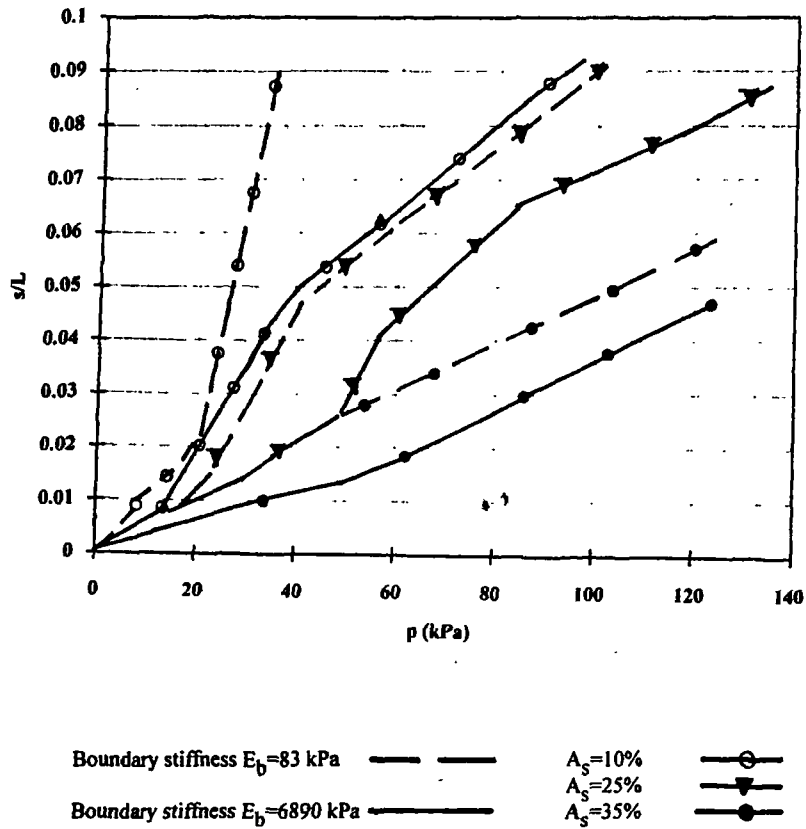
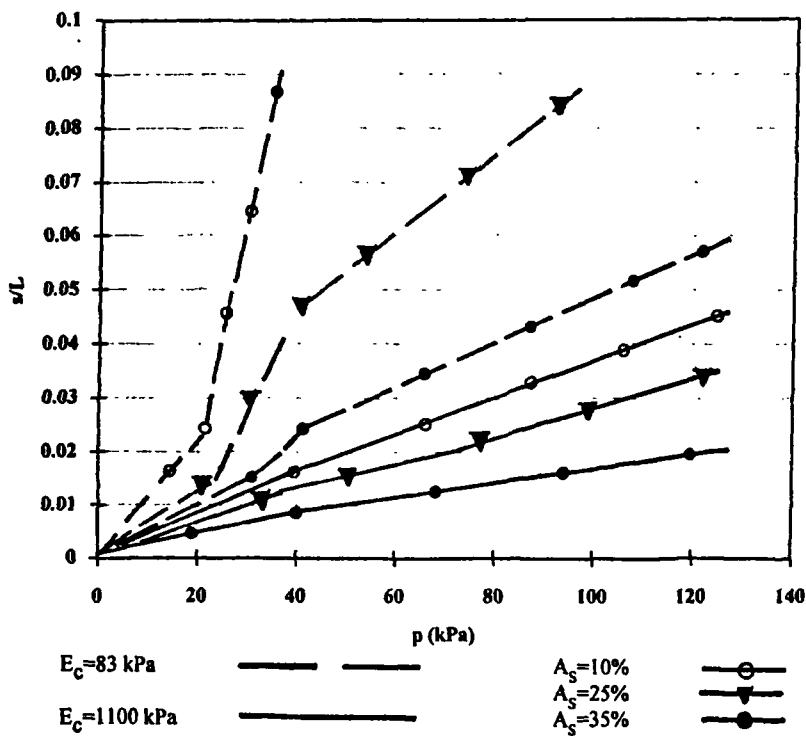


Fig 5.6: The load : displacement response from non-linear unit cell finite element analyses (after Barksdale & Bachus 1983)



(a)



(b)

Fig 5.7: The load : displacement response from non-linear unit cell finite element analyses (a) effect of area ratio; (b) effect of clay compressibility, after Barksdale & Bachus 1983

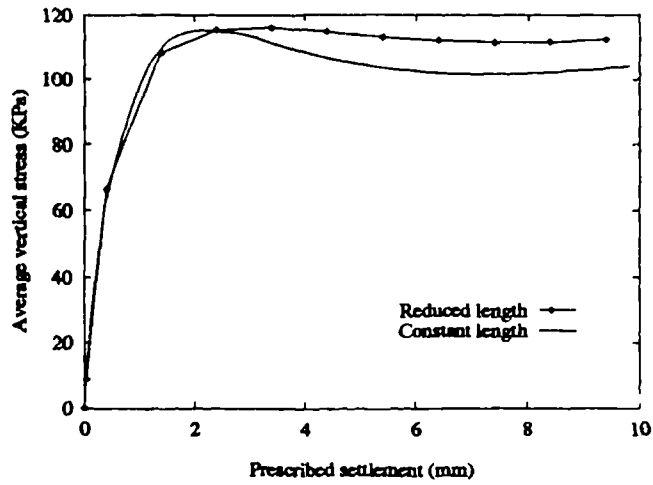
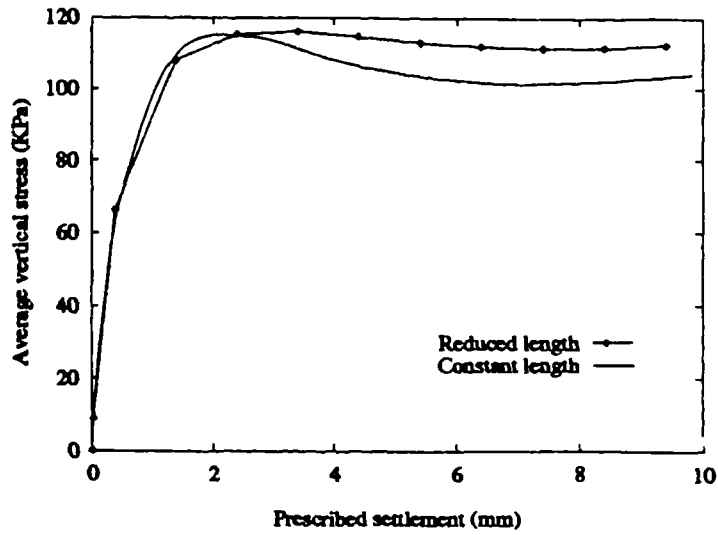
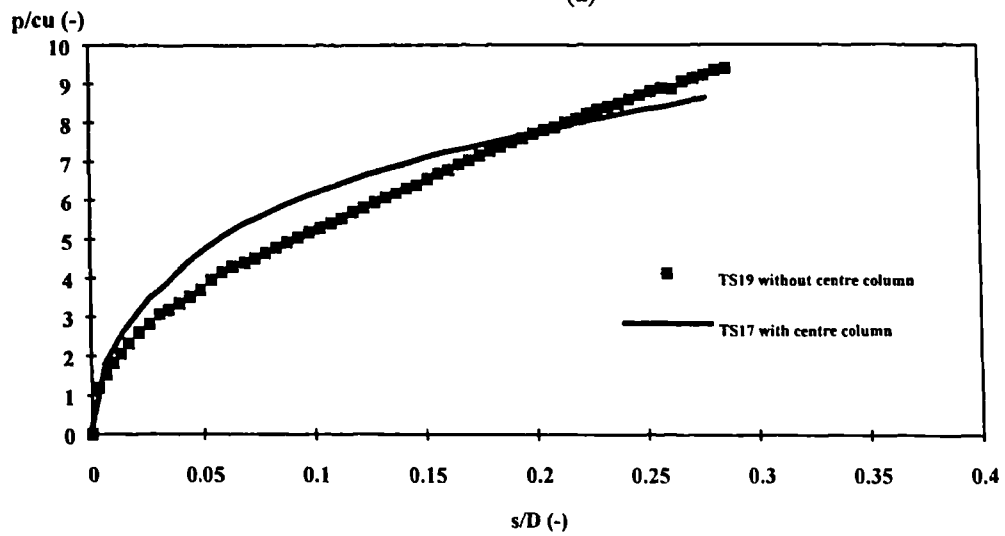


Fig 5.8: Effect of L/d ratio on the load ; displacement response (tests TS05 & TS10, after Lee & Pande 1994)

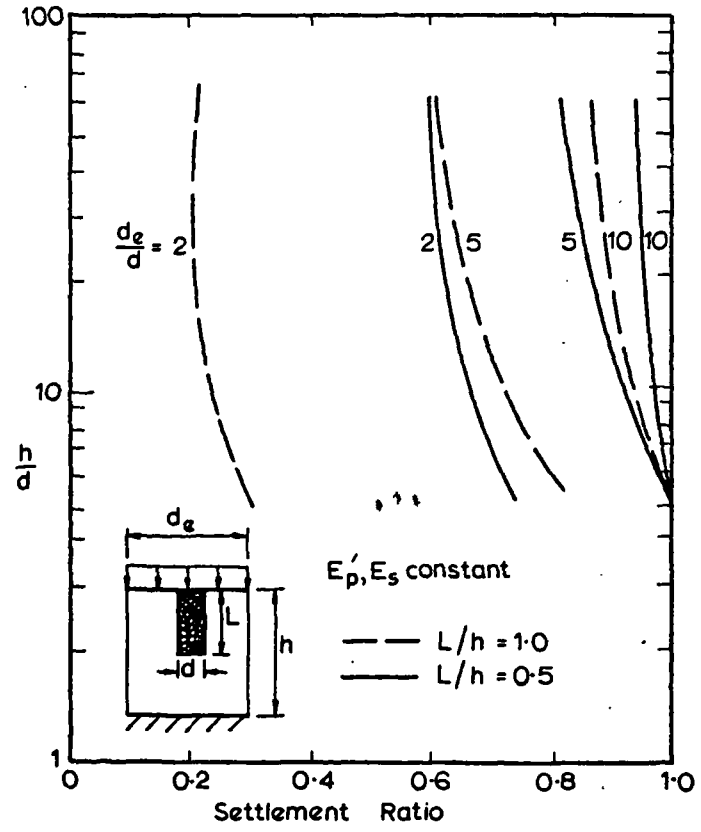


(a)

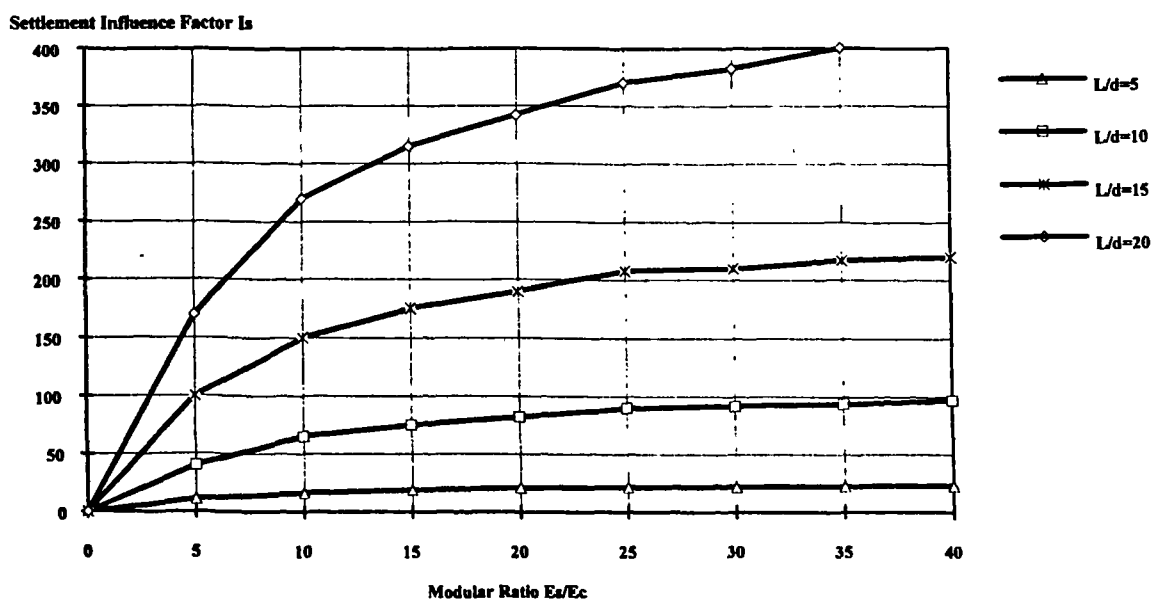


(b)

Fig 5.9: Effect of the length of central column on the load ; displacement response (a) numerical response with the length of central column reduced, after Lee & Pande 1994; (b) result from the author's model tests with central column omitted, tests TS09 & TS19

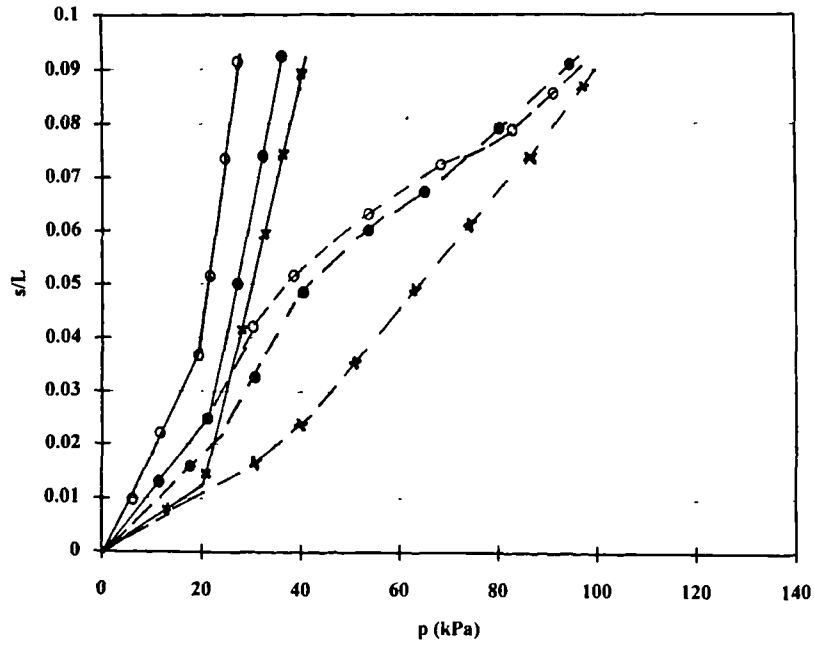


(a)

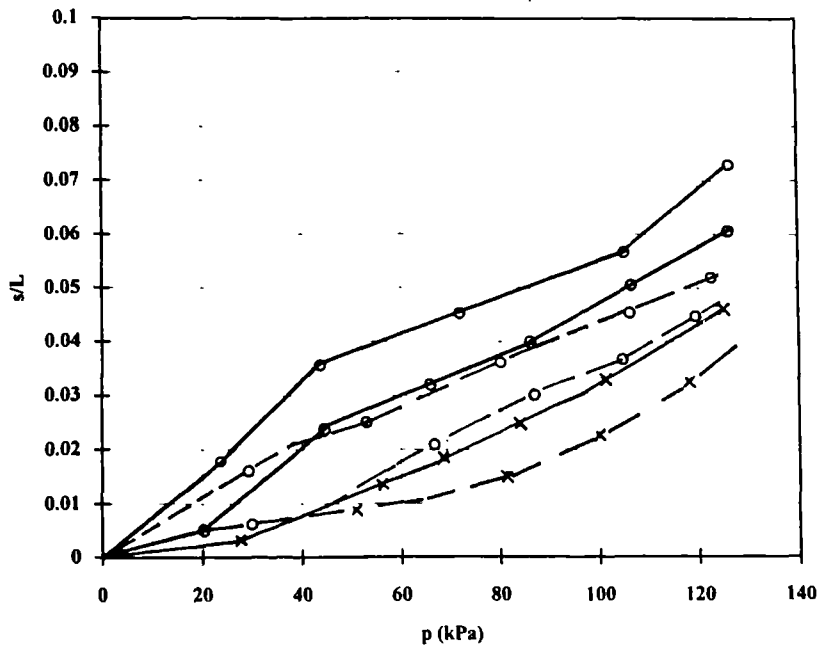


(b)

Fig 5.10: The settlement reduction ratio predicted by unit cell analyses (a) Effects of the area ratio and column length on the predicted settlement reduction ratio, after Balaam 1978; (b) Effects of the column length and modular ratio on the predicted settlement reduction ratio, after Barksdale & Bachus 1983



(a)



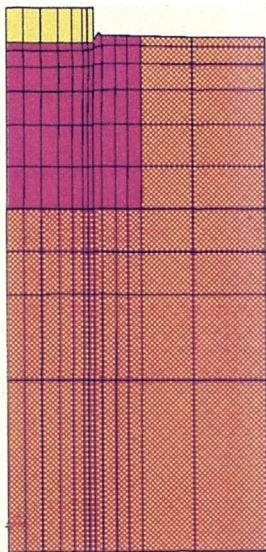
(b)

Boundary stiffness $E_b = 83$ kPa	—	$L/d = 5$	○
	—	$L/d = 10$	●
Boundary stiffness $E_b = 6890$ kPa	- - -	$L/d = 20$	×

Fig 5.11: Effect of column length on the load : settlement response predicted by modified unit cell analyses (a) $A_s = 10\%$; (b) $A_s = 35\%$, data deduced from Barksdale & Bachus 1983 Fig 29-37

Normalised Vertical Stresses (TS05)

Deformed Pattern

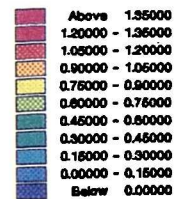


(a)

σ_v^{av} ($\delta_o = 2.5 \text{ mm}$)



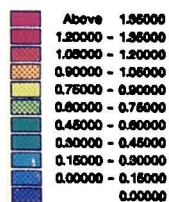
(b)



σ_v^c ($\delta_o = 2.5 \text{ mm}$)



(c)



σ_v^s ($\delta_o = 2.5 \text{ mm}$)



(d)

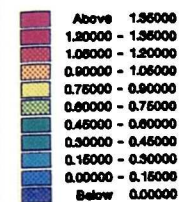
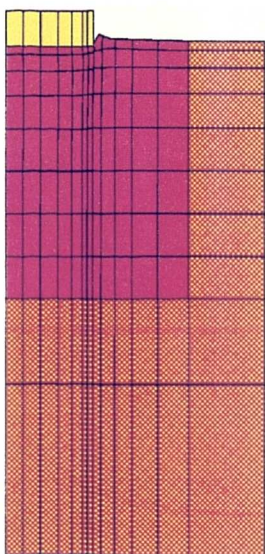


Fig 5.12: Results from Swansea homogenised analyses (test TS05), (a) deformed pattern; (b) distribution of normalised average vertical stresses; (c) distribution of normalised vertical stresses in clay; (d) distribution of normalised vertical stresses in column, after Lee & Pande 1994

Normalised Vertical Stresses (TS07)

Deformed Pattern

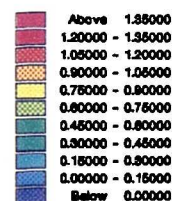


(a)

σ_v^{av} ($\delta_o = 2.5 \text{ mm}$)



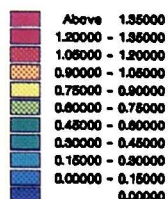
(b)



σ_v^c ($\delta_o = 2.5 \text{ mm}$)



(c)



σ_v^s ($\delta_o = 2.5 \text{ mm}$)



(d)

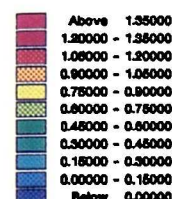


Fig 5.13: Results from Swansea homogenised analyses (test TS07), (a) deformed pattern; (b) distribution of normalised average vertical stresses; (c) distribution of normalised vertical stresses in clay; (d) distribution of normalised vertical stresses in column. after Lee & Pande 1994

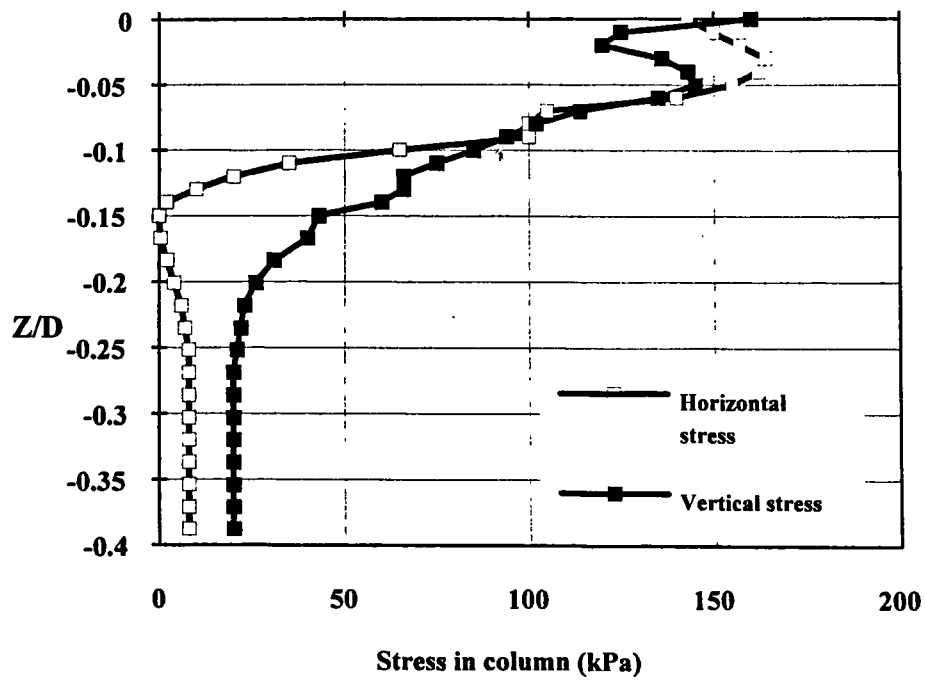
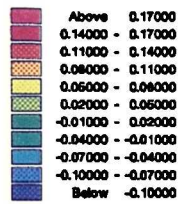
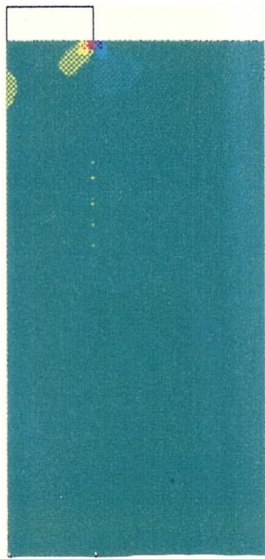


Fig 5.14: Numerical prediction of vertical and horizontal stress distribution with depth (test TS02, data from Amaniampong & Pande 1993)

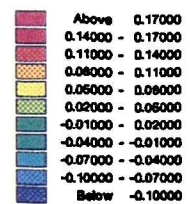
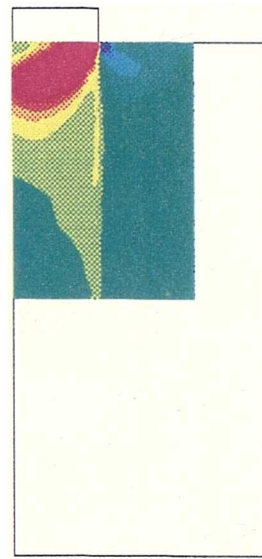
Plastic Strains (TS07)

$$\epsilon_{r,c}^p (\delta_o = 2.5 \text{ mm})$$



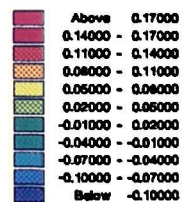
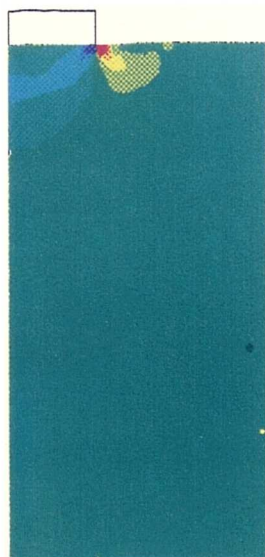
(a)

$$\epsilon_{r,s}^p (\delta_o = 2.5 \text{ mm})$$



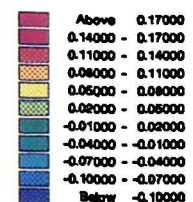
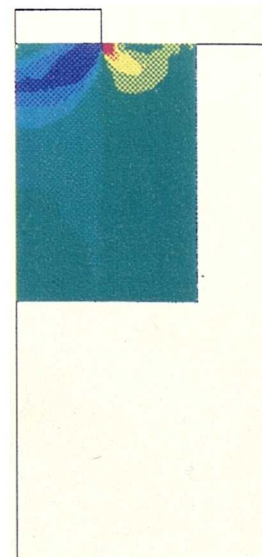
(b)

$$\epsilon_{v,c}^p (\delta_o = 2.5 \text{ mm})$$



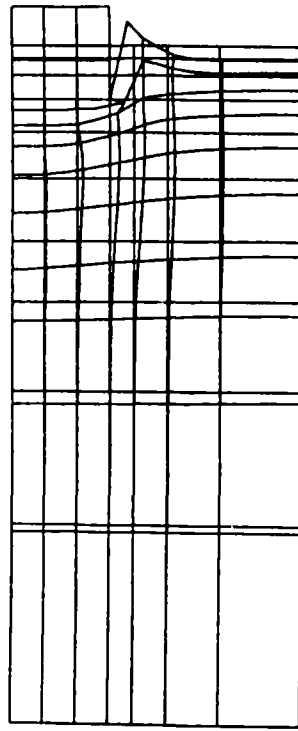
(c)

$$\epsilon_{v,s}^p (\delta_o = 2.5 \text{ mm})$$

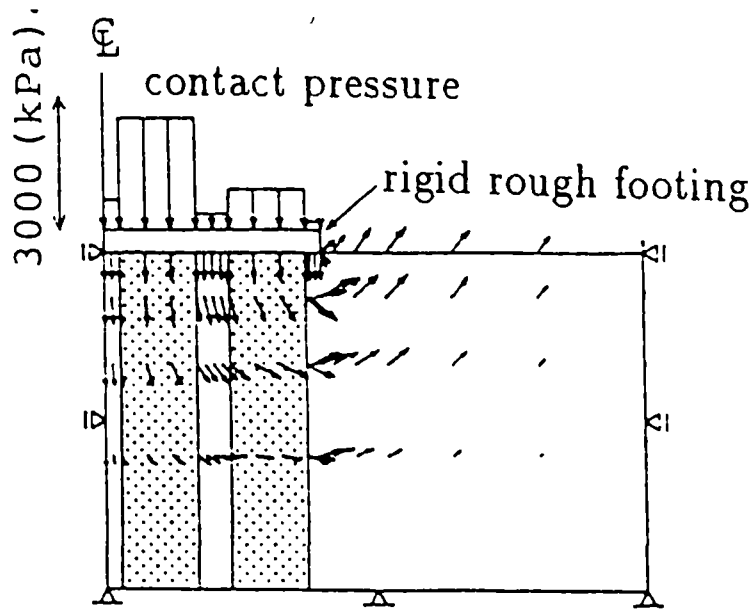


(d)

Fig 5.15: Plastic strain results from Swansea homogenised analyses (test TS07), (a) radial strain in clay; (b) radial strain in column; (c) vertical strain in clay; (d) vertical strain in column, after Lee & Pande 1994



(a)



(b)

Fig 5.16: Deformation behaviour produced by numerical analyses (a) deformed mesh from homogenised analysis, after Amaniampong & Pande 1993; (b) vertical displacement vectors, after Asaoka et al 1994

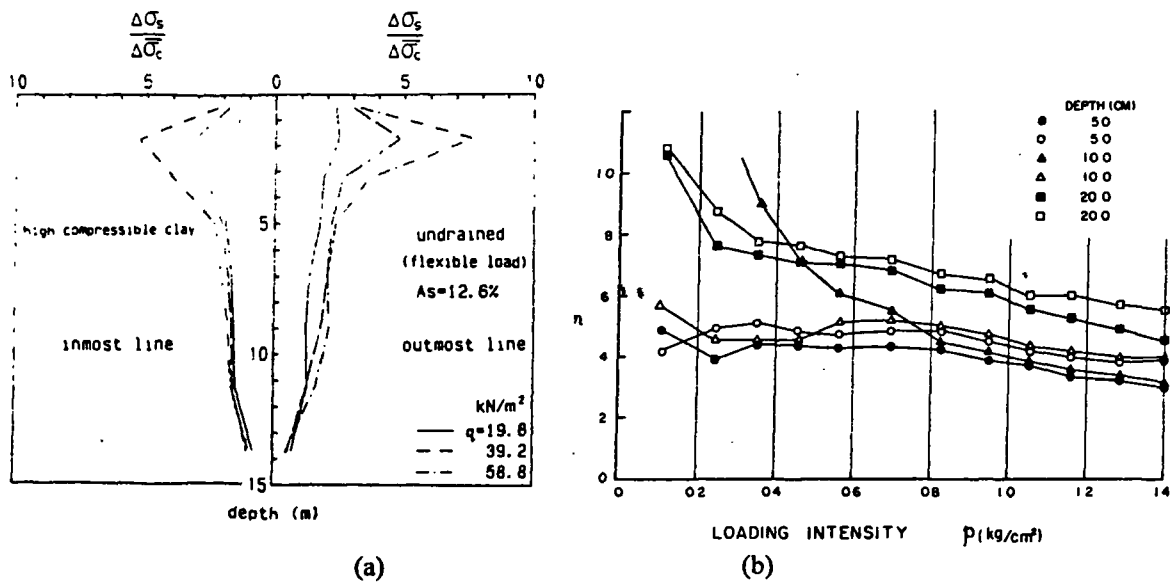


Fig 5.17: Distribution of stress concentration ratio with depth (a) Numerical prediction, after Ishizaki, 1992; (b) measurements from model test, after Aboshi 1979

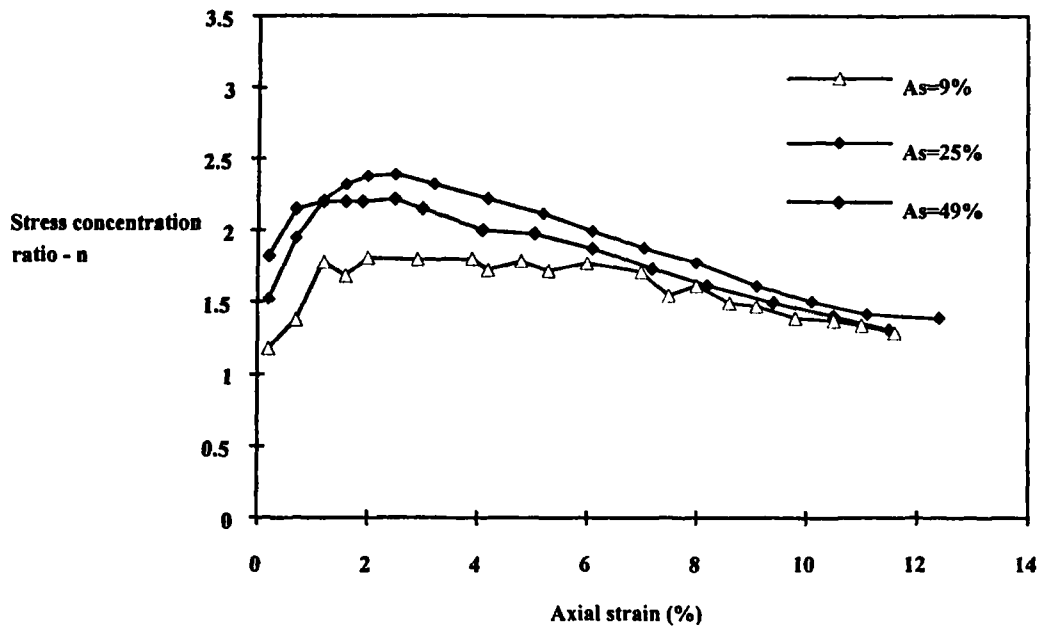
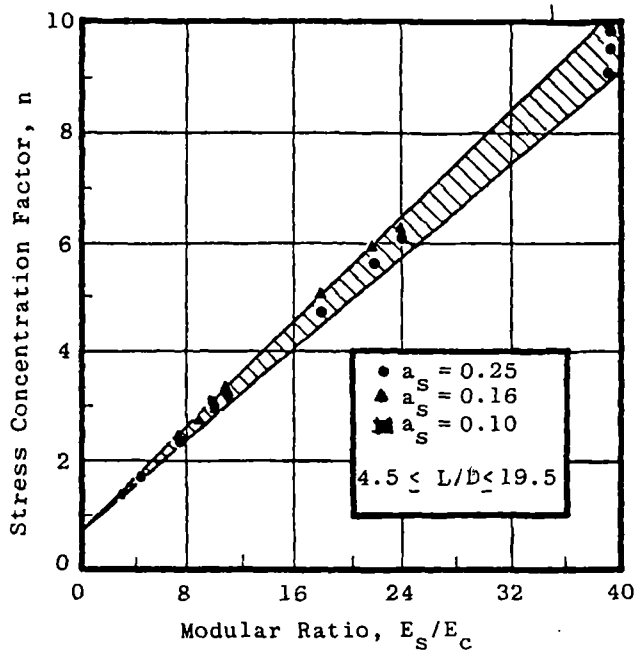
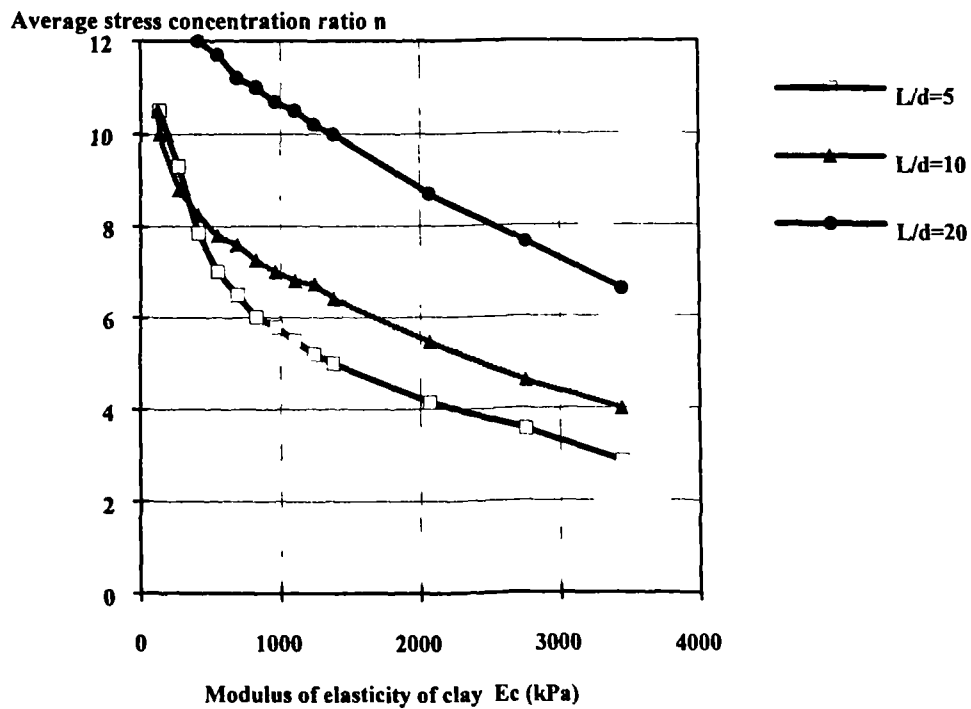


Fig 5.18: Effect of area ratio on the stress concentration ratio : strain response in triaxial tests (data from Ishizaki et al 1989)

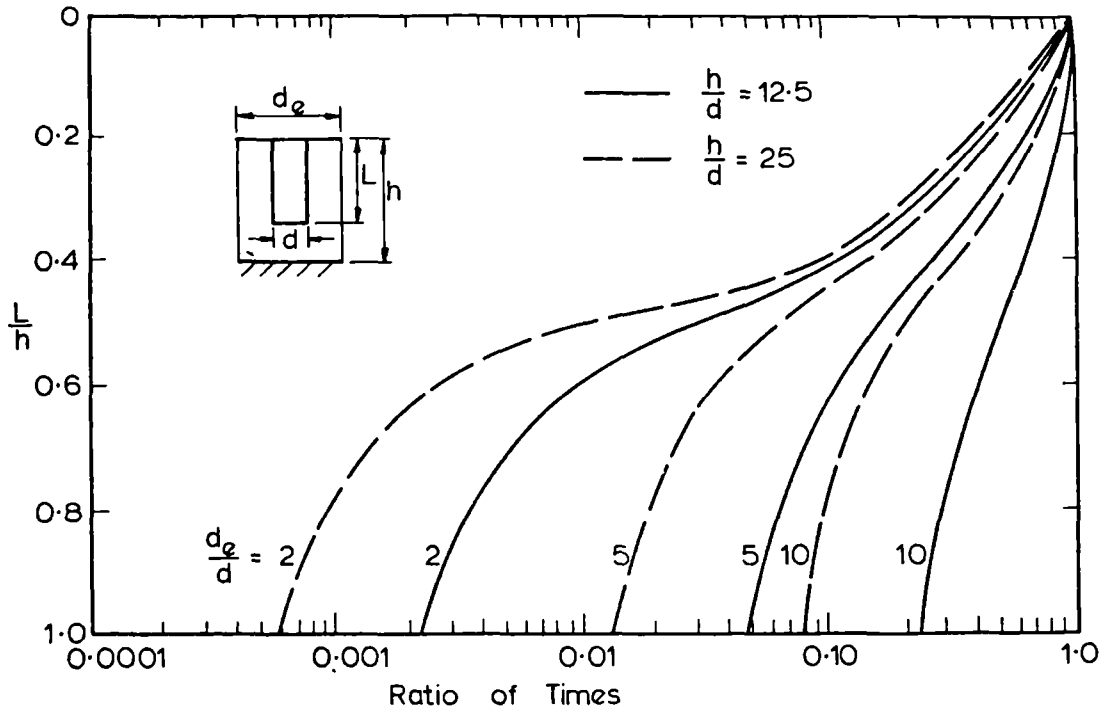


(a)



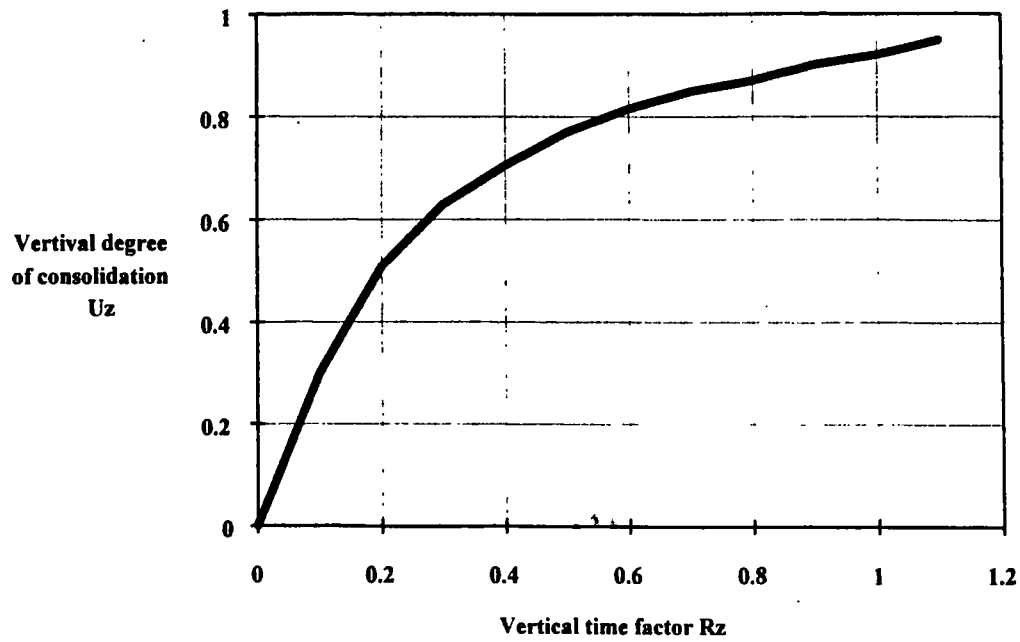
(b)

Fig 5.19: Stress concentration ratio profile (a) effect of modular ratio E_s/E_c , (b) effect of elasticity modulus of clay E_c , after Barksdale & Bachus 1983

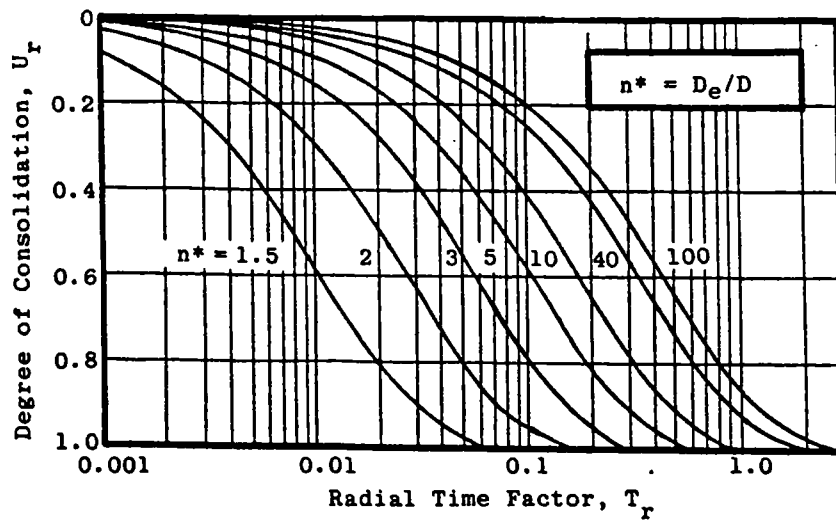


$$\frac{d_e}{d} = \frac{1}{\sqrt{A_s}}$$

Fig 5.20: Effect of column length and area ratio on the degree of consolidation predicted by unit cell analyses (after Balaam 1978)



(a)



(b)

$$n^* = \frac{1}{\sqrt{A_s}}$$

Fig 5.21: Degree of consolidation predicted by unit cell analyses (a) vertical consolidation, (b) effect of area ratio on the horizontal consolidation, after Barksdale & Bachus 1983

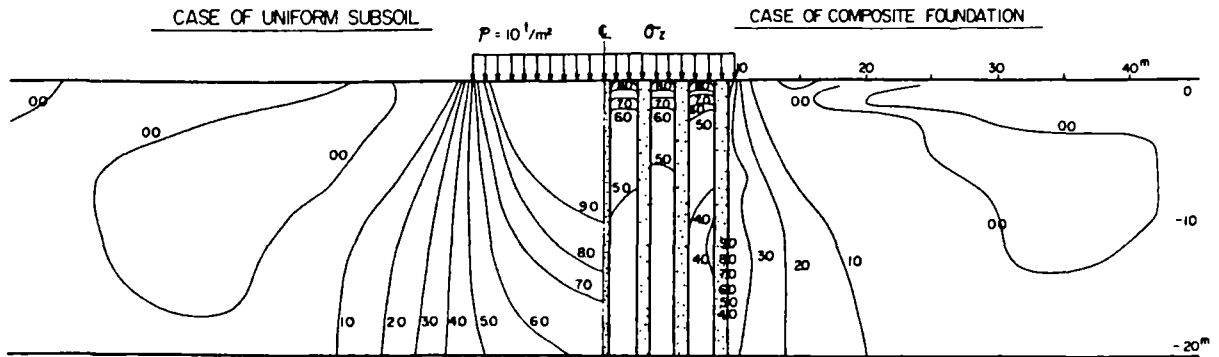


Fig 5.22: Stress distribution in a composite foundation under a flexible load compared with a homogeneous case predicted by a plane strain FE analysis (after Aboshi 1979)

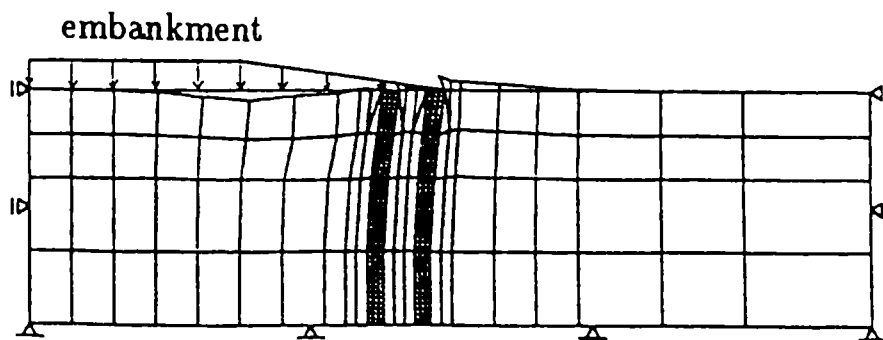


Fig 5.23: Numerical prediction of deformation at failure under a flexible load (after Asaoka et al 1994a)

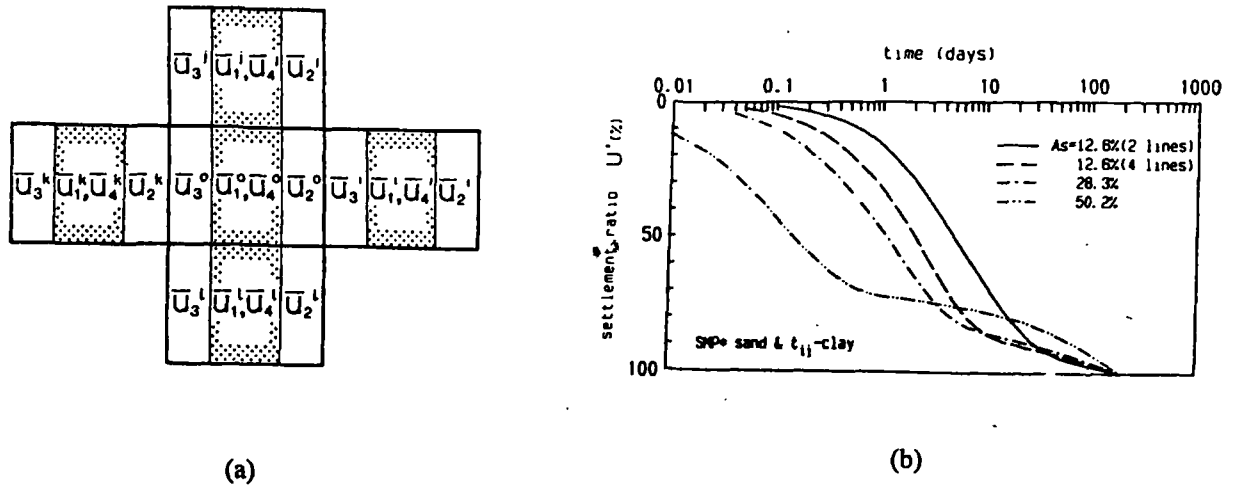


Fig 5.24: FE analyses of soft ground reinforced by sand compaction piles (a) multi-link elements; (b) effect of the area ratio on the foundation settlement, after Ishizaki 1992

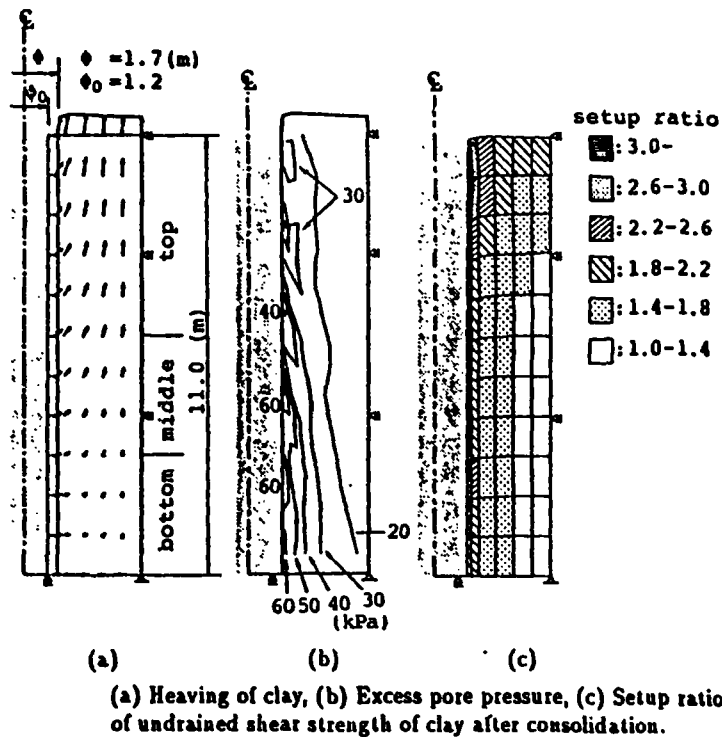
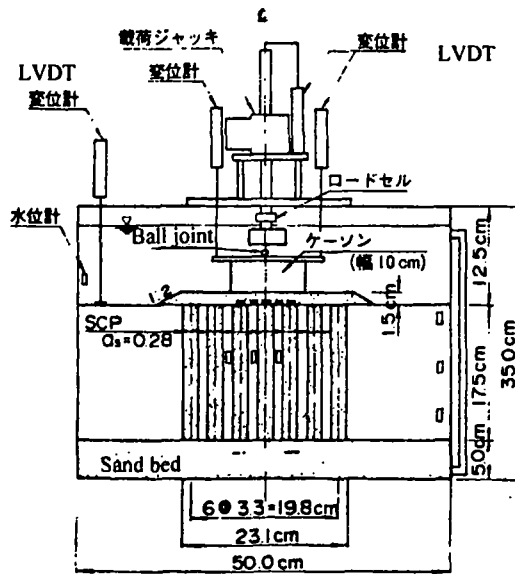
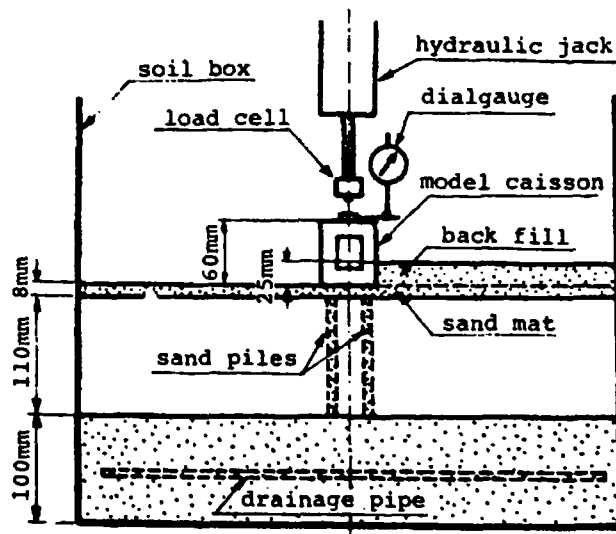


Fig 5.25: Numerical analyses on the effect of column installation using displacement method on (a) heaving of clay; (b) excess pore pressure; (c) set-up ratio of undrained shear strength of clay after consolidation, after Asaoka 1994b

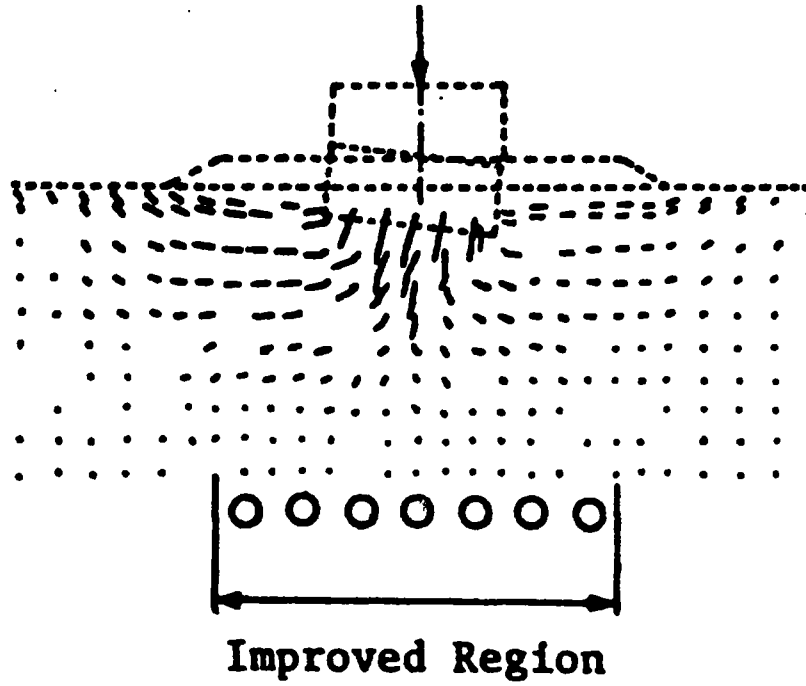


(a)

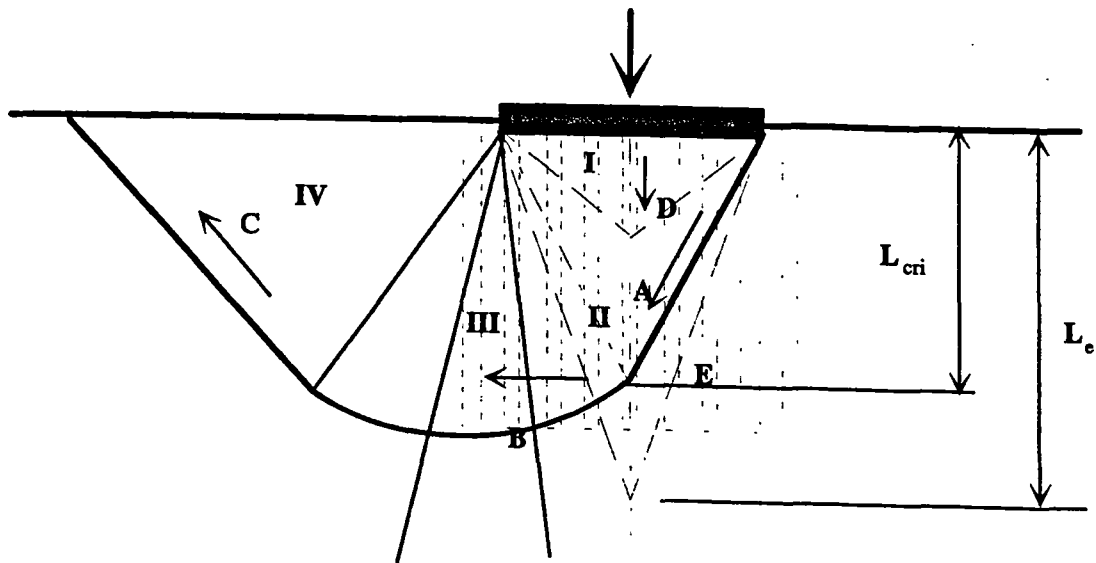


(b)

Fig 6.1: (a) Set up of centrifuge test on model sand compaction piles in PHRI (after Terashi et al 1991) (b) set up of centrifuge test on model sand compaction piles in TIT (after Kimura et al 1983)

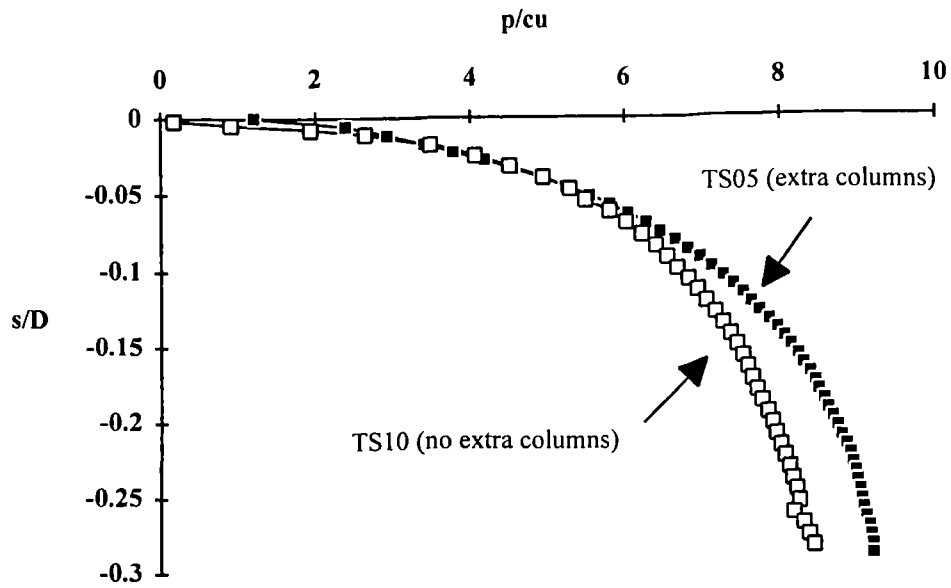


(a)

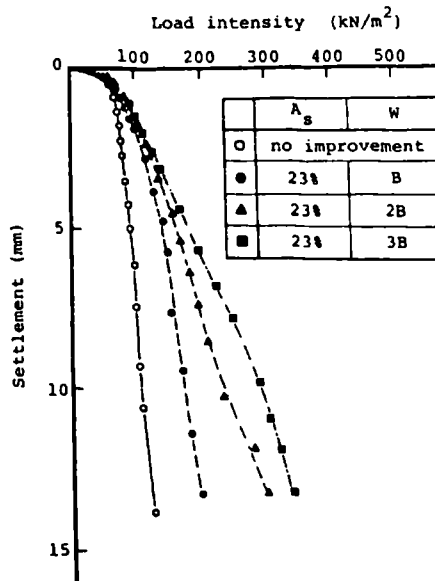


(b)

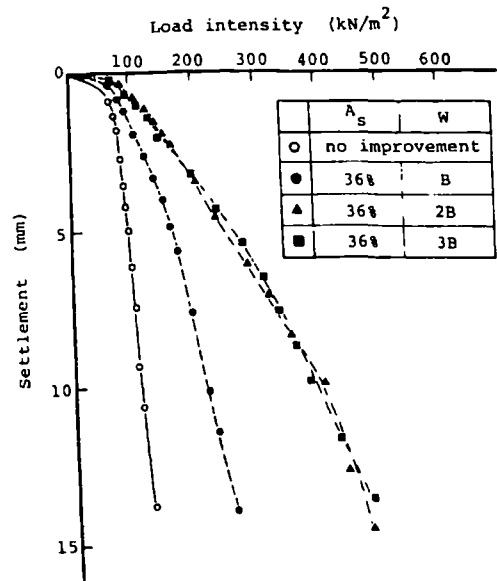
Fig 6.2: (a) Displacement vectors of model composite ground from centrifuge test, after Terashi et al 1991; (b) failure mechanism proposed by the Author for the model stone column foundation



(a)



(b) $A_s = 23\%$



(c) $A_s = 36\%$

Fig 6.3: Comparison of the effect of extra reinforced region on the load : displacement response (a) result of the Author's model tests, TS05 & TS10; (b) result from centrifuge tests $A_s = 23\%$, after Kimura et al 1983; (c) result from centrifuge tests $A_s = 36\%$, after Kimura et al 1983.

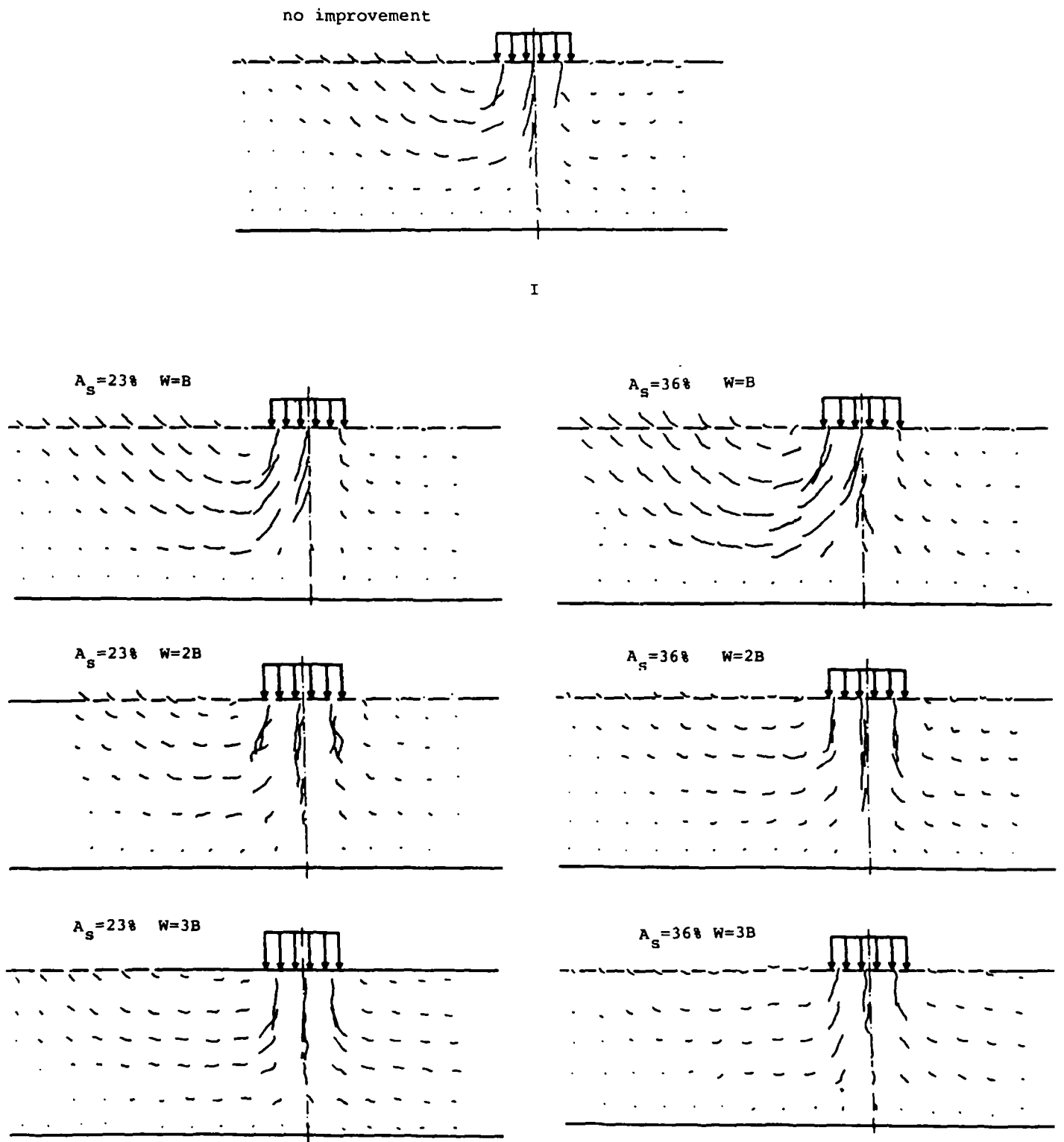


Fig 6.4: Displacement vectors obtained from centrifuge tests (after Kimura et al 1983)

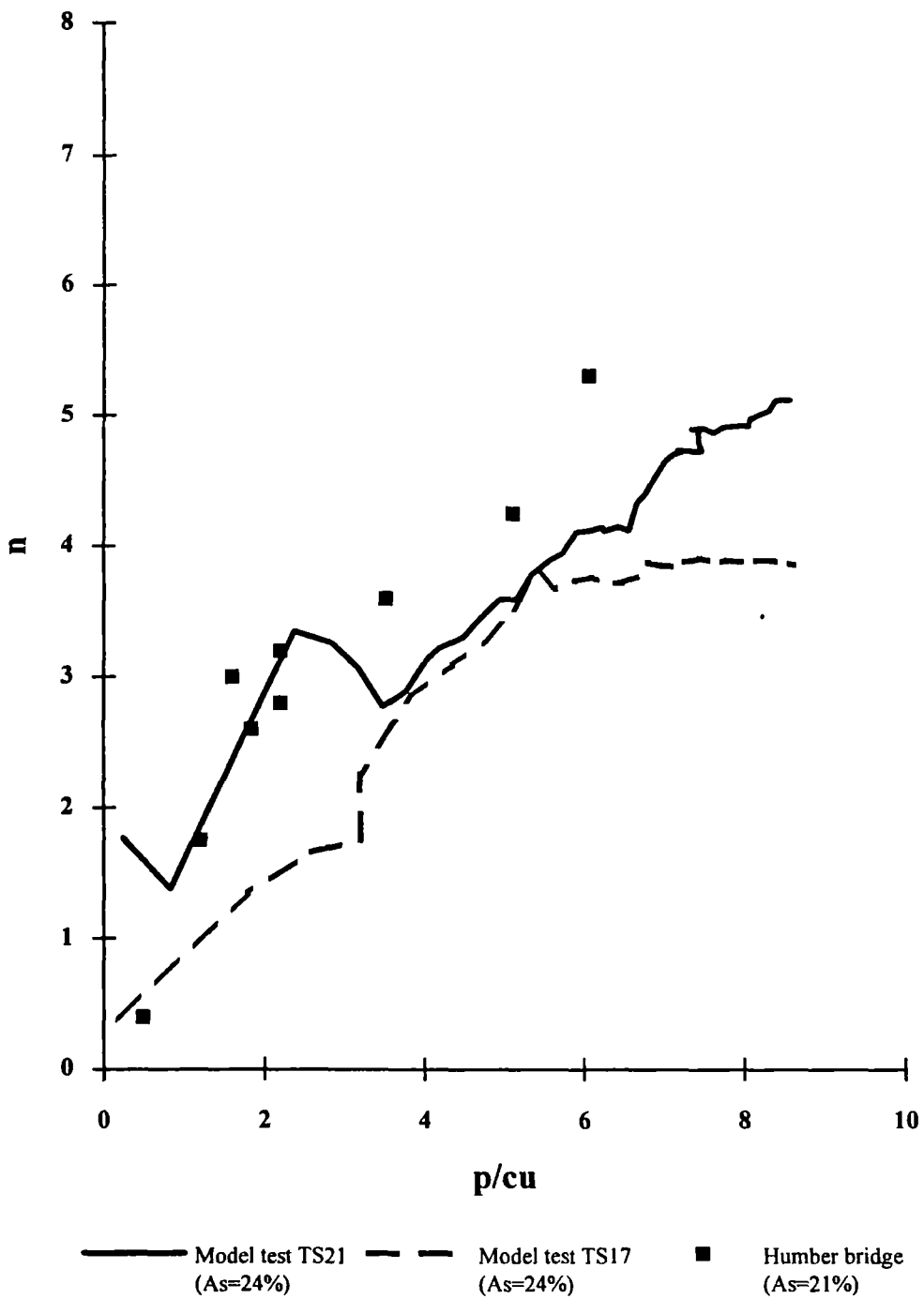
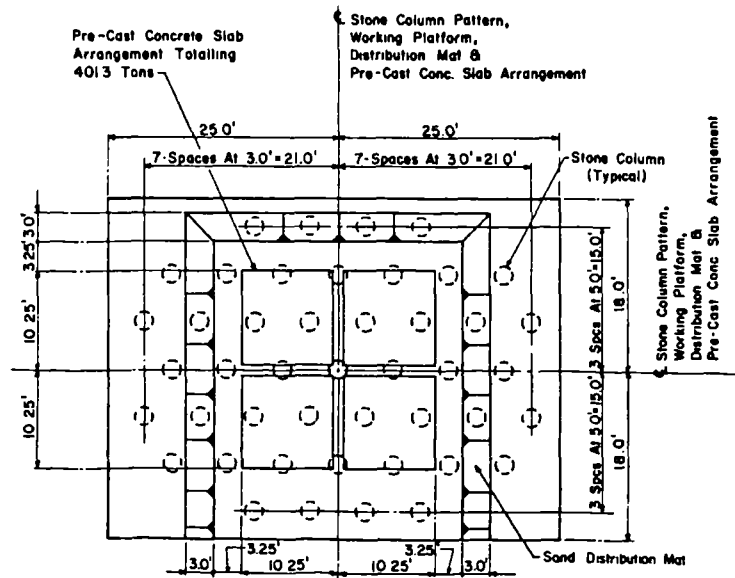
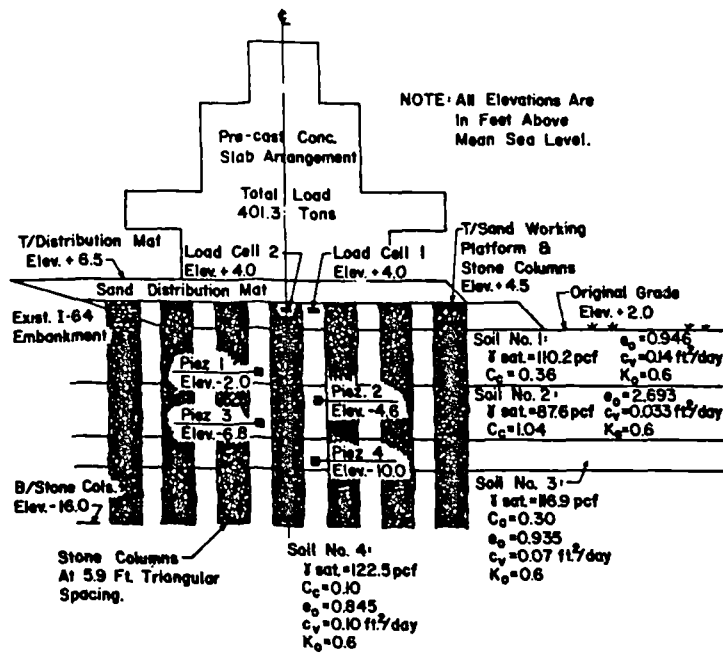


Fig 6.5: Comparison of stress concentration ratio : load response between the results from the Author's model tests and from field (Humber bridge case, after Greenwood 1991)



(a)



(b)

Fig 6.6: Hampton field test on stone column reinforced foundation (a) plan; (b) section, after Goughnour & Bayuk 1979b

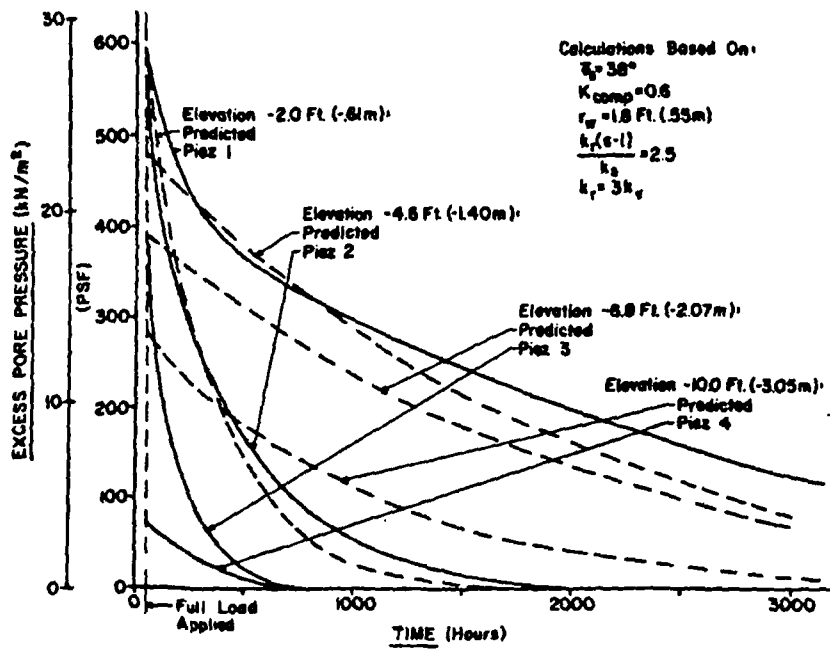
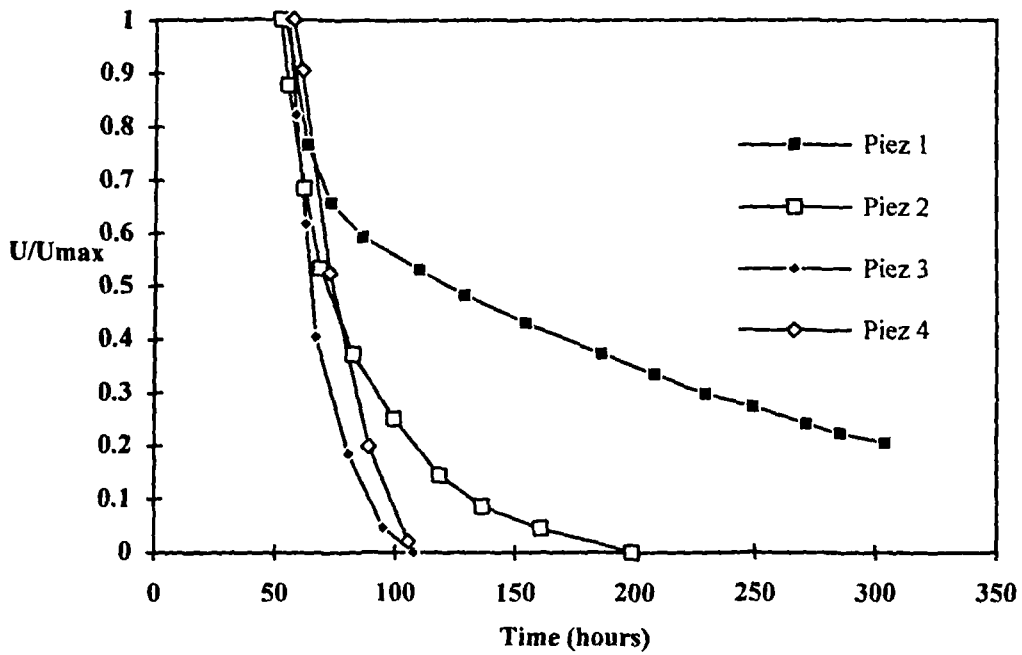


Fig 6.7: Piezometer response and predictions (after Bayuk & Goughnour 1979)



(b)

Fig 6.8: Rate of excess pore pressure dissipation : time (data deduced from Bayuk & Goughnour 1979)

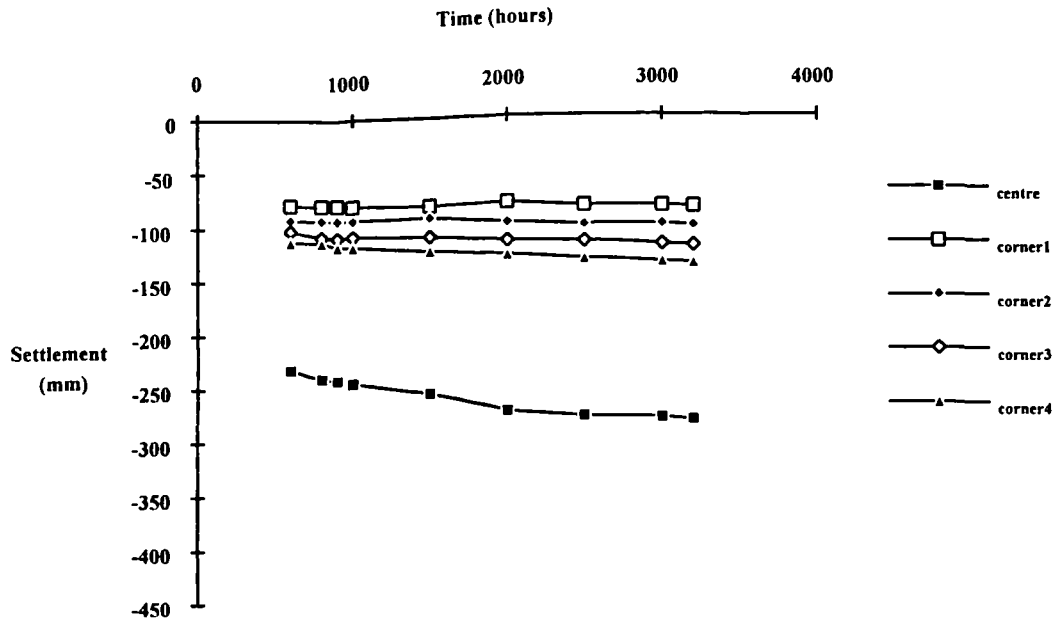


Fig 6.9: Surface settlement : time response measured from Hampton field test (reproduced from Goughnour & Bayuk 1979b)

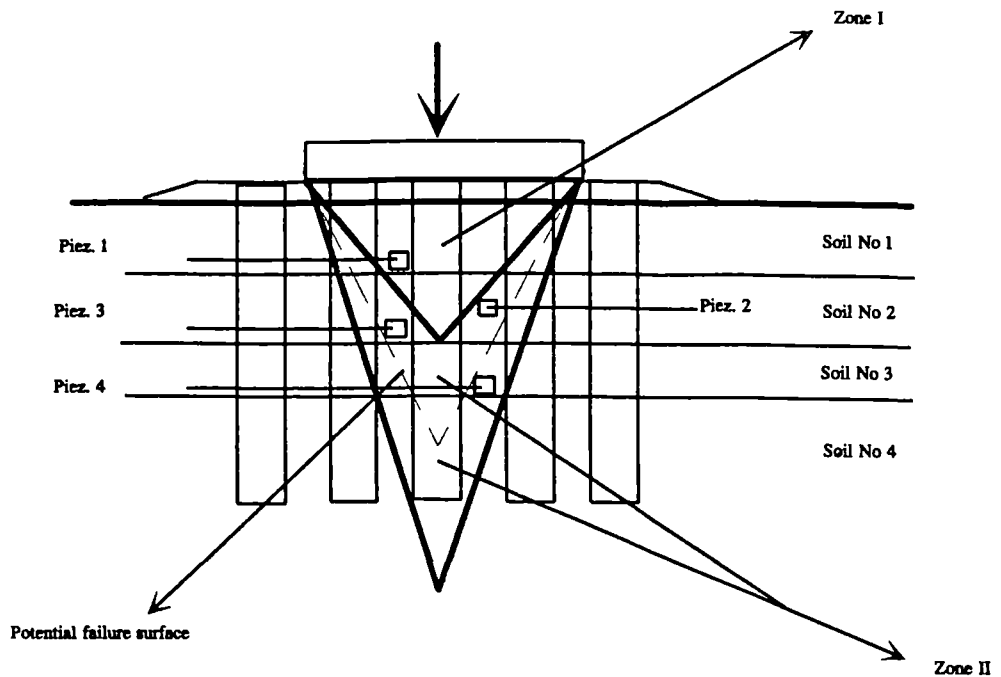


Fig 6.10: Analysis of the failure mechanism of Hampton field case

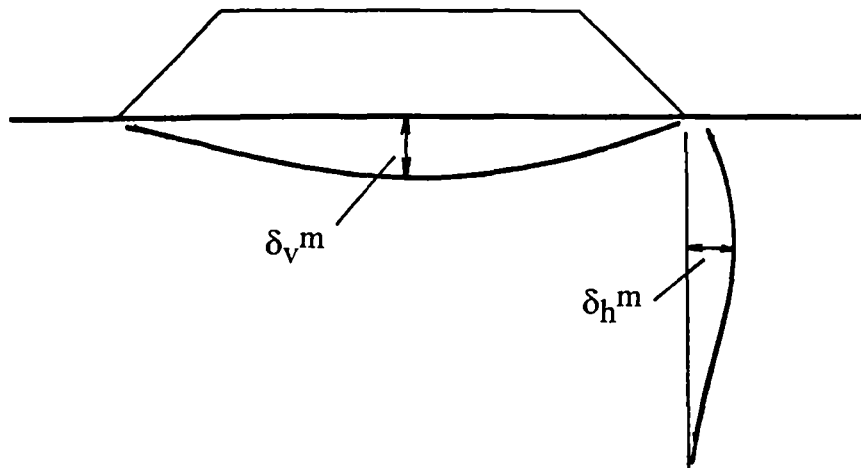


Fig 6.11: Deformations in a soft ground beneath an embankment

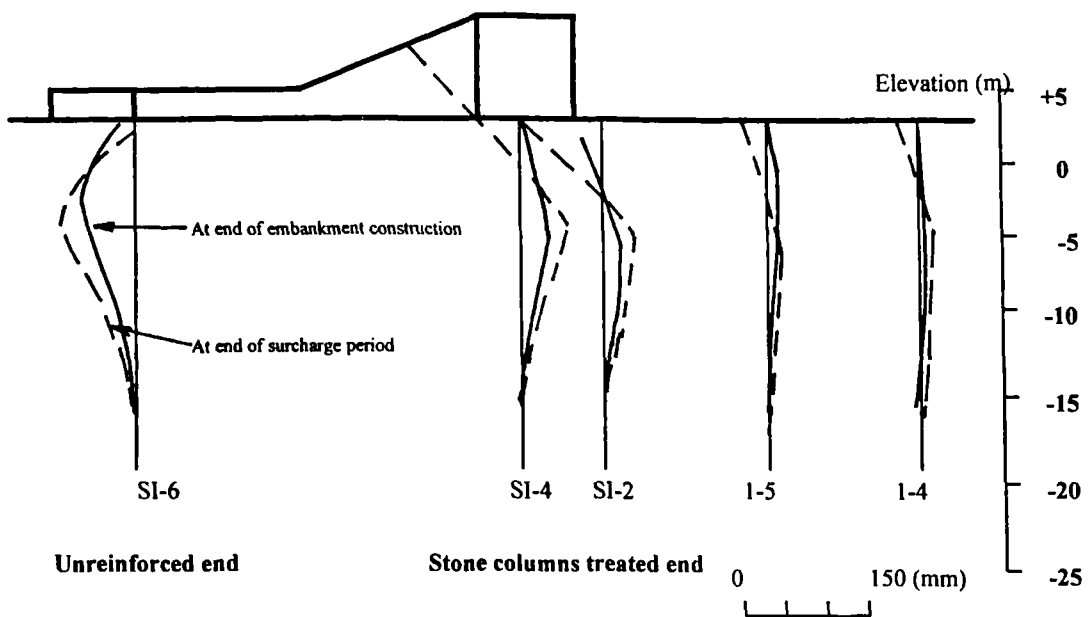


Fig 6.12: Ground horizontal movement profile beneath a trial embankment (Jourdan Road Terminal Project, reproduced from Munfukh et al 1984)

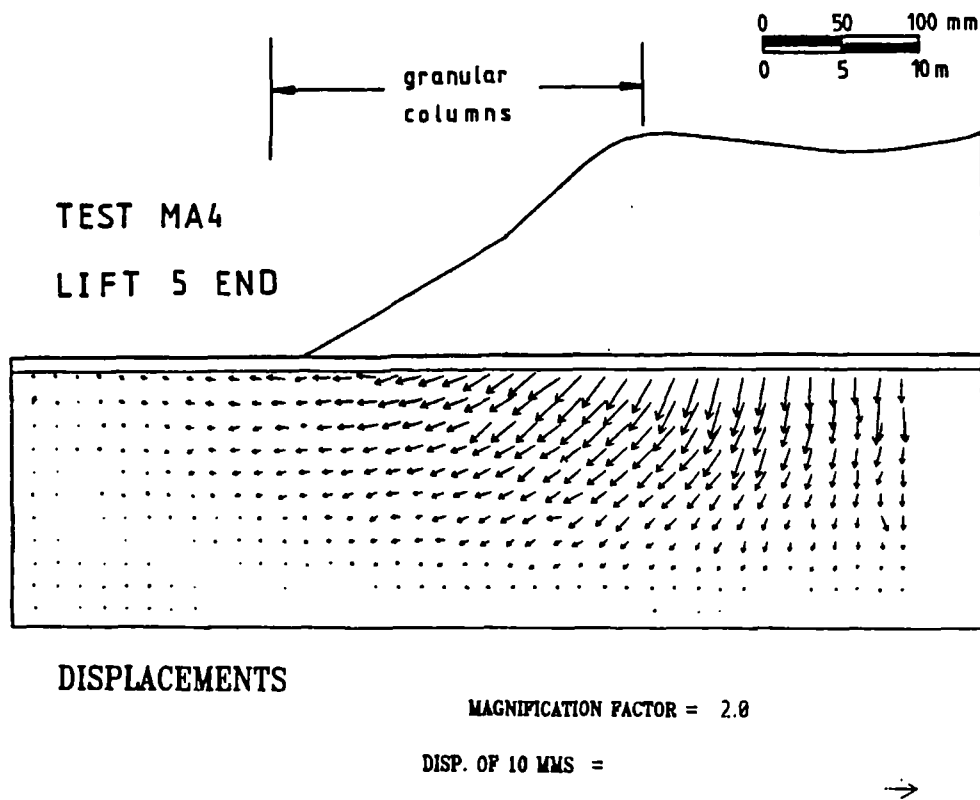


Fig 6.13: Displacement vector of a centrifuge model (after Almeida 1984)

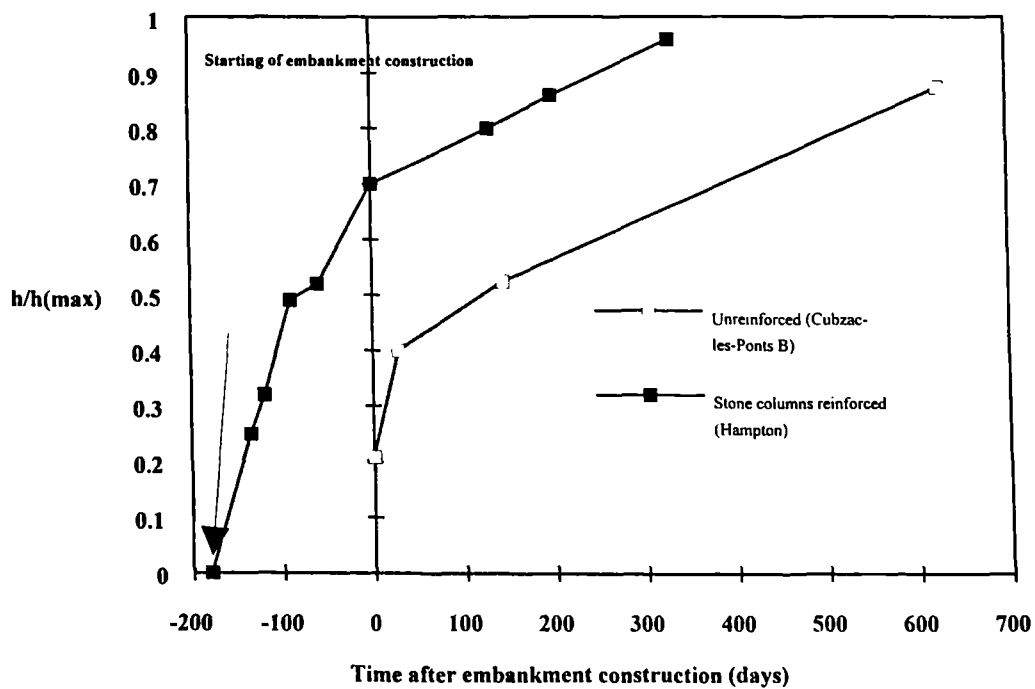
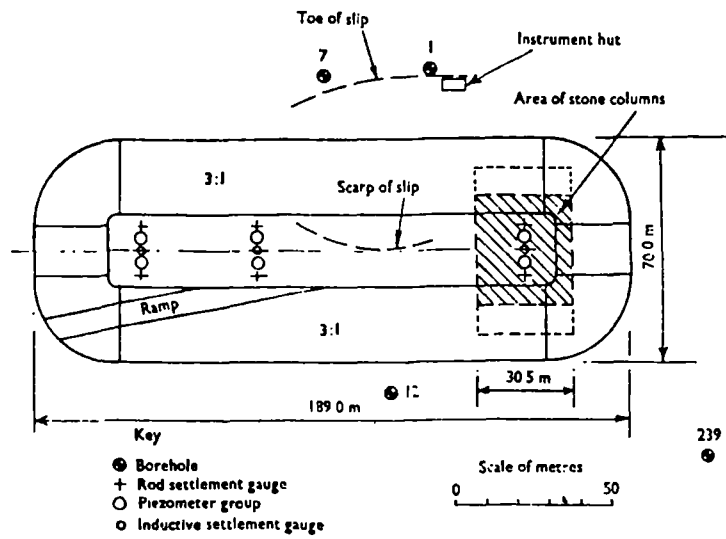
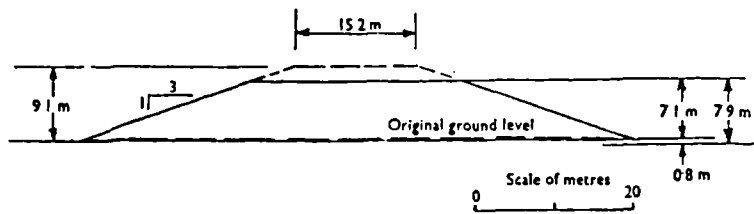


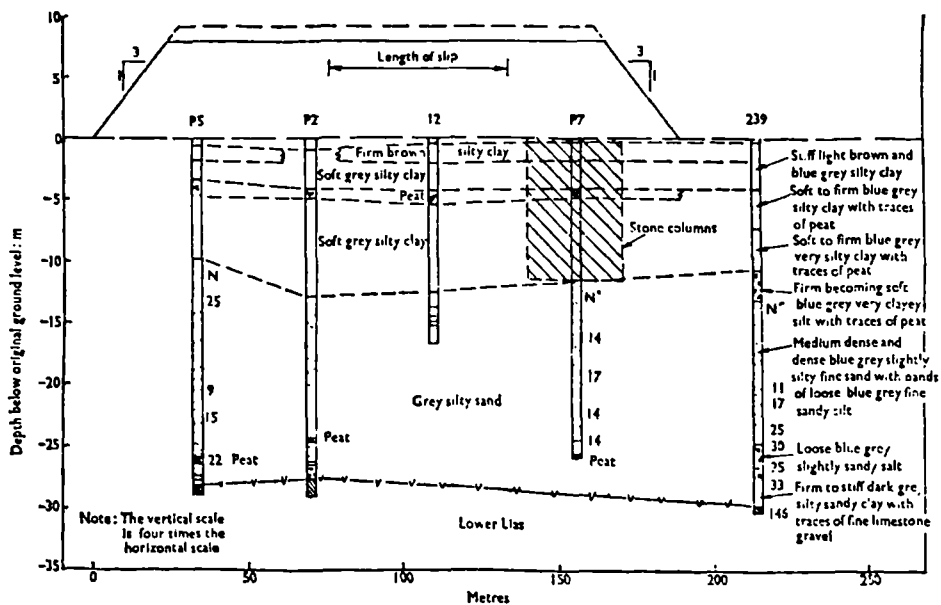
Fig 6.14: Development of maximum horizontal displacement in soft ground under embankment load (data from Tavenas 1979 and Goughnour & Barksdale 1984)



(a)

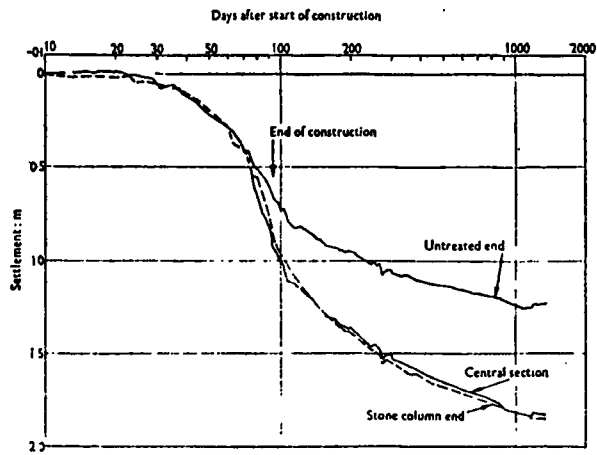


(b)



(c)

Fig 6.15: East Brent trial embankment (a) plan; (b) section of embankment; (c) longitudinal section, (after McKenna et al 1975)



(a) Settlement of the three centre line rod settlement gauges against log time

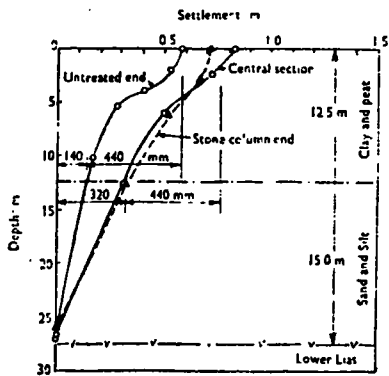


Fig. 11. Inductive settlement gauge readings on day 90, two days before the slip

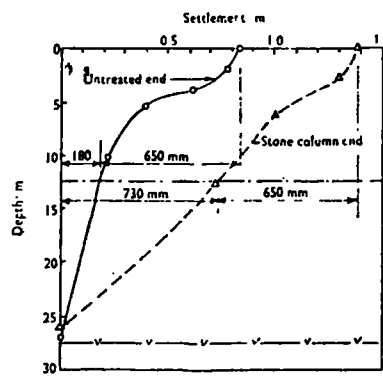
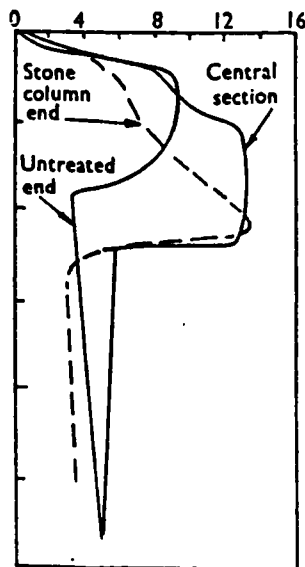


Fig. 12. Inductive settlement gauge readings on day 188

(b)

(c)



(d)

Fig 6.16: The measurements from East Brent trial embankment (a) readings from rod settlement gauges (b) readings from inductive settlement gauges on days 90 (c) readings from inductive settlement gauges on days 188; (d) readings from piezometer, Greenwood 1991

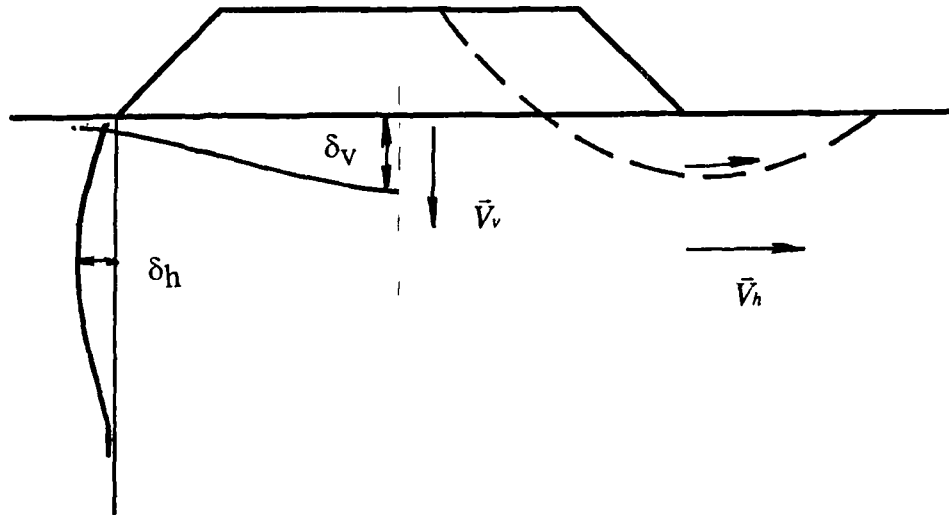


Fig 6.17: Analysis of failure mode of a soft ground under embankment load

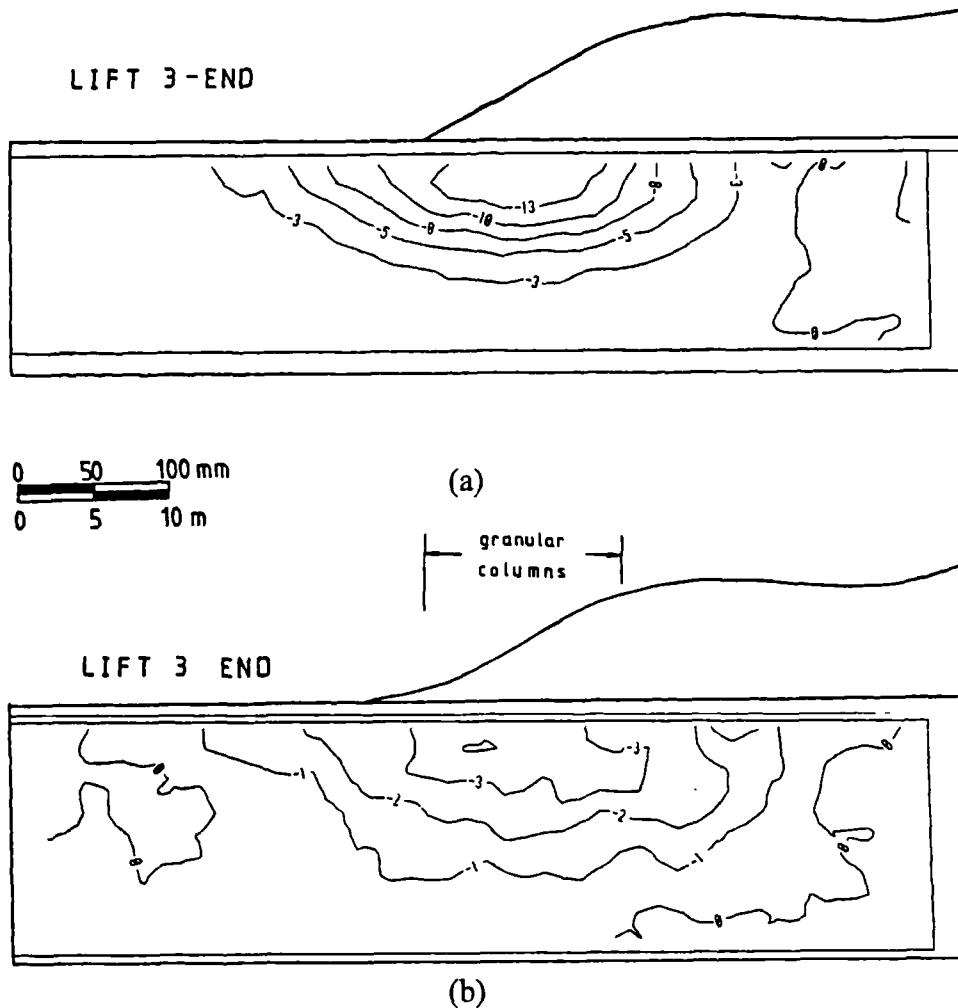
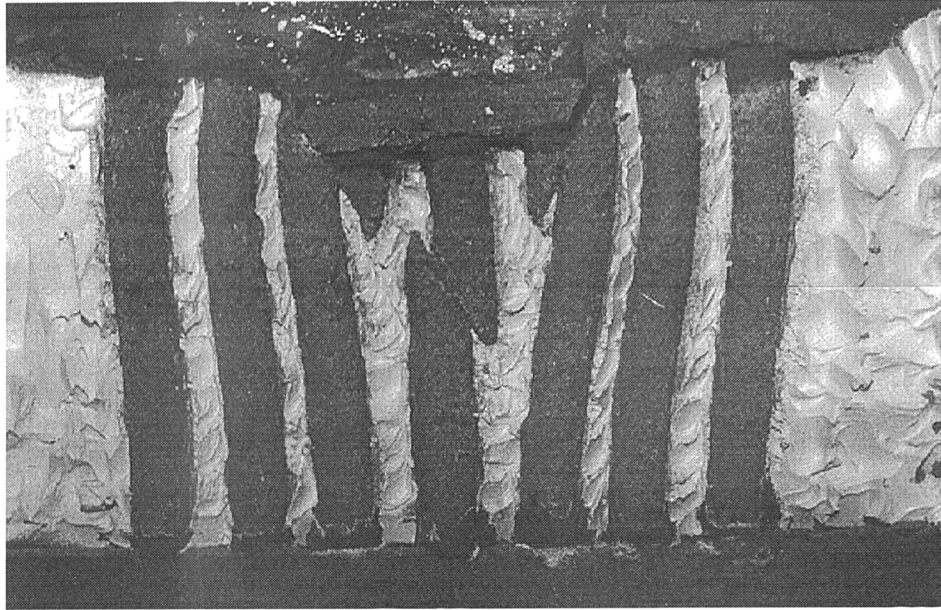
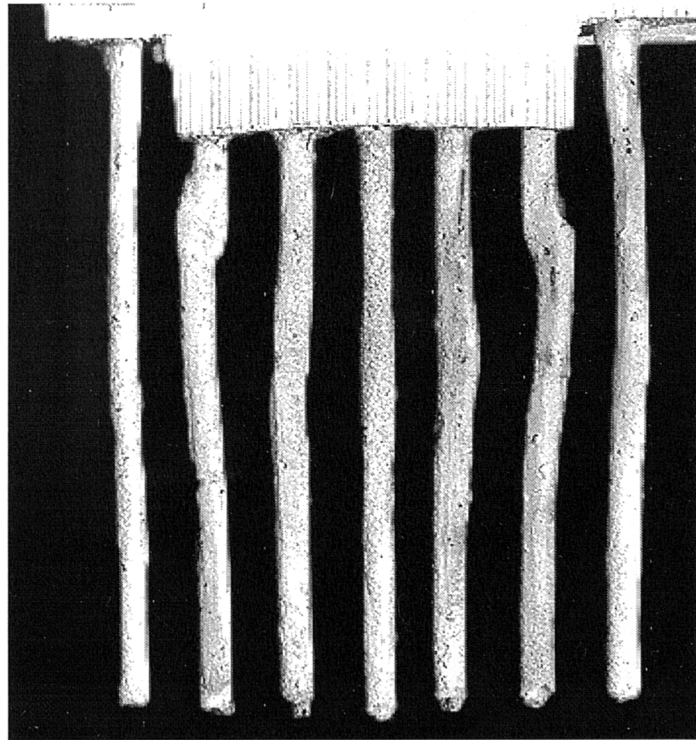


Fig 6.19: Horizontal displacement contours of centrifuge tests on model embankment built on (a) unreinforced clay bed (b) clay bed partly reinforced by granular columns, after Almeida 1984



(a)



(b)

Plate 6.1: The shapes of the model stone columns after test (a) centrifuge test, picture supplied by Terashi & Kitazume Japanese PHRI (b) the Author's model TS17



GLASGOW
UNIVE
LIBRARY

Plate 6.2: The deformation shape of model stone columns after test (TS10)